University of Reading

Crosstalk of oestrogen receptors in the male mouse brain

Thesis Submitted in fulfilment for the degree of PhD.
School of Biological Sciences, University of Reading

DeAsia Davis

May 2024

Declaration

I confirm that this is my own work and the use of all material from other sources has been properly and fully acknowledged.

Signed: DeAsia Davis

Covid Mitigation Statement

There were three main objectives to this thesis: 1) investigate crosstalk between oestrogen receptors and the signalling within multiple cell types 2) investigate the production and regulation of neurosteroids in the SBN of the male mouse 3) investigate the relevance of the production of neuroestrogens in the SBN using aromatase – flox mice model. Our work was significantly delayed 4 months due to university closure and lab capacity restrictions. The third objective of this thesis was to take place with our collaborator Professor Sonoko Ogawa at the University of Tsukuba, Japan April 2020. This unfortunately did not take place due to the COVID-19 pandemic and the resultant travel and work restrictions. After severe travel restrictions were lifted in Japan in 2022, we applied for certificate of eligibility per Japan regulations. The new date for travel was May 2022- July 2022, however, I had been offered a job with a major pharmaceutical company and chose not to extend my 4th year lab work.

Acknowledgements

Firstly, I would like to thank my supervisor, Dr. Nandini Vasudevan for her support, guidance, and patience over these past five years. I would not have made it through this PhD without your support and your guidance. Thank you for constantly pushing me to be the best version of myself and the best scientist I can be. I would like to extend my gratitude to Professor Phil G. Knight, thank you for all your help and support the last five years. I wouldn't have gotten through my thesis without Dr. Evangelos Delivopoulos and Dr. Francesco Tamagnini. Thank you for teaching me the techniques I've used during this project. It would not have been possible without the two of you so thank you! A very special thank you to Dr. Ruby Vajaria and Dr. Janine Dovey. Thank you for being my friends and support system throughout the years. Thank you to the entire Vajaria family for supporting me and always driving me to the airport. Thank you, Hong and all of the lab support staff who kept everything together. Finally, thank you to my mom and my sisters for their constant love and support throughout the years, I couldn't have done this without their devotion. Also, a special thanks to my grandmother who is no longer here but who provided me with the foundation I needed to start and finish this PhD.

Contribution Statement

Data in this thesis is presented in Chapter 2-4.

1. Chapter 2: Most of the data in Chapter 2 with the exception of Figures 2.8-2.10 are published in the following publication:

Publication: Davis D, Vajaria R, Delivopoulos E, Vasudevan N. Localisation of oestrogen receptors in stem cells and in stem cell-derived neurons of the mouse. J Neuroendocrinol. 2023 Feb;35(2):e13220. doi: 10.1111/jne.13220. Epub 2022 Dec 12. PMID: 36510342.

Expanded data: Figure 2.8-2.10.

Figures: All figures represent data collected, analysed and generated by Ms. DeAsia Davis's except Figure 2.4 which was done in collaboration with Ms. Ruby Vajaria, a PhD student co-supervised by Dr. Nandini Vasudevan and Dr. Evangelos Delivopoulos.

Intellectual contribution: The work in the paper was originally conceived and supervised by Dr. Nandini Vasudevan and expanded by Ms. DeAsia Davis to include ERα-36. Ms. DeAsia Davis also independently learnt and proposed the use of EZ-coloc software to analyse these sets of data.

Writing: The results and methods were written by Ms. DeAsia Davis as well as parts of the introduction and discussion and expanded data, with discussion by all co-authors. Some parts of the introduction and discussion were written by Dr. Nandini Vasudevan and Dr. Evangelos Delivopoulos in collaboration with Ms. Davis.

2. Chapter 3: Most of the data in this Chapter 3 is being prepared for publication.

Figures: All figures represent data collected, analysed and generated by Ms. DeAsia Davis.

Intellectual contribution: Using the techniques in Chapter 2, Ms. DeAsia Davis independently initiated this project due to interest in ER-GPER1 crosstalk. This was expanded and supervised by Dr. Nandini Vasudevan.

Writing: The results and methods were written by Ms. DeAsia Davis as well as parts of the introduction and discussion, in discussion with Dr. Nandini Vasudevan. Some parts of the introduction and discussion were written by Dr. Nandini Vasudevan.

3. Chapter 4: This has been submitted for publication in Endocrinology.

Submitted publication: Neurosteroids in the social behaviour network of the mouse.

Dovey, Janine., Davis, DeAsia., Knight, P., and Vasudevan, N. Submitted to Endocrinology, November 2023.

Figures: All figures that relate to the male mouse represent data collected, analysed and generated by Ms. DeAsia Davis. All figures that relate to the female mouse represent data collected, analysed and generated by Ms. Janine Dovey, a student in the laboratory supervised by Nandini Vasudevan. Hence, this paper has equal contributions from Ms. Janine Dovey and Ms. DeAsia Davis and is submitted as such to Endocrinology.

Intellectual contribution: The work in the paper was originally conceived and supervised by Dr. Nandini Vasudevan and Professor Phil Knight. Ms. DeAsia Davis also independently optimised and validated the acute slice technique that is integral to this paper. Many of the ideas in this chapter was honed by discussion amongst Ms. Janine Dovey, Ms. DeAsia Davis and Dr. Nandini Vasudevan.

Writing: The results and methods were written by Ms. DeAsia Davis and Ms. Janine Dovey as well as parts of the introduction and discussion, in discussion with Nandini Vasudevan. Some parts of the introduction and discussion were written by Dr. Nandini Vasudevan with discussion with both Ms. Janine Dovey and Ms. DeAsia Davis.

This has been agreed to by my supervisor, Dr. Nandini Vasudevan.

Signed:

Dr. Nandini Vasudevan

Contents

Abbreviations

Abstract

Locally produced neuroestrogens are crucial in the development of sexually dimorphic brain regions and drive sex-typical social behaviours. These behaviours are due to the signalling of oestrogens via its receptors in a set of interconnected nuclei called the social behaviour network (SBN). This thesis investigated the molecular interactions between classical oestrogen receptor(s) (ERs) ERα and ERβ and novel member ER G-Protein-Coupled-Oestrogen-Receptor 1(GPER1) through investigation of localization and crosstalk of receptors within cell lines and the production and regulation of neurosteroids in the SBN of male mice.

For the first time the subcellular localization of ERα, its variant ERα 36 and GPER1 was reported in mouse embryonic cells (mES) and mES derived motor neurons, although their functional roles remain to be investigated. Next, we treated a mouse embryonic hypothalamic neuronal cell (m-Hypo N42) with either vehicle (DSMO), E2, E2-BSA, G1 (GPER1 agonist), PPT (ERα agonist), or DPN (ERβ agonist) and measured aromatase expression through RT-qPCR. We also identified translocation of oestrogen receptors from the nucleus to the plasma membrane in two set of embryonic cell lines: mES and m-Hypo N42. For the first we demonstrate that ERβ and GPER1 may collaborate by signalling in the same pathway to rapidly increase aromatase expression in a mouse hypothalamic cell line. Using a novel *ex vivo* slice culture system, we show that the production of neuroestrogens - Estradiol (E2) and neurotestosterone- Testosterone (T) increases within 24 hours in all SBN nodes. Secretion of neurosteroids were measured by ELISA and RTqPCR and used to examine expression of steroidogenic enzymes and steroid receptors at various timepoints. Data presented in this thesis show that the expression of neurosteroids and steroidogenic enzymes are sexually dimorphic and increase with respect to time suggesting de novo synthesis. Lastly, we used the *ex vivo* slice culture system to examine the regulation of aromatase and subsequent oestrogen production in Medial Preoptic Area (MPOA) and Ventromedial Hypothalamus (VMH), two regions of the SBN associated with sexual and aggressive behaviour in male mice. However, the mechanism of action of aromatase regulation remains unclear. Collectively, these studies expand our knowledge of the function relevance of ERs in multiple systems and how they develop and maintenance the function of the SBN.

1.Introduction

1.1 General Introduction

Although generally thought to be a female sex hormone, oestrogen plays a critical role in the maintenance and regulation of reproductive and non-reproductive functions in both males and females. Oestrogen is a multifunctional steroid hormone that is critical for the sexually dimorphic organization of the brain and activation of sex-specific behaviours in both males and females by signalling via oestrogen receptors (ER)(Marrocco & Davidson, 1996). Oestrogen receptors are expressed throughout the central nervous system (CNS) particularly in sexually dimorphic regions; some of these regions of the brain are part of the interconnected set of nuclei called the Social Behaviour Network (SBN) that drive several social behaviours (O'Connell & Hofmann, 2011); (Ogawa et al., 2020);(Newman, 1999) . The SBN is conserved amongst vertebrate species and key to the regulation of common sexually dimorphic reproductive and aggressive behaviours (Newman, 1999), Goodson et al, 2005). The actions of oestrogen are thought to be mediated mainly by three oestrogen receptors (ERs), the classical intracellular nuclear hormone receptor oestrogen receptors alpha (ERα), an isoform of the ERα, the oestrogen receptor beta (ERβ), and the novel G protein-coupled oestrogen receptor 1/ 30 (GPER1/GPR30). The predominantly studied signalling pathway for oestrogens is the genomic pathway where oestrogens bind ERα and ERβ to activate transcriptional events that control gene expression (Fuentes & Silveyra, 2019). However, over the last two decades, studies have found that rapid membrane-initiated signalling via Membrane oestrogen receptors (mERs) such as GPER1 but also via ERα and ERβ is also physiologically significant, particularly in the central nervous system (Ruby Vajaria & Nandini Vasudevan, 2018) and in the cardiovascular system (Fuentes & Silveyra, 2019; Saczko et al., 2017; Vrtačnik et al., 2014).

Non-genomic signalling mediated via from mERs have shown to regulate aggressive behaviour in male rodents and sexual behaviour in females (Ervin, Mulvale, et al., 2015).For example, in *Peromyscus polionotus* male mice, estradiol injections increased aggression within 15mins via ERα or ERβ (Trainor, Rowland, et al., 2007). However, the molecular mechanisms that underlie oestrogen control of social behaviours are still not fully understood (Ervin, Mulvale, et al., 2015; Fuentes & Silveyra, 2019; Goodson, 2005; J. L. Goodson & D. Kabelik, 2009) .In this introduction, we will focus on a) the different ERs, particularly the mERs as a prelude to Chapter 2 b) nongenomic signalling, particularly as it pertains to social behaviours as a prelude to Chapter 3 and c) the role of aromatase and neuroestrogens in social

behaviours as a prelude to Chapters 4 and 5. We will focus on CNS examples of non-genomic and genomic signalling wherever possible.

1.2 Oestrogen

Steroids are organic compounds that belong to a sterol group of lipids. All steroids are composed of four domains (A, B, C, D) in a tetracyclic sterane structure(Nes, 2011). A, B, and C are full six-carbon cyclohexane rings, ring D contains the five-carbon cyclopentane(Norman & Litwack, 1997). There are six classes of steroid hormones (1) oestrogen (2) androgens (3) progestins (4) glucocorticoids (5) mineralocorticoids (6) Vitamin D steroids(Hall, 1984; Villee, 1972). In human adrenals cholesterol can be synthesized de novo via acetate, however most cholesterol is derived from dietary cholesterol plasma-low density lipoproteins (LDLs) (Giatti et al., 2019). The biosynthetic pathway of cholesterol is facilitated by more than 27 enzymes from cytochrome 450s (CYPs) and hydroxysteroid dehydrogenase (HSDs) that aid in the structural modifications necessary to form pregnenolone , a precursor for steroid hormones(Giatti et al., 2019; Nes, 2011). In the mitochondria, StAR (steroidogenic acute regulatory protein) transfers free cholesterol from the outer mitochondrial membrane to the inner mitochondrial membrane(Kallen et al., 1998; Miller, 2007). Cholesterol is then used as a substrate by cleavage enzyme P450scc, which catalyses the conversion of cholesterol to either 17- alpha hydroxy pregnenolone (eventually leading to vitamin D and its isoforms) or progesterone leading to the other steroids (Giatti et al., 2019; Miller, 2007).

Oestrogens are lipophilic molecules that are synthesized in the gonads or in the brain itself from cholesterol(Giatti et al., 2019).Oestrogens are synthesized via catalysation of C^{19} androgenic steroids to C^{18} estrogenic steroids by the enzyme aromatase(Chan et al., 2016; Stocco, 2012). In mammals, there are four forms of oestrogen (Kuiper et al., 1997): oestrone (E1) 17β-oestradiol (E2) oestriol (E3) and 17α- oestradiol (17α) (Figure 1.1). E2 is the most potent form of oestrogen and has been the focus of studies on the function of oestrogens both in oestrogen-dependent and oestrogen-independent cancers (Chen et al., 2008; Hayashi et al., 2003) and in the CNS (Charlotte A Cornil et al., 2012; C. A. Cornil et al., 2012; Cui et al., 2013; Honda et al., 2011).

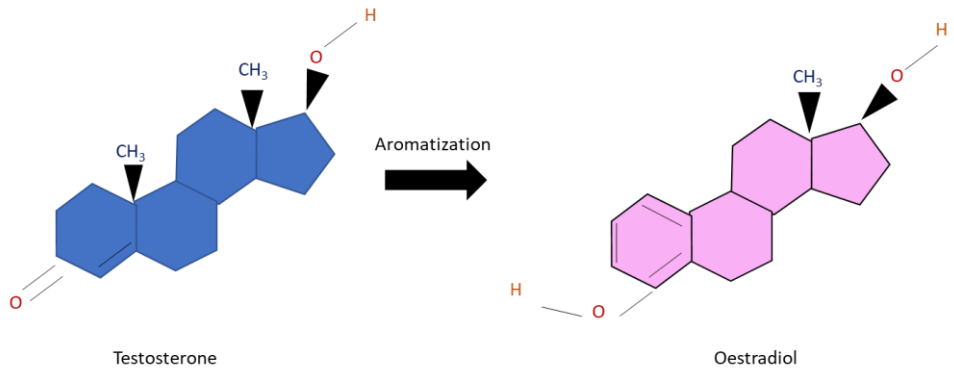

Figure 1.1 Chemical structure and conversion of testosterone to oestradiol. *C-19 steroids are aromatized via the oxidation of a methyl group. Subsequent oestrogen have a ' aromatic A- ring structure . The oestrogens are unique among the steroid hormones in that they have an aromatic and 18- carbon structure.*

1.2.1 Structure of classical oestrogen receptors

Estrogenic signalling is mediated in part by transcription factors i.e. two distinct isoforms of the nuclear oestrogen receptors (ERs) known as ERα and ERβ. ERα (Figure 1.2) and ERβ (Figure1.2) are encoded by two distinct genes: ESR1 and ESR2 respectively, that are differentially expressed through the body and CNS. Like other members of the nuclear receptor superfamily of transcription factors, ERs contain 5 regions - A/B, C, D and E/F that correspond to distinct structural domains that have specialized functions (Figure 1.2). The A/B region, a N terminal hypervariable domain, is involved in the activation of gene transcription .The C domain is the DNA binding domain (DBD) and can bind to oestrogen response elements (ERE) in the chromatin of target sequences (Enmark & Gustafsson, 1999; Mueller & Korach, 2001; Pike et al., 2000). The C domain is also responsible for the dimerization function. The Ligand Binding Domain (LBD) , Region E/F) is comprised of a ligand binding pocket as well as critical for coactivator and co-repressor binding. The ligand-independent activation (AF)-1 and ligand-dependent activation (AF)-2 work to recruit coregulatory protein complexes that facilitate transcriptional regulation (Heldring et al., 2007).

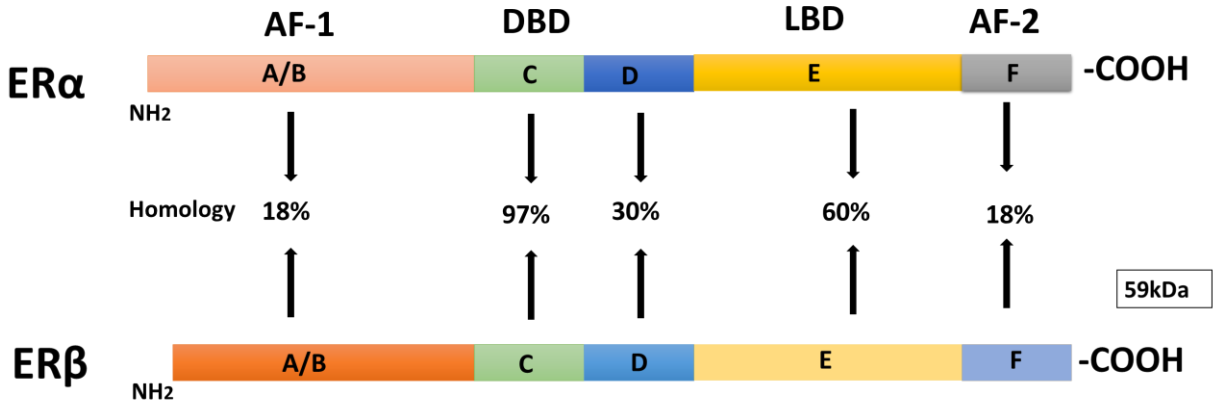

Figure 1.2 Oestrogen receptor structure. Schematic structure of the nuclear oestrogen receptors ERα and ERβ and the percentage of homology between the domains annotated by regions A-F. These domains correspond with the function : N-terminal activation function 1 region (AF)-1, DNA-binding domain (DBD), ligand-binding domain (LBD), and C-terminal function 2 domain (AF)-2.

Classical ERα is a 66kDA protein coded by ESR1 in contrast to the ERβ that is a 59kDA protein encoded by ESR2 gene that is on a different chromosome (Kuiper et al., 1996; Mosselman et al., 1996)Though this receptors share a high degree of homology in their DBD (97%), there are structural differences in their (AF)-2 (less than 18% homology) which accounts for differences in transcriptional activity(Enmark & Gustafsson, 1999). Additionally, ERβ lacks (AF)-1 activity which reduces their transcriptional activation. Differences in LBD amino acid sequences between ERα and ERβ also decrease the affinity of ERβ for E2 compared to other oestrogens. In addition to full length ERα and ERβ there are several alternatively sliced isoforms. The full length ERα66 has three known slice variants ERαΔ4 (ERα52), ERα46 and ERα36. ERα46 is a 46kDA associated with human breast cancer cells, where it is localized at the plasma membrane of epithelial (L. Li et al., 2003). ERα36 is a 36- kDa protein that lacks the transcriptional activation domains (AF)-1 and (AF)-2 though there exists a DNA binding domain (Wang et al., 2005).ERα36 is notably detected in both the cytoplasm and the plasma membrane in breast cancer and endothelial cells (Penot et al., 2005; Wang et al., 2006)and recently the CNS. ERαΔ4 has been found in high levels in the membrane subfractions of neurons and (Penot et al., 2005; Wang et al., 2005).In the hypothalamic cell lines N-38 ERαΔ4 is found at higher levels than full length ERα(Dominguez et al., 2013).

There are five known slice variants of ERβ in the brain, with the type and amount of the splice variant dependent on the brain region (Weiser et al., 2008).ER-β1 has been shown to be the most abundant variant throughout the brain, it is expressed in the meAMY(extended Medial Amygdala) and LS (lateral septum) of the Social Behaviour Network, discussed further in

Section 1.4.2 . At the membrane oestrogens can act via several ERs- ERα 36, ERαΔ4, Erβ and its splice variants. Since several ERs have been shown at the plasma membrane in different cell types, it is conceivable that they initiate rapid non-genomic signalling (Chaban et al., 2004) though the physiological significance of the presence of these variants and their relative levels in any cell type remain poorly understood.

1.3 Oestrogen Signalling

1.3.1 Genomic Signalling

Direct genomic signalling occurs E2 interacts with ERα and ERβ within the nucleus and cytosol which then binds to DNA sequences and modulates gene expression (Bjornstrom & Sjoberg, 2005). There are two major types of genomic signalling 1) ligand –dependent 2) ligand-independent (Bjornstrom & Sjoberg, 2005). Ligand – dependent genomic signalling requires hormone-bound receptors ERα and ERβ to bind directly to specific enhancer elements in the promotor region of target genes. Ligand – independent signalling can occur without specific enhancer elements (i.e. EREs) or via activated growth factor receptors/growth factors that crosstalk with nuclear ERs as illustrated in Figure 1.3. Genomic effects can occur via direct binding to specific ERE (oestrogen response elements) or binding of ER to DNA-bound transcription factors such as AP-1 which may bind to non-ERE-containing enhancer elements (Dickens et al., 2011) (figure 3). A number of genes such as oxytocin and oxytocin receptor, the enkephalins are transcriptionally regulated by E2 to drive female reproductive behaviour or lordosis in the (Bale et al., 2001) (Bale et al., 1995) (Sinchak et al., 2000). On the other hand, E2 can also exert action via rapid non-genomic effects that involves the indirect regulation of gene expression via activation of multiple intracellular cascades; this is termed coupled or integrated signalling and is important in the induction of the progesterone receptor (PR) by oestrogen in breast cancer cells (Vasudevan & Pfaff, 2007) (Vasudevan & Pfaff, 2008)in lordosis (discussed further in section 1.5.2.1).

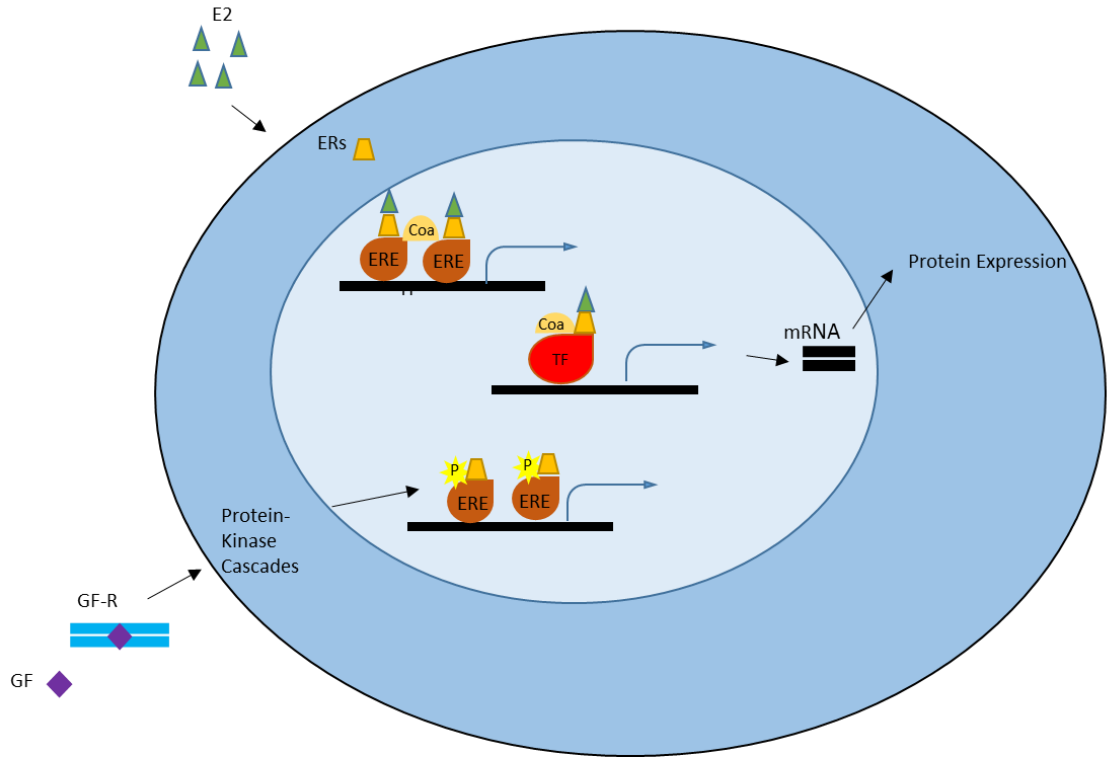

Figure 1.3. Illustration of genomic signalling by nuclear oestrogen receptors. Receptors are bound to cognate ligands that act as transcription factors in the nucleus by binding to specific enhancer elements in promoter genes. (2) ERE- independent action, receptors bind to other transcription factors, that then binds to enhancer-elements specific for that transcription factor (Kuiper et al., 1997). Growth factors activate protein cascades that leads to the phosphorylation and activation of oestrogen receptors at specific enhancer elements(Bjornstrom & Sjoberg, 2005; Giatti et al., 2019; Simoncini et al., 2002).

1.3.1.2 Non-genomic Signalling

The first evidence of non-genomic signalling was reported by (Szego & Davis, 1967), who observed a rapid increase in uterine cyclic adenosine monophosphate (cAMP) of ovariectomized female mice within 15 mins of E2 stimulation. In a variety of cell types, non-genomic signalling of oestrogen action involves the activation of protein kinase cascades (Giatti et al., 2019; Losel et al., 2003; Wehling & Lösel, 2006), by activation of a membrane ER (mER) at the plasma membrane (Vasudevan & Pfaff, 2007, 2008)). In many cases, this has been shown using a membrane limited E2-BSA conjugate, which is 17β Estradiol linked to benzoate preventing estradiol from entering the cell due to the large size of BSA (Vasudevan & Pfaff, 2007). In addition, the identity of the mER initiating this cascade was shown by the use of pharmacological agonists or antagonists or by the use of knockout animals (Rainville et al., 2015).In two nuclei of the female SBN, namely the medial preoptic area (mPOA) and

the bed nucleus on the stria terminalis (BNST), E2 treatment to ovariectomized rats rapidly increased the phosphorylation of CREB (Zhou et al., 1996). Additionally, E_2 treatment caused an increase in immunoreactive phosphorylated CREB (pCREB) cells in the anteroventral periventricular nucleus, suggesting CREB phosphorylation has an effect on E2 mediated gene expression (Figure 1.4) (Gu & Moss, 1996). In both male and female gonadectomized mice, E2-BSA administration for 1 hour increased pCREB in the mPOA, ventromedial hypothalamus (VMH), medial septum as well as in GnRH neurons indicating rapid non-genomic signalling (Abraham et al., 2004). In addition, phospho-CREB could be increased by either ERα or ERβ; in the mPOA, a region that expresses both receptors, pCREB increases were normal upon EB administration in either the ovariectomized ERαKO or ERβKO female mice. In regions where ERβ or ERα was the sole ER, pCREB did not increase on E2-BSA administration (Abraham et al., 2004). Moreover, in some cases this could be due to an increase in protein translation for e.g. in NG108 neuroblastoma cells, E2 rapidly increases in postsynaptic density protein 95 (PSD-95) via the increased phosphorylation of elongation factor 4E-BP1 in a PKB-dependent fashion without changing the level of PSD-95 mRNA (Akama & McEwen, 2003). PSD-95 is required for the synthesis of new spines and synaptic activity indicating that rapid action of E2 may effect cognitive (Akama et al., 2013). Similarly , in midbrain dopaminergic neurons`, both protein kinase B (PKB) (Ivanova et al., 2001) and protein kinase A (PKA) pathways (Beyer & Karolczak, 2000) were rapidly induced by E2 and blocking these pathways resulted in a reduction of neurite outgrowth. In some studies, the rapid signalling cascade has been linked to a behavioural change; this has been most often shown in the hippocampus where oestrogen generally is beneficial for cognition or in the cortex for neuroprotection (Frick & Kim, 2018).

In the dorsal hippocampus, activation of GPER1/GPR30 (Section 1.3.1.3), a GPCR and a putative mER, or activation of ERα using pharmacological agonists for GPER-1 such as G-1 rapidly increased social recognition, object recognition and dendritic spine density within 40 minutes in female ovariectomized mice(Ervin, Lymer, et al., 2015; Christopher Gabor et al., 2015; Lymer et al., 2017; Phan et al., 2012), with the time frame suggesting that this is due to rapid, non-genomic action. In contrast to this, the ERβ agonist, DPN, impaired social recognition and increased object placement at higher doses and decreased spine density in the stratum lacunosum-moleculare layer of the hippocampus (Phan et al., 2011). However, in the medial amygdala, infusion of pharmacological agonists to all three ERs, i.e. ERα, ERβ and GPER1 could increase social recognition in ovariectomized female mice (Lymer et al., 2018)demonstrating that the differential contribution of ERs appears to depend on brain region. Though the mechanisms that underlie the rapid increase in spine density remain

unclear, both protein synthesis inhibitors and actin polymerization inhibitors decrease social recognition when infused into the dorsal hippocampus prior to testing but DNA transcription inhibitors do not decrease social recognition (Sheppard et al., 2018). In addition, post-training infusion of a JNK inhibitor but not an ERK inhibitor into the dorsal hippocampus of female ovariectomized mice abolished GPER-1 mediated object recognition memory, suggesting that GPER1 used a different MAPK pathway for memory retrieval (Kim et al., 2016). The rapid effect of oestrogens on male aggressive behaviour in the *Peromyscus* species is described in Section 1.5.2.1.2.

In some cases, integration of these two pathways by a coupled signalling pathway can exist. For example, E2-BSA addition for 20 minutes in a neuroblastoma cell line increases transcription from a consensus ERE by increasing phosphoinositide 3-kinase (PI3K) and ras-raf-mEK-ERK pathway (ERK) activation which in turn phosphorylate the ERα (Figure1.4)(Clark et al., 2014). In, SK-N-SH, a neuroblastoma cell line, E2 treatment rapidly increases PKA activation and CREB phosphorylation, both of which are needed for the upregulation of the neurotensin gene; upregulation does not occur when the protein kinase A (PKA) pathway is blocked or in the preoptic area of PKA-deficient mice (Watters & Dorsa, 1998). E2-BSA activated mitogen-activated protein kinase (MAPK) pathways (Figure1.4) in human neuroblastoma cells and this signalling pathway was required to upregulate a c-fos promoter linked to a reporter gene (Watters et al., 1997); c-fos is often used as a candidate to measure activation of different brain nuclei, including those in the SBN (Davis et al., 2004; Kalinichev et al., 2000). In the arcuate nucleus of the hypothalamus (ARH), spine density, particularly of mushroom shaped spines is increased by E2 treatment over 48 hours in female rats and is correlated with the increase in female sexual receptivity also known as lordosis. However, the first phase of this process is the generation of filamentous spines, a process promoted by the activation of protein kinases C (PKC) and LIM domain kinase (LIMK) by the ERα-mGluR1 (Figure 1.4) complex at the cell membrane. LIMK is a kinase that phosphorylates and inactivates the actin depolymerization factor, cofilin and allows for branching and stabilization of spines. Supporting this, administration of a Metabotropic glutamate receptor 1(mGluR1) antagonist into the ARH decreases the levels of phosphorylated cofilin within an hour of infusion. However, the appearance and increase of mature, mushroom shaped spines in ARH neurons of the female rat requires longer time scales – approximately 48 hours after E2 administration, in parallel with the E2 induction of lordosis – and requires genomic transcription, including an increase in CREB-mediated (Christensen et al., 2011) (Micevych & Christensen, 2012). In another nucleus critical for lordosis, the ventromedial hypothalamus (VMH), application of ligands that bind G-protein coupled

receptors (GPCR) such as oxytocin, vasopressin or acetylcholine increase frequency of action potentials (Kow & Pfaff, 1988). Together, these data suggest that these rapid effects that emanate from E2 stimulation of mERs induces changes in long-term transcription and alters CNS function to drive a physiologically relevant behaviour.

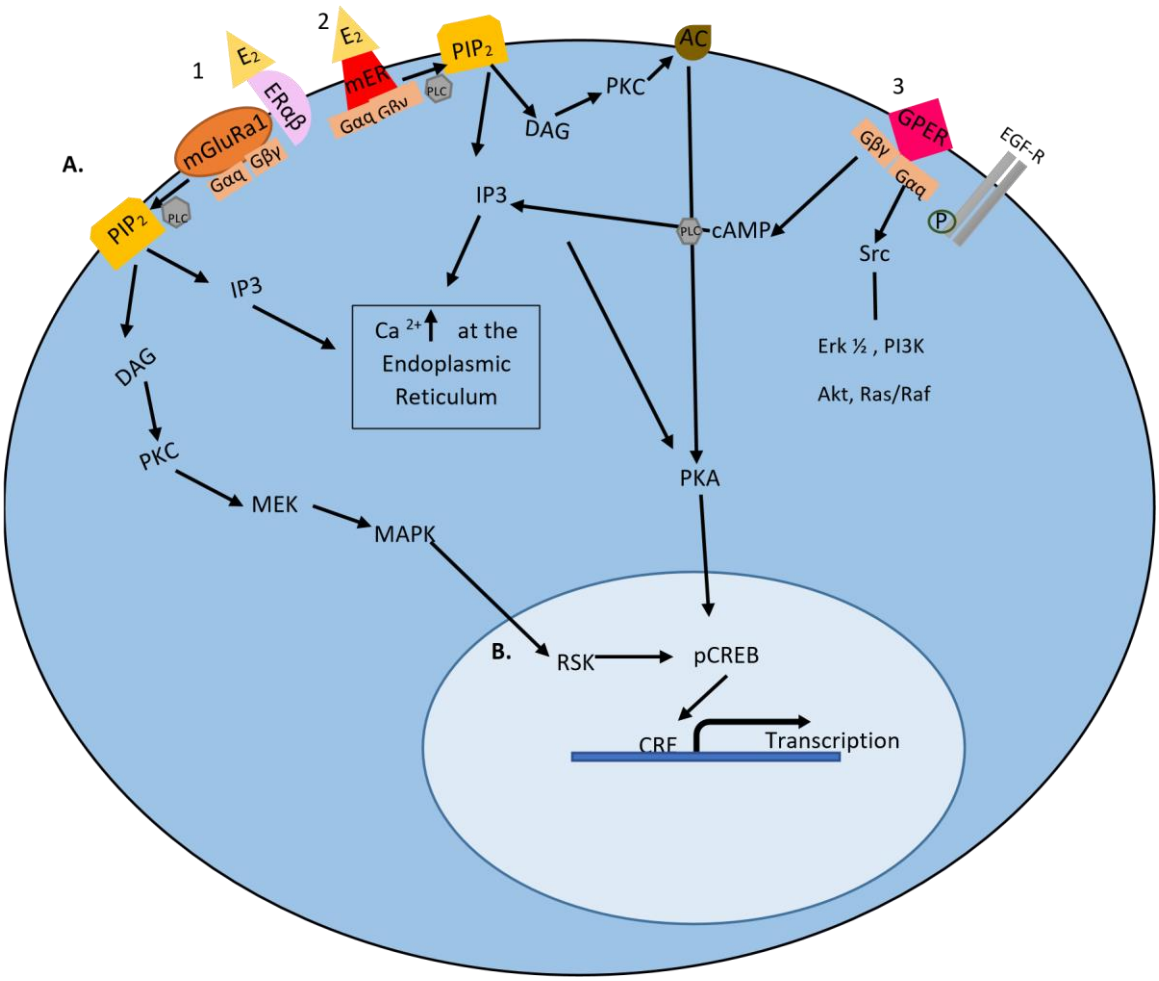

Figure 1.4. Illustration of membrane-initiated signalling of estradiol and initiation of transcription. (A Multiple membrane initiate non – genomic actions of E_2 and secondary proteins. (B) Pathway of nongenomic initiated cell changes. 1. At the plasma membrane oestrogen receptors (αlpha and βeta) are coupled with membrane associated protein metabotropic glutamate receptors and G- proteins. mGluR1a activation leads to phospholipase C (PLC) stimulation and hydrolysis of phosphatidylinositol 4,5- biphosphate (PIP2)this ultimately leads to the activation of multiple protein kinase and MAPK (mitogen-activated protein kinase). MAPK activates ribosomal s6 kinase, which in turn induces phosphorylation of CREB and transcription 2. E2 activates membrane associated oestrogens (mERs) coupled with G-proteins to activate PLC generating IP3 stimulating the release of Ca^{2+} from the endoplasmic reticulum (ER). DAG activates protein kinase C-delta which generates cAMP activity via adenylyl cyclase activating PKA mediating CREB phosphorylation and transcription 3. E2 activates GPER coupled with G- coupled proteins at the plasma membrane or cytosol activating cAMP which generates IP3 via PLC increasing Ca^{2+} at the ER. Gβγ activates increase Src kinase leading to the phosphorylation of epidermal

growth factor receptor (EGF-R) channel activating multiple protein kinase pathways inducing transcription of c-fos and (Girgert et al., 2019; Micevych & Christensen, 2012).

1.3.1.2.1 Membrane Oestrogen Receptors

Oestrogen receptors acting as membrane ERs (mER) have been shown to induce neuronal and behavioural changes in rodents and birds (Charlotte A Cornil et al., 2006; Qiu, Bosch, Jamali, et al., 2006). For example, castrated male quail with a testosterone implant but administered an inhibitor to aromatase show no appetitive or consummatory reproductive behaviour; the appetitive component is restored by intracerebroventricular administration of E2-BSA (Cornil et al., 2018). Appetitive and consummatory behaviour in rodents is the two-step process of mating, appetitive behaviour is sniffing and investigating before approach, whereas consummatory behaviour is physical mounting/mating (Cornil et al., 2018; Hashikawa et al.). This suggests that membrane-initiated signalling by oestrogen can initiate the first part of a complex behavioural sequence. Oestrogens can exert physiologically relevant rapid actions through membrane-localized nuclear ERs or through the membrane-initiated action from GPER1 or in some cases ERs anchored to the plasma membrane by other secondary proteins (Liu & Brent, 2005) (Doolan & Harvey, 2003)that normally localise at the plasma membrane.

The localization of ERs (ERα or ERβ) appears to be dependent on cell type. For example, in endothelial cells both receptors are present at the membrane as both homo and heterodimers (Lei Li et al., 2003)while in human breast cancer cells ERα is abundant, ERβ is scattered in smaller amounts (Ali Pedram et al., 2006; Mahnaz Razandi et al., 2004). Western blot analysis shows that estradiol significantly increased the level of ERα 66 and variant ERα52 at the plasma membrane in a hypothalamic neuronal cell line after 30 mins of (Dominguez et al., 2013). In astrocytes ERα, but not ERβ, was shown to be coupled with tyrosine-protein kinase (Src) and MAPK pathways to initiate rapid estradiol effects that were linked to (Pawlak et al., 2005). Consistent with this data, in a breast cancer cell line MDA-MB- cells 17β- estradiol and ERα/β agonist ICI did not activate cells that express only ERβ, suggesting there may be higher affinity for oestrogen binding to ERα at the cell membrane than for ERβ (Edward J Filardo et al., 2000).In MCF-7 cells that were immune-panned for ERα, cells with higher levels of ERα at the membrane supported higher adenylyl cyclase activation but lower proliferation(Zivadinovic & Watson, 2005) though this kind of correlation has not been done in the CNS.

In many cell lines, mERs are coupled to G-proteins at the plasma membrane, though this has predominantly been shown with ERα. For example, ERα induction of phospho-ERK (pERK) in cortical neuronal cultures is pertussis-toxin sensitive, indicating an interaction with a Gai/o protein that mediates neuroprotection. This induction was also dependent on ERα binding to a series of protein responsible for signal transduction of GPCRs including β-arrestin (b-arrestin) and subsequent proto-oncogene tyrosine-protein kinase Src (c-src) recruitment since siRNA to b-arrestin abrogated this interaction and pERK activation (Dominguez et al., 2009). In guinea pig arcuate nucleus preopiomelanocortin (POMC) neuron, E2 rapidly uncouples the G-protein coupled inward rectifying K+ channel (GIRK) from the inhibitory μ-opioid receptor, increasing depolarization, a phenomenon that can be attenuated by PKC, PKA and PLC antagonists and mimicked by STX (a novel oestrogen membrane receptor ligand) in an ICI independent manner. Since STX targets Gaq-PLC-PKA-PKC pathway and this uncoupling by STX occurs in ERαKO, ERβKO and GPER1 KO mice, it can be inferred that a novel mER couples to Gaq in these hypothalamic neurons (Qiu, Bosch, Tobias, et al., 2006).In SK-N-BE(2)C neuroblastoma cells, potentiation of transcription from a consensus ERE by E2-BSA using a two-pulse regimen can be abolished by a dominant negative Gaq mutant suggesting that ER in this cell is coupled to a Gaq protein (Clark et al., 2014). In some cases, the classical ERs are coupled to the p85 subunit of PI3K sequestered in the caveolae of endothelial cells where E2 application rapidly induces endothelial nitric oxide synthase (eNOS) (Haynes et al., 2000) while ERβ in caveolae may also activate eNOS via the ERK pathway(Chambliss & Shaul, 2002); these interactions are dependent on the presence of the caveolin-specific protein caveolin 1 (CAV1) (Schlegel et al., 1999). Though caveolae are less abundant in neurons, a similar scenario may also occur in lipid rafts that are ubiquitous in neurons. Recently, it was demonstrated that reduction in CAV1 levels in neurons impaired synaptic vesicle exocytosis and endocytosis, suggesting that caveolae formation in neurons is central to their (Koh et al., 2021).

The presence and importance of caveolar proteins in anchoring ERs to the membrane has been investigated initially in a breast cancer cell line MCF-7 cells and hippocampal neurons. Membrane factions of MCF-7 cells show the presence of ERα at the membrane (Ali Pedram et al., 2006)at a level of around 5-10% of all ERα molecules in the cell (Levin, 2009b); this is possibly by trafficking of transmembrane gyproteins through a process of palmitoylation . Palmitoylation depends on the conserved cysteine at position 451 in mouse ERα (residue 447 in human ERα); mutation of this residue results in lower palmitoylation, less association with caveolin and less membrane localization in Chinese hamster ovary (CHO) cells and in HepG2 liver cells (Acconcia et al., 2005). This had biological consequences – for example, in HepG2

cells, this abrogated rapid nongenomic signalling i.e. ERK and PKB activation by E2(Acconcia et al., 2005) as well as genomic transcription from the cyclin D1 promoter. A second mutation at position 522, a nonclassical palmitoylation site, where a serine had been mutated to alanine S522A, resulted in 62% less binding of ERα to CAV1 at the CHO cell membrane and lower ERK activation (Razandi et al., 2003).Interestingly, it was found that the palmitoylation of CAV1 protein is also required for ER transport to the membrane (Pedram et al., 2007) and that E2 treatment decreased palmitoylation and subsequent association with CAV1 in a time and dose-dependent manner, suggesting that this could be a self-regulated system in some cells(Acconcia et al., 2005). However, in CHO cells, E2 addition does not regulate palmitoylation(Razandi et al., 2003)and in both an immortalized hypothalamic neuronal cell line mHypo-38 and in rat primary hypothalamic neurons, short term E2 treatment increased ERα levels both at the membrane and increased internalization via β-arrestin tagging rapidly, suggesting that E2 can, within acute time-frames, increase non-genomic signalling from the plasma membrane(Dominguez et al., 2013; Dominguez & Micevych, 2010). Additionally, Gilad and Schwartz found that in HEK-293 clones, ERβ expression at the membrane was highest when caveolin expression was high, and ERK activation and transcriptional upregulation of the Vitamin D receptor promoter occurred only in this condition (Gilad & Schwartz, 2007). These studies demonstrate that CAV-1 is a) required by all nuclear ERs for membrane localization b) biologically significant and c) required for both rapid non-genomic signalling and genomic transcription, at least in some cell lines.

CAV-1-3 has been found in neurons and glia (Galbiati et al., 1998). In a series of experiments from the Mermelstein lab, in hippocampal cells, it was shown that downstream signalling cascades resulted from a unique combination of caveolin proteins in a signalosome with the ERα. As can be seen in Figure 1.5, CAV1 sequesters ERα and brings it in contact with mGluR1, resulting in recruitment of Gaq protein and PLC/MAPK/PKC activation that increases CREB phosphorylation (Boulware et al., 2007; Boulware et al., 2005). On the other hand, CAV3 binding to ERα or ERβ allows for the recruitment of mGluR2/3 which in turn leads to Gai/o activation and PKA inhibition, leading to inhibition of CREB-dependent transcription(Luoma et al., 2008). Apart from hippocampal neurons, mGluR1a interaction with ERα mediated by CAV1 is required for PLC activation, elevation of intracellular calcium and an increase in neuroprogesterone production from hypothalamic astrocytes in the female; this is important in negative feedback as well as in facilitating lordosis behaviour (Micevych & Sinchak, 2008). Predictably, trafficking of the ERα to the membrane and internalization of the receptor within astrocytes was blocked by both the mGluR1 antagonist and the ERα/β

antagonist, ICI 182, 780(Bondar et al., 2009). Caveolins have also been shown to couple ERα with Gaq proteins in striatal neurons where CAV1 promotes binding of the ERα to mGluR5; E2 increases ERK-dependent CREB phosphorylation. However, ERβ and ERα can also couple to mGluR3 to decrease L-type channel dependent CREB phosphorylation(Grove-Strawser et al., 2010). In the female hippocampus, ERα is found in large dense core vesicles and in both glutamate and GABA neurotransmitter vesicles (Tabatadze et al., 2013). These findings demonstrate that at least ERα can be compartmentalized into different subcellular locations based on the association with different CAV-mGluR combinations with ultimately differing functional consequences.

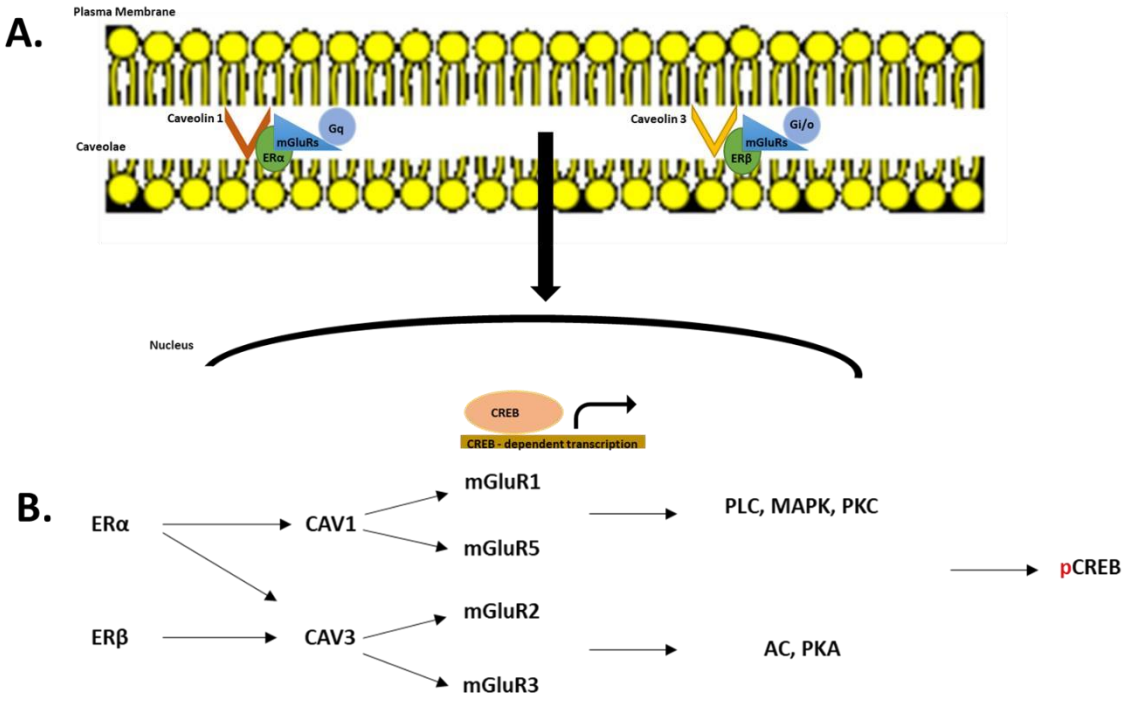

Figure 1.5. Oestrogen receptors activation via mGluRs is organised via caveolins 1 and 3 in neurons. (A) Caveolin activates ERα and ERβ for signalling mGluRs and g proteins. Caveolin 1 and 3 is responsible for recruiting ERα to the plasma membrane for signalling via mGluR1 and 5, Gq to activate the PLC, MAPK, PKC pathway which induces CREB phosphorylation. Caveolin 3 is responsible for recruiting ERβ to the plasma membrane for signalling via mGluR2 and 3, Gi/o to activate the AC, PKA pathway which induces CREB phosphorylation. AC, adenylyl cyclase; PKA, protein kinase A; PLC, phospholipase C; MAPK, mitogen-activated protein kinase; PKC, protein kinase C. (B) Summary depicting oestrogen receptors links to different caveolins and mGluRs in the brain.

1.3.1.3 GPER1/ 30

GPER1 or GPR30 a former orphan G- protein coupled receptor has been demonstrated to bind to 17β-estradiol at 3.3nM binding affinity and has been implicated in cancer progression, neuroprotection, behaviour and cardiovascular health(Hadjimarkou & Vasudevan, 2018; Thomas et al., 2005). GPCRs are the largest class of signalling molecules in humans; they function as heptahelical transmembrane proteins that are expressed on the cell surface, though GPER1 localization is up for debate. (Thomas et al., 2005), found that 17β-estradiol could bind to the plasma membrane of a human breast cancer cell line, SKBR3 do not express ERα or ERβ and could increase adenylyl cyclase and cyclic adenosine monophosphate (cAMP) with these cells, suggesting an interaction with Gas. Silencing GPER1 abolished this increase in cAMP in SKBR3 cells (Thomas et al., 2005). However, apart from the PKA pathway, the other main pathway activated by GPER1 is the ERK pathway though Gbg subunits that activate c-src/Shc. This in turn activates a matrix metalloprotease (MMP) which cleaves heparin-bound epidermal growth factor (HB-EGF) to active epidermal growth factor (EGF), resulting in the activation of EGF receptor (EGFR) and downstream ERK activation, including calcium increase in a ryanodine receptor (RyR)- dependent (Ariazi et al., 2010; E. J. Filardo et al., 2000). In COS-7, calcium increase upon GPER1 activation is also EGFR-dependent though calcium increase via ERα activation is phospholipase C (PLC)-dependent (Chetana M. Revankar et al., 2005). The PKA and ERK pathways are interlinked – PKA activation inhibits the ERK pathway by inhibiting RAF proto-oncogene serine (c-Raf) in SKBR3 cells (Filardo, 2002). In both SKBR3 cells which endogenously express GPER1 and in a monkey fibroblast cell line, COS-7 cells were GPER1 was transfected, GPER1 also activates PI3K/PKB signalling (Chetana M. Revankar et al., 2005). In MDAMB-231 cells that overexpress GPER1, EGFR activation of the ERK pathway is sensitive to pertussis toxin, indicating that GPER1 can couple to a GaI protein (E. J. Filardo et al., 2000). Moreover, GPER1-mediated neuroprotection in cultured cortical neurons is via downregulation of NR2B subunits mediated by death activated protein kinase, suggesting that different cell types support different downstream pathways from GPER1 activation (Liu et al., 2012).

The subcellular localization of this receptor is controversial, as is its internalization and recycling(Ruby Vajaria & Nandini Vasudevan, 2018). In SKBR3 cells that express lower levels of GPER1 endogenously, it has been detected in both the plasma membrane (Filardo et al., 2007) and in the endoplasmic reticulum (Prossnitz & Maggiolini, 2009a; Chetana M. Revankar et al., 2005) by using cellular fractionation and immunocytochemistry. Although, GPER1 appears to be at the plasma membrane in some breast cancer cell lines, in MDA-MB231 and HEC50 cells or in COS cells that overexpress the receptor, GPER1 was found to

be localized in the nearby endoplasmic reticulum and not the plasma membrane(Chetana M. Revankar et al., 2005) (Otto et al., 2008). It may be that GPER1 localization is cell-type specific or that there are other proteins involved in the translocation of GPER1 to the cell surface(Prossnitz & Maggiolini, 2009a) .For example, in human embryonic kidney 293 cells (HEK293) it was found that GPER1 interacts with the C-terminal PDZ motif of a-kinase-anchoring protein (AKAP) which maintains GPER1 at the plasma membrane(Broselid et al., 2014; de Valdivia et al., 2017). Similarly, GPER1 has been detected in the CA1 region of the hippocampus by electron microscopy anchored to the cell membrane of the dendritic spine by the spine protein PSD-95(Akama et al., 2013). Furthermore, GPER1 has been shown at the Golgi apparatus and endoplasmic reticulum in cultured hippocampal (Matsuda et al., 2008)and in oxytocin neurons from the paraventricular nucleus(Sakamoto et al., 2007). How these atypical sites of localization couple to different signal transduction pathways in different cell types is not known (Ruby Vajaria & Nandini Vasudevan, 2018).

As is evident in the preceding sections, contributions of various receptors to downstream signalling or cellular phenotype can be influenced the use of pharmacological inhibitors and activators as well as using tissue or cell lines that are devoid of those receptors or treated with siRNA to knockdown the receptor. In some studies, specificity i.e use of the antagonist in addition to receptor agonists was not carried out and hence results should be interpreted with caution. Many of the studies use ICI 182,780 to rule out the involvement of the classical ERα and ERβ ; however, it should be noted that the ICI compound is a GPER agonist(Petrie et al., 2013). Table 1 below shows some of the properties of commonly used agonists and antagonists to the ERs, used in several studies to show the contribution of receptors to cell and organismal phenotypes

.

Receptor	**Agonists**	**Antagonists**
ERα	PPT	ICI 182,780
ERβ	DPN	ICI 182,780
GPR30	G-1, PPT, ICI 182,780	G-15
ERα-36 variant	G-1,PPT?	?

Table 1.1 Specific Agonists and Antagonists for Oestrogen Receptors/. ?, represent unknown function .

1.4 Oestrogen in the brain

1.4.1 Introduction

Steroid action in the brain is the result of neuroactive steroids (steroids that are produced in the peripheral endocrine glands or locally synthesized (Baulieu et al., 1999) (Do Rego et al., 2009). (are three major classes of sex-steroid hormones, oestrogens androgens and progestins that control sexual differentiation and highly influence brain development, social and reproductive behaviour (Lenz et al., 2012). Early in normal development during critical in utero and/or in perinatal periods, oestrogen acts on the brain to organise a male or female-typical phenotype. Further during development, puberty and throughout life/adulthood, oestrogen, testosterone, and progesterone act via their cognate receptors to organise sexual dimorphic framework of the CNS and produce sex-specific behaviour; this concept is known as the organizational/activational hypothesis (Figure 1.6) (Lenz et al., 2012; Mccarthy, 2008; Phoenix et al., 1959).This influential hypothesis has been borne out by a number of hormone manipulation studies in rodents where a neonatal testosterone surge (Dovey & Vasudevan, 2020)is required to cement organizational effects(Harris & Gorski, 1978);(Hines et al., 1992);(Hines et al., 1985);(Simerly et al., 1985).

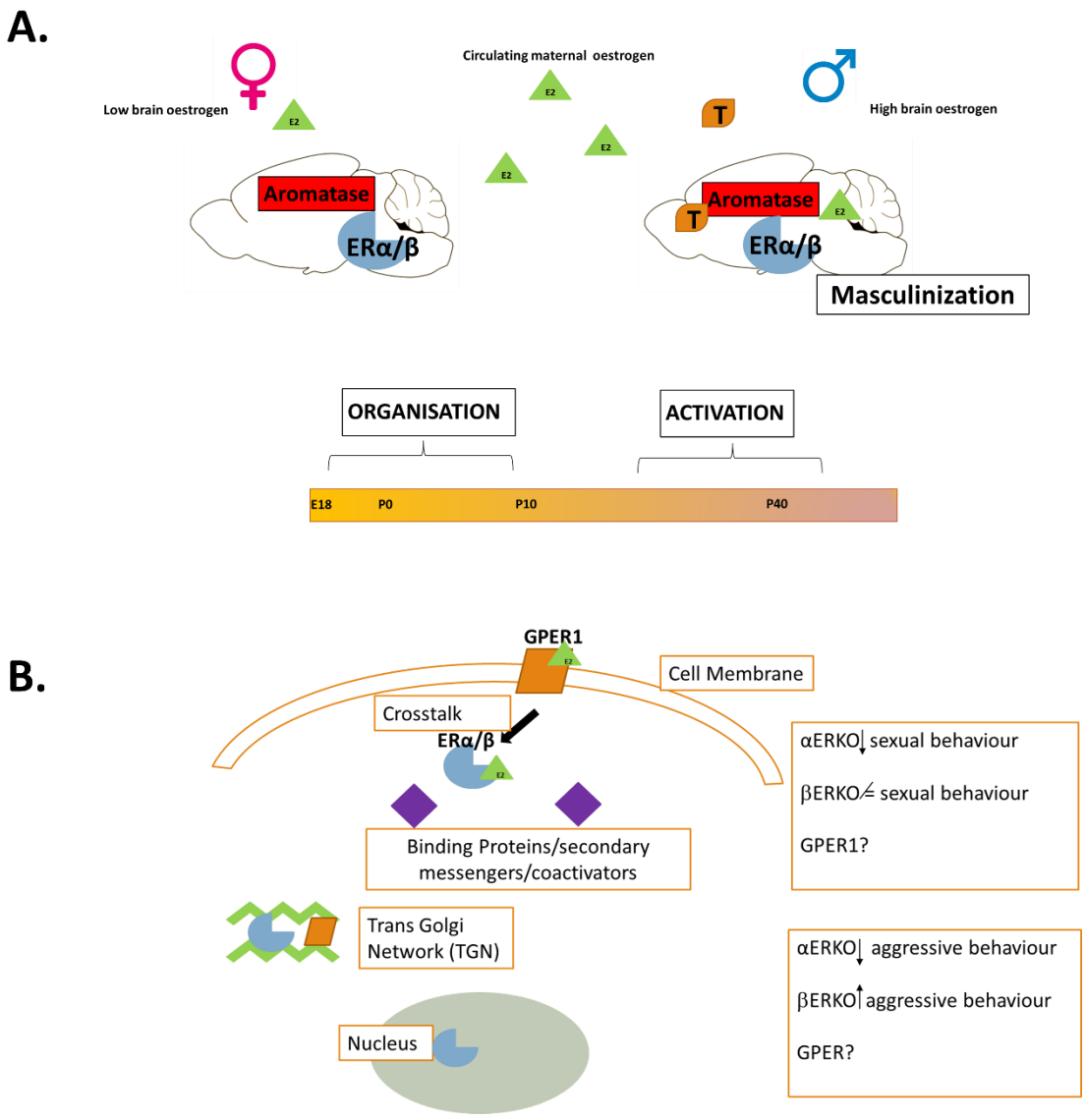

Figure 1.6. Organization and activational stages of male and female brain. (A) In male rodents, there is a perinatal surge of androgens from the testes, this peaks at the end of the embryonic period. Once in the brain testosterone is converted to by (p450c) aromatase to oestrogen (E_2) . Oestrogen then organizes the brain via its receptors leading to the masculinization/ defeminization of the male brain. In females during the post-natal period, there is low oestrogen in the brain, in contrast there is high oestrogen in the male brain during this period. During the activational stage (puberty) there is high testosterone in the male brain and high progesterone and oestrogen in the female brain. (B) Oestrogen activates these neural circuits that allow for the expression of sexual and aggressive behaviour in specific areas of the brain. Oestrogen action can be activated via is classical receptors ERα or ERβ or GPER1. Recent studies have shown that these two may crosstalk together to bind to secondary proteins, such as G proteins and mGlurs throughout the cell to increase or decrease phenotypic expressions of sexual or aggressive behaviour.

1.4.2 The Social Behaviour Network

The social behaviour network (SBN) was first introduced by (Newman, 1999),who identified a 'core' functional and connective construct in mammalian brains that is key to the regulation of common sexually dimorphic reproductive and aggressive behaviours(Goodson, 2005; Newman, 1999). The SBN consists of six bidirectional nodes : (1) the extended medial amygdala (medial amygdala and the bed nucleus of stria terminalis) MeAMY (2) lateral septum- LS (3) medial preoptic area- MPOA (4) anterior hypothalamus- AH (5) ventromedial hypothalamus –VMH and (6) the midbrain sections that include the periaqueductal gray- PAG (Newman, 1999)(Figure 1.7). The role of each node was first inferred by the presence of lesions that would present behavioural deficits during social interactions (Newman, 1999).

There are two general characteristics for the SBN namely that all nuclei are reciprocally connected and secondly, that these nuclei must share similar cell morphology and neurochemistry that initiate and regulate sexual(Charlier et al., 2005; Taziaux et al., 2006) , aggressive (Wu & Shah, 2011; Xu et al., 2012; Yang et al., 2017) and parental behaviours in males and females(Coolen et al., 1998; Newman, 1999). Comparative endocrinology and neuroendocrine studies demonstrate these nuclei are: a) hormonally sensitive and therefore possess hormone receptors b) present in all vertebrate species(Balthazart et al., 1996; Goodson, 2005; Newman, 1999).

Figure 1.7 Schematic representation of the neuroanatomical pathways of the social behaviour network. Arrows indicate the bidirectionality of the connection between the six brain regions 1) meAMY (medial amygdala) & BNST (bed nucleus of the stria terminalis) which is a part of the extended amygdala network 2) LS (lateral septum) 3) POA(preoptic area) 4) AH (anterior hypothalamus) 5) VMH (ventromedial

hypothalamus) 6) PAG (periaqueductal grey or midbrain area). Note that the PAG is a convergent nuclei for all others in the node and directs motor output that is critical for the display of social behaviour. (Modified from Goodson, 2005)

In rodents, mPOA, BNST, and meA regions are larger in males than in females. Sexual dimorphism in the mPOA is largely due to the increase in aromatization of testosterone to oestrogen in males during the critical postnatal differentiation period (Arai et al., 1996) despite no difference in the levels of the ERα (Cintra et al., 1986) (Scott et al., 2000). While the MeA is anatomically dimorphic, the dimorphism arises because the posterior dorsal region has neurons with greater soma size in males, presumably due to relatively high concentration of androgen and oestrogen receptors in the male which may reduce apoptosis (Sheridan, 1979; Simerly, 1990). The sexually dimorphic posterior division of the BNST also shows greater projection density in males than females, presumably due to both increased aromatization and increased AR and ER density(Commins & Yahr, 1985; Simerly et al., 1990). In general, the mechanisms by which the increased levels of ER and AR promotes larger mPOA and BNST areas are unknown. This suggest that regions of the SBN are sexually dimorphic as a result of differential sensitivity to hormones that subsequently regulate patterns of activity (Newman, 1999)but may also be dependent on the type of behaviour expressed . For example in male rodents, mPOA lesions inhibited all copulatory behaviour (Hull & Dominguez, 2007), but had no effect on lordosis in females (Greenberg & Trainor, 2016; Kirn & Floody, 1985). Though the posterior regions of the BNST and meA modulates aggressive behaviour in both male and female rodents, however there are differences in the relative contribution (Greenberg & Trainor, 2016). The VMH also appears to be larger in male rats than females though this is not due to greater neuron number but rather greater neuron size and higher numbers of synaptic afferents, possibly due to longer dendritic lengths(Dulce Madeira et al., 2001; Flanagan-Cato et al., 2001) ; males also show higher spine density that is decreased by estradiol treatment unlike in females where spine density increases and dendrite length decreases (Frankfurt, 1994; Frankfurt et al., 1990). Though males have higher levels of lordosis-promoting nitric oxide synthase neurons (Martini et al., 2008; Martini et al., 2011)and aromatase (Roselli, 1995; Simerly et al., 1990; Wagner & Morrell, 1997)in the VMH than females, oestrogen upregulates the progesterone receptor (PR) (BOGIC et al., 1988; Lauber et al., 1990), enkephalin (Romano et al., 1990)to a greater extent in females than in males possibly due to the higher expression of ERα, PR and ERβ in the female than in the male VMH (Orikasa et al., 1996).

Neonatally castrated male rats or male pups treated with an aromatase inhibitor showed a demasculinized VMH with lower spine density and area (Feder & Whalen, 1965) and synaptic

afferents (Ogawa et al., 2020). ERα plays an important role in masculinizing the BNST, the meA and the mPOA; the perinatal testosterone surge at E18 was instrumental in reducing apoptosis in the male mPOA(Davis et al., 1996). Targeted knockdown of ERα using siRNA in the neonatal male rat mPOA reduced volume and apoptosis, resulting in a demasculinized (McCarthy et al., 1993). In the mPOA, this is presumably via non-genomic signalling since an ERα-mutant incapable of membrane-initiated signalling showed a smaller (Khbouz et al., 2020). Though the mode of signalling by oestrogen to masculinize the meA is not known, knockdown of ERα in the pubertal male mEA reduces the volume of the extended amygdala (Sano, Tsuda, et al., 2013). However, ERβ may also play a role in the BNSTp (a part of the extended amygdala) since both ERα and ERβ agonists administered during the perinatal period to females increased the volume (Hisasue et al., 2010). Similarly, testosterone propionate administration to neonatal females could also increase BNSTp volume and prevent apoptosis of cells (Rosie et al., 1993). These studies show that sexually dimorphic neuroanatomy and synaptic connectivity in the SBN is a consequence of ER signalling.

1.4.3 Characteristics of the SBN and Sexual Dimorphism

Although the core regions of the SBN are relatively conserved across all vertebrate classes, both species and sex influence the activation of nodes in the SBN and the initiation and maintenance of sociosexual behaviours (Goodson, 2005);(James L Goodson & David Kabelik, 2009);(Newman, 1999) (Wullimann & Mueller, 2004). Morphologically homologous brain regions (Table 1.2) across vertebrate class are functionally different, and each node contains sex steroid receptors that are required for sexual differentiation and the temporal coordination of social communication (Goodson, 2005). Evidence supports the idea of a sexually dimorphic SBN including hormonal manipulation experiments and by monitoring immediate early gene expression (IEG) via the activation of the SBN nodes during social behavioural studies (Kollack-Walker & Newman, 1995). In rodents, c-fos, an IEG marker that is expressed within 1hr of behavioural test is an indirect indicator of neuronal activity (Kollack-Walker & Newman, 1995), c-fos immunoreactivity increased dramatically in MPOA, BSNT and meA after mating activity (mounting and ejaculation) in male rats (Coolen et al., 1997);(Coolen et al., 1996);(Hull & Dominguez, 2007; Veening et al., 1998)but increased slowly in these areas in the female. In addition, the VMH in females, but not males, showed increases in c-fos in response to male copulatory behaviour (Coolen et al., 1996), indicating that nodes of the SBN between sexes differ in relative contribution depending on the type of behaviour.

Mammalian	Aves	Osteichthyes*	Reptilia*	Amphibia*
Extended medial amygdala: Medial amygdala and medial bed nucleus of the stria terminalis	Nucleus taeniae	Supracommissural nucleus of the ventral telencephalon	Extended medial amygdala: Medial amygdala and medial bed nucleus of the stria terminalis	Extended medial amygdala: Medial amygdala and Bed nucleus of the stria terminalis
Medial Preoptic area	Medial Preoptic area	Medial Preoptic area	Medial Preoptic area	Medial Preoptic area
Anterior hypothalamus	Anterior hypothalamus	Anterior hypothalamus (plus ventral tuberal region)	Anterior hypothalamus	Anterior hypothalamus
Lateral septum	Lateral septum	Ventral nucleus of the ventral telencephalon	Lateral septum	Lateral and dorsal septum
Ventromedial hypothalamus	Substantia grisea centralis	Ventromedial hypothalamus	Ventromedial hypothalamus	Ventromedial hypothalamus
Periaqueductal gray (midbrain)	Periaqueductal gray (midbrain)	Anterior tuberal nucleus	Periaqueductal gray	Currently not known

Table 1.2. Homologs across vertebrate class in the social behavioural network . modified from (Goodson, 2005). Recorded homology is determined by the relative position and distribution of sex steroid hormones. * Will not be discussed further in this review since our work will focus on mammals.

Although most work has been done in rodents, the SBN is present in all vertebrate species that share overlapping but distinct patterns of activity in the SBN upon the display of social behaviours(O'Connell & Hofmann, 2011) (Table 1.3). Across mammals, the meA is the first to receive environmental inputs from the main olfactory bulb (L. Kang et al., 2010); those signals in turn project simultaneously to all regions of the SBN though further contribution of other nodes in the SBN appears to be species-specific. In rodents, the LS seems to have a large impact on the initiation of aggressive behaviour(Nelson & Trainor, 2007), this may be due to the differences in the promotion of behavioural outputs by the LS across different species. In rats, LS lesions decreased resident aggression during a territorial intruder test (Blanchard & Blanchard, 1977), but rats exposed to conditioned stimuli displayed an increase in aggressive/ defensive behaviours (Singewald et al.; Sparks & LeDoux, 1995). The role of the LS may also vary with social organization in field sparrows (a territorial species) where LS lesions increased aggressive behaviours while lesions in male zebra finches (a gregarious species) caused a reduction in courtship and aggression(Thompson et al., 1998). Collectively, this data

indicates that behavioural outputs may not be linked to a single node in the SBN but rather the pattern of activity across the SBN that contributes to species and sex specific outputs referred to as functional connectivity (J. L. Goodson & D. Kabelik, 2009) which could be dependent on steroid hormone signalling in an incompletely understood manner.

Region	Mammals	Birds	Teleost
meAMY	motivation, parental care, reproduction, stress response, aggression, social recognition	aggression, motivation, reproduction	aggression, reproduction
LS	emotional learning, social recognition, reproduction, parental care	aggression, reproduction stress response	Reproduction
MPOA	aggression, reproduction, parental care	aggression, reproduction, parental care	aggression, reproduction, parental care
VMH	aggression, reproduction, parental care	aggression, reproduction, parental care	
AH	aggression, reproduction, parental care		
PAG	reproduction, vocalization	vocalization	vocalization

Table 1.3. Proposed roles of each region in the SBN in the regulation of behaviours in mammals, birds, and teleost. Roles of each 'core' region first identified by the absence or presence of lesions. Subsequent studies provided evidence showing differential patterns of c-fos expression in response to sex typical behaviours or encounters. : (1) the extended medial amygdala (medial amygdala and the bed nucleus of stria terminalis) MeAMY (2) lateral septum- LS (3) medial preoptic area- MPOA (4) anterior hypothalamus- AH (5) ventromedial hypothalamus –VMH and (6) the midbrain sections that include the periaqueductal gray- PAG (Modified from O'Connell and Hofmann 2011; Goodson, 2005)

1.5 Oestrogen action in the SBN

Oestrogen not only regulates neuronal networks that control social behaviours but also contributes to the formation of the SBN. Since the concentration of ERs appear relevant in sexual differentiation of the brain and subsequent dimorphism seen in the regions of the SBN, it is important to understand the distribution of oestrogen receptors (Section 1.5.1) as well as aromatase that produces the ligand i.e. neuroestrogens (Section 1.7) in these areas as they provide insight in the physiological relevance of oestrogen in sex-typical social behaviours.

1.5.1 Distribution of ERs in the SBN of the mouse and rat brain

ERα, ERβ and GPER1 are differentially distributed throughout the SBN (Table 1.4) with most of the data currently available for female rodents, though some papers now also include the male. Using immunocytochemistry for ERα and ERβ, (Merchenthaler et al., 2004), compared the distribution of both receptors throughout the central nervous system of the female mouse. ERα and ERβ distribution is described in terms of the number of immunoreactive cells and relative intensity of the cells within that region. In the medial amygdala, subtle differences were observed in distribution of ERα and ERβ with ERβ- immunoreactive cells nearly undetectable in the basolateral and basomedial nucleus and significantly less than ERα in the central and cortical nucleus of the amygdala(Shughrue et al., 1996; Shughrue et al., 1997). There was scattered immunoreactivity throughout the lateral septum for both receptors. There were no major differences in the distribution between receptor isoforms in the anterior hypothalamus, BNST or medial preoptic area (Dovey & Vasudevan, 2020). However, (Patisaul et al., 1999), found that in female rats ERβ mRNA was more abundant throughout the mPOA than ERα though the function of the increased ERβ remains unclear. However, like the mouse, there were a large number of ERα-positive immunoreactive cells in the rat female VMH as compared to a very sparse distribution of ERβ (Patisaul et al., 1999) and as compared to males. Overall, the female rat midbrain contained more ERα-immunoreactive region than any another region, with most cells clustered within the PAG, similarly to the mouse. Since ERα and ERβ show differential distribution in some nuclei within the female mouse and rat brain, it is thought that these nuclei may mediates oestrogen-dependent processes that differ between species (Patisaul et al., 1999). Some of these differences in receptor concentrations also depend on an interaction between developmental; this has been summarized in our laboratory (Dovey & Vasudevan, 2020) and can be one reason for sexual dimorphism for activity and neuroanatomy in the SBN. For the purposes of this thesis, we will focus on the distribution of ERs in adult male and female rodents (mice and rats).

Some of these results may be affected by the reliability and relative affinities of antibodies to ERα and ERβ and to post-translational modifications and translational efficiency between these two isoforms in studies that measured solely mRNA concentrations. For more than 10 years, the distribution of ERβ has also been difficult to examine due to the lack of a specific antibody (Melissa A Snyder et al., 2010). The recent availability of a ERβ-RFP transgenic mouse and reliable ERα antibodies have allowed for dual immunocytochemistry. (Sagoshi et al., 2020), shows that many neurons in the mPOA and mEA expressed both ERα and ERβ while neurons in the PVN and dorsal raphe expressed mostly ERβ; strong ERβ signal was also seen in the BNST with males showing more ERβ positive cells when intact or gonadectomized than females (Sagoshi et al., 2020). Gonadectomised but not intact males showed more ERβ-

RFP positive cells in the meA than females. There was very little ERβ in the hippocampus, the VMH or in the PAG (Sagoshi et al., 2020).

The distribution of the GPER1 in the brain does not appear to show much sexual dimorphism and has been explored in detail in a review published by our laboratory (Dovey & Vasudevan, 2020). GPER1 distribution is present in both the male and female SBN with high levels present in the VMH, mPOA and meA and lower levels in the BNST and lateral and anterior hypothalamic nuclei (Brailoiu et al., 2007; Hazell et al., 2009). In both studies, GPER1 has been reported to colocalise with oxytocin and vasopressin neurons in the PVN but the significance of this remains unclear. In addition, GPER1 colocalisation with the other nuclear receptors is also not determined.

Area	**ERα**	**ERβ**	**GPER1**
LS	?	?	=
MPOA	?	M>F	=
BNST	M<F	M<F	=
MeA	M<F	?	=
VMH	=	?	=

Table 1.4. Relative expression of oestrogen receptors in male and female adult mice or rats. Expression levels of oestrogen receptors were determined by mRNA, protein expression or a combination of both. "?" denotes unknown levels in males or females, "=" equal levels of expression in the brain area. Adapted from (Dovey & Vasudevan, 2020)

1.5.2 Oestrogen regulated behaviours

The pattern of activity in each SBN node following or during a behavioural interaction is dependent on the availability of hormone receptors in that region(Goodson, 2005; Newman, 1999). For example, in male rodents after engaging in sexual behaviour the meAMY is the first to receive inputs from the olfactory bulb and signals are then relayed to the other regions of the SBN. However, in female sexual behaviour hypothalamic areas are proposed to receive inputs first given the density and type of sexual hormones available in the area (Li & Dulac, 2018). While studies show that oestrogen is an important regulator of social and sexual behaviour, they also support the notion that are differences across the SBN that are sex and species dependent such that different nodes of the SBN are differentially utilised to produce sex-typical behaviours(Gegenhuber & Tollkuhn, 2022; Goodson, 2005). Oestrogen receptors

ERα and ERβ regulate gene expression differently and has also been proven to have some tissue and temporal variation in expression. This section will review the differences in function and structure across SBN regarding aggressive, male reproductive and female reproductive behaviour.

1.5.2.1 Sexual behaviour in females

In females the VMH is considered essential for the expression of lordosis behaviour. (Pfaff, 1973) found that the VMH nuclei contained oestrogen concentrating cells and that the oestrogen injection directly into the VMH of female rats facilitate lordosis (Davis et al., 1979). During a study of male copulatory behaviour, partnered female rats saw an increase in c-fos activity in the VMH, but in no other areas of the SBN (Coolen et al., 1996). In female mice, there was a decreased level of ERα in the VMH using silencing RNA abolished lordosis (Musatov et al., 2006), suggesting that E2 acting via ERα in the VMH is necessary for lordosis to occur. In 17β- estradiol-3-benozate (EB) -primed ovariectomized (OVX)\ female rats that were infused via intracerebroventricular injection (i.c.v) with PPT and DPN (ERα and ERβ agonist respectively) show an increase in lordosis behaviour compared to DMSO-infused controls at 30 mins, 120 mins and 240 mins(Dominguez-Ordonez et al., 2016). Injections of selective antagonists of ERα (MPP) and ERβ (PHTPP) significantly decrease lordosis behaviour induced by subsequent E2 administration (Dominguez-Ordonez et al., 2016). This data suggests that activation of both ERα and ERβ are required for rapid facilitation in lordosis behaviour, implying that non-genomic signalling by these receptors contributes to lordosis. Consistent with this inference, PKA, ERK and c-src antagonists infused into the VMH 30 mins before testing inhibited EB-primed lordosis behaviour in female rats (Domínguez-Ordoñez et al., 2021). Similarly in female whiptail lizards EB injections after VMH lesions did not rescue the loss in receptivity, suggesting that the VMH is also important in female sex behaviour in a nonmammalian species (Kendrick et al., 1995).

Other hypothalamic nuclei expressing ERs are also important in the display of lordosis behaviour and coupled signalling that is critical in this behaviour. Indeed, E2-BSA administration alone in two pulses with the administration of membrane-permeant EB does not induce any lordosis; indicating that non-genomic signalling contributes but is not sufficient for lordosis behaviour (Kow & Pfaff, 2004). A two-pulse priming paradigm in female rats where membrane-impermeant E2-BSA injected into the VMH prior to administration of EB and progesterone could drive lordosis to the same extent as traditional

longer-priming EB regimens, suggesting that membrane-initiated rapid non-genomic signalling potentiated lordosis behaviour (Kow & Pfaff, 2004).

How does nongenomic signalling contribute to this behaviour? In the arcuate nucleus (ARH), a microcircuit that is responsible for the activation of lordosis behaviour in the mPOA(Christensen & Micevych, 2013); E2 administration into the ARH rapidly activated protein kinase C theta (PKCq)(Dewing et al., 2008), leading to the release of neuropeptide Y and the subsequent activation of b-endorphin afferents into the mPOA(Sodersten & Eneroth, 1981). In the mPOA, this led to the internalization of the μ-opioid receptor (MOR) after 30 minutes of E2-BSA administration in the ARH; this non-genomic signalling occurring in SBN nuclei activates and internalises MOR and transiently inhibits lordosis until progesterone signalling relieves this inhibition. Pharmaceutical experiments such as the administration of a PKC inhibitor (BIS) in the ARH 30 mins prior to E2-BSA administration reduced MOR internalization in the mPOA (Dewing et al., 2008). In addition, in the ARH, 22% of mGluR1a positive neurons were ERα-positive suggesting that this interaction at the membrane is important in initiating the rapid non-genomic signalling cascade (Christensen et al., 2011; Dewing et al., 2007). Indeed, CAV1 siRNA or an antagonist to mGluR1a in the arcuate nucleus not only reduced MOR internalization in the mPOA but also reduced lordosis (Christensen & Micevych, 2012; Dewing et al., 2007).

In OVX female rats, there was a significant increase in dendritic spine density i.e. filamentous spines the neurons of the ARH after EB treatment (Christensen et al., 2011)within 4 hours, with increase in phosphorylated cofilin with an hour (Christensen et al., 2011). This suggests that, in the ARH, ERα increases spinogenesis and drives lordosis behaviour. Consistent with this, cytochalsin B, an inhibitor that depolymerises actin, inhibited lordosis when injected into the ARH (Christensen et al., 2011). Though rapid non-genomic signalling in the ARH is important for initiating the sequence of events, genomic signalling via ERα-mediated transcriptional upregulation of the progesterone receptor in the VMH is needed for lordosis (Parsons et al., 1982). The two-pulse paradigm where E2-BSA in the first pulse is followed by E2 in the second pulse also potentiates transcription of the progesterone receptor gene (Sa et al., 2014). A female mouse that has a mutation in the ERα DBD region and cannot bind the ERE was deficient in lordosis behaviour(McDevitt et al., 2008). It is clear from these studies that ERα plays a dominant role in increasing lordosis in female rodents by initiating both genomic and non-genomic events. Further supporting the role of ERα in lordosis, ERαKO female mice showed no lordosis behaviour(Ogawa et al., 1998), while ERβKO female mice with normal levels of ERα show no change in lordosis behaviour from wild-type mice(Ogawa et al., 1999). However, subsequent studies have shown that EB increases spines in the VMH

in neurons that are ERα-positive; it is possible that this could be via GPER1 since G-1 (GPER1 agonist) administration in OVX female mice increased lordosis behaviour (Anchan et al., 2014). Though GPER1 can phosphorylate ERα in the male hippocampus, this interaction has not been shown in SBN nuclei (Hart et al., 2014). Interactions between ERs has been hinted at in previous studies. For example, in OVX female rats, only the ERα agonist (PPT) and not the ERβ agonist (DPN) induced sex behaviour when injected on two consecutive days prior to testing; the combination of both these agonists reduced sex behaviour suggesting that ERβ can modulate ERα's role in inducing sex behaviour (Mazzucco et al., 2008). Given that both ERα and ERβ can induce lordosis behaviour rapidly, but ERα does so over longer time scales, it is possible that the contributions of receptors vary depending on the type of signalling i.e. genomic or non-genomic that is predominant.

The role of aromatase in rodent behaviour has been studied using both global knockout (ArKO) and forebrain-aromatase knockout models. In the ArKO model, OVX female mice treated with EB in adulthood showed reduced sex behaviour, suggesting that organizational effects of EB are important in the display of this behaviour. This was shown to be perhaps due to a loss of discrimination of volatile odours emitted by males(Bakker et al., 2003). The deletion of aromatase in the forebrain of both male and female mice resulted in decreased spine density, hippocampal dependent memory, and loss of PKB and ERK signalling in the cerebral cortex(Lu et al., 2019).

1.5.2.1.2 Sexual behaviour in males

The relative contribution of each region of the SBN regarding sexual behaviour is sexually dimorphic (Goodson, 2005). During mating activity male rats displayed an increase in c-fos activity in the MPOA, BNST, MeA all areas which are significantly larger and contain greater levels of ERs and androgen receptors (AR) than that of their female (Greenberg & Trainor, 2016). Consistent with this, male rats treated with the aromatase inhibitor fadrozole showed low levels of sex behaviour compared with fadrozole-treated males with E2 injected into the mPOA which showed increased sex behaviour (Clancy et al., 2000).

(Cross & Roselli, 1999), were the first to demonstrate that E2 can exert rapid action on male reproductive behaviour; within 35 minutes of estradiol stimulation, castrated but sexually experienced male rats showed an increase in chemoinvestigation and mounting, along with a reduction in the latency to mount (Cross & Roselli, 1999). This suggests that oestrogen non-genomically increases both male sexually motivation and appetitive behaviours towards receptive females. Using ArKO male mice that were administrated EB in adulthood still resulted in reduced mounting frequency since less than half of the male mice mounted

receptive females during the 30 mins(Clancy et al., 1984). In addition, ArKO male mice also displayed longer latency to initiate mounts than WT mice. ArKO males still showed sexual interest by licking or sniffing genital area of receptive females, suggesting that sexual motivation itself was not affected by the deletion of aromatase (Honda et al., 1998). Similarly to female mice, ERαKO male mice showed no sex behaviour while ERβKO male mice showed no differences from WT mice in the ejaculation frequency or latency of mounting (Ogawa et al., 1999). These finding suggest that ERα but not ERβ is critical for the display of male-typical sexual behaviour and sexual motivation as well. Male sexual behaviour requires ERα expression in MPOA and VMH since knockdown of ERα in these regions using siRNA decreases m ale sexual behaviour in mice (Sano, Vasudevan, et al., 2013). Additionally, silencing ERα in the mPOA of male rats also decreased sex behaviour(Paisley et al., 2012), suggesting that oestrogen signalling mediated by ERα in the mPOA is critical. This contrasts with the quail, where ERβ may play an important role in male sexual behaviour. After inhibition with aromatase specific inhibitor, vorozole (VOR), male Japanese quail showed significantly reduced rhythmic cloacal sphincter movements (RCSM) (Seredynski et al., 2015), an appetitive sexual behaviour in birds. Administration of DPN prevented the reduction in the frequency of RCSM after VOR injections within 30 minutes, while there were no changes in the reduction of RCSM when the ERα agonist PPT was injected(Seredynski et al., 2015). Together this data suggest that sexual motivation in quail may largely depend on nongenomic signalling by ERβ via locally synthesized oestrogens(Seredynski et al., 2015). This is interesting as studies using rodents suggest that sexual motivation is independent of ERβ activation; a comparative endocrine study needs to be conducted to determine the relative contribution of each region in the SBN and ERs in male sexual behaviour across all vertebrae species.

1.6 Aggression in males

For the purpose of this thesis, aggression will relate to male rodents, as female rodents generally do not show aggressive behaviour outside of maternal and post-partum aggression(Ervin, Lymer, et al., 2015). Aggression in the rodent model in the lab is generally measured in a resident-intruder paradigm that is repeated across days (Koolhaas et al., 2013).

1.6.1 The contribution to ERα and ERβ in aggression

Though ERα expression is positively correlated with aggressive behaviour in LS, BNST, and AH (Trainor et al., 2006), knockdown studies pinpoint critical areas for this behaviour in rodents to be the VMH. For example, (Sano, Tsuda, et al., 2013), found that when ERα is suppressed in the MPOA there was a reduction in sexual behaviour, but not aggressive behaviour. Additionally, there was and a reduction in both aggression and sexual behaviours

in males with ERα suppression in the VMH. There were no changes in ERα knockdown in the meAMY for either behaviour. This suggest that ERα expression is required in the MPOA and VMH for normal sexual behaviour but only in the VMH for aggressive behaviour (Sano, Tsuda, et al., 2013). When ERα was deleted in GABergic, but not glutamatergic neurons in the BNST and mPOA, there was attenuation of aggressive and sex behaviour, as well as an increase in ERβ expression suggesting that ERα and ERβ are linked transcriptionally (Wu et al., 2017). However, though adult ERβKO male mice did not show any differences in aggression when compared to WT mice (Ogawa & Pfaff, 1999), when treated with EB, they showed an increase in the number of aggressive bouts compared to WT (Nomura et al., 2006). ERβ may also be a regulator of aggressive behaviour in an age-dependent manner. ERβ knockout male mice showed significantly increased aggressive behaviour and shorter latency periods when compared to wildtype during puberty and young adulthood, though the mechanism is unclear (Nomura et al., 2002).

(Trainor, Lin, et al., 2007), have explored the effect of photoperiod on aggression using several species of *Peromyscus* which show parental care and aggression. In short photoperiods, male California mice (*Peromyscus californicus*), beach mice (*Peromyscus polionotus*) and deer mice (*Peromyscus maniculatus*) all show increased aggression as compared to mice in longer photoperiods. In beach and deer mice but not in California mice, this is correlated with an increase in ERα in the lateral septum and a decrease of Erβ in the BNST and a decrease in circulating testosterone (Trainor, Lin, et al., 2007). In addition, in beach mice, both PPT and DPN could restore aggression in fadrozole (aromatase inhibitor) treated mice housed in short photoperiods, suggesting that both ERα and ERβ play a role in this species (Trainor, Lin, et al., 2007). In the beach mouse and California mouse, fadrozole-treated mice could show normal aggression within 15 mins of E2 injection only when housed in short photoperiods, with the time frame following injection suggesting that non-genomic signalling is sufficient for aggression (Trainor, Lin, et al., 2007). This was borne out by the fact that cycloheximide treatment did not change the rapid E2 facilitation of aggression (Laredo et al., 2013). In California mice`, aggression in the short photoperiod but not long photoperiod is correlated with increased p-ERK expression in the meA and BNST as detected by immunocytochemistry(Trainor et al., 2010), reinforcing the idea that E2 facilitation of aggression is via rapid, non-genomic signalling pathways.

The importance of ERα in VMH neurons has been elegantly demonstrated by optogenetic activation and inhibition of these neurons in the laboratories of David Anderson and Dayu Lin (Falkner et al., 2014). For example, optogenetic activation of ventral lateral ventromedial hypothalamus (vlVMH) neurons expressing ERα elicited attacks from male mice towards

male and female conspecifics including towards a glove, while inhibition of these neurons reduces inter-male attack demonstrating that these neurons are in the final pre-motor module of the neuronal circuitry (Davis, Dovey, et al., 2023) (Falkner et al., 2014). Therefore, direct high-intensity photostimulation activated these neurons and uncoupled them from the preceding modules that gather sensory information about the opponent i.e. VNO/AOB and the decision-making module; i.e. the meA and the BNST to attack intruders that would not normally be the subject of aggression (Falkner et al., 2014). In addition, VMH neurons expressing ERα of the resident male fire and show increased calcium during both the social appraisal and attack stages in intermale-aggression and ablating these neurons does not decrease conspecific sex recognition (Lee et al., 2014) (Leroy et al., 2018). Interestingly, low intensity photostimulation of these vlVMH neurons that express ERα allowed for mounting both male and female conspecifics, showing that ERα-expressing neurons from the VMH (around 40%) control both mounting and aggression, suggesting that activation intensity of overlapping neurons in the VMH can drive different social behaviours (Lee et al., 2014). In rats, the vlVMH lies within a defined hypothalamic attack area (HAA) and electrical and pharmacological stimulation elicited intermale aggression, suggesting that ERα signalling in the vlVMH is conserved across species (Yang et al., 2017). Optogenetic activation of anterior vlVMH neurons expressing ERα project primarily to the PAG increased self-defence behaviours by the resident in the face of intruder attack while activation of posterior vlVMH neurons expressing ERα project primarily to the mPOA and increased driving attacks (Wang, 2018). The molecular mechanisms that underlie the rapid control of aggression by E2 remain unclear.

1.7 The influence of ligand on behaviour

The role of locally synthesized ligand i.e. E2 in the brain has been explored using both pharmacological and genetic models. There is a relatively large body of work that investigates the role of neuroestrogens on cognition, focusing on the hippocampus. This was one of the first regions of the brain where *de novo* synthesis of oestrogen and other steroidogenic pathway precursors was identified using LCMS and solid phase extraction(Hojo & Kawato, 2018). Using immunohistochemical and RT-PCR techniques, the presence of steroidogenic enzymes was also shown in the pyramidal cells of the hippocampus (Hojo et al., 2004; Hojo & Kawato, 2018; Hojo et al., 2008). This has been discussed in detail in Chapter 4 and hence we will not describe it here. In this section, I will focus on describing the phenotypes obtained either when aromatase is genetically deleted or modified or when it is inhibited using pharmacological means. *In vivo*, since males have very little E2 in their blood, phenotypic characterization of the loss of aromatase is easier to interpret in male models.

Pharmacological models have relied on the addition of an aromatase inhibitor (AI) either chronically in cell cultures or administered to animals.

.

1.7.1. Role of neuroestrogens in the hippocampus: a role for cognition?

Some of the first studies that suggests a role for locally produced neuroestrogens were from the Rune group and used both dissociated cultures or hippocampal slices from males and female postnatal and adult animals. In hippocampal slices derived from either males or females, estradiol was secreted into the steroid free and serum free medium over a period of seven days(Kretz et al., 2004; Prange-Kiel et al., 2003). In mixed-sex dissociated cultures, addition of cholesterol and testosterone increased E2 while siRNA transfection with StAR and chronic application of letrozole (aromatase inhibitor) decreased it (Fester et al., 2009), suggesting *de novo* steroidogenesis. However, though production of neurosteroids appears to sex independent, there was sexual dimorphism when the role of this local hippocampal neuroestrogen was investigated. Letrozole decreased spine density and spine synapses on long term (7days) exposure in slices derived from females but not from males, likely due to a decrease in long term potentiation (LTP) in females but not in males (Vierk et al., 2012) (Kretz et al., 2004). This suggest that the response of spines was sensitive to local estradiol concentrations though several published reports show that the spine density fluctuates across the female oestrous cycle with the highest spine density shown at proestrus (Woolley & McEwen, 1992). Together, this suggest that spine density is sensitive to gonadally produced oestrogen. To resolve this discrepancy, detailed studies from the Rune lab showed that GnRH release at proestrous may synchronise the peripheral oestrous cycle with an internal "hippocampal" cycle since the application of GnRH rescued the inhibition of spine density seen with letrozole. GnRH stimulation of hippocampal neuroestrogen synthesis was via GnRH receptors localized in hippocampal neurons (Prange-Kiel et al., 2008).

In the global aromatase knockout mouse, social recognition, and spatial memory(Martin et al., 2003) was severely impaired in males but social recognition could be rescued in adulthood (Pierman et al., 2008).A comprehensive study was carried out recently by the Brann group which looked at a number of different cognitive phenotypes, along with associated neuromorphological parameters in both sexes in the mouse. Conditional knockout mice that did not possess aromatase in the forebrain neurons i.e. FBN-AroKO (hippocampus and cerebral cortex) showed several different phenotypes(Rosenfeld et al., 2018). The showed a deficit in cognitive tests as measured by the Barnes Maze and the novel object recognition test as well as a deficit in context but not cued conditioning, suggesting that hippocampal synapses are important. Consistent with this, hippocampal neurons showed lower spine density in both

hippocampus and cortex, with a decrease in mushroom, thin and stubby types(Lu et al., 2019). Synaptic density (as measured by PSD-95 and synaptophysin colocalisation) was also decreased in both the hippocampus and cortex of the FBN-aroKO compared to the WT(Lu et al., 2019). The amplitude of hippocampal LTP generated by high frequency stimulation in brain slices was lower in the FBN-AroKO than the WT. This could be rescued by E2 and abrogated by treatment with a MEK inhibitor implying that rapid nongenomic signalling by neuroestrogens in the forebrain was responsible for generating LTP. Similarly, implantation of a E2 capsule 7 days prior to testing allowed for rescue of the cognitive deficit in the novel object recognition and Barnes Maze tests, as well as the normalization of synaptic density. These phenotypes were not sexually dimorphic since males and female conditional KO show the same phenotype and the loss of neuroestrogens in the forebrain does not control either exploration or anxiety (Lu et al., 2019).

1.7.2 Role of neuroestrogens in social behaviour

Initial studies in the rat and quail used both non-steroidal and steroidal aromatase inhibitors to achieve a decrease in aromatase activity. In the male rat, administration of fadrozole for a week inhibited approach and copulatory behaviour though all behaviours except ejaculation were rescued by implantation of a silastic capsule with oestrogen over weeks (Roselli et al., 2003). In the quail, acute single administration of vorozole to the castrated, testosterone-supplemented male quail reduced the appetitive component of male sex behaviour called the rhythmic cloacal sphincter movement (RCSM) strongly within 30 minutes and weakly reduced the consummatory component called the cloacal contact movement (CCM) (C. A. Cornil et al., 2006). The RCSM could be restored rapidly within 30 minutes by the concomitant injection of estradiol, suggesting that the initial part of the male mating behaviour sequence in the quail is critically dependent on non-genomic signalling (C. A. Cornil et al., 2006). Similarly, a single administration of aromatase inhibitor to the male mouse also decreased sex behaviour within 10 mins, similar to the quail, with a decrease both appetitive and consummatory components i.e. in the number of mounts and intromissions, as well as in anogenital investigation. This could be rapidly restored within 10 mins after an injection of E2 (Taziaux et al., 2007). Since RCSM but not CCM in the castrated/testosterone supplemented male quail that had been administered vorozole could be restored by membrane-limited E2BSA within 30 mins of administration icv, this suggests that male sex behaviour in the quail has both non-genomic (RCSM) components and genomic components (CCM), reminiscent of lordosis behaviour in the female mouse (Seredynski et al., 2013). This effect was replicated by DPN but not by ERα or GPER1 agonists, suggesting that RCSM in the male quail is driven by ERβ at the membrane (Seredynski et al., 2015).

1.7.3 Use of genetically modified aromatase gene in mouse models

With respect to genetic ablations of aromatase, the first models used mice where aromatase was deleted globally. Results obtained using this model, particularly in the realm of sexually dimorphic behaviours can be difficult to interpret because of developmental effects of oestrogen on the brain to organize male-specific behaviours such as aggression and sex in the rodent. For example, male mice that lack the aromatase gene in all tissues and in all stages of life showed loss of aggression in adulthood which cannot be rescued if E2 (7.5 µg/mouse) was given after 7 days postnatally, suggesting that this behaviour is developmentally organized and then activated later during adulthood by oestrogen. Sex behaviour was also greatly reduced as was discrimination between oestrous females and intact males(Bakker et al., 2004; Bakker et al., 2002). However, unlike aggression, sex behaviour could be rescued by injection of 17b-estradiol in adulthood, though olfactory investigation of volatile odours, an initial event important for interaction with conspecifics was not rescued in adulthood(Bakker et al., 2004) . A brain-specific aromatase KO (brArKO) male mouse also showed decreased number of mounts and intromission that was only partially rescued with testosterone supplementation and not recovered by systemic oestrogen administration alone. Full recovery of the behaviour required both testosterone and oestrogen supplementation suggesting that brain derived oestrogen from testosterone is required for the full display of male sex behaviour in the mouse (Brooks et al., 2020). In female ArKO mice, lordosis was reduced and is not rescued by the administration of oestrogen in adulthood; this was correlated with the loss of preference for non-volatile odours emitted by oestrous females or males (Bakker et al., 2002). This phenotype was rescued by E2 administration in the prepubertal period, suggesting that oestrogen has an organizational effect in females for this behaviour (Brock et al., 2011). Neither female (Dalla et al., 2004)nor male ArKO mice (Dalla et al., 2005)differed from WT mice in anxiety, exploration and motor activity but show a phenotype in the forced swim test that denotes depression. In females, this was correlated with increased serotonin in the hippocampus and the phenotype is not rescued by estradiol treatment in adulthood (Dalla et al., 2004).

More recent studies have used chemo or optogenetics to control the activity of different neuronal subtypes. Controlling aromatase in two nodes of the SBN nuclei i.e. BNST or meA could elicit different effects on social behaviours in males and females. Aromatase expressing neurons in the BNST are required for intermale aggression and sex behaviour since silencing of these neurons using chemogenomic means resulted in a decrease in both these behaviours and loss of social recognition. In females, loss of these neurons did not alter maternal aggression or mating, suggesting that aromatase activity in the BNST is important for

recognition of same sex males and potential partners only in males (Bayless et al., 2019). In addition, silencing of meA aromatase neurons in males and females reduced aggression in mice, without altering mating behaviour, marking behaviour, locomotor, or anxiety behaviours (Unger et al., 2015).

All studies present using inhibitors or genetically modified animals show that local production of oestrogen is capable of driving both spatial memories and social behaviours.

1.8 Relevance of non-genomic signalling

Why does non-genomic signalling initiated by mERs exist? In many cases, e.g. lordosis or spinogenesis, it appears to be the initiating step in a sequence of events as part of a coupled signalling pathway. This initiating step could either prime or potentiate the later steps or could be antagonistic. For example, work from our laboratory has shown that in neuroblastoma cells, E2-BSA potentiated transcription from a consensus ERE by phosphorylation of the ERα by activated PKB and ERK (Clark et al., 2014). Studies from the Dorsa laboratory have shown that rapid activation of PKA by E2-BSA may potentiate transcription from non-ERE containing promoters such as those with cis-regulatory element (CRE) enhancer elements(Watters & Dorsa, 1998). Hence, one function of non-genomic signalling and the rationale for the existence of the mERs is the ability of mER-mediated action to prime transcription from both ERE and non-ERE containing promoters, increasing the number of genes responsive to oestrogen. This may occur by the mER, and ER being arranged in series as shown in Figure 1.8 B. However, mERs may also antagonize the transcriptional activity of the classical ERs though antagonism of classical ERs by GPER1 activation has been mostly shown in cancer cells with not many examples in the CNS (Hadjimarkou & Vasudevan, 2018). In breast cancer cell line (MCF7) , GPER1 activation by G-1 decreased proliferation that was increased by ERα activation while in MDA-MB-231 cells, GPER1 activation lowered Akt signaling that is critical to Erβ-mediated ezrin phosphorylation that promotes cell invasion (Zhou et al., 2016)(Figure 1.8 C).

These studies suggest that activation of mERs and subsequent rapid non-genomic signalling can act as as gain amplifier or dampener of genomic effects. Depending on the relative levels of ERs and their combinations as well based on temporal kinetics, the same ligand i.e. E2 could generate different responses in the same cell (Rainville et al., 2015). Our laboratory has outlined several scenarios where GPER1 as a mER may act as a “collaborator” to ERα or ERβ (Hadjimarkou & Vasudevan, 2018) (Ruby Vajaria & Nandini Vasudevan, 2018) where GPER1 may act in series or in parallel to increase final output which could be an alteration in cell phenotype e.g. spinogenesis or an alteration in behaviour e.g. lordosis. For example, in OVX

female rats, activation of both ERα and GPER1 using PPT and G-1 respectively decreased food intake within 1 hr (Butler et al., 2018). Blockade of GPER1 using G-15 decreased the PPT effect within 1hr suggesting that activation of GPER1 is necessary for ERα to exert rapid non-genomic anorexigenic effects (Butler et al., 2018). Moreover, the variant ERα-36 isoform may also influence ERα66-dependent responses. Inhibition of LPS-induced TNFα expression in MCF7 cells was dependent on the full length ERα66 isoform, the variant ERα- 36 isoform and GPER1. When ERα-36 or the GPER1 was knocked down, the anti-inflammatory effects of oestrogen was lost (Notas et al., 2021).

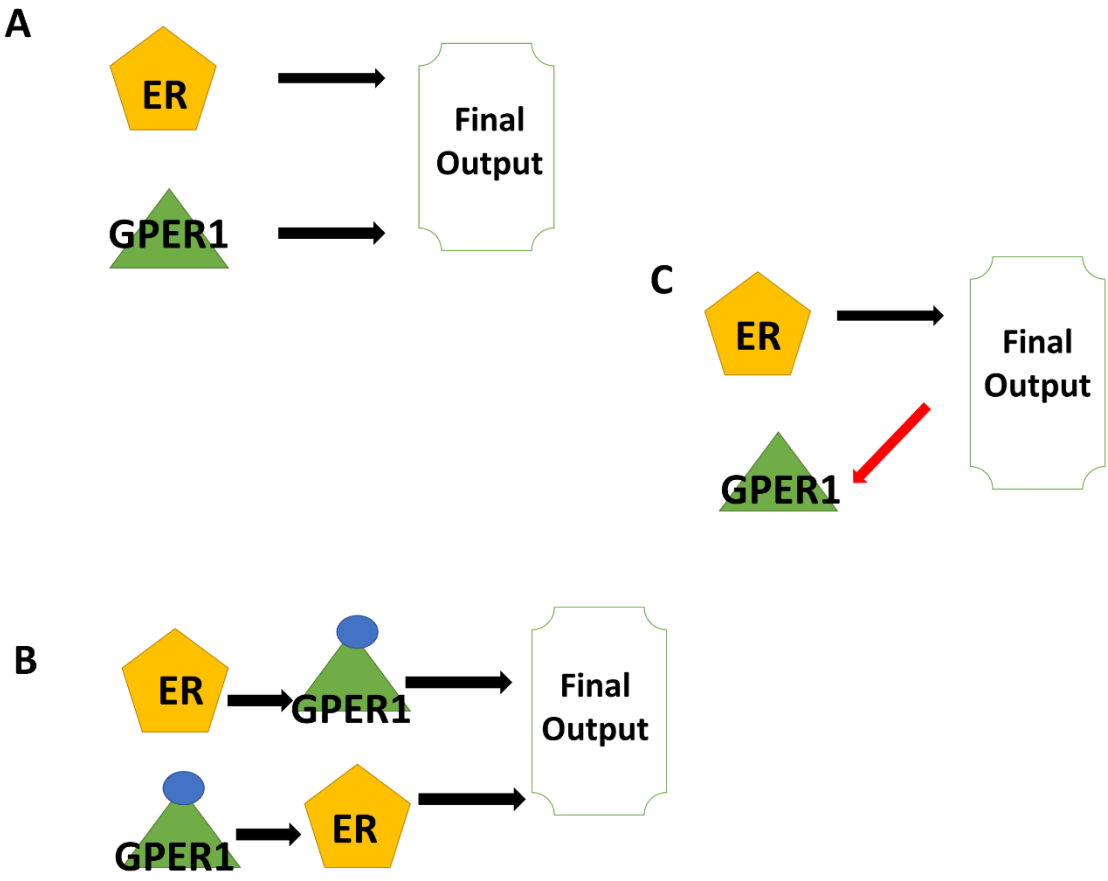

Figure 1.8 Schematic Crosstalk of ERs and GPER1 to reach an output. Classical ERs (ERα or ERβ) and GPER1 can signal in a parallel manner (A) or in a series (B) .In these scenarios both receptors are required for the final output. In contrast GPER1 may antagonize ER mediated signalling (C), in this scenario the final output is decreased or abolished. Adapted from (Ruby Vajaria & Nandini Vasudevan, 2018).

GPER1 may have an important collaborative role in two processes – spinogenesis and lordosis. In the VMH, though EB increases spine density, this is not on ERα+ neurons and could be on GPER1+ neurons. Secondly, G-1 administration to ovariectomized mice is sufficient to increase lordosis, a behaviour for which it is known that ERα is critical (Anchan et al., 2014). It is possible that these two receptors are positioned in the same pathway to promote behaviour. For example, G1, like EB can facilitate lordosis behaviour via deactivation of the MOR in the mPOA when infused into the third ventricle 47 hours after a suboptimal priming dose of EB, suggesting that there is an interaction between GPER1 and other ERs in the ARH (Long et al., 2014). Furthermore, infusion of ICI and tamoxifen (ERα antagonist) , both shown to be GPER1 agonists but ER antagonists could also facilitate lordosis in the same paradigm and these effects could be abolished with infusion of a specific GPER1 antagonist, G15 (Long et al., 2017; Long et al., 2014).

1.9 Objectives and Aims

The molecular interaction between GPER1 and ERα remains unknown and colocalisation of these receptors is the first step in understanding how these two receptors may collaborate or signal. Secondly, despite the progress made in understanding the role of different regions of the brain and the contribution of different receptors in social behaviour, several questions remain. For example, in the mouse, the functional relevance of neurosteroids in social behaviour has only been studied using genetic knockouts and a narrow range of behaviours, while most of the physiological significance of neurosteroids in ethologically relevant behaviours have been studied in birds. The regulation of neurosteroids synthesis and the production by different SBN nuclei in the mouse is not known.

The main objectives of this thesis are:

a) To investigate crosstalk between the GPER1 and the ERα in two contexts (i) localization in organelles and ii) signalling within cells.
b) To investigate the production and regulation of neurosteroids in the SBN of the male mouse.

A secondary objective is to devise a system where this can be more easily studied. Therefore, a two relatively novel systems a) stem cell differentiated neurons and b) acute slice cultures where neurosteroids could be measured. An original objective i.e. to understand the relevance of the production of neuroestrogens in the SBN in the male mouse

was to be investigated in collaboration with Professor Sonoko Ogawa at the University of Tsukuba, Japan using an aromatase-flux model (area specific aromatase knockout). This could not be done due to the COVID-19 pandemic and the resultant travel and work restrictions.

2. Localisation of oestrogen receptors in stem cells and in stem cell derived neurons of the mouse.

DeAsia Davis1, Ruby Vajaria1, Evangelos Delivopoulos1 and Nandini Vasudevan1

1: School of Biological Sciences, University of Reading, United Kingdom RG6 6GAS.

Corresponding author:

Dr. Nandini Vasudevan,

School of Biological Sciences, University of Reading, United Kingdom RG6 6GAS

Email: n.vasudevan@reading.ac.uk

Running title: Oestrogen receptor localisation in neurons

Keywords:

Oestrogen receptors, stem cells, subcellular localisation, neuronal differentiation

Acknowledgments/Funding statement

This work was partly funded by a Project Grant from the British Society for Neuroendocrinology to NV, a grant from the Centre for Integrative Neuroscience (CINN,

University of Reading, UK) to ED and an EPSRC Doctoral Training Partnership Fellowship to RV.

Conflict of interest statement

The authors declare that we have no conflict of interest.

Most of the data in Chapter 2 with the exception of Figures 2.8-2.10 are published in the following publication:

Publication: Davis D, Vajaria R, Delivopoulos E, Vasudevan N. Localisation of oestrogen receptors in stem cells and in stem cell-derived neurons of the mouse. J Neuroendocrinol. 2023 Feb;35(2):e13220. doi: 10.1111/jne.13220. Epub 2022 Dec 12. PMID: 36510342.

Expanded data: Figure 2.8-2.10.

Figures: All figures represent data collected, analysed and generated by Ms. DeAsia Davis's except Figure 2.4 which was done in collaboration with Ms. Ruby Vajaria, a PhD student co-supervised by Dr. Nandini Vasudevan and Dr. Evangelos Delivopoulos.

Intellectual contribution: The work in the paper was originally conceived and supervised by Dr. Nandini Vasudevan and expanded by Ms. DeAsia Davis to include ERα-36. Ms. DeAsia Davis also independently learnt and proposed the use of EZ-coloc software to analyse these sets of data.

Writing: The results and methods were written by Ms. DeAsia Davis as well as parts of the introduction and discussion and expanded data, with discussion by all co-authors. Some parts of the introduction and discussion were written by Dr. Nandini Vasudevan and Dr. Evangelos Delivopoulos in collaboration with Ms. Davis.

2.1 Abstract

Oestrogen receptors (ER) transduce the effects of the endogenous ligand, 17β-estradiol in cells to regulate a number of important processes such as reproduction, neuroprotection, learning and memory and anxiety. The ERα or ERβ are classical intracellular nuclear hormone receptors while some of their variants or novel proteins such as the GPCR, GPER1/GPR30 are reported to localise in intracellular as well as plasma membrane locations. Though the brain is an important target for oestrogen with oestrogen receptors expressed differentially in various nuclei, subcellular organisation and crossttalk between these receptors is under-explored. Using an adapted protocol that is rapid, we first generated neurons from mouse embryonic stem cells. Our immunocytochemistry approach shows that the full length ERα (ERα-66) and for the first time, that an ERα variant, ERα-36, as well as GPER1 is present in embryonic stem cells. In addition, these receptors typically decrease their nuclear localisation as neuronal maturation proceeds. Finally, though these ERs are present in many subcellular compartments such as the nucleus and plasma membrane, we show that they are specifically not colocalised with each other, suggesting that they initiate distinct signalling pathways.

2.2 Introduction

Oestrogen (17β-E; E2) plays an important role in reproduction, neuroprotection, vascular and cognitive function (Brann et al., 2012; Ervin, Lymer, et al., 2015; K. S. Ervin et al., 2013; Pfaff et al., 1994) and in the maintenance of sexually dimorphic behaviours by both genomic and non-genomic signalling (Ogawa et al., 2020). Genomic signalling is a slow signalling mechanism by which oestrogen on binding the nuclear oestrogen receptors ERα and ERβ regulates transcription from target genes (Mangelsdorf et al., 1995; Nilsson & Gustafsson, 2011). Oestrogen also initiates rapid, non-classical signalling that involves the activation of multiple protein kinase cascades from plasma- membrane localised oestrogen receptors (mERs), particularly in endothelial cells (Prossnitz & Maggiolini, 2009b), breast cancer cells (A. Pedram et al., 2006; M. Razandi et al., 2004) and neurons (Vasudevan & Pfaff, 2007, 2008). In the central nervous system (CNS), rapid signalling by mERs in the nuclei of the social behaviour network regulates sex-typical social behaviours such as aggression and copulation whereas signalling in limbic nuclei facilitates hippocampus-dependent learning and memory formation (Fernandez et al., 2008; Rainville et al., 2015; Trainor et al., 2008).

Though the common isoform of ERα i.e. full length ERα-66 and ERβ were thought initially to be intracellular receptors, a number of studies have shown localisation of these receptors at the plasma membrane, with functional implications (Rainville et al., 2015). For example, in astrocytes, the arcuate nucleus and in striatal and hippocampal neurons, ERα can couple to different metabotropic glutamate receptors (mGluR) that is a result of ERα anchoring at the plasma membrane to specific caveolin (CAV) subtypes (reviewed in (Meitzen & Mermelstein, 2011)). Silencing of CAV1 (Christensen & Micevych, 2012) or blockade of mGluR1 (Dewing et al., 2007) in the arcuate nucleus leads to lower localisation of ERα at the plasma membrane, decreases μ-opioid receptor internalisation in the medial preoptic area and lowers lordosis, a measure of female sexual receptivity, in response to E2. Similarly, in astrocytes, the rapid increase in calcium required for the neuroprogesterone release that is important for reproduction is synergistically increased with a combination of mGluR1 agonists and 17b-E (Micevych et al., 2007) as well as by ERα-selective agonists such as PPT ((1,3,5-tris (4-hydroxyphenyl)-4-propyl-1H-pyrazole) (Kuo et al., 2009). This suggests that ERα is anchored at plasma membrane and can functionally act as a mER that initiates rapid nongenomic signalling in the CNS. Consistent with this, a ERα522 mutant incapable of being palmitoylated loses membrane localisation and rapid activation of the pCREB pathway upon 17b-E treatment (Boulware et al., 2005) in hippocampal neurons. A variant of ERα called ERα-36 that lacks the AF-1 N-terminal domain is a cytoplasmic/plasma-membrane localised ER, detected in endothelial cells as well as in ERα-

66 positive and ERα-66-negative breast cancer cell lines (Zhang et al., 2011);(Vranic et al., 2011). In triple negative (ERα-, PR-, HER2-) breast cancer cell lines, ERα-36 promotes proliferation via rapid epidermal growth factor receptor (EGFR)-ERK signalling (Zhang et al., 2011). In Hec1A endometrial cancer cells, tamoxifen, a first-line therapy for breast cancer and a mixed agonist/antagonist for ERα-66 could activate PI3K/PKB signalling in an ERα-36 dependent manner (Lin et al., 2010). Yet another mER is the G-protein coupled receptor, GPER1/GPR30, localised at the plasma membrane of SKBR3 cells, which activates EGFR-ERK signalling via the release of the heparin-bound EGF (E. J. Filardo et al., 2000); in COS-7 cells, this interaction with EGFR by GPER1 localised to the endoplasmic reticulum increases calcium flux (C. M. Revankar et al., 2005). In the rat CA1, GPER1 at the cell membrane of the dendritic spine is anchored to PSD-95 (Akama et al., 2013) or to SAP97 (Waters et al., 2015) and increases social and spatial cognition in mice by rapidly signalling in the hippocampus (C. Gabor et al., 2015). These studies show that apart from the classical nuclear localisation of ERa that is related to its transcriptional role (Nilsson et al., 2001; Vasudevan & Pfaff, 2007, 2008), ERs have also been investigated for their presence on the plasma membrane as a prerequisite for membrane-initiated rapid signalling. Therefore, subcellular localisation is relevant to the type of signalling pathway utilised by these receptors i.e. rapid non-genomic signalling in contrast to slower regulation of cellular and behavioural phenotypes.

Investigating the subcellular colocalisation of these receptors also allows us to understand crosstalk between these receptors (Hadjimarkou & Vasudevan, 2018). For example, G-1, a selective GPER1 agonist, deactivates μ-opioid receptor (MOR) internalisation in the medial preoptic area, signalling in tandem with ERα, in the arcuate nucleus of the hypothalamus (ARH), to facilitate lordosis in female rats (Long et al., 2014). In non-neuronal cells, the ability of G-1 to rapidly increase c-fos expression within an hour in the mouse spermatogonial cell line GC-1 is dependent on ERα, suggesting that these receptors may signal via in the same pathway (Sirianni et al., 2008). Recently, ERα-36 has been shown to physically interact with GPER1 in SKBR3 (ERα-66 negative) and MCF-7 breast (ERα-66 positive) cancer cell lines to inhibit proliferation. This novel GPER1-ERα-36 interaction in the cytoplasm is required for the oestrogen inhibition of LPS-induced inflammation via the inhibition of NF-κB, suggesting that these receptors can interact with each other in a complex with a cytokine (Notas et al., 2021).

Though GPER1, a putative mER, has been localised to the plasma membrane of the dendritic spine, (Funakoshi et al., 2006; Waters et al., 2015) endoplasmic reticulum (Waters et al., 2015) and Golgi apparatus (Sakamoto et al., 2007) (Matsuda et al., 2008) in hippocampal and hypothalamic neurons, subcellular localisation of endogenous ERα-36 has been studied mostly in cancer cell lines (Qu et al., 2019) with no report in the CNS. Moreover, subcellular

colocalisation of these putative mERs, with the classical receptor ERα has not been studied, though signalling from these receptors may antagonise or synergise with each other to govern final cellular output to oestrogen stimulation (Hadjimarkou & Vasudevan, 2018) (Notas et al., 2021). In part, this is due to the difficulty and cost of maintaining primary neuronal cultures from embryonic or neonatal rodent sources.

Neural differentiation protocols predominantly rely on growth factors to induce neural lineage specification. The main morphogens usually employed for motor neuron differentiation are retinoic acid (RA), sonic hedgehog (SHH) and its agonists: smoothened agonist (SAG) and purmorphamine. In most protocols, neural precursor cells (NPC) are first derived from pluripotent stem cells in a process called neural induction. NPC are then patterned into a desired neural lineage with the use of RA and SHH at specific concentrations, followed by the addition of neurotrophic factors which ensures neuronal maturation. The entire process to generate β-tubulin positive neurons requires 20 days or more (Qu et al., 2014). In this study, we committed mouse embryonic stem cells to neural lineages, by fine tuning a mass suspension protocol by Wichterle et al (Wichterle & Peljto, 2008) to generate embryoid bodies within 5 days. This fast and efficient adaptation has produced both astrocytes (Juneja et al., 2020) and neurons (Delivopoulos et al., 2015; Fannon et al., 2020). Hence, the objectives of this study were to examine the subcellular localisation and colocalisation of endogenously expressed ERα, GPER-1 and ERα-36 in neurons differentiated from pluripotent mouse stem cells.

2.3 Material and Methods

2.3.1 Cell culture

The male mouse embryonic stem cell line (mES) CGR8 (from inner cell mass of day 3 mouse embryo, strain 129) was obtained from Sigma, Aldrich UK. mES were plated between passage 7 and 13 at 10^6 cells in gelatine-coated (0.1%) tissue culture flasks ($25cm^2$) and maintained in SNL media composed of Dulbecco's modified Eagle medium (DMEM)(Gibco, UK), 10% fetal bovine serum (FBS) (Biosera, UK), 1% Penicillin/Streptomycin(P/S) (Gibco,UK), 1%L-Glutamine (Gibco,UK), 100μM 2-Mercaptoethanol (Gibco, UK) and 10^6 Leukaemia inhibitory factor (LIF) (Calbiochem,UK) (Fannon et al., 2020). They were incubated at 37°C at 95% O_2, 5% CO_2. Stem cells were passaged at a ratio of 1:8 at 80% confluence (approximately every 2 days) to maintain pluripotency. They were then used to plate on 0.1% gelatinized glass coverslips in 24 well plates for immunocytochemistry (Section 2.3.3) or in 60 mm non-adherent Petri dishes for neuronal differentiation (Section 2.3.2).

2.3.2 Neuronal Differentiation from mES cells

mES were plated (Day 0) at 50,000 cells per/ml ($0.5 * 10^6$) onto non-adherent 60mm Petri dishes in ADFNK medium composed of Advanced DMEM/F12 – Neurobasal (1:1) (Gibco, UK) , 10% Knockout Serum Replacement (KSR) (Gibco, UK), 1% P/S, 1% L-Glutamine (Gibco, UK), 100µM 2-Mercaptoethanol (Gibco, UK) and maintained at 37°C in a 95% O_2, 5% CO_2, for the formation of embryoid bodies (EBs). The medium was changed on Day 2 and supplemented with 1 µM all-trans retinoic acid/1 µM purmorphamine, which are known neuralizing agents. On Day 4 medium was changed back to ADFNK without RA or purmorphamine. On Day 6, EBs were washed in Phosphate Buffered Saline (PBS), re-pelleted and resuspended in 5 ml of 0.25% trypsin-EDTA (1X) on a rocker for 10 min at 37°C. 5 ml of ADFNK was added to neutralize the trypsin-EDTA. The EB suspension was then triturated with a series of three progressively smaller in diameter fire-polished glass Pasteur pipets, passed through a 70 µm cell strainer to remove large aggregates, centrifuged for 5 min at 180 rcf, resuspended in 5 ml ADFNB medium (Advanced D-MEM/F12: Neurobasal (1:1) (Gibco, UK), 1x B27 supplement (Invitrogen), 200 mM L-Glutamine (Gibco, UK), 1x Pen/Strep (Gibco,UK), 10 ng/ml βFGF (Gibco UK), 10 ng/ml BDNF (Gibco, UK)) and counted using trypan blue exclusion. Individual cells were replated onto either 0.1% gelation or laminin-coated (2 µg/cm^2) coverslips (13 mm) at 200 cells/mm^2 (30000 cells) in 24-well tissue culture plates and allowed to grow till D (day) 7, D14 and D21, with media changes every 2 days. This method of neuronal differentiation is a modification of the Peljto et al. protocol which has been shown to produce motor neurons (M. Peljto et al., 2010).

2.4 Immunocytochemistry

mES CGR8 cells at a density of 0.3x 10^6 were plated on gelatinised 13mm coverslips in 24 well plates and fixed on day 2 for 20 mins in 4% paraformaldehyde (PFA) at room temperature (RT) for immunocytochemical analyses. Similarly, cultured differentiated neurons (mESn) (Section 2.3.2) were fixed in 4% PFA/RT for 20 mins at room temperature at day 7,14 and 21 of culture, as standard timepoints of examining neuronal maturation (Delivopoulos & Murray, 2011). Fixed cells were then permeabilized in 10% normal goat serum (NGS) (Fisher, UK) containing 0.1 % Triton X-100(Sigma, UK) in PBS for 10 minutes at RT. For experiments where target antigens need to be visualised at the cell membrane, CellBrite® Cytoplasmic Membrane Dye (Biotium,UK) was incubated with fixed cells for 10 mins at RT at the dilution shown in Table 2.1, prior to permeabilization. This timeframe is kept short so that the dye remains at the membrane and image analyses of target antigen (detected by antibody) localised with the membrane dye reveals the extent of colocalisation. After permeabilization, cells were washed

again thrice for 5 minutes each in PBS, then incubated with primary and secondary antibodies (Table 2.1). Primary antibodies (Table 2.1) that detect the ERα-66 and the mERs, ERα-36 and GPER1, diluted in 10% NGS in PBS were applied to cells overnight on a shaker at 4°C. After 3 washes (5 min each) in PBS, cells were incubated with secondary antibodies (Table 2.1) in 10% NGS in PBS for 1hr. To detect the endoplasmic reticulum or the Golgi apparatus, we used stains that we could apply to fixed cells rather than available live stains (e.g., BoDIPY) to be compatible with prior antibody application. Stock solutions for concanavalin A conjugated to Alexa Flour 594 to detect the endoplasmic reticulum were prepared at 1mg/ml in 0.1 M sodium bicarbonate and stored at -20°C. 1mg of Lectin HPA-Alexa Fluor™647 Conjugate to detect the Golgi apparatus was dissolved in 1ml of PBS and stored at -20°C. These organelle stains were then added at the concentrations and times shown in Table 2.2. After application of the organelle stain, cells were washed again thrice for 5 minutes each in PBS and coverslips mounted onto glass slides with Fluromount-G Mounting Media with DAPI (Invitrogen, UK) and sealed with DPX mountant (Sigma, UK). Slides were left to dry for at least 30 mins before imaging cells on the microscope. Negative controls omitted the primary antibody/antibodies.

2.4.1 Conjugation of antibodies with fluorophore

Since antibodies to the oestrogen receptor were raised in the same species, Anti-ERα(Saint John's Laboratory, UK) and Anti-GPER1(Saint John's Laboratory, UK) were conjugated to Fluorescein isothiocyanate (FITC) (Thermofisher, UK), as per the suppliers protocols (Thermofisher UK). Briefly, anti- ERα and anti-GPER1 were initially concentrated using Amicon Ultra centrifugal filter units (Ultra 4 MWCO 30KDA) (Merck Millipore, UK) to generate stock solutions of concentrated Anti-ERα and Anti-GPER1 at 2mg/ml in 0.1 M sodium bicarbonate. FITC stock solution was prepared at 1mg/ml in anhydrous dimethyl sulfoxide (DMSO). 50µl of FITC solution was slowly add to the 2mg/ml of antibody solution and incubated at 4º C for 1hr with continuous stirring. Free fluorophores was separated from conjugated antibody using PD-10 column, Sephadex G-25M (BioRad, UK) and conjugated ERα/ FITC and GPER/FITC was eluted with PBS. In order to determine the labelling efficiency and concentration, absorbance values were measured at A280 and A495. For effective labelling, the degree of labelling should fall within 2-6 moles of FITC per one mole of antibody; typical concentrations were in the range of 0.2 mg/ml. The newly conjugated antibody was stored at -20° C until use.

Antibody Name/ Target/(Cat #)	Source	Host Species	Dilution
ERα (STJ97499)	St. John's Laboratory, UK	Rabbit	1:300
GPER1 (STJ192629)	St. John's Laboratory, UK	Rabbit	1:300
ERα-36 (ERA361-1)	Alpha Diagnostics, USA	Rabbit	1:300
b-tubulin-III /neuronal marker (ab 18207)	Abcam, UK.	Mouse	1:300
MAP2/neuronal marker (AB_2313549)	Aves Lab. Davies, CA	Chicken	1:300
Neu-N (Fox 3)/neuronal marker (AB_2313556)	Aves Lab, Davis, CA	Chicken	1:300
Goat anti-Rabbit IgG (H+L) Secondary Antibody, DyLight 488 (11800074)	Invitrogen, Thermo-Fisher Scientific, UK	Goat	1:300
Goat anti-Rabbit IgG (H+L) Cross-Adsorbed Secondary Antibody, Alexa Fluor 568 (A-11011)	Invitrogen, Thermo-Fisher Scientific, UK	Goat	1:300
Goat anti-Rabbit IgG (H+L) Cross-Adsorbed Secondary Antibody, Alexa Fluor 647 (19123672)	Invitrogen, Thermo-Fisher Scientific, UK	Goat	1:300
Goat anti-Mouse IgG (H+L) Cross-Adsorbed Secondary Antibody, Alexa Fluor 568 (A-11004)	Invitrogen, Thermo-Fisher Scientific, UK	Goat	1:300

Goat anti-Chicken IgY (H+L) Cross-Adsorbed Secondary Antibody, DyLight 350 (SA5-10069)	Invitrogen, Thermo-Fisher Scientific, UK	Goat	1:300
Goat anti-Chicken IgG (H+L) Cross-Adsorbed Secondary Antibody, Alexa Fluor 647 (A-21449)	Invitrogen, Thermo-Fisher Scientific, UK	Goat	1:300

Table 2.1. Details of primary and secondary antibodies used for immunocytochemistry in mES and mESn. Primary antibodies were bought from various sources and used at the dilution described at the table. Goat anti-rabbit secondary antibodies conjugated to different fluorophores was used to obtain localisation of different antigens from the same coverslip.

Antibody Name/ Stain/(Cat #)	Source	Time (mins)	Dilution /Concentration
CellBrite® Cytoplasmic Membrane Dye (30022)	Biotium Inc, UK	10	1:200 in PBS
Concanavalin A, Alexa Fluor™594 Conjugate/Endoplasmic reticulum marker(C11253)	Invitrogen, Thermo-Fisher Scientific, UK	20	50µg/ml
Lectin HPA From *Helix pomatia* (edible snail), Alexa Fluor™647 Conjugate/Golgi apparatus marker (L32454)	Invitrogen, Thermo-Fisher Scientific, UK	20	5µg/ml

Table 2.2 . Organelle and cell membrane stains used in experiments to determine subcellular localisation of the antigens in mES and mESn. Stains were used for the times specified at the dilution specified either prior or after antibody application as detailed in Methods.

2.5 Image Analysis

Images were acquired using a Zeiss AxioImager Epiflourescent (Carl Zeiss MicroImaging GmbH) microscope with 20x objective under identical exposure times, gain and threshold with exposure times set by negative controls (no primary antibody added). Monochromatic images were analysed with EZcolocalisation (image processing plugin for Image J/Fiji, NIH Image) (Schneider et al., 2012) using methods previously described in (Stauffer et al., 2018). Since quadcolour experiments were possible, for mES cells that are homogenous, we analysed the presence of each oestrogen receptors in two or three different organelles in the same cell – i.e. for e.g. ERα (green) in plasma membrane (red) and nucleus (DAPI blue) or ERα (green) in the nucleus (DAPI blue), endoplasmic reticulum (ConA-red) and Golgi apparatus (HPA-far red) in the same cell. However, not all cells in mESn cultures are neurons and must be identified by a neuron-specific stain such as b-III Tubulin (far red) or NeuN (blue) that also stains the nucleus. Cells identified as neurons by these methods were then further analysed for the presence of oestrogen receptors in various organelles, using the EZcolocalisation (EZcoloc) plugin.

Manders coefficients determine the degree of overlap between fluorophores in a region delineated by the organelle stain even when signal intensities differ and this Ezcoloc plugin can be expanded to include more than two fluorophores. Hence, Manders coefficients M1 and M2 are pixel intensities, auto-corrected for background, and describe the intercept of both fluorophores divided by either fluorophore 1 or fluorophore 2 whereby

$$M_x = \frac{\sum_{i=1}^{n} N_{i,coloc}}{\sum_{i=1}^{n} N_i}$$

(Manders et al., 1993; Stauffer et al., 2018) (See Supplementary figure 1 for details). For our experiments, M1 was consistently used to denote the organelle/cellular stains, while M2 and M3 represented the oestrogen receptor antibodies, as denoted in the legends.

For ratio analyses of the distribution of target antigen between two organelles, organelle stains (Table 2.2) were used to identify the region of interest (ROI) in Fiji (NIH Image). The organelle outlines were overlaid on the channel containing the antigen of interest and mean intensity of the fluorescence signal in the nucleus, endoplasmic reticulum, Golgi apparatus and plasma membrane measured. For mES cells, between 45-50 cells were analysed for each target antigen localised at a particular site. For differentiated neurons (mESn), at least 20 neurons from each stage i.e. D7, D14, D21 – positive for a neuronal marker (NeuN or bIII-tubulin) - were analysed for each target antigen or at a particular subcellular site.

2.6 Statistical Analysis

Neurons were analysed separately at different stages as D7, D14 and D21 and if there were no significant differences between days of differentiation i.e., D7, D14 or D21, neurons were combined across stages, for ease of comparison to mES cells. All data are presented as mean ± SEM with graphs and statistics performed using Prism 9.0 (Graph Pad Software, CA, USA); numbers within columns or above columns refer to the number of cells analysed for each target antigen at a particular cellular location. Two-way ANOVA followed by either Sidak's or Tukey's post-hoc tests were used to compare between groups in experiments examining localisation of each ER within different organelles and for ratio analyses (Figure 2.4). For colocalisation of different ERs with each other in various organelles, differences between colocalisation in selected organelles was examined using Kruskal Wallis non-parametric test followed by the Dunn's posthoc test, since data was not normally distributed. In all cases, $p<0.05$ deemed statistically significant. Manders correlation coefficients ^{3} 0.5 were considered localised (Manders et al., 1993). Determination if colocalisation was statistically different ($p<0.05$) from this threshold value was carried out using one sample t test and Wilcoxon's test.

2.6 Results

2.6.1 Increase of ERα localisation in the nucleus and plasma membrane in mES-derived neurons (mESn)

compared to mES cells.

Since most studies have characterized ERα-66 as a nuclear receptor with small traces being found in the cytoplasm and plasma membrane (reviewed in (Rainville et al., 2015)), we first decided to determine the localisation of ERα in mES cells and mESn (Figures 2.1A-D), before proceeding to ERα-36 (Figure 2.2A-D) and GPER1 (Figure 2.3A-D). For the purposes of these experiments, the M1 overlap coefficient is better suited to understand the localisation of the target antigen within each cellular compartment, since this denotes the level of antigen in that compartment.

ERα-66 localises differentially in mES and mES derived neurons. Analysis of nuclear and membrane localisation revealed a significant increase in colocalisation in mESn in both these compartments compared to mES cells (Figure 2.1A and 2.1C). There are also higher levels of ERα-66 colocalisation in the plasma membrane of D21 mESn compared to D7 mESn (Figure 1A; $F(5,757)=87.14$; $p<0.0001$). Previous studies have localized minor amounts of ERα in the endoplasmic reticulum (Kelly & Levin, 2001), but to date no study has quantified ERα in the Golgi apparatus. Results reveal high localisation of the ERα-66 in both the endoplasmic reticulum and Golgi apparatus across both cell types. Though there are minor differences between mES and mESn in endoplasmic reticulum localisation of ERα-66 (Figure 2.1B and D),

there is a decrease in localisation of ERα in the Golgi apparatus in neurons at the Day 14 stage (Figure 2.1B; $F(7,760)=40.73$, $p<0.0001$ and 1D).

2.6.2 The localisation of ERα-36 and GPER1 in subcellular compartments is similar in mES and mESn cells

Both ERα-36 and GPER1 are localised in the nucleus in mES and mESn (Figure 2.2A and C for ERα-36; Figure 2.3A and C for GPER1) to a similar extent. For both these receptors, there is a transient increase in localisation in the plasma membrane from mES, where there is no appreciable localisation, to D7-mESn. However, as differentiation of neurons proceeds, there is a decrease in plasma membrane localisation of both ERα-36 and GPER1 to levels similar to those found in mES cells (Figure 2.2A; $F(7,658)=17.30$, $p<0.0001$ and 3A; $F(5,683)=17.22$, $p<0.0001$). Though there are no differences in localisation of either of these receptors in the endoplasmic reticulum between mES and mESn, there is a decrease in localisation of these receptors in the Golgi apparatus as neuronal differentiation proceeds (Figure 2.2B; $F(5,776)=38.95$,$p<0.0001$ and 2D for ERa-36 and 3B; $F(5,762)=41.38$, $p<0.0001$ and 3D for GPER1)

The relative levels of the oestrogen receptors between the nucleus and the other organelles (plasma membrane, endoplasmic reticulum, Golgi apparatus) is shown in Figure 2.4A-C. As can be seen, there are higher relative levels of all the oestrogen receptors in the nucleus as compared to the endoplasmic reticulum (Figure 2.4A; $F(1,570)=2043$, $p<0.0001$). Though there are higher levels of ERα-66 in the nucleus compared to the ERa-66 in the Golgi apparatus in both mES and mESn cells (Figure 2.4B; $F(1,571)=619.9$, $p<0.0001$), there are lower levels of ERα-36 and GPER1 in the nucleus compared to the Golgi apparatus of mESn cells compared to mES cells (Figure 2.4B). As differentiation proceeds, the level of ERs in the nucleus decrease, as they rise in the endoplasmic reticulum and the Golgi apparatus. However, levels of ERα-66, ERα-36 or GPER-1 are roughly equally distributed between nucleus and plasma membrane in mES cells and this does not change in mESn for either ERα or GPER1 (Figure 2.4C; $F(1,286)=6.242$, $p=0.0130$). For ERα-36, there is more protein at the plasma membrane in mESn than in mES cells, compared to levels in the nucleus (Figure 2.4C).

2.6.3 Though oestrogen receptors are present in the same organelle they are differentially distributed in mES and mESn

Our data so far reveals localisation of oestrogen receptors in all four subcellular compartments i.e. nucleus, endoplasmic reticulum, plasma membrane and Golgi apparatus. Do these receptors

colocalise with each other? There is low colocalisation (<0.5) of ERα and the variant ERα-36 or ERα and GPER1 within mES cells, independent of compartment (Figure 2.5A and B; Supplementary data 1A) To evaluate this, we used heat maps to observe differential distribution of these receptors within an organelle (Figure 2.5C and 2.5D). Similar patterns were observed in the mESn where there was no colocalisation in nucleus or plasma membrane (Figure 2.6A; Supplementary data 1B and 6C) or endoplasmic reticulum or Golgi apparatus (Figure 6B; Supplementary data 1B and 6D) for ERα/ERα-36 or ERα/GPER1. We next investigated the colocalisation of the two membrane ERs i.e., ERα-36 with GPER1. Independent of organelle, there was very little colocalisation of these two receptors in either mES (Figure 2.7A, B and C) or mESn (Figure 2.7A, B and D). Therefore, despite the presence of these oestrogen receptors capable of rapid non-genomic signalling in each organelle, they appear to occupy distinct spaces within the organelle, independent of neuronal development.

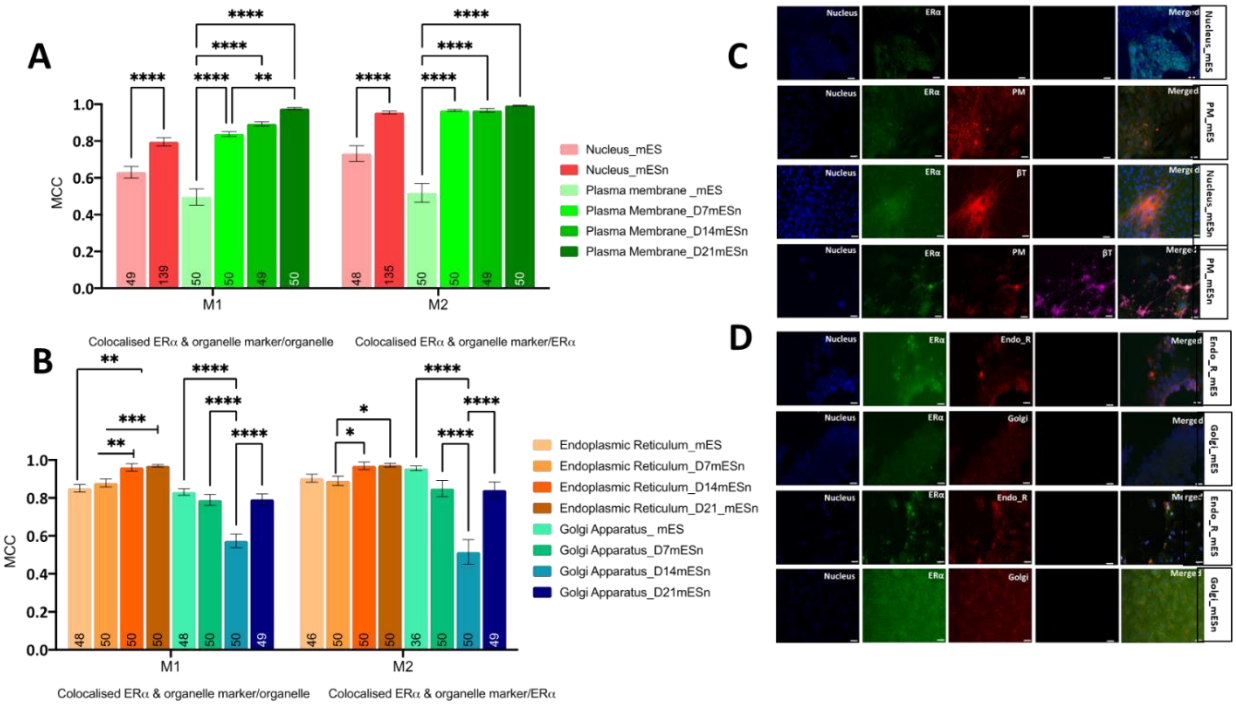

Figure 2.1. Subcellular localisation of ERα in mES and mESn. Quantification of ERα-66 in various organelles was carried out using image analyses using EZcoloc plugin (Fiji, NIH Image) to obtain Manders Correlation Coefficient (MCC) presented as M1 and M2 (Details in methods). MCC values ranging from 0 to 1 represent no colocalisation (0) or complete colocalisation with 0.5 as the threshold for colocalisation (Supplementary Figure 1). A two-way ANOVA followed by Tukey's posthoc comparison compares between groups (A) Comparison of localisation of ERα in the nucleus and plasma membrane of mES and mESn. (B) Comparison of localisation of

ERα in the endoplasmic reticulum and Golgi apparatus of mES and mESn. Data is presented as the mean ± SEM. (n = 36-48 mES, n=49-139 mESn); number of analysed cells inside each bar. (C) Representative images (20x objective) of ERα (green), nuclear DAPI stain (blue), plasma membrane (red) in mES cells (first two rows). The third and fourth row show ERα (green), nuclear stain (blue), plasma membrane (red) and neuronal markers β-tubulin (red or far red) in Day 14 mESn. (D) Representative images (20x objective) of ERα (green), nuclear DAPI stain (blue), endoplasmic reticulum or Golgi apparatus (red) in mES cells (first two rows). The third and fourth row show ERα (green), NeuN staining indicating neurons (blue), endoplasmic reticulum or Golgi apparatus (red) in Day 14 mESn. Scale bar, 100 µm. *:p<0.05, **:p<0.01; ***: p<0.001; **** P ≤ 0.0001, Abbreviations: PM: Plasma membrane; EndoR: Endoplasmic reticulum; Golgi: Golgi apparatus; bT: bIII-tubulin.

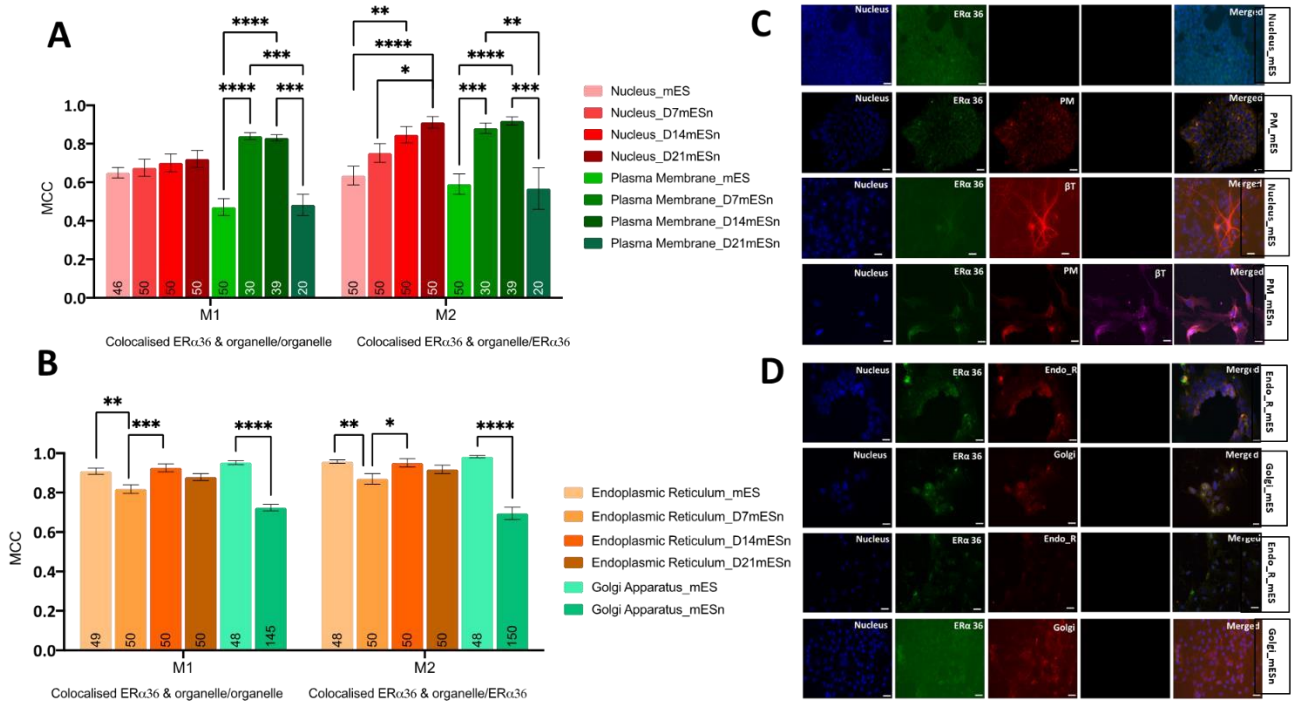

Figure 2.2. Subcellular localisation of ERα-36 in mES and mESn. Quantification of ERα-36 in various organelles was carried out using image analyses using EZcoloc plugin (Fiji, NIH Image) to obtain Manders Correlation Coefficient (MCC) presented as M1 and M2 (Details in methods). MCC values ranging from 0 to 1 represent no colocalisation (0) or complete colocalisation with 0.5 as the threshold for colocalisation (Supplementary Figure 1). A two-way ANOVA followed by Tukey's posthoc comparison compares between groups. (A) Comparison of localisation of ERα-36 in the nucleus and plasma membrane of mES and mESn. (B) Comparison of localisation of ERα-36 in the endoplasmic reticulum and Golgi apparatus of mES and mESn. Data is presented as the mean ± SEM. (n = 46-50 mES, n=20-150 mESn); number of analysed cells is within each bar (C) Representative images (20x objective) of ERα-36 (green), nuclear DAPI stain (blue), plasma membrane (red) in mES cells (first two rows). The third and fourth row show ERα-36 (green), nuclear stain (blue), plasma membrane (red) and neuronal markers β- tubulin (red or far red) in Day 14 mESn. (D) Representative images (20x

objective) of ERα-36 (green), nuclear DAPI stain (blue), endoplasmic reticulum or Golgi apparatus (red) in mES cells (first two rows). The third and fourth row show ERα-36 (green), NeuN staining indicating neurons (blue), endoplasmic reticulum or Golgi apparatus (red) in Day 14 mESn. Scale bar, 100 µm. *:p<0.05, **:p<0.01; ***: p<0.001;**** P ≤ 0.0001. Abbreviations: PM: Plasma membrane; EndoR: Endoplasmic reticulum; Golgi: Golgi apparatus; bT: bIII-tubulin.

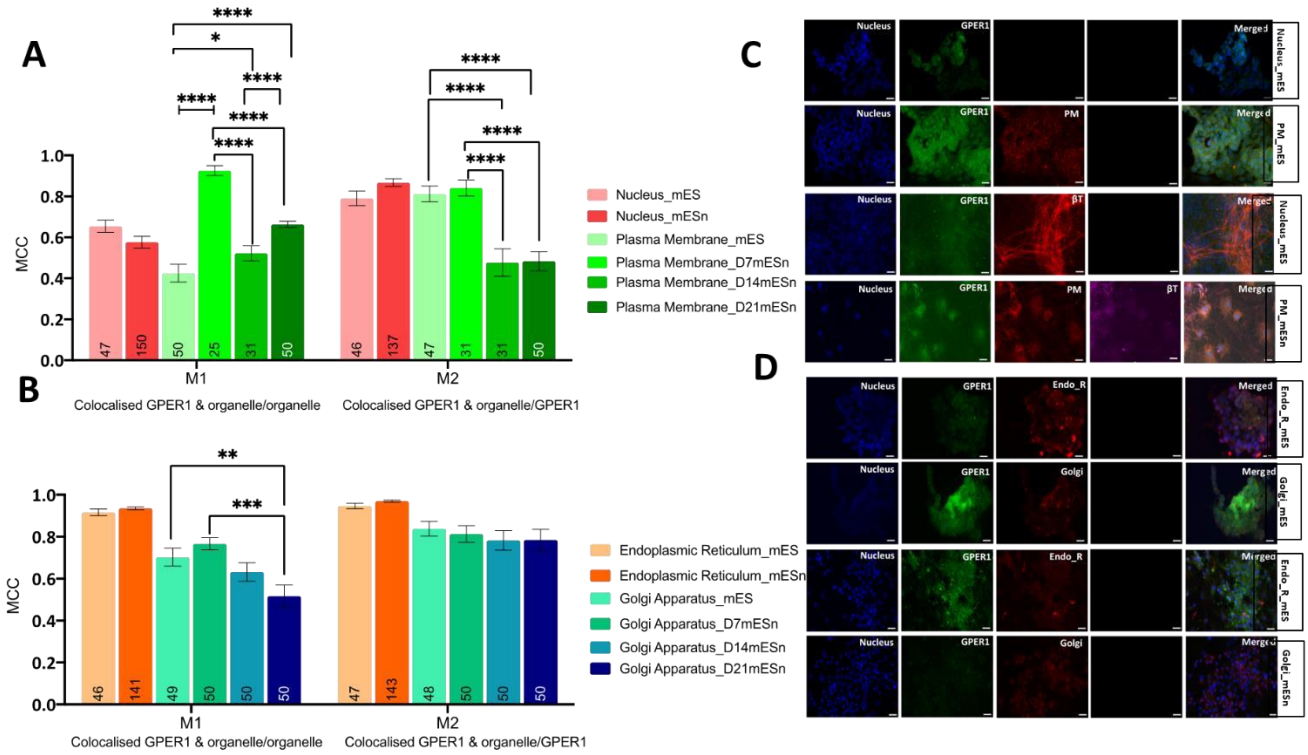

Figure 2.3. Subcellular localisation of GPER1 in mES and mESn. Quantification of GPER1 in various organelles was carried out using image analyses using EZcoloc plugin (Fiji, NIH Image) to obtain Manders Correlation Coefficient (MCC) presented as M1 and M2 (Details in methods). MCC values ranging from 0 to 1 represent no colocalisation (0) or complete colocalisatio with 0.5 as the threshold for colocalisation (Supplementary Figure 1). A two-way ANOVA followed by Tukey's posthoc comparison compares between groups. (A) Comparison of localisation of GPER1 in the nucleus and plasma membrane of mES and mESn. (B) Comparison of localisation of GPER1 in the endoplasmic reticulum and Golgi apparatus of mES and mESn. Data is presented as the mean ± SEM. (n = 46-50 mES, n=31-150 mESn); number of analysed cells is within each bar. (C) Representative images (20x objective) of GPER1 (green), nuclear DAPI stain (blue), plasma membrane (red) in mES cells (first two rows). The third and fourth row show GPER1 (green), nuclear stain (blue), plasma membrane (red) and neuronal markers β- tubulin (red or far red) in Day 14 mESn. (D) Representative images (20x objective) of GPER1 (green), nuclear DAPI stain (blue), endoplasmic reticulum or Golgi apparatus (red) in mES cells (first two rows). The third and fourth row show GPER1 (green),
NeuN staining indicating neurons (blue), endoplasmic reticulum or Golgi apparatus (red) in Day 14 mESn. Scale bar, 100 µm. *:p<0.05, **:p<0.01; ***: p<0.001;**** P ≤ 0.0001. Abbreviations: PM: Plasma membrane; EndoR: Endoplasmic reticulum; Golgi: Golgi apparatus; bT: bIII-tubulin.

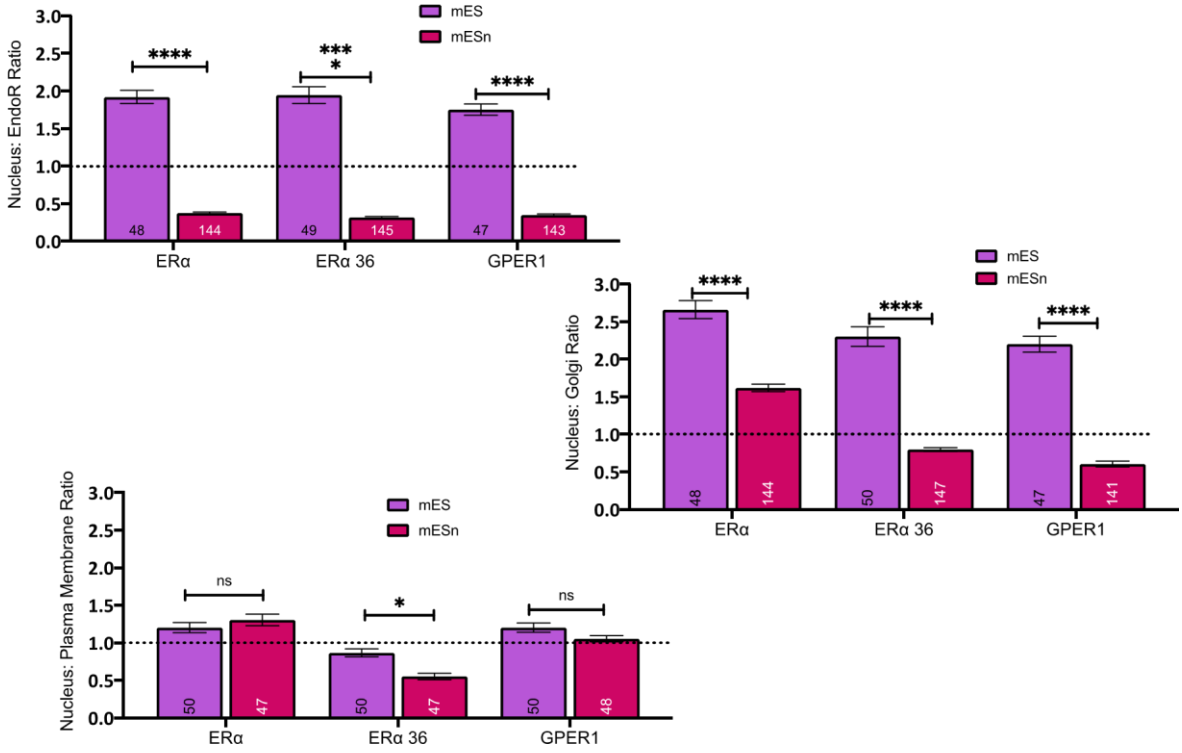

Figure 2.4. The distribution of oestrogen receptors in mES and mESn cells. (A) The distribution of ERα-66, ERα-36 and GPER1 in the nucl3.eus vs. the endoplasmic reticulum is shown by the Nuclear: Endoplasmic reticulum ratio in mES cells compared to mESn cells. (B) Similarly, the distribution of ERα-66, ERα-36 and GPER1 in the nucleus vs. the Golgi apparatus is shown by the Nuclear: Golgi apparatus ratio in mES cells compared to mESn cells. (C) The distribution of ERα-66, ERα-36 and GPER1 in the nucleus vs. the plasma membrane is shown by the Nuclear: plasma membrane ratio in mES cells compared to mESn cells. For A) and B), mESn represents data, combined from all stages of neuronal differentiation while for C), mESn represents data from Day 7 differentiated neurons only. *:$p<0.05$; **** $P \leq 0.0001$. No of analysed cells are given within each bar. Two-way ANOVA followed by Sidak's multiple comparison test compares between groups.

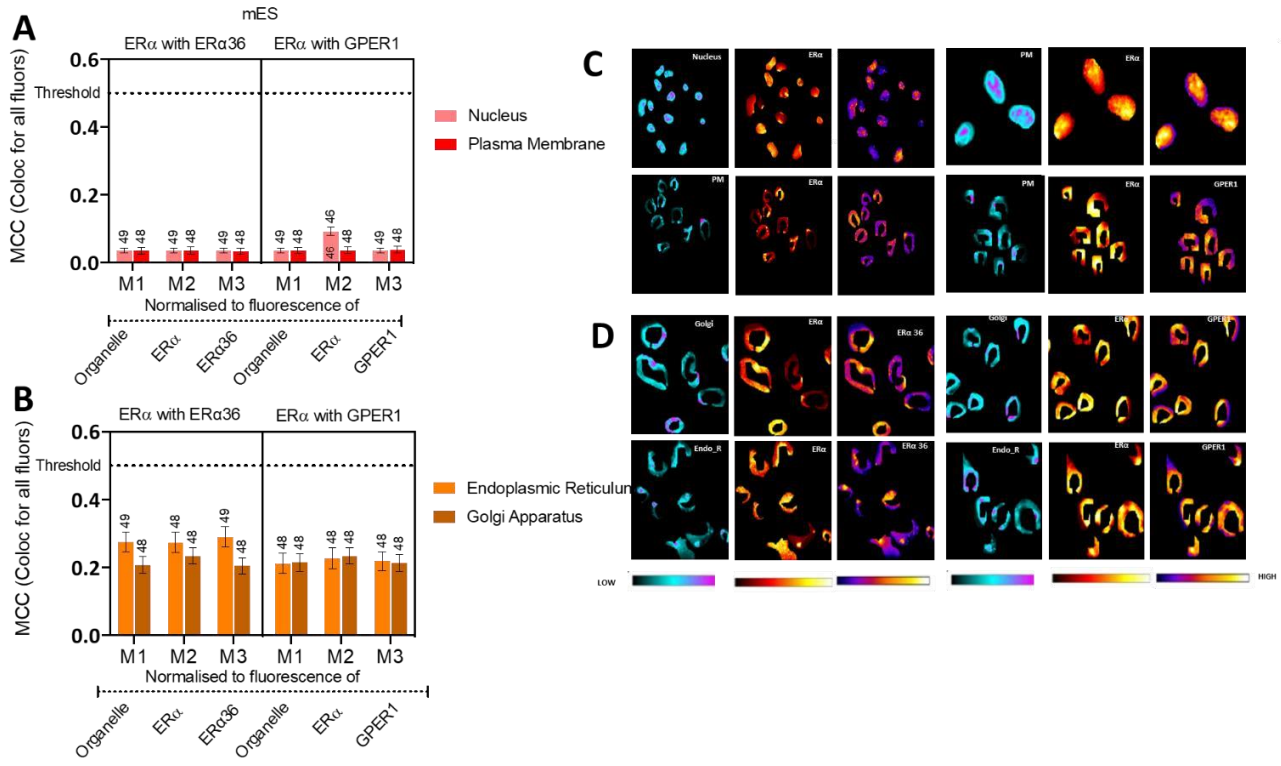

Figure 2.5. Colocalisation of ERα-66 with ERα-36 and GPER1 in mES cells. Quantification of colocalisation between ERα66 and each of the other oestrogen receptors i.e., ERα-36 and GPER1 was carried out using Manders Correlation Coefficient (MCC) presented as M1, M2, and M3, whereby M1 values represent intersection of all fluorophores in the organelle, M2 values represent the intersection of all fluorophores in ERα-positive pixels and M3 represent the intersection of all fluorophores in either ERα 36 or GPER1-positive pixels. MCC values ranging from 0 to 1 represent no colocalisation (0) or complete colocalisation with 0.5 as the threshold for colocalisation (Supplementary Figure 1). (A) Comparison of colocalisation of ERα36 (left) and GPER1 (right) with ERα-66 in the nucleus and plasma membrane of mES. (B) Comparison of colocalisation comparison of ERα-36 (left) and GPER1(right) with ERα-66 in the Golgi apparatus and endoplasmic reticulum of mES. Data is presented as the mean ± SEM. (C) Heatmaps of ERα-36 (left) and GPER1 (right) quantifying the amount of each antigen in nucleus (first row) and plasma membrane (second row). (D) Heatmaps of ERα-36 (left) and GPER1 (right) quantifying the amount of each antigen in the endoplasmic reticulum and Golgi apparatus. All MCC values are significantly below 0.5 MCC (dotted line; Supplementary data 1A). Abbreviations: PM: Plasma membrane; EndoR: Endoplasmic reticulum; Golgi: Golgi apparatus. The number of cells analysed is given above each bar.

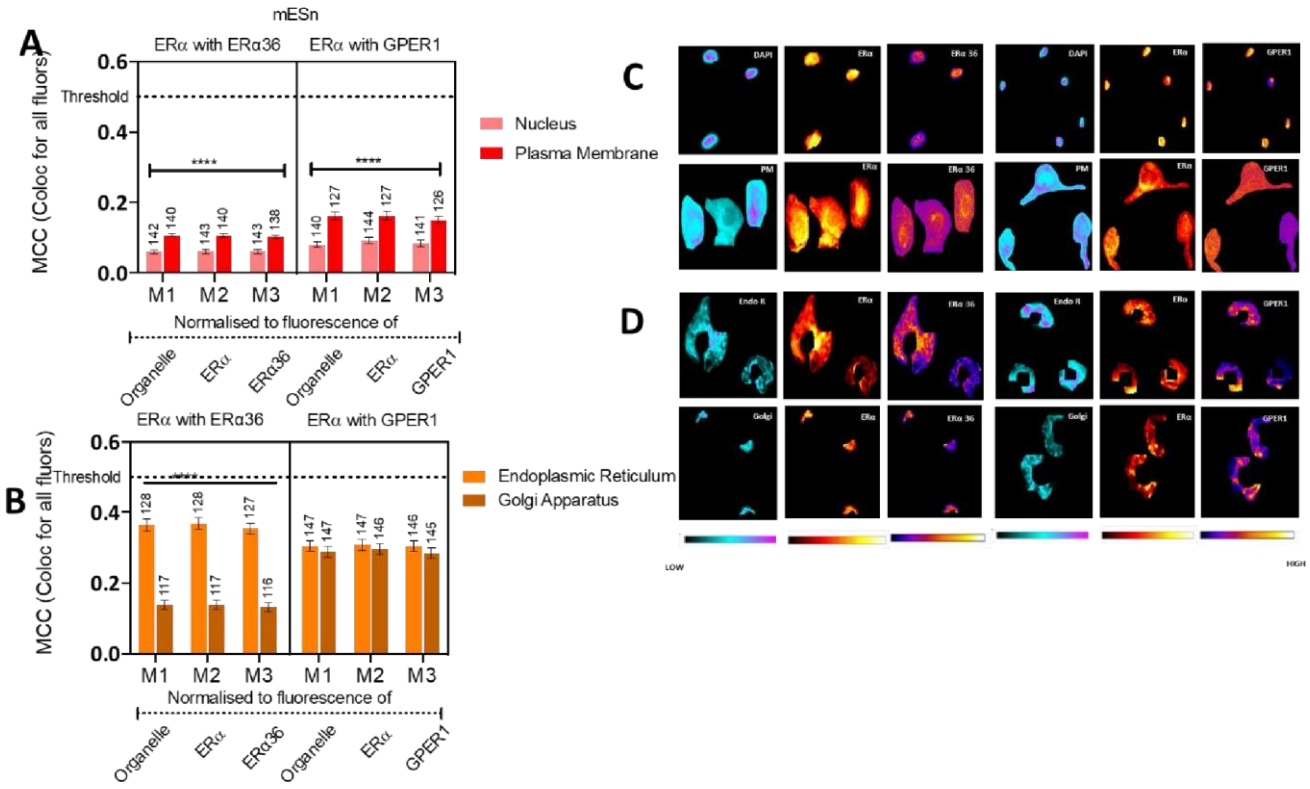

Figure 2.6. Colocalisation of ERα-66 with ERα 36 and GPER1 in neurons derived from mES cells (mESn). Quantification of colocalisation between ERα-66 and each of the other oestrogen receptors i.e., ERα-36 and GPER1 was carried out using Manders Correlation Coefficient (MCC) presented as M1, M2, and M3, whereby M1 values represent intersection of all fluorophores in the organelle, M2 values represent the intersection of all fluorophores in ERα-positive pixels and M3 represent the intersection of all fluorophores in either ERα 36 or GPER1-positive pixels. MCC values ranging from 0 to 1 represent no colocalisation (0) or complete colocalisation with 0.5 as the threshold for colocalisation (Supplementary Figure 1). (A) Comparison of colocalisation of ERα-36 (left) and GPER1 (right) with ERα-66 in the nucleus and plasma membrane of mESn. (B) Comparison of colocalisation comparison of ERα-36 (left) and GPER1(right) with ERα-66 in the Golgi apparatus and endoplasmic reticulum of mES. Data is presented as the mean ± SEM. (C) Heatmaps of ERα-36 (left) and GPER1 (right) quantifying the amount of each antigen in nucleus (first row) and plasma membrane (second row). (D) Heatmaps of ERα-36 (left) and GPER1 (right) quantifying the amount of each antigen in the endoplasmic reticulum and Golgi apparatus. Day 14 neurons are shown in (C) and (D). **** $P \leq 0.0001$, cf the other organelle in the same MCC group using non parametric Kruskal Wallis test followed by Dunn's posthoc comparison between groups. For ERα colocalised with ERα-36, the Kruskal Wallis test shows a statistically different median between colocalisation in the nucleus versus the membrane ($H(5)=148.7$, $p<0.0001$) and between the endoplasmic reticulum and the Golgi apparatus ($H(5)=251.2$, $p<0.0001$). For ERα colocalised with GPER1, the Kruskal Wallis test shows a statistically different median between colocalisation in the nucleus versus the membrane ($H(5)=123.5$, $p<0.0001$). All MCC values are significantly below 0.5 MCC, the threshold for colocalisation (dotted line; Supplementary data 1B). Abbreviations: PM: Plasma membrane; EndoR: Endoplasmic reticulum; Golgi: Golgi apparatus. The number of cells analysed is given above each bar.

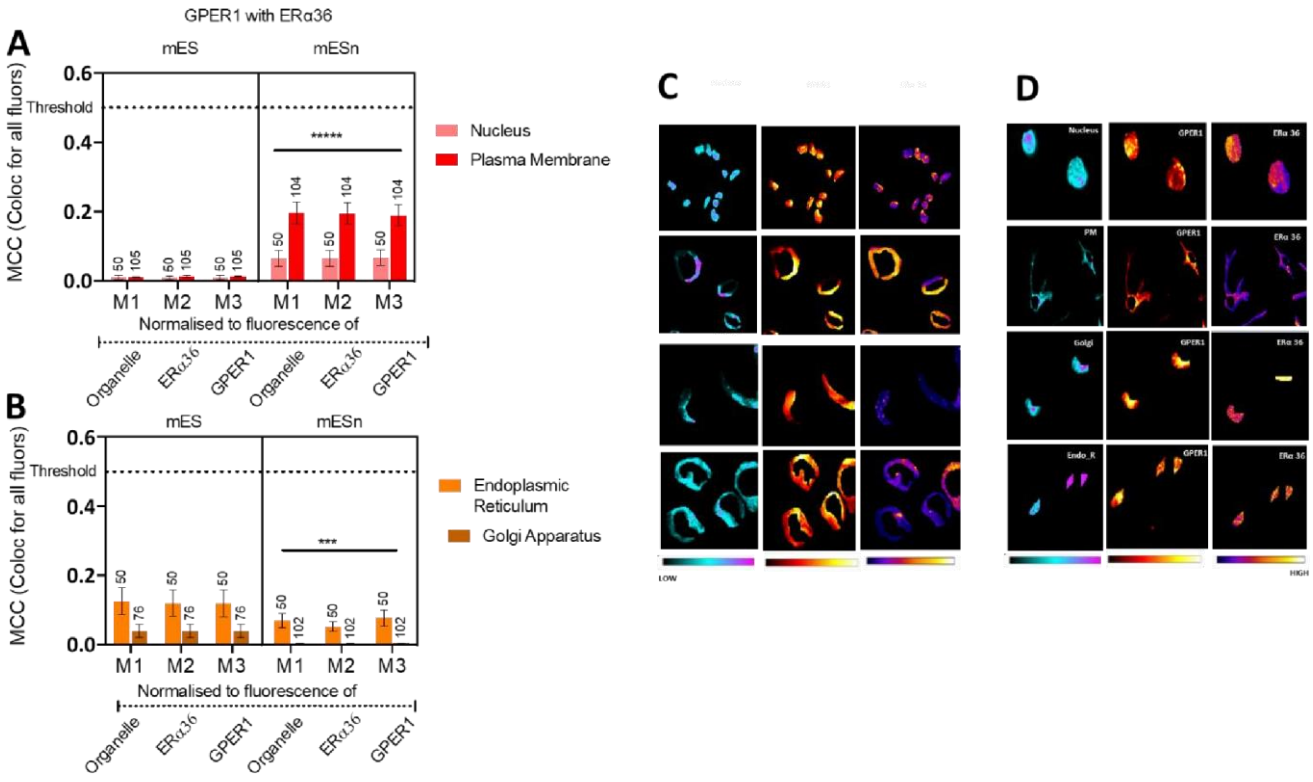

Figure 2.7. Colocalisation of ERα-36 with GPER1 in mES and neurons derived from mES (mESn). Quantification of colocalisation between ERα-36 and GPER1 was carried out using Manders Correlation Coefficient (MCC) presented as M1, M2, and M3, whereby M1 values represent intersection of all fluorophores in the organelle, M2 values represent the intersection of all fluorophores in GPER1-positive pixels and M3 represent the intersection of all fluorophores in ERα-36-positive pixels. MCC values ranging from 0 to 1 represent no colocalisation (0) or complete colocalisation with 0.5 as the threshold for colocalisation (Supplementary Figure 1). (A) Colocalisation of ERα-36 and GPER1 in the nucleus and plasma membrane of mES (left panel) and mESn (right panel). (B) Colocalisation of ERα-36 and GPER1 in the Golgi apparatus and endoplasmic reticulum of mES (left panel) and mESn (right panel) (C) Heatmaps of ERα-36 and GPER1 quantifying the amount of each antigen in nucleus and plasma membrane (first two rows) and in Golgi apparatus (3rd row) and endoplasmic reticulum (4th row) in stem cells (mES). (D) Heatmaps of ERα-36 and GPER1 quantifying the amount of each antigen in nucleus and plasma membrane (first two rows) and in Golgi apparatus (3rd row) and endoplasmic reticulum (4th row) in neurons derived from mES cells (mESn). ****: $p<0.001$ cf the other organelle in the same MCC group using non-parametric Kruskal Wallis tests followed by Dunn's posthoc test. For ERα-36 and GPER1 colocalised in mES cells, there is no statistically significant difference in colocalisation between nucleus and plasma membrane as determined by posthoc tests ($H(5)=12.21$; $p=0.0320$). For ERα-36 and GPER1 in mESn cells, there is significantly increased colocalisation in plasma membrane than in nucleus ($H(5)=150.8$; $p<0.0001$). For ERα36 and GPER1 in mESn cells, there is significantly more colocalisation in the endoplasmic reticulum than the Golgi apparatus ($H(5)=50.09$; $p<0.0001$). All values are significantly below the threshold of 0.5 MCC (dotted line; Supplementary data 1C). Abbreviations: PM: Plasma membrane; EndoR: Endoplasmic reticulum; Golgi: Golgi apparatus. The number of cells analysed is given above each bar.

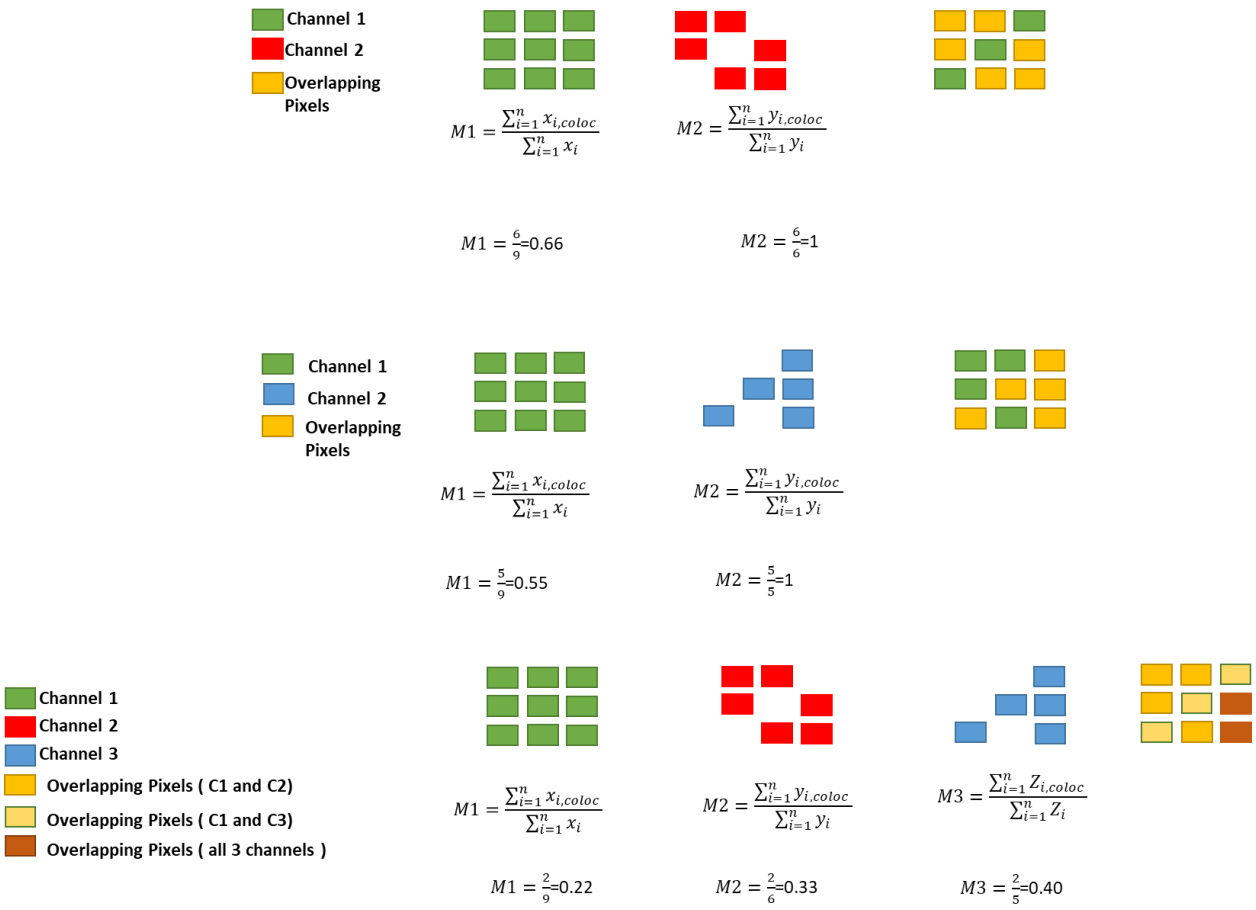

Supplementary Figure 1: An example workflow showing the intercept of different fluorophores (red, green, blue) and how colocalisation of these leads to the calculation of Manders Correlation Coefficients (M1, M2 or M3). For M3, the overlapping pixels for all three fluorophores is used as the numerator (C). In Figures 1-3, we sought to determine if ERs were present in different organelles. M1 always denoted the organelle stain while M2 denoted the specific oestrogen receptor antibody (ERα-66, GPER1 and ERα-36). Supplementary Figure 1A is an example of these type of experiments If we wanted to determine if ERα was at the membrane, M1 would represent all overlapping pixels for the membrane stain and ERα as the numerator divided by the denominator i.e. all pixels of the membrane stain. M2, on the other hand, would represent all overlapping pixels for the membrane stain and ERα as the numerator divided by all the pixels of ERα. If every pixel stained by the membrane stain also stained for ERα, M1 would be 1 and would represent complete colocalisation. If no pixel stained by the membrane stain overlapped with ERα staining, the numerator would be 0 and M1 would be zero.

2.7 Discussion

In the present study, we used two cell types, the mouse embryonic stem cells (mES) CGR8 and differentiated neurons, both of which express ERα-66, ERα-36 and GPER1.

Our data reveal three findings – namely (1) ERα-66 localisation in both nucleus and membrane increases as neuronal maturation proceeds (2) GPER1 and ERα-36 localise similarly -i.e. in the nucleus and endoplasmic reticulum independent of stem cell or neuronal status with transient increases in the plasma membrane and decreases in the Golgi apparatus as neuronal maturation proceeds (3) ERα-66, ERα-36 and GPER1 are not colocalized with each other in any subcellular compartment despite the presence of all receptors in these compartments. Finally, for the first time we identify and characterise ERα-36 localisation in mES derived neurons in four subcellular compartments visualised i.e., the nucleus, plasma membrane, endoplasmic reticulum and Golgi apparatus.

2.7.1 The presence of ERα-66 and mERs in stem cells

One of our objectives was to provide a model neuronal system for the study of oestrogen receptor signalling, in particular for rapid, non-genomic signalling. We used the CGR8 mES cell line, which does not require a feeder layer to sustain pluripotency. Instead, stemness is maintained with the addition of LIF in the media. With this protocol, we generated bIII-tubulin positive cells by D7 (13 days total). This is one of the fastest and simplest methods for neural differentiation available since unlike other methods, we do not need to seed the generated EBs on adherent plates or harvest neural rosettes, which are additional complex steps often used (Shparberg et al., 2019). A similar technique to ours has been employed recently by Hanafiah *et al.* to obtain NPCs by Day 8 and neurons by Day 12, as demonstrated via the expression of nestin and neurofilament markers (Hanafiah et al., 2020). In our protocol, we obtain NPCs by Day 6 and supplement BDNF and βFGF in the neuronal media to ensure neuronal maturation over the following 3 weeks. Though the three selected timepoints for neuronal characterization (D7, D14 and D21) do not correspond to any specific embryonic or postnatal developmental stage, in the vast majority of neuronal studies that contain a developmental element, characterization is carried out within this timeframe (Gu et al., 2016) (Albers & Offenhäusser, 2016);(Murray & Delivopoulos, 2021);(Delivopoulos & Murray, 2011)

Our data clearly show the presence of all receptors in the mES and in neurons derived from mES. Human ES and embryoid bodies express both ERα-66 and ERβ(Hong et al., 2004); however, ERβ is not reliably detectable with currently available antibodies and hence not assayed in this study (M. A. Snyder et al., 2010). GPER1 has been recently shown to be

expressed by neural stem cells in the rat embryo (Zhang et al., 2019) but to the best of our knowledge, neither GPER1 or ERα-36 has not been demonstrated in the mES. Furthermore, no previous study has shown the subcellular localisation of these receptors within mES, or neurons derived from stem cells (Section 2.8).

2.8 Subcellular localisation of the ERα, GPER1 and ERα-36 in mES or in neurons derived from mES

2.8.1 Localisation at the ERs in the plasma membrane

Our study shows that only ERα-66 is reliably present in the plasma membrane of mES. In mES, a membrane limited conjugate E2-BSA increases cell motility and F-actin in a Src-EGFR dependent manner, suggesting that rapid signalling from the membrane has functional relevance, though the receptor mediating this was not identified (Yun et al., 2012). Our data suggests that this is most likely ERα. In a hypothalamic cell line, mHypo-38 (Dominguez et al., 2013) and in neurons (Dominguez & Micevych, 2010) and astrocytes (Bondar et al., 2009), ERα-66 levels at the plasma membrane are increased by 17b-oestradiol, rapidly within 30 minutes. This shows that this full-length ERα-66 can be targeted to the plasma membrane in neurons. Similarly, though there is low localisation of GPER1 and ERα-36 (MCC<0.5) in the plasma membrane of mES, plasma membrane localisation increases for all oestrogen receptors as neuronal maturation proceeds, suggesting that GPER1 and ERα-36 can also be tethered to the membrane. In SKBR3 breast cancer (L. Kang et al., 2010) and HEK cells (Wang et al., 2006), around 50% of the ERα-36 is at the membrane where it increases ERK signalling rapidly similar to GPER1-induced EGFR-dependent ERK signalling (E. J. Filardo et al., 2000); tethering at the membrane thus may provide an opportunity to access growth factor receptors. Rapid signalling by ERK due to activation of growth factors is linked to maturation of neurons from stem cells (Tzeng et al., 2015) (Yin et al., 2014) and it is possible that increased plasma localisation during neuronal maturation for the classical ERα-66 as well as the mERs in this study may result in increased non-genomic signalling by crosstalk with growth factor receptors.

2.8.2 Localisation of the ERs in the nucleus

Our results also show that though all oestrogen receptors are present in the nucleus, ERα-66 uniquely amongst the three oestrogen receptors increases its localisation in the nucleus, as maturation proceeds. 40% of the ERα-36 variant has been shown in the nucleus in HEK cells, where it can act as a dominant negative mutant and decrease transcriptional activation by ERα-66 from a luciferase reporter (Wang et al., 2006). Since nuclear ERα-66 increase but levels of nuclear ERα-36 and GPER1 remain the same as neurons differentiate, it is possible that transcriptional signalling by ERα-66 increases as neuronal maturation proceeds. However, it is

important to note that despite high localisation of every oestrogen receptor in the endoplasmic reticulum, nucleus and Golgi apparatus in mES cells, the distribution of all oestrogen receptors appears to be nucleus-biased (Figure 2.4) and may reflect studies that show that global transcriptional activity is higher in stem cells than in differentiated cells (Efroni et al., 2008);(Turner, 2008).

In breast cancer cells, the majority of GPER1 appears to be intracellular with minor amounts on the cell membrane (Filardo et al., 2007); in COS cells, it is primarily seen in the endoplasmic reticulum where it mediates calcium release in response to oestrogen (C. M. Revankar et al., 2005). The distribution of GPER1 in mES cells where it appears to show significant nuclear localisation is unusual but not unreported. Also, other G-protein coupled receptors such as muscarinic acetylcholine receptors (Lind & Cavanagh, 1993), adrenergic receptors (Buu et al., 1993) and endothelin receptors (Boivin et al., 2003) can localise in the nucleus in multiple cell lines across various species (Bhosle et al., 2019);(Boivin et al., 2008) and nuclear translocation of GPER1 with a single nucleotide polymorphism (SNP) in cancer associated fibroblasts increases the migration of neighbouring cells (Madeo & Maggiolini, 2010);(Pupo et al., 2013). Though deglycosylation of this mutant GPER1 increases GPER1 binding to chromatin and transcription from the *c-fos* promoter (Pupo et al., 2013), the function of wildtype GPER1 in the nucleus and perinuclear compartments (Cheng, Graeber, et al., 2011) remains elusive.

Our data show that ERα-66 and GPER1 are equally distributed between the nucleus and plasma membrane in mES cells or in differentiated neurons, suggesting that both non-genomic and genomic signalling occur. Our data also suggest that as neuronal differentiation proceeds, ERα-66 is the dominant player driving transcription in the nucleus, but all oestrogen receptors decrease their nuclear localisation and redistribute to the other cellular compartments such as the plasma membrane to possibly increase non-genomic signalling. In support, ERα-36 distribution shows a decrease in nuclear localisation and movement towards the membrane (Figure 2.4C).

2.9 There is no colocalisation amongst receptors in any subcellular compartment

The heatmap distribution (Figures 2.5-2.7) shows that despite the presence of ERα-66, ERα-36 and GPER1 in all cellular compartments studied, they do not colocalise, with MCC values in the range of 0 to 0.3. What are the reasons for this further spatial organisation into microdomains? Functional microdomain organisation of receptors into caveolae has been suggested by the interaction of full-length ERα with different caveolin isoforms. For e.g., CAV1 allows ERα to couple to Ga_q via mGluR5 in the striatum but via mGluR1A in the arcuate

hypothalamus and hippocampus, to activate ERK signalling. However, in the dorsal root ganglion, ERα coupling to CAV3 may allow for interaction with mGluR2/3 to activate Ga_i and subsequent reduction in PKA signalling (Meitzen & Mermelstein, 2011). Though GPER1 coupling to caveolin has not been shown in the CNS, this separation into microdomains could allow ERα-66 or ERα-36, where colocalisation with caveolin is seen in Hec1 cells (Lin et al., 2010), to activate Gα proteins.

Our previous review (Hadjimarkou & Vasudevan, 2018) suggested several scenarios in which GPER1 could interact with ERα-66, with the focus on GPER1 being a "collaborator" (Levin, 2009a). One scenario is to increase the level of a convergent output by using two different signalling pathways and separating these receptors into microdomains within these subcellular compartments may allow for access to these different pathways. For example, calcium increase in COS cells is mediated by both ERα-66 and GPER1 in response to oestrogen but ERα-66 uses a PLC-dependent mechanism whereas GPER1 uses a EGFR-mediated mechanism (C. M. Revankar et al., 2005). Hence, calcium increases are large in this cell line and are due to both receptors acting via spatially distinct pathways in an additive manner. In the cortex, where ERα-66 and IGFR interaction mediates neuroprotection via inhibition of GSKβ (Garcia-Segura et al., 2007; Sohrabji, 2015), GPER1 achieves neuroprotection via activation of death activated protein kinase 1 (DAPK1) (Liu et al., 2012), suggesting again that various signalling pathways could be used by differently located oestrogen receptors to facilitate a common cellular endpoint (R. Vajaria & N. Vasudevan, 2018). Spatial separation within subcellular compartments may also be a way to achieve either independent outputs or sequential activation from each receptor. For example, mGluR1-mediated long-term depression (LTD) and synapse silencing by oestrogen in the hippocampal CA3 is via GPER1, independent of ERα and ERβ though all these receptors are expressed in this region (Briz et al., 2015). Coupled signalling where activation of one receptor leads to the regulation of the other may also be a consequence of unique compartmentalisation. For example, priming of lordosis or female sex behaviour by GPER1, acting as a "gain amplifier" at a cytoplasmic location may be coupled to ERα-mediated activation of transcription in the nucleus by an intervening signal transduction cascade (Anchan et al., 2014; R. Vajaria & N. Vasudevan, 2018). Though GPER1 and ERα-36 are implicated predominantly in non-genomic signalling, they are not colocalised in either mES or mESn. Both receptors bind a plethora of ligands, including some aromatic plant compounds (GPER1) (R. Vajaria & N. Vasudevan, 2018),17a-oestradiol, estriol, estrone (ERα-36) (Wang et al., 2015), with a wider spectrum of ligand specificity than full length ERα and spatial separation in the same organelle may also be a way to allow for discrete access to different ligands.

2.10 Summary

Most studies in this field detail the translocation of nuclear receptors, in the presence of some typical stimulus, such as endogenous ligand or antagonist but do not explore colocalisation. Our results, in an accessible system of differentiated neurons from embryonic stem cells show, for the first time, expression of these endogenous oestrogen receptors in different subcellular compartments and demonstrates, at least in this cell system, that colocalisation appears to be low. Currently, the mechanisms or reasons for such differential localisation are unclear and have not been explored for most nuclear hormone receptors. The distribution of GPER-1 has also been controversial with some studies showing predominantly localisation in the endoplasmic reticulum, or in the perinuclear space or in the cell membrane in a possibly cell-specific manner (R. Vajaria & N. Vasudevan, 2018) (and refs therein). Our data show that many subcellular locations are possible with the function of nuclear localisation of this GPCR unknown.

Quantitative protein colocalisation for biomarkers, including nuclear hormone receptors and mERs is now being explored for more precise breast cancer therapy (Cheung et al., 2021);(Meattini et al., 2017). Our study supports the contention that such compartmentalisation and colocalisation analyses is, as argued by some other investigators (Acconcia et al., 2021), a field ripe for investigation since it is relevant to biological function.

2.11 Supplementary methods for chapter 2

This section is an overview of material and methods in chapter 2, describing in detail optimisation and supplementary methods. This section will expand on the published work of (Davis, Vajaria, et al., 2023) that comprises of background, supplementary results, and conclusions.

2.11.1 Neuronal cell culture

Neuronal cell cultures originating from mES cells were grown in two different growth media to achieve optimal culture conditions for neural differentiation outlined in (Davis, Vajaria, et al., 2023). The method described is a modified version of the protocol described in (Mirza Peljto et al., 2010). As previously reported in (Ray et al., 1993) bFGF can increase survival and proliferation of embryonic hippocampal neurons in vitro. To promote higher efficiency of neuronal differentiation a second batch of neuronal cells was grown using ADFNB medium (advanced D-MEM/F12: Neurobasal (1:1) (Gibco, UK), 1x B27 supplement (Invitrogen), 200 mM *L*-glutamine (Gibco, UK), 1x Pen/Strep (Gibco, UK), 10 ng/ml Beta fibroblast growth factor (βFGF) (Gibco, UK), 10 ng/ml brain-derived neurotrophic factor (BDNF)

(Gibco, UK)) resulting in a culture with 50-60% of cells with neuronal morphology (Figure 2.9). Neuronal cells were detected using neuronal marker β-Tubulin III via immunocytochemistry described in(Davis, Vajaria, et al., 2023). β-Tubulin III is a commonly used neuronal marker that exhibits temporal spatial gradients that are typical for neuronal and glial precursor cells (Katsetos et al., 2003). Neuronal cultures yielding higher neuronal-like cells (Figure 2.8) using this modified method were used for all experiments in Chapter 2.

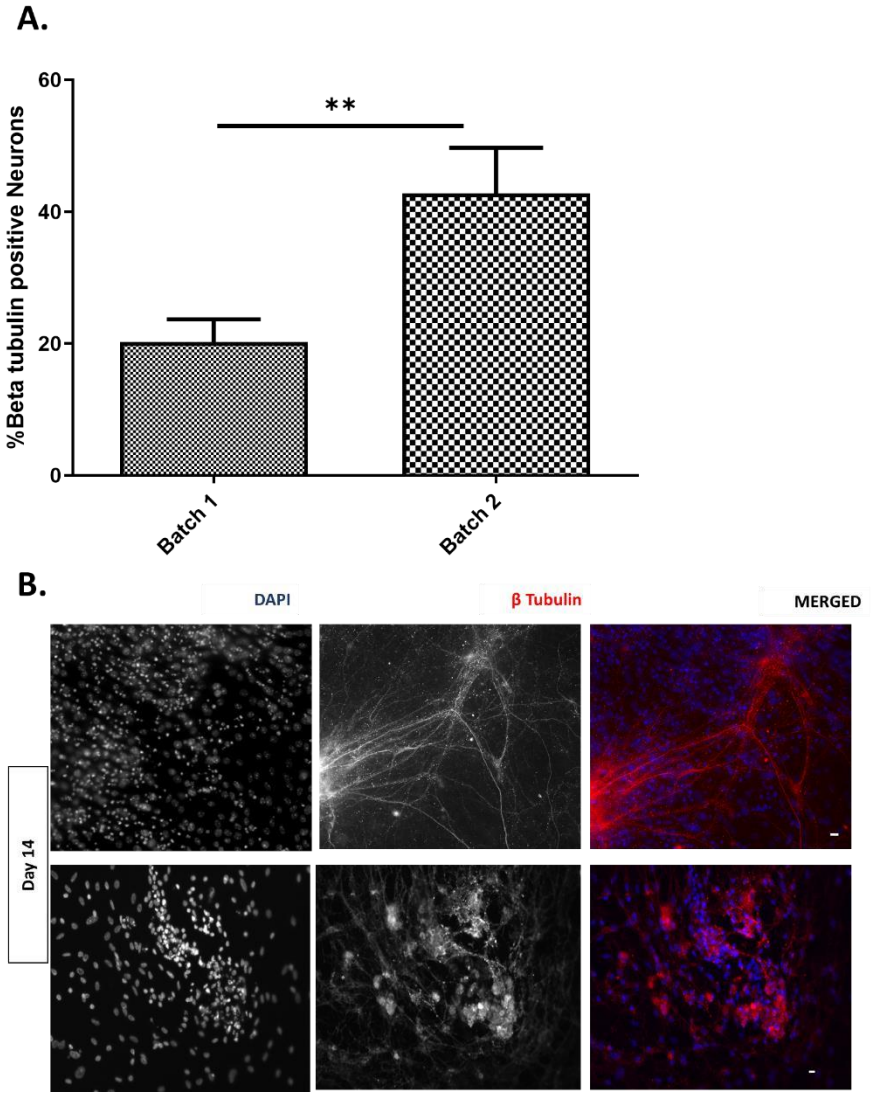

Figure 2.8 Differences in Neuronal Cultures. (A) Percentage of neurons that stained positive for β Tublin III from two different batches (D14 used as a representative). Batch 1 neurons were cultured with ADFNB medium containing 5 ng/ml Beta fibroblast growth factor (βFGF) and 5 ng/ml brain-derived neurotrophic factor (BDNF) and yielded 20%-40% of cells with neuronal morphology. Batch 2 neurons were cultured with ADFNB medium containing 10 ng/ml Beta fibroblast growth factor (βFGF) and 10 ng/ml brain-derived neurotrophic factor (BDNF) and yielded 50-60% of cells with neuronal morphology. (B) Representative images of Day 14 neurons (top row) Batch 1, (bottom row) Batch 2 neurons.

2.11.2 Antibodies

Two antibodies Anti- GPER(STJ192629) and Anti- ERα (STJ97499) that were validated for Western.

Blotting (WB), Immunohistochemistry (IHC) and Immunofluorescence (IF) were used for this study. To validate these antibodies for usage with ICC, we conducted ICC experiments to investigate specificity and comparable staining patterns shown with antibodies previously published and validated for use in ICC experiments.

ERα Antibody (H-184) (Santa Cruz Laboratory, USA) was validated for use with ICC, but discontinued.

Here, we detected full length- ERα in mES cells at 1:100 dilution using the rabbit ERα Antibody (H-184) and Anti- ERα (STJ97499). Approximately 50 cells of mES cells were selected and analysed for a similar distribution within these cells by employing nuclear: cytoplasmic(N:C) ratio analyses using Image J(Fiji/ NIH, USA) . Results revealed that there were no significant differences between ERα Antibody (H-184) and Anti- ERα (STJ97499) N:C ratio (Figure 2.9).

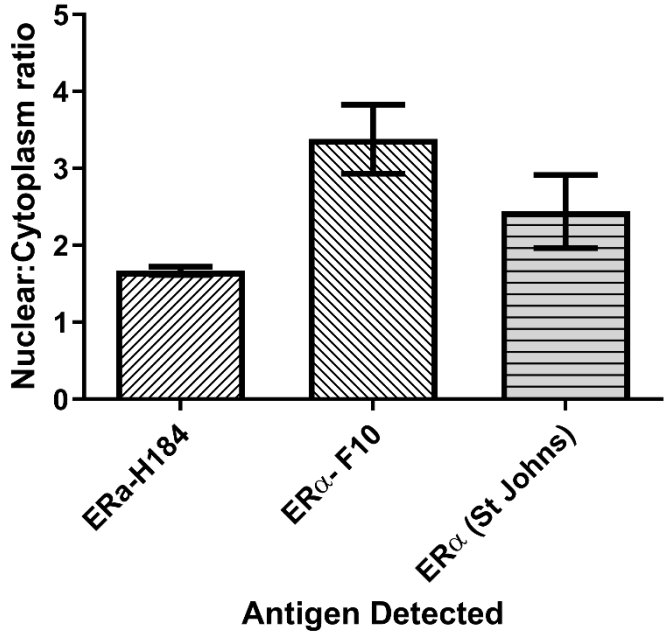

Figure 2.9. Validation of the ERα from St Johns Labortaory, UK in mES cells. This rabbit polyclonal antibody is compared against previously reported antibodies in literature. These are the H184 antibody raised in rabbit

against the N-terminal A/B domain of ERα and the F10 antibody raised in rabbit against the DNA binding domain of ERα. Both are polyclonal antibodies made and sold by Santa Cruz Biotechnology which were discontinued. Hence, we used an available antibody from a local source i.e. St Johns Laboratory, UK but compared it against existing aliquots of the Santa Cruz antibodies. In the lab, we calculated the nuclear: cytoplasmic ratio (N:C ratio) of this ERα in mES cells using all three ERα antibodies in parallel, to demonstrate similar distribution. One way ANOVA reveals no significant differences between the three antibodies. All data was collected by a colleague in the laboratory, Ms. Ruby Vajaria in in fulfilment of MRES in Biomedical Sciences, University of Reading (2018). N=35-48 cells/antibody.

2.11.3 Antibody conjugation

Since antibodies linked to oestrogen receptor that were being used by us were raised in the same species, i.e. rabbit Anti-ERα (Saint John's Laboratory, UK- STJ97499).) and Anti-GPER1(Saint John's Laboratory, UK- STJ192629) were conjugated to fluorescein isothiocyanate (FITC) (Thermofisher, UK), as per the suppliers protocols (Thermofisher UK). To determine the labelling efficiency, absorbance values were measured at A280 and A495. First, we determined the molarity using equation 1, whereby, ε= protein molar extinction (for IgG- 210,000 M-1 cm), A max=absorbance of the dye solution , CF= correction factor of dye absorbance at 280nm(provided by supplier) Next, we calculated the degree of labelling using equation 2, whereby ε′ = molar extinction coefficient of the fluorescent dye. For effective labelling, the degree of labelling should fall within 2-6 moles of FITC per one mole of antibody. Finally, we determined the protein concentration using equation 3. The newly conjugated antibodies which we present here as ERα-FITC and GPER1-FITC were compared for labelling efficiency against unconjugated AntiGPER1(Figure 2.10) to ensure similar distribution.

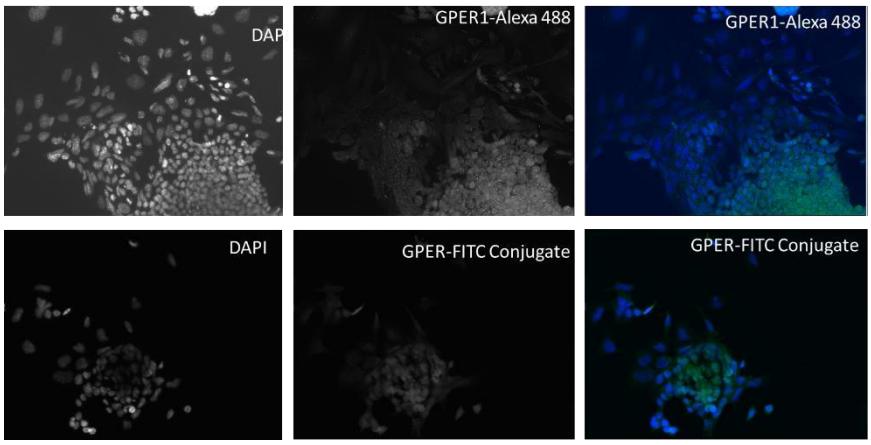

Figure 2.10 Comparison of GPER1 with GPER1-FITC conjugate used by immunocytochemistry. mES cells stained with Anti-GPER1 antibody obtained from St Johns Laboratory UK, followed by the goat anti-rabbit and Alexa 488 secondary antibody (top row) or GPER FITC conjugate, synthesized by us (bottom row) showing similar distribution..

2.12 Supplementary results for chapter 2

2.12.1 The use of PCC to correlate the ERS to different organelles

Immunocytochemistry was used followed by image analyses using EZ colocalisation to show that oestrogen receptors are differentially localised in organelles, with ERα-36 and GPER1 localised similarly both mES and mESn. ERα-66 full length show increases in both the plasma membrane and nucleus as mES differentiates to mESn. Thirdly, all ERs are present in the nucleus, Golgi, endoplasmic reticulum and plasma membrane but are not colocalized with each other.

For the paper we used Manders Coefficient to measure the co-occurrence of oestrogen receptors in the nucleus, plasma membrane, endoplasmic reticulum, and Golgi apparatus. In (Davis, Vajaria, et al., 2023), a threshold (cut-off) level of 0.5 was used to denote colocalization on a scale of 0 to 1 (Davis, Vajaria, et al., 2023)We also detected nuclear to organelle ratios for receptors in both cell types using mean integrated density analyses. In addition to MCC, we also determined correlation of antigen in organelles in mES and mESn using Pearson Correlation Coefficient (PCC). Although MCC is more accurate for determining the relative position of receptors at a subcellular level and hence was used in the publication(Davis, Vajaria, et al., 2023), correlation coefficients (PCC and SRC) relay information about how two variables are related to one another. Since values of PCC range from -1 to 1 there is no auto threshold for correlations that corresponds to a threshold for colocalisation. However, values from 0.25 to 0.5 are considered weakly corelated.

Here, we present supplementary data using PCC where we investigate correlation of ERα-66 full length in various organelles (Figure 2.11), ERα-36 in various organelles (Figure 2.12) and GPER1 in various organelles (Figure 2.13). In some figures, we collapsed the neurons across differentiation days (D7, D14, D21) for simplicity. Therefore, Figure 2.11 that depicts the correlation of ERα 66 in various organelles using PCC could be compared to Figure 2.1 that depicts the cooccurrence of ERα in various organelles using MCC. Similarly, Figure 2.12 could be compared to Figure 2.2 where both investigate the correlation and cooccurrence of ERα-36 respectively in various organelles. Also, Figure 2.13 could be compared to Figure 2.3 where both investigate the correlation and co-occurrence of GPER1 respectively in various organelles. Since Correlation Coefficients are not extended to three channels, they cannot be used to measure correlation of two different receptors in the same organelle.

2.12.2 PCC reveals similar results to MCC for localization of ERs in organelles

Analysis of nuclear and membrane correlation using PCC revealed a significant increase in correlation in mESn in both organelles compared to mES cells for full length ERα-66 (Figure 2.11A) with low levels of this receptor in the nucleus of mES cells. There are also higher levels of ERα-66 colocalisation in the plasma membrane of D21 mESn compared to D7 and D14 mESn. The results reveal higher correlation of the ERα-66 in the endoplasmic reticulum (Figure 2.11B) of mESn compared to mES cells. In contrast, ERα66 correlates with a significant decrease in mES cells compared to mESn in the Golgi apparatus. In both endoplasmic reticulum and Golgi apparatus, high correlation of ERα-66 with these organelles can be seen. These results are similar to what is seen when we use MCC to analyse the data and therefore, the same conclusions can be drawn.

Similarly, both ERα-36 (Figure 2.12A) and GPER1 (Figure 2.13A) are correlated in the nucleus to a similar extent in mES and mESn. For both these receptors, there is a transient increase in the plasma membrane from mES to mESn, similar to what is seen when we use MCC. For ERα-36, the endoplasmic reticulum and Golgi apparatus ERα-36 correlates slightly higher in mES cells compared to mESn (Figure 2.12B) while there is no difference with GPER1 (Figure 2.13B). There is a decrease in correlation of ERα-36 (Figure 2.12B)and GPERR1 in the Golgi apparatus (Figure 2.13B) in mESn compared to mES cells.

Correlation only measures how well the intensities in one image predict the other and could be dependent on antigen affinities to the antibody used. In principle, high correlation with low cooccurrence could be obtained (Aaron et al., 2018). However, in this study, inferences obtained from using cooccurrence (MCC) and correlation (PCC) are closely matched for all three ERs studied.

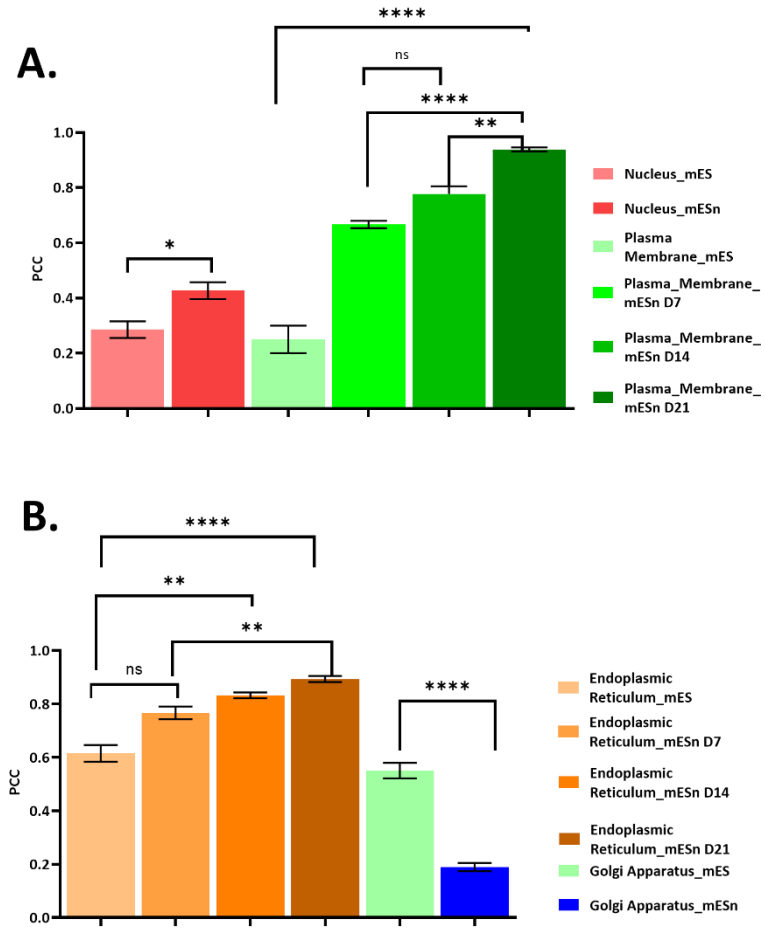

Figure 2.11 Subcellular localisation of ERα-66 in mouse embryonic stem cell line (mES) and cultured differentiated neurons (mESn). Quantification of ERα in various organelles was carried out using image analyses using EZcoloc plugin (Fiji, NIH Image) to obtain Pearson correlation coefficient (PCC) presented. PCC values ranging from -1 to 1 represent negative correlationanticorrelation (-1) , no colocalisation (0) or positive correlation .one ANOVA followed by Dunn's multiple comparison test compares between groups. (A) Comparison of localisation of ERα in the nucleus and plasma membrane of mES and mESn. (B) Comparison of localisation of ERα in the endoplasmic reticulum and Golgi apparatus of mES and mESn. Data is presented as the mean ± SEM. (n = 50 mES, n = 49-50 per D7,14,21 mESn)(*p < .05, **p < .01; ***p < .001; ****p ≤ .0001.

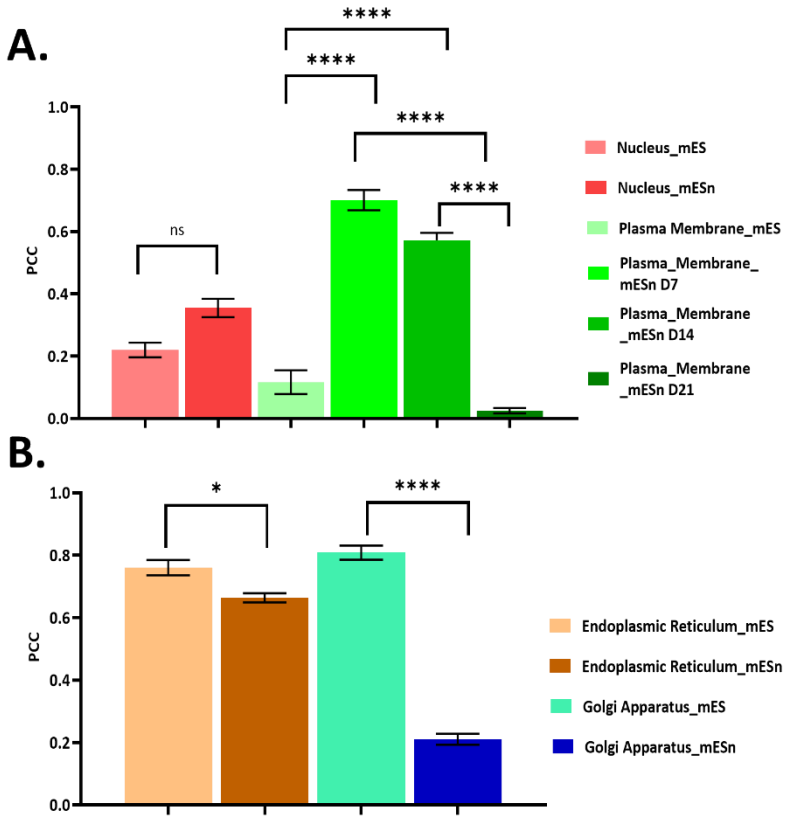

Figure 2.12. Correlation of ERα-36 in mouse embryonic stem cell line (mES) and cultured differentiated neurons (mESn). Quantification of ERα 36 in various organelles was carried out using image analyses using EZcoloc plugin (Fiji, NIH Image) to obtain Pearson correlation coefficient (PCC) presented. PCC values ranging from -1 to 1 represent negative correlationanticorrelation (-1) , no colocalisation (0) or positive correlation.one ANOVA followed by Dunn's multiple comparison test compares between groups. (A) Comparison of localisation of ERα 36 in the nucleus and plasma membrane of mES and mESn. (B) Comparison of localisation of ERα 36 in the endoplasmic reticulum and Golgi apparatus of mES and mESn. Data is presented as the mean ± SEM. (n = 50 mES, n = 49-50 per D7,14,21 mESn)(*p < .05, **p < .01; ***p < .001; ****p ≤ .0001.

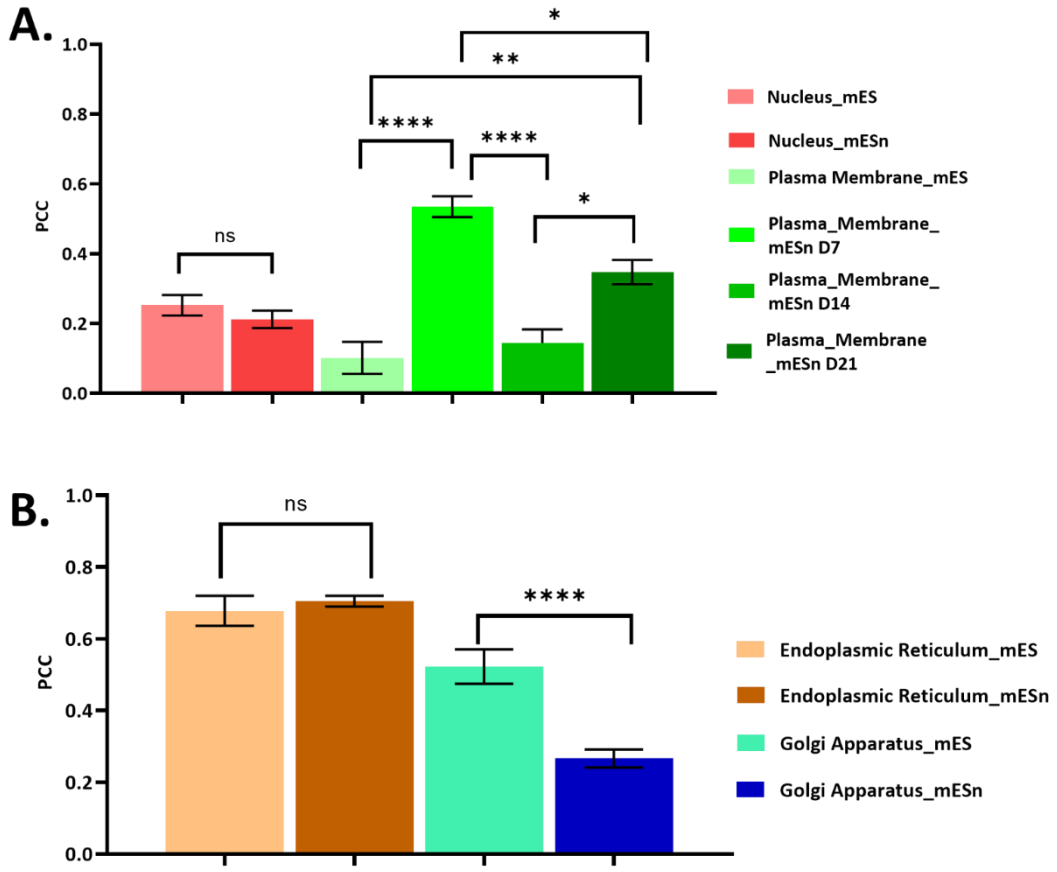

Figure 2.13. Correlation of GPER1 in mouse embryonic stem cell line (mES) and cultured differentiated neurons (mESn). Quantification of GPER1 in various organelles was carried out using image analyses using EZcoloc plugin (Fiji, NIH Image) to obtain Pearson correlation coefficient (PCC) presented. PCC values ranging from -1 to 1 represent negative correlation (-1) , no colocalisation (0) or positive correlation . one ANOVA followed by Dunn's multiple comparison test compares between groups. (A) Comparison of localisation of GPER1 in the nucleus and plasma membrane of mES and mESn. (B) Comparison of localisation of GPER1 in the endoplasmic reticulum and Golgi apparatus of mES and mESn. Data is presented as the mean ± SEM. (n = 50 mES, n = 49-50 per D7,14,21 mESn)(*p < .05, **p < .01; ***p < .001; ****p ≤ .0001.

Supplementary data published with (Davis, Dovey, et al., 2023)is included in Appendix 1.

3. The membrane estrogen receptor, GPER1 collaborates with classical ERs via rapid non-genomic signalling

Chapter 3: Most of the data in this Chapter 3 is being prepared for publication.

Figures: All figures represent data collected, analysed and generated by Ms. DeAsia Davis.

Intellectual contribution: Using the techniques in Chapter 2, Ms. DeAsia Davis independently initiated this project due to interest in ER-GPER1 crosstalk. This was expanded and supervised by Dr. Nandini Vasudevan.

Writing: The results and methods were written by Ms. DeAsia Davis as well as parts of the introduction and discussion, in discussion with Dr. Nandini Vasudevan. Some parts of the introduction and discussion were written by Dr. Nandini Vasudevan.

Abstract

Aromatase (Cy19A1) catalyzes the conversion of testosterone to estrogens which regulate sexually dimorphic behaviour by signalling in the social behaviour network, a collection of interconnected nuclei in the brain. Though ERα and GPER1 may interact in response to E2, and influence oestrogen-mediated phenotypes, including the modulation of synaptic transmission in adult female mice. Although the interaction between ERβ and GPER1, is underexplored. To understand the role of oestrogen receptors in rapid non-genomic regulation of aromatase expression, we treated a mouse embryonic hypothalamic neuronal cell (N42) and a mouse embryonic stem cell line (mES) with either vehicle (DSMO), E2, E2-BSA, G1 (GPER1 agonist), PPT (ERα agonist), or DPN (ERβ agonist) and measured either aromatase expression or ERα translocation at 20 mins. GPER1 activation decreased the nuclear localization of ERα in mES cells. In N42 cells, aromatase expression increased nearly 20-fold after 20 mins of treatment with G1 and DPN, but not with PPT. Additional treatments with GPER1 antagonist and DPN reversed these effects, suggesting that increases in aromatase expression requires both GPER1 and ERβ to be active. Surprisingly, treatment with G1 and DPN together, decreased aromatase expression, suggesting that GPER1 and ERβ 'crosstalk' to mediate rapid increases in aromatase expression. Our results show that ERβ and GPER1 may collaborate by signalling in the same pathway to rapidly increase aromatase expression and GPER1 may impact ERα translocation in a cell type specific manner.

3.1 Introduction

Oestrogens synthesis is facilitated by cholesterol entry into the mitochondria, followed by a series of enzymatic steps (Ghosh et al., 2009);(Boon et al., 2010). Oestogen is a steroid hormone that signalls via ERs whose expression is in several peripheral tissues in the body inlcuding ovaries, placenta, bone, muscle tissues and testis (Nelson & Bulun, 2001). In the vertebrate brain, oestrogen is crucial for social behavior (Beyer, 1999) including social recognition (K. Ervin et al., 2013), learning and memory(Gervais et al., 2013),aggression(Yang et al., 2013);(Chen & Hong, 2018)and sexual behavior (Court et al., 2022);(Balthazart & Surlemont, 1990);(Yang et al., 2017). Generally, the effects of oestrogen are mediated by ligand-activated binding of nuclear classical oestrogen receptors (ERs) ERα and ERβ (Enmark & Gustafsson, 1999);(Kuiper et al., 1997). However, several studies showed a small percentage of classical receptors are localized at the plasma membrane (mERs) (Ervin, Lymer, et al., 2015; Micevych & Christensen, 2012). Along with these typically intracellular ERs that may act as mERs, a relatively novel GPCR called G protein-coupled ER 1 (GPER1) can also function as the mER (reviewed in (Rainville et al., 2015)). These ERs may act together or independently of one another to facilitate rapid oestrogen action that is initiated at the cell membrane by the binding of 17β-estradiol to a mER (E. J. Filardo et al., 2000; Hadjimarkou & Vasudevan, 2018; C. M. Revankar et al., 2005).

Aromatase (cytochrome P450), a product of the Cyp19a, converts C19 steroids to estrone or estradiol (Boon et al., 2010). Aromatase activity was first detected by Nafotlin et al in the rat hypothalamus and has long been established as a crucial play in the development and functionality of the CNS (Naftolin & MacLusky, 1982).Consistent with several of these functions, aromatase is highly expressed throughout the vertebrate brain including the BNST, mPOA, amygdala and ventromedial hypothalamus (Lephart, 1996; Naftolin & MacLusky, 1982), which are essential for reproductive and social behaviour (Bayless et al., 2019; Pfaff & Sakuma, 1979). Using immunohistochemistry (IHC) and ELISA , a 65-70 % decrease in neurooestrogen in the hippocampal CA1 region was seen n the forebrain-specific aromatase knockout mice(FBN-ARO-KO) Both male and female mice displayed a significant decrease in spaital memory compared to wild-type (Lu et al., 2019) using both the Barnes Maze and the novel object recognition test. In addition, though there is no difference in motility or exploratory behaviour, mice showed a phenotype in the forced swim test that indicates increased depression; these phenotypes are correlated with decreased spine density in the hippocampus (Lu et al., 2019). These data suggest that neuroestrogen and aromatase activity in the forebrain is

important to the maintenance of memory, at least partially via regulation of neuronal connectivity.

Neuronal aromatase expression is controlled by conserved promoter region I.F region. In the embryonic cell culture of male and female amygdala treated with E2, there was a significant increase in *Cyp19a1* expression compared to vehicle only in female cultures, though male cultures displayed higher levels overall (Cisternas et al., 2017). When treated with ERα, ERβ and GPER1 specific agonist, only cell cultures treated with the ERβ specific agonist DPN for 2 hours were able to demonstrate an increase in *Cyp19a1* expression levels similar to E2. This suggest that ERβ plays a role in the acute regulation of aromatase (Cisternas et al., 2017) in neuronal culture. In the mHypo-E42 (N42) hypothalamic cell line derived from embryonic mouse, real time PCR revealed that aromatase mRNA expression significantly increased compared to vehicle after 6hrs of treatment with 17β-estradiol. Further investigation revealed that this transcriptional increase in aromatase mRNA was facilitated by ERα binding to the JUN complex at the AP-1 site in the i.f promoter region of the aromatase gene(Yilmaz et al., 2009). Taken together, these data suggest that regulation of aromatase in the brain could be nuclei-specific and temporally different, though the signaling pathways and mechanisms that regulate this specificity are still not well understood.

Here we study the contribution of oestrogen receptors in the rapid regulation of aromatase and the translocation of ERα in two different cell lines – a mouse embryonic stem cell line (mES) and in hypothalamic N42 cells – using receptor-specific agonists. Several common environmental pollutants decreased aromatase expression in human granulosa cells within 48 hours and this was reversed by silencing GPER1(Zajda & Gregoraszczuk, 2020). Understanding the mechanism by which these ERs regulate aromatase would allow us to infer pathways by which endocrine disruptors may act within cells.

3.2 Material and Methods

3.2.1 Maintenance and culture of cell lines

Two different cell lines, mHypo-42 (N42) Hypothalamic cell line and a mouse embryonic stem (mES) cell line (CGR8) were used. Cryopreserved mouse embryonic hypothalamic neuronal cell lines N42 were reanimated in Dulbecco's modified Eagle medium (DMEM)(Gibco, UK), supplemented with 10% fetal bovine serum (FBS) (Biosera, UK) and 1% Penicillin/Streptomycin(P/S) (Gibco,UK) in tissue culture flasks (25cm2). mES were plated between passage 2 and 13 at 106 cells in 0.1% gelatin-coated (0.1%) tissue culture flasks (25cm2) and maintained in SNL media composed of Dulbecco's modified Eagle medium

(DMEM)(Gibco, UK), 10% fetal bovine serum (FBS) (Biosera, UK), 1% Penicillin/Streptomycin(P/S) (Gibco,UK), 1%L-Glutamine (Gibco,UK), 100µM 2-Mercaptoethanol (Gibco, UK) and 106 Leukaemia inhibitory factor (LIF) (Calbiochem,UK) (Fannon, 2021). Both cell lines were incubated at 37°C at 95% O2, 5% CO2. Stem cells were passaged at a ratio of 1:8 at 80% confluence (approximately every 2 days) to maintain pluripotency. They were then used to plate at a density of 200 cells/mm2 (30,000 cells/well) on 0.1% gelatinized glass coverslips in 24 well plates for immunocytochemistry or on 0.1% gelatinized 12 well plates for RNA isolation on Day 1. Prior to the addition of hormones, media from cells were removed and washed with warmed PBS, and media that is phenol red free and 10% charcoal stripped sera (hormone-free media) was added to ensure the removal of all exogenous hormones for 24 hours. For mES cells, this media is phenol red free DMEM (Gibco, UK), 10% characol stripped fetal bovine serum (csFBS) (Biosera, UK), 1% Penicillin/Streptomycin(P/S) (Gibco,UK), 1%L-Glutamine (Gibco,UK), 100µM 2-Mercaptoethanol (Gibco, UK) and 106 Leukaemia inhibitory factor (LIF) (Calbiochem,UK). For N42 cells, phenol-red free DMEM supplemented with 10% csFBS (Biosera, UK), and 1% P/S (Gibco,UK) was added. On Day 3, hormones or other agonists/agents were diluted in hormone-free medium at the desired concentrations (Table 3.1) and placed on a rocker for 30 minutes before being added directly to cells. Cells were rinsed with warm PBS before media was changed.

3.2.2 Treatment of cells with agonists and antagonists

Antagonist, agonist, inhibitors, and activators were prepared at concentrations and dissolved in dimethylsulfoxide (DMSO) at concentrations that are 10-fold or 100-fold of those described in Table 3.1 and stored at -20 °C. Antagonist were added 10 mins prior to 20 minutes of hormone or agonist treatment at 37°C at 95% O2, 5% CO2. Final concentration of DMSO in the media was 0.1%.

3.2.3 Translocation of receptors measured by immunocytochemistry (ICC)

mES and N42 cells were plated on 0.1% gelatinized 13mm glass coverslips in 24 well plates in maintenance media described in Section 3.2.1. The next day (Day 2) this media was removed, cells were washed with warmed PBS, before adding hormone-free medium for 24 hours. On Day 3, to test the trafficking of receptors initially, cells were treated with E2, E2- BSA, G1, PPT and DPN dissolved in 1 % DMSO to a final concentration of 10-8 M for 10 mins, 20 mins, 30 mins, 60 mins, and 2 hours (Section 3.3.2 for results). In all experiments in this chapter, cells

were processed for immunocytochemistry using rabbit Anti- ERα (STJ97499, 1:300) and Anti-GPER1 (STJ192629, 1:300) (Table 2.1 and Table 2.2), 20 minutes after agonist treatments. Images were acquired at 20x using a Zeiss AxioImager Epiflourescent (Carl Zeiss MicroImaging GmbH) microscope with identical gain and exposure times. We set exposure times to be lower than any autofluorescence seen in negative controls (no primary antibody added). We analysed the presence of each receptor in N42 cells in three different organelles in the same cell at the same time using green (ERα) filters, red (plasma membrane) and blue (nucleus) or GPER1 (green), nucleus (DAPI blue), endoplasmic reticulum (ConA-red) and Golgi apparatus (HPA-far red) in the same cell. Monochromatic images were then analysed with EZcolocalisation (image processing plugin for Image J/Fiji, NIH Image) to generate Manders coefficients (MCC) that measure colocalisation of these receptors in different subcellular organelles. This ICC protocol has been described in detail in (Davis, Vajaria, et al., 2023)as well as in Section 2.4. The analyses of localization using MCC has also been described in Section 2.5 as well as in (Davis, Vajaria, et al., 2023).

Treatment	Pathway	Diluent	Concentration	Time (Mins)
Phorbol 12 myristate 13 acetate (PMA)	PKC inhibitor	DMSO	10µm	10
KT570	PKA inhibitor	DMSO	50nm	10
PD98059	MEK inhibitor	DMSO	50µm	10
BAPTAM-AM (BAPTA)	Calcium inhibitor	DMSO	5µm	10
G1	GPER1 agonist	DMSO	0.001µm (10-8M)	20
G15	GPER1 antagonist	DMSO	1µm	10
PPT	ERα-selective agonist	DMSO	0.001µm (10-8M)	20
DPN	ERβ-selective agonist	DMSO	0.001µm (10-8M)	20
E2BSA (17β-estradiol conjugated to bovine serum albumin (BSA)	mER agonist	DMSO	0.001µm (10-8M)	20
ICI 182,780	ER antagonist	DMSO	1µm	10
17β-estradiol (E2)	ER agonist	DMSO	0.001µm (10-8M)	20

Table 3.1: Both mouse cell lines (mHypo-42 or mES CGR8 cells) were treated with 17β-estradiol or the membrane-limited E2-BSA conjugate which are agonists to all ERs or any mER respectively and translocation or aromatase expression measured after 20 minutes of treatment. In some experimental conditions, receptor specific agonists and/or antagonists to the ERs were added. To investigate signalling pathways that are involved in stimulation of aromatase expression, antagonists to those pathways were added. Antagonists were added 10 minutes prior to the 20-minute incubation with agonists.

3.2.4 RNA Isolation and Real-Time (RT)-PCR for aromatase

mES and mHypoE-42 cells were treated as outlined in Section 3.2.1 and 3.2.2 and total RNA was extracted using RNeasy Plus Micro Kit (Qiagen , UK) per manufacturer's instruction, 20 minutes after treatment. DNase digestion was carried out using RNase-Free DNase Set (Qiagen) . RNA integrity and concentration was determined by Nanodrop (ThermoFisher Inc, UK). 50 ng of total RNA was used for cDNA synthesis for a final volume of 20µl using *Quanta cDNA synthesis kit* per manufacturer's instructions. cDNA was diluted to a final concentration of 5ng in sterile 1X TE and stored at -20°C until use. 5ng of was used for real-time RT-PCR using the Power SYBR green kit (Fisher, UK) in a 14 µl total volume which also contained 380 nm of forward and reverse primers. The primers were synthesized by IDT and stored at 5 µM stock concentrations in TE in -20C. The sequences of *ActD* or β-actin forward primer are 5' TGTGCTGTCCCTGTATGCCTCTGG *3' and ActD* reverse primer are 5'GGGAGAGCATAGCCCTCGTAGATGG 3'. Similarly, the sequences for aromatase i.e. Cytochrome P450, family 19, subfamily a, polypeptide 1 (*Cyp19a1*) forward primer are 5'GGACACCTCTAACATGCTCTTCCTGGG 3' and *Cyp19a1 reverse* primer are 5' *TGATGAGGAGAGCTTGCCAGGC* 3'. Reactions are run on StepOnePlus Real Time PCR machine (ABI Biosystems). PCR profiles were as follows: Initial Hold: 95ºC for 10 min, followed by denaturation at 94ºC for 15s , Anneal/Extend 60ºC, 1min for 40 cycles, followed by a standard melt curve. Threshold cycles CT were automatically determined by StepOnePlus System. Aromatase expression was normalized to expression levels of an endogenous control gene, β-actin and expressed using the 2-ΔΔCt comparative method compared to the vehicle control. 3-7 independently prepared samples were used to demonstrate reproducibility.

3.2.5 Statistical Analysis

For image analyses, EZcolocalisation software generates both M1 and M2 Manders coefficients (MCC). M1 is the intercept of all fluorescent channels/organelle wherease M2 is the intercept of all fluorescent channels/target antibody (Section 2.5, Supplementary Figure 1) All data are presented as mean ± SEM with graphs and statistics performed using Prism 9.0 (Graph Pad

Software); Data was analysed using Kruskal Wallis nonparametric test followed by the Dunn's post hoc test, since data was not normally distributed. In all cases, $p < .05$ was deemed statistically significant. Manders correlation coefficients > 0.5 were considered localised (Manders et al., 1993). Determination if colocalisation was statistically different ($p<0.05$) from this threshold value was carried out using one sample t test and Wilcoxon's test. For some data, we used only M1 since we were primarily interested in the localisation of ERs in the organelle.

Data on aromatase expression: Differences between treatment groups were analysed by Kruskal Wallis nonparametric test followed by the Dunn's post hoc test, since data was not normally distributed. In all cases $p<.05$ was deemed significant. With some experiments, we need to increase the number of replicates but could not do so since we ran out of time, due to delays caused by the COVID pandemic.

3.3 Results

We previously determined the distribution of ERs in mES cells in the nucleus , plasma membrane, endoplasmic reticulum and Golgi apparatus compared with neurons derived from mES cells (Davis, Vajaria, et al., 2023). Since we concluded that ERs localises differentially in mES and mES derived neurons, this led us to conclude that ERs may exhibit differential distribution and different biological effects that is dependent on cell type. .

3.3.1 ERα and GPER1 localisation in different organelles in N42 cells

Similar to Chapter 2, we first determined the subcellular localization of oestrogen receptors in N42 cells using ICC. Since there is no reliable antibody for ERβ, we did localization analyses only for the classical ERα-66 (herewith referred to as ERα) and GPER1. Though the N42 cell lines is known to possess these receptors, subcellular localization has not been done . For comparison between organelles, we used Manders coefficient with a focus on M1 as the metric for colocalisation within the same organelle with a 0.5 threshold (Davis, Vajaria, et al., 2023). We found that ERα-66 localises in N42 cells at roughly equal measure in the plasma membrane, endoplasmic reticulum, and Golgi apparatus. We also detected lesser amounts of ERα-66 in the nucleus, though still above the 0.5 threshold (Figure 3.1A). When compared with mES cells, there were similar amounts of antigen detected in the nucleus, endoplasmic reticulum and Golgi apparatus. Pairwise comparison using Dunn's test indicated that there is higher localisation of ERα-66 in the plasma membrane of N42 cells compared to mES cells; $p <0.0001$. Interestingly, we found GPER1 mainly localised in the plasma membrane with trace amounts in the nucleus

< 0.5 (Figure 3.1B). There were significant differences between GPER1 localisation between mES and N42 cells(de Valdivia et al., 2017);(Sandén et al., 2011).

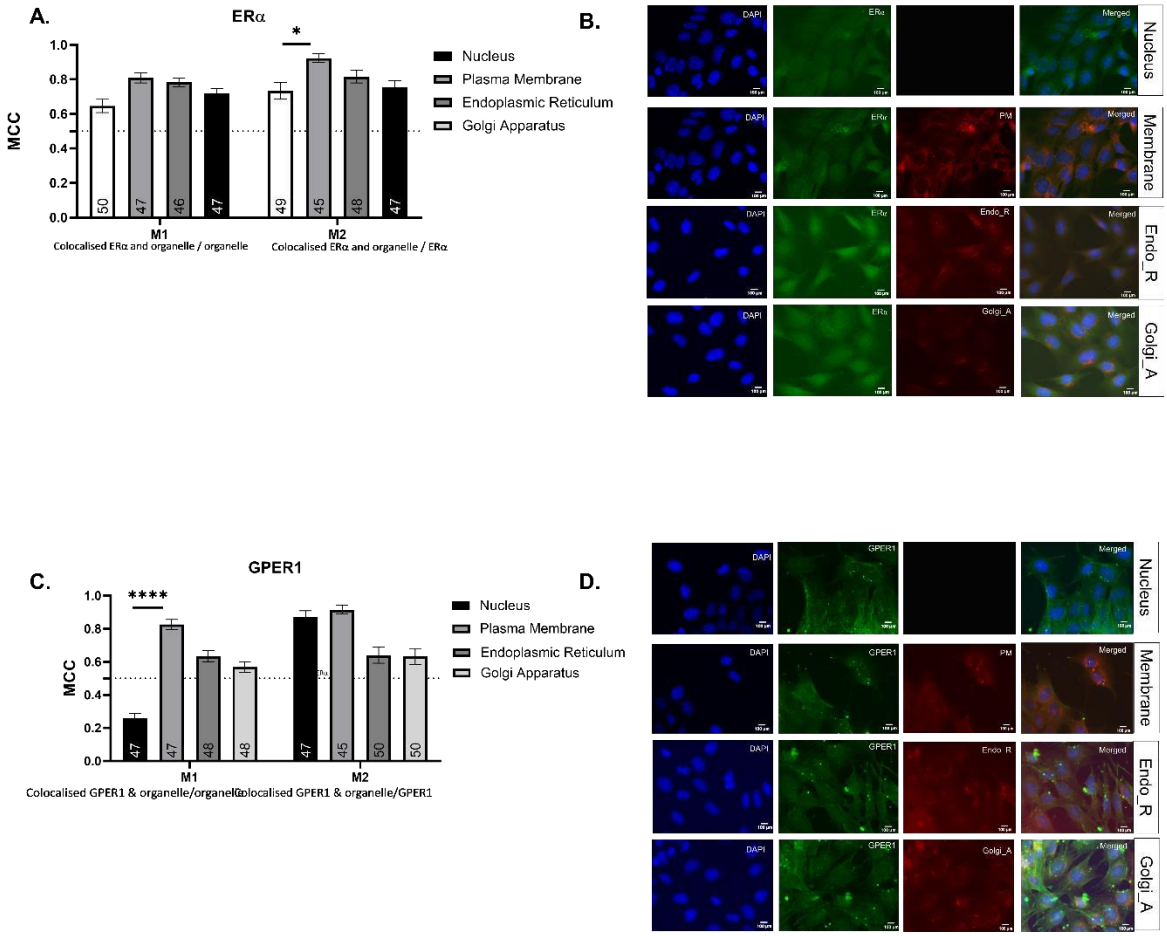

Figure 3.1 . Subcellular localisation of ERα and GPER1 in mouse embryonic hypothalamic neuronal cells *(*mHypoE-42 or N42). Quantification of ERα-66 and GPER1 in various organelles was carried out using image analyses using EZcoloc plugin(Stauffer et al., 2018) (Fiji, NIH Image) to obtain Manders correlation coefficient (MCC) presented here as M1 and M2 . MCC values ranging from 0 to 1 represent no colocalisation (0) or complete colocalisation with 0.5 as the threshold for colocalisation). Kruskal – Wallis One- Way ANOVA followed by multiple comparisons Dunn test between groups was used for analyses. (A) Comparison of localisation of ERα in the nucleus, plasma membrane, endoplasmic reticulum, and Golgi apparatus . (C) Comparison of localisation of GPER1 in the endoplasmic reticulum and Golgi apparatus. Data is presented as the mean ± SEM (n = 46-50). (B) Representative images (20x objective) of ERα (green), nuclear DAPI stain (blue), plasma membrane (red) in mES cells (first two rows). The third and fourth row show ERα (green), nuclear stain (blue), Endoplasmic Reticulum or Golgi Apparatus (red) . (D) Representative images (20x objective) of GPER1 (green), nuclear DAPI stain (blue), plasma membrane (red) in mES cells (first two rows). The third and fourth row show GPER1 (green), nuclear stain (blue), Endoplasmic Reticulum or Golgi Apparatus (red). Numbers within columns refer to the number of cells analysed. Scale bar, 100 μm. *p < .05, **p < .01; ***p < .001; ****p ≤ .0001, EndoR, endoplasmic reticulum; Golgi_A, golgi apparatus; PM, plasma membrane.

3.3.2 A change in nuclear localisation of ERα with G1 and DPN in mES cells but not in N42 cells.

Nuclear localisation of ERα-66 and GPER1 was measured by exposure to DMSO (control), the endogenous ligand 17β-oestradiol (E2) and E2-BSA (membrane-impermeant E2) as well with receptor specific agonists such as G1 (GPER1 selective agonist), PPT (ERα-selective agonist), and DPN (ERβ-selective agonist). Treatment with ligand or agonist for 20 mins resulted in an increase in nuclear localisation of ERα-66 in mES, but not N42 cells (Figure 3.2). It was previously shown that Dex, a synthetic glucocorticoid receptor (GR) agonist could stimulate nuclear translocation of the GR in N42 cells within 30 minutes(Rainville et al., 2019). To test specificity of ERα translocation in mES and N42 cells, we treated cells with Dex. Neither DMSO nor dexamethasone changed colocalisation when compared to naïve cells (Appendix 2, Supplementary Figure 1 and 2) In addition, GPER1 and ERβ appeared to decrease and increase nuclear localisation of ERα respectively. We next tested if GPER1-mediated decrease in nuclear localisation of ERα is specific by using the antagonist, G-15. This reversed the decrease (Figure 3.3A) though the plasma membrane is not the location of ERα when cells are treated with G-1 or with G-15 (Figure 3.3B).

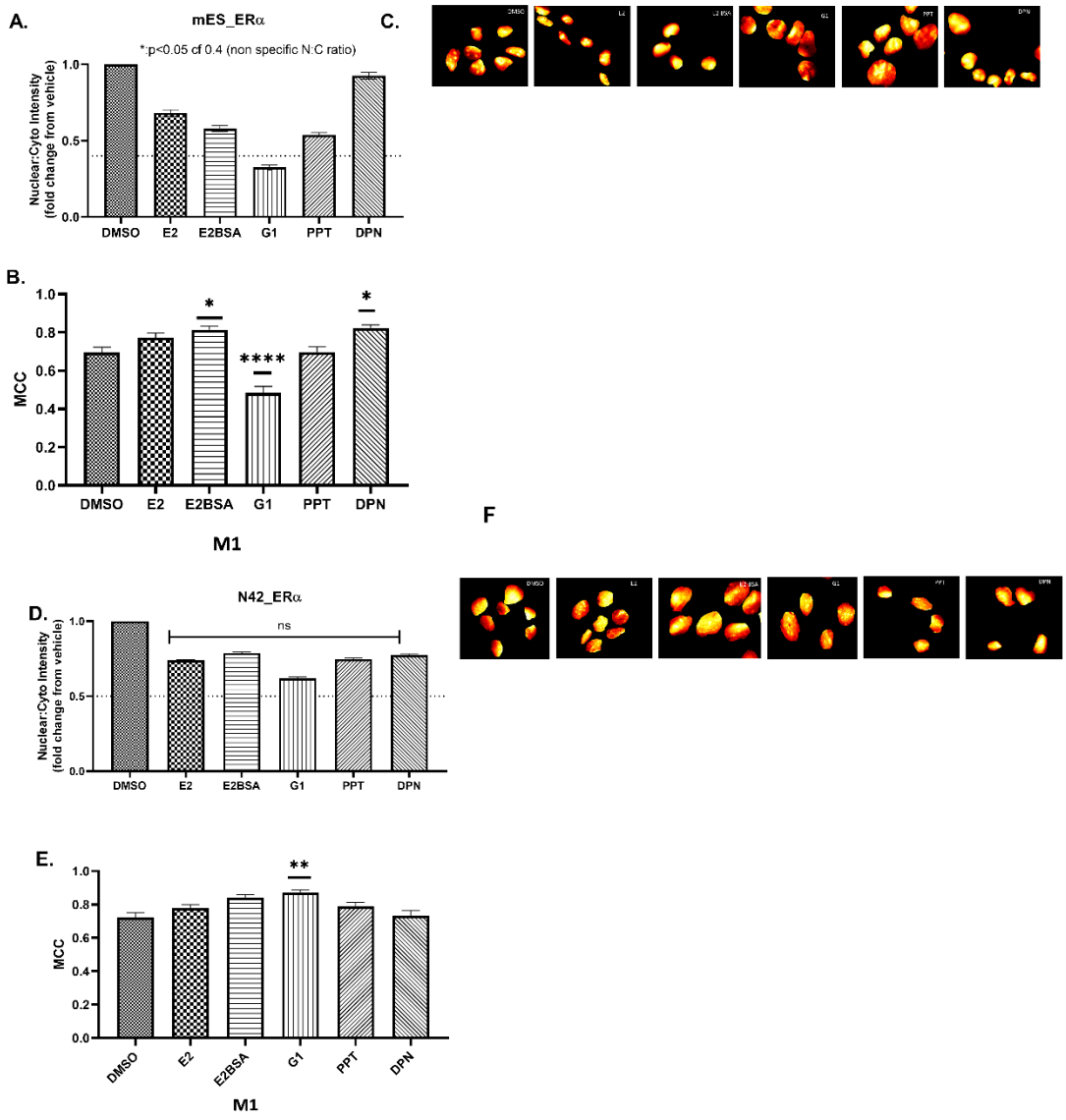

Figure 3. 2 . Nuclear localisation of ERα by G1 . This is measured by two methods: nuclear: cytoplasmic ratio (N:C) and by MCC. A & D) Nuclear-to Cytoplasmic Ratio of ERα in mES cells (A) and in N42 (D) cells in control media (DMSO- vehicle treatment) and media containing E2, E2-BSA, G1, PPT or DPN. Concentrations of agonists are in Methods. Nuclear localization was decreased following 20 mins of treatment with G1 in mES cells only (10-8M). To obtain a more accurate reading of nuclear localization we used M1(Manders Correlation Coefficient)(B & E), which measures the localisation of the target antigen within the nucleus. C & F) Heat maps showing antigen distribution in the nucleus . ****p <0.0001 , one-way ANOVA.

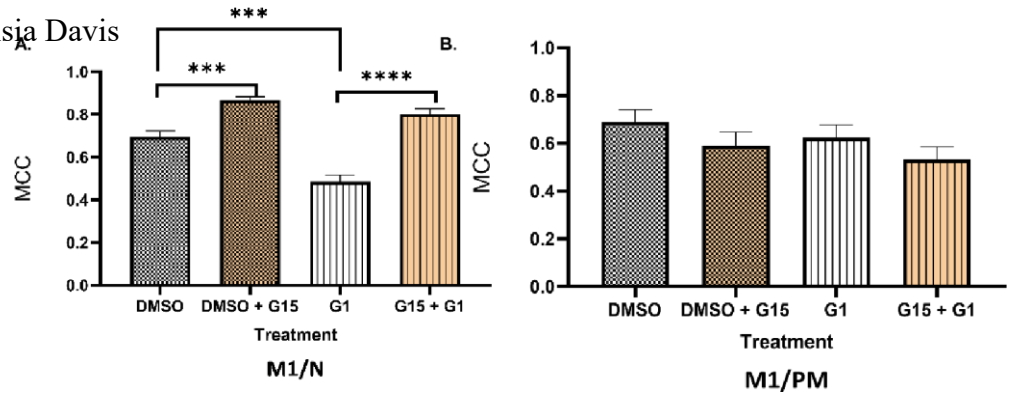

Figure 3.3. Nuclear localisation of ERα by G1 was reversed by G15 in mES cells. (A) Nuclear(N) localization using M1 (Manders Correlation Coefficient) after 10-minute incubation with antagonist G15 (10-6M) ,followed by 20-minute incubation with G1 (10-8M). (B) Plasma Membrane (PM) localization using M1 (Manders Correlation Coefficient) after 10-minute incubation with antagonist G15 followed by 20-minute incubation with G1. In both cases, this is compared to cells to which the DMSO vehicle control is added and also to cells where both DMSO and G-15 (antagonist only control) are added. . $P \leq 0.001$****$p \leq 0.0001$, one-way ANOVA.

3.3.3 Rapid increase in aromatase mRNA expression is facilitated by DPN and G1 via calcium mediated or PKA pathways.

A second output that was tested within the same timeframe is the induction of aromatase using qPCR. In this case, the ERβ-selective agonist DPN and the GPER1 agonist, G-1 both showed an increase in aromatase mRNA expression within 20 minutes in the hypothalamic N42 cell line but not in mES cells (Figure 3.4A-B). This increase could be abrogated by the addition of both agonists, suggesting that both receptors signalled in the same pathway to increase aromatase mRNA (Figure 3.4C). In addition, the specific antagonist G-15 also decreased DPN-mediated increase in aromatase mRNA, suggesting that these two receptors ERβ and GPER1 use the same pathway to increase aromatase expression. Since GPER1 can act via MAPK, calcium and PKA pathways, we decided to test the dependence of induction on these pathways by using inhibitors. Both the calcium chelator BAPTA-AM (Figure 3.5A) and the PKA inhibitor, Rp-cAMPS (Figure 3.5C) could inhibit the increase in aromatase expression obtained with either DPN or G-1. However, the MEK inhibitor did not decrease aromatase expression mediated by either GPER1 or ERβ, suggesting that this induction is specific to PKA and calcium pathways (Figure 3.5B).

Our next series of experiments using GPER1 siRNA to confirm the results of the inhibitor experiments and to further reveal the signalling mechanism could not be completed due to the shortage of time and the COVID pandemic.

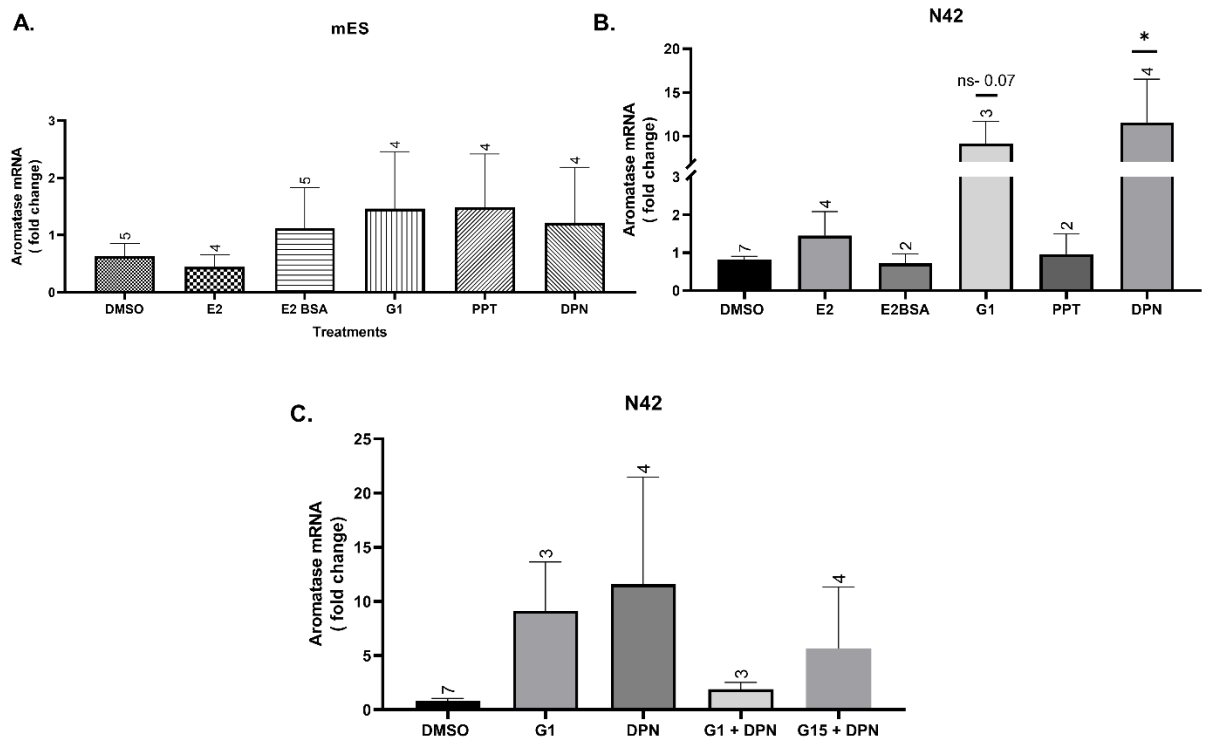

Figure 3.4 Receptor-specific regulation of aromatase mRNA in N42 , but not mES cells.(A) Real time RT-PCR was performed to measure aromatase mRNA expression in mES B) N42 after 20-minute incubation with either DMSO, E2, E2-BSA, G1, PPT, and DPN (10-8M) . Aromatase levels were normalized to control gene β-actin levels; details are in Methods. Results are expressed as the mean ± SEM, n=3-7, n's (# of replicates analysed) are displayed at the top of error bars. *P < 0.02. C) Real time RT-PCR of aromatase mRNA expression in N42 cells after 10 mins of antagonist G15 (10-6M) followed by 20 min treatment with the Erβeta agonist DPN (10 -8M) or 20 min treatment of the receptor agonists for GPER1 G1 (10-8M) and DPN (10-8M) added simultaneously. Results are expressed as the mean ± SEM, n=3-7, n's (# of replicates analysed) are displayed at the top of error bars

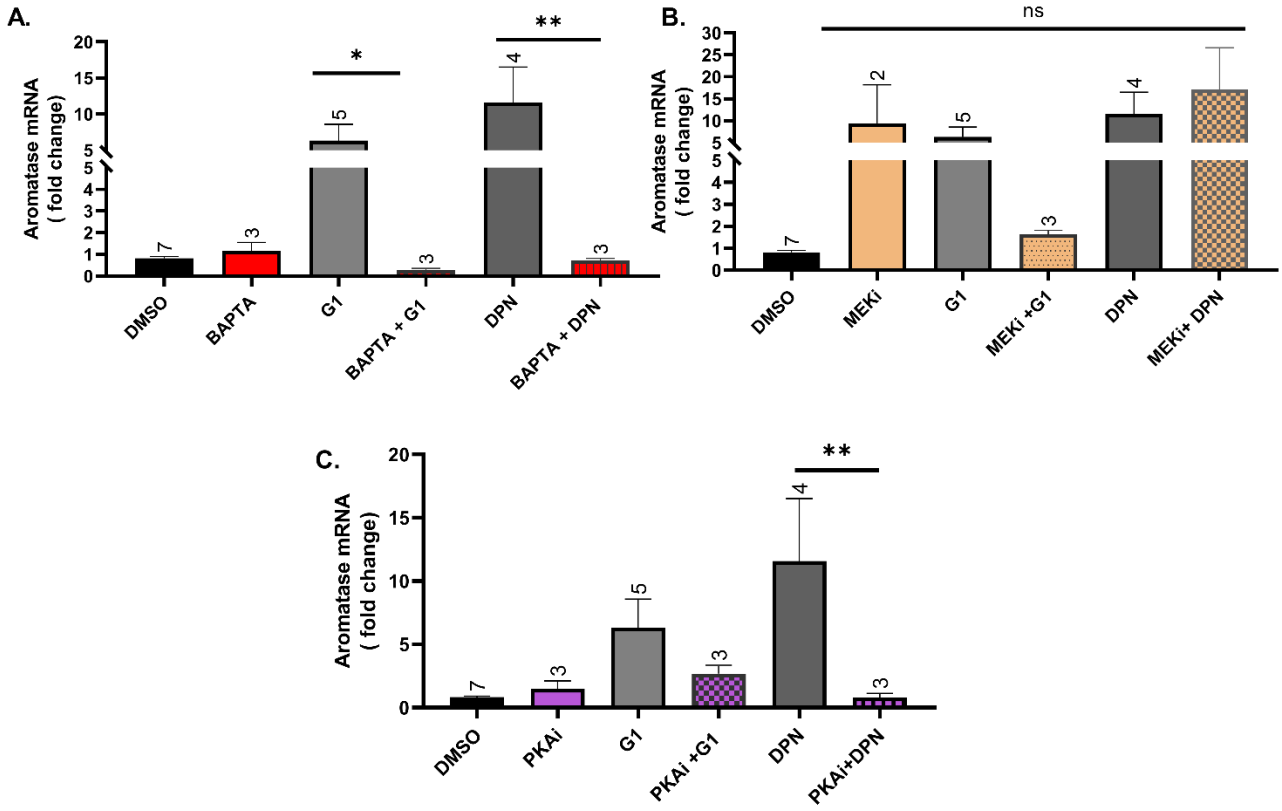

Figure 3.5. Effects of protein kinase inhibitors on aromatase mRNA expression in N42 cells (A) Real time RT-PCR was performed to measure aromatase mRNA expression in N42 after 10-minute incubations of BAPTAM AM (5µm) (selective CA2+ chelator) followed by 20 mins incubations with either DMSO, or the receptor agonists G1 or DPN (10-8M). (B) Real time RT-PCR was performed to measure aromatase mRNA expression in N42 after 10-minute incubations of MEK(50µm)(mitrogen –activated protein kinase) inhibitor followed by 20 mins incubations with either DMSO, G1 or DPN(10-8M) (C) Real time RT-PCR was performed to measure aromatase mRNA expression in N42 after 10-minute incubations of PKA inhibitor (50nm) followed by 20 mins incubation with either DMSO, G1 or DPN(10-8M). Aromatase levels were normalized to control gene β-actin levels. Results are expressed as the mean ± SEM, n=3-7, n's (# of replicates analysed) are displayed at the top of error bars. * P ≤ 0.05. **P ≤ 0.01, one-way ANOVA.

3.4 Discussion

Previously, we showed ERα and GPER1 expression, using specific antibodies to these proteins, in both mES cells and neurons that were differentiated from mES cells. In this study, we compared mES cells with a hypothalamic cell line, mHypoE-42 (N42) cells that are responsive to 17β-estradiol since they show upregulation of aromatase mRNA by a number of different steroids (Brooks et al., 2012; Yilmaz et al., 2009; Yilmaz et al., 2011; Yilmaz et al., 2015). This cell line as well as a closely related line, mHypoE-38 (N38) expresses both ERα and ERβ; in addition, mHypoE-38 has also been demonstrated to express the mER, GPER1 as well as several

ERα variants (Dominguez et al., 2013). In this study, we show crosstalk by GPER1 with the other classical ERs, using two different outputs: translocation and regulation of mRNA.

3.4.1 ERα and GPER1 localisation in mHypo-E42 cells

ERα has been localized by us to the plasma membrane, nucleus as well as being highly localized in the endoplasmic reticulum and the Golgi apparatus in mES cells (Davis, Vajaria, et al., 2023). In hypothalamic N42 cells, ERα was also predominantly expressed in the plasma membrane, the endoplasmic reticulum and in the Golgi apparatus, with some localization in the nucleus. The localization of ERα at the plasma membrane suggests that this ER may mediate non-genomic signalling by estrogen in this cell line; in the N38 cell line, 17β-estradiol rapidly activated PKC and calcium flux (Dominguez et al., 2013). Due to the non-specific nature of all commercially available ERβ antibodies, we were unable to localize this receptor but previous studies and our data on aromatase regulation in this study showed that this receptor is expressed and functional in N42 cells.

We previously reported that GPER1 localised to an equal extent in both the nucleus and plasma membrane in mES cells using the same colocalisation parameter i.e. Manders colocalisation coefficient (MCC). However, we saw very little nuclear localization in N42 cells in this study, suggesting that GPER1 nuclear localization may be cell type dependent. GPER1 has been shown in a variety of different subcellular locations in different cell types. In HeLa cells (Funakoshi et al., 2006) and in breast cancer SKBR3 cells (Thomas et al., 2005), GPER1 showed plasma membrane localization, that is typical of GPCRs. However, in COS-7 cells, it was shown in the endoplasmic reticulum (C. M. Revankar et al., 2005) and in magnocellular neurons, in both the Golgi apparatus and in the endoplasmic reticulum (Sakamoto et al., 2007). In both mES cells (Davis, Vajaria, et al., 2023) and in this present study in N42 cells, there was significant localization of this receptor in the endoplasmic reticulum. It is possible that N-linked glycosylation of this receptor, known to occur in the endoplasmic reticulum and trans-golgi network (Pupo et al., 2013) may be the rationale for localisation of this receptor at these sites in both mES and N42 cells. Unlike in mES cells where there was significant localization of GPER1 to the Golgi apparatus (Davis, Vajaria, et al., 2023), in N42 cells, GPER1 was mostly distributed in the plasma membrane and endoplasmic reticulum. The ubiquitous distribution of GPER1 in the endoplasmic reticulum in most cells could be due to the stimulatory role of GPER1 in rapid, estrogen-induced calcium release; this could be a common rapid signalling pathway within cells for estrogen.

3.4.2 Trafficking of ERα and GPER1 by estradiol in mES cells

For translocation of receptors from the nucleus, we used a stringent cut-off i.e., 0.5 with the MCC to understand if receptors were moving out of the nucleus (Davis, Vajaria, et al., 2023). E2-BSA and 17β-estradiol (E2) increased the movement of ERα-66 to the plasma membrane in hypothalamic astrocytes and in the N38 (Dominguez et al., 2013) cell line as well as in neurons (Dominguez & Micevych, 2010) within 30 minutes, suggesting that translocation of the ERα could be non-genomically mediated. The timeframes used in our study i.e., 20 minutes indicates that translocation of this receptor by GPER1 agonism may also be mediated by non-genomic signalling. In the N42 cell line, only the GPER1 agonist, G-1 decreased nuclear localisation of ERα; G-15, the GPER1 antagonist, reversed this effect demonstrating specificity. However, unlike in N38 cells, ERα did not translocate out of the nucleus to the cell membrane; the location of the ERα after 20 minutes of G-1 application is not known. There are only a few studies that demonstrate direct crosstalk between GPER1 and the ERs. For example, we have previously shown that G-1 increased the phosphorylation of ERα in the male mouse ventral hippocampus (Hart et al., 2014). In testicular cancer cells, GPER1 stimulation of a PKA pathway rapidly induced the expression of ERα-36 isoform (Wallacides et al., 2012). As far as we are aware, there is no other report of GPER1-mediated translocation of ERα. Our data also suggests that this could be cell line specific since this is seen in mES but not in N42 cells.

In contrast, both the ERβ agonist, DPN and E2-BSA slightly increased nuclear localization within 20 minutes when compared to the DMSO control. It is possible that the reason that there was no translocation by 17β-estradiol itself because of the opposing actions of ERα and ERβ. In many cell contexts, ERβ can oppose ERα-mediated transcriptional activity (Matthews & Gustafsson, 2003) (Pettersson et al., 2000) and both isoforms had opposing roles in proliferation in the prostate epithelial cells (Ellem & Risbridger, 2009).

3.4.3 Regulation of aromatase mRNA by ERβ and GPER1

A second output of non-genomic signalling is the rapid upregulation of aromatase mRNA within 20 minutes by both ERβ and GPER1 agonists in N42 hypothalamic cells but not in mES cells. Most of the regulation of aromatase within similar time frames has been studied in terms of aromatase activity. For example, the provision of calcium/ATP or glutamate in quail mPOA explants inhibited aromatase activity and this inhibition could be relieved by inhibitors to PKA, PKC, tyrosine kinase and ser/threonine kinases. This demonstrated that aromatase activity could

be decreased by phosphorylation of the enzyme (Balthazart et al., 2003a, 2003b). *In vivo*, this decrease in aromatase activity was seen in the mPOA of the male quail after visualization of the female, and was restored to basal levels within 2 hours, by a mechanism that is believed to be non-transcriptional and is most likely a post-translational change (de Bournonville et al., 2013). However, this remains to be tested further, at the level of the aromatase protein.

GPER1 has been reported to increase aromatase mRNA and aromatase activity in 24 hours in tamoxifen-resistant MCF-7 cells and does so, in a tamoxifen-dependent manner, within 12 hours in another cancer cell line i.e., SKBR3 cells, to increase invasiveness. However, this is not rapid regulation; this is thought to be due to transcriptional upregulaton of aromatase mRNA and posttranslational modifications of aromatase protein to enhance aromatase activity (Catalano et al., 2014). In contrast to this upregulation of aromatase, another study demonstrated that GPER1 antagonism with G-15 increased aromatase mRNA in both mature mouse testis and a Leydig cell line within 24 hours, suggesting that GPER activation suppresses aromatase mRNA in the male reproductive tract. The mechanism that underlies this is also unknown (Kotula-Balak et al., 2018).

As far as we are aware, no study has reported the *rapid* regulation of aromatase mRNA in any tissue by any ER. A single study in female mouse neuronal embryonic cultures derived from the amygdala showed that the addition of 17β-estradiol induced aromatase mRNA via a ERβ-dependent mechanism within 2 hours (Cisternas et al., 2017). The time frame in our study i.e., 20 mins suggests that this is most likely due to stabilisation of the aromatase mRNA. Though this mechanism has not been reported for ERβ and/or GPER1, aromatase mRNA is capable of being stabilized by several other agents. For example, macrophage inhibitory factor stabilised aromatase in endometrial cells (Veillat et al., 2012), dioxin slowed down the degradation of the aromatase transcript in MCF-7 breast cancer cells (Chan et al., 2010), and trichostatin decreased the stability of the aromatase transcript in MCF-7 cells (Łuczak & Jagodziński, 2009).

3.4.4 Mechanisms of ERβ and GPER1-mediated upregulation of aromatase mRNA

Uniquely, we showed that GPER1 rapidly increased aromatase, most likely initiated from the plasma membrane, since this is the predominant location for this receptor in N42 hypothalamic cells. G-15, the GPER1 antagonist also decreased the ERβ-mediated increase of aromatase mRNA, suggesting that there is crosstalk between these two receptors. Consistent with this, G-1 decreased DPN-mediated upregulation of aromatase mRNA, suggesting that these receptors were using the same downstream pathway. What is the mechanism by which G-1 and DPN increase aromatase mRNA? Both a PKA inhibitor and a calcium-chelator i.e., BAPTA-AM but

not MEK inhibitors decreased aromatase mRNA that was increased by GPER1 or ERβ, suggesting that these pathways are important. Though how aromatase mRNA is regulated by rapid signalling pathways is poorly studied, data suggests that PKA activation can increase aromatase expression. For example, PKA activation by forskolin also increased aromatase in granulosa cells (Luo & Wiltbank, 2006) while dexamethasone, a GR agonist synergistically increased aromatase activity with forskolin in an osteoblastic cell line (Watanabe et al., 2007). Since GPER1 is linked to a Gαs protein and can activate PKA signalling (Thomas et al., 2005), this could be a probable pathway in the N42 cell line. As far as we are aware, there is no data on how calcium regulates aromatase mRNA expression though calcium is known to increase stability of some transcripts such as parathyroid hormone (Naveh-Many & Nechama, 2007), brain derived growth factor (BDNF) (Fukuchi et al., 2005) by the induction of protective binding proteins.

3.4.5 Temporal control of aromatase mRNA by ER isoforms

This study shows that ERβ and GPER1 can acutely regulate aromatase mRNA. However, regulation of aromatase mRNA in the same mHypo-42 cell line had previously been shown to be upregulated within a longer time period i.e., 6 hours and 24 hours via ERα mediated binding to an AP1 element. siRNA to ERα or ICI 182,780 administration abolished this estrogen-mediated induction of aromatase (Yilmaz et al., 2009). Consistent with these reports, trophoblast cells aromatase mRNA increased because of higher binding of ERα to enhancer elements in the aromatase promoter in 72 hours (Kumar et al., 2009). However, in our study, PPT, an ERα-selective agonist did not increase aromatase expression within 20 minutes. It is possible that aromatase mRNA is being stabilized within these short timeframes by ERβ and GPER1 while it is being induced transcriptionally by ERα over longer time frames. A more in-depth analyses using ERβ specific antagonists, siRNA to ERβ and GPER1 and dissection of signal transduction pathways remains to be performed to understand the temporal regulation of aromatase mRNA.

3.4.6 Physiological relevance of ERβ and GPER1-mediated regulation of aromatase

What is the physiological relevance of ERβ and GPER1-mediated rapid increase of aromatase mRNA expression? This is more difficult to answer without *in vivo* experiments. However, it is possible that the rapid increase of aromatase by mERs control initial sequences of social behaviours which need to occur quickly upon appropriate stimuli. For example, in the male

quail, acute inhibition of brain aromatase decreased the appetitive sex behaviour (ASB) but not the consummatory sex behaviour in the presence of the female, within 30 minutes of i.c.v injection. Similarly, ICI 182,780 and tamoxifen, ERα and ERβ antagonists, injected i.c.v also inhibited ASB but not consummatory sex behaviour within 30 minutes of injection. This ASB but not consummatory sex behaviour was however restored if E2-BSA or ERβ-agonist was given i.c.v 15 mins after the aromatase inhibitors (Seredynski et al., 2015; Seredynski et al., 2013). These elegant experiments clearly demonstrate that this part of the mating behaviour sequence i.e., sexual motivation is dependent on rapid non-genomic signalling initiated by neuroestrogens acting at membrane-bound ERβ.

This is consistent with our novel data on ERβ-induced regulation of aromatase mRNA. In addition, mice with a mutation of ERα that does not allow it to anchor to the plasma membrane show reduced sex behaviour in males (Khbouz et al., 2020) demonstrating that membrane-initiated actions from both ERα and ERβ appear to be important in male sex behaviour in vertebrates.

3.5 Summary

This study is important because it demonstrates that a mER, GPER1, is a collaborator to the classical ERs to increase the final output (R. Vajaria & N. Vasudevan, 2018). Importantly, we show for the first time that GPER1 can collaborate or interact with *both* classical ERs within acute timeframes. For example, GPER1 mediates ERα translocation in mES cells. We also demonstrated a nonclassical action of GPER1 and ERβ in mediating ligand-independent regulation of aromatase mRNA expression through a convergent calcium/PKA/CREB pathway in a mouse hypothalamic neuronal cell lines. Though the mechanism remains largely unknown, this is similar to the mGluR1 receptor which acts in concert with ERα in the female rat arcuate nucleus to increase lordosis (Dewing et al., 2007; Micevych & Dewing, 2011) and with ERβ in the male quail mPOA to increase male sex behaviour (Seredynski et al., 2015). Importantly, our current study suggests that different isoforms of the ER are used at various timepoints to provide temporal control.

3.6 Supplementary methods for chapter 3

This section is an overview of material and methods in chapter 2, describing optimisation for the translocation of ERs .

3.6.1 Preliminary data

Preliminary data showed that the highest nuclear trafficking for all agonists towards the nucleus occurred in mES cells at 30 minutes after hormone/agonist treatment before returning to baseline after 1 hour (Figure 3.6 and Figure 3.7). Interestingly, we also observed significant differences in no treatment vs DMSO-treated cells, suggesting that concentrations of DMSO has an impact on translocation of these receptors.

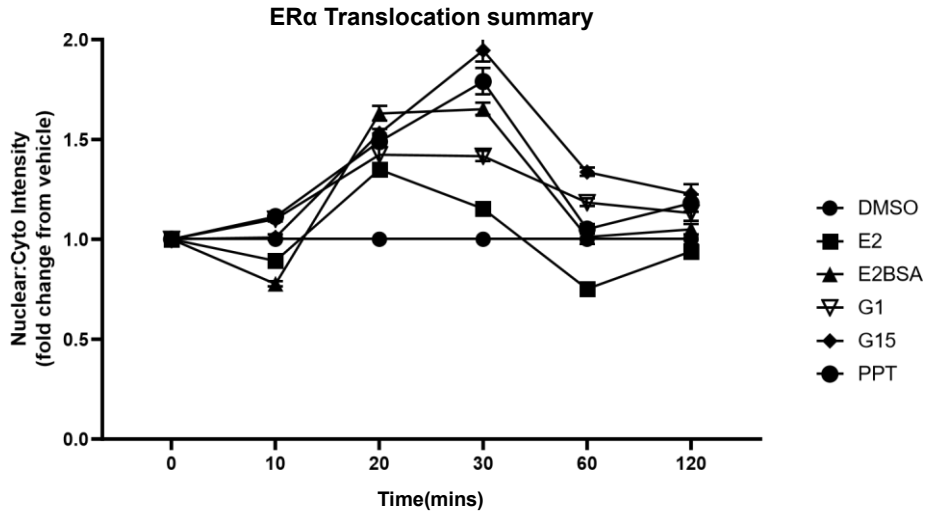

Figure 3.6. Optimisation of the translocation of ERα in mES cells. Cells were treated with vehicle (1% DMSO), or 10-8M E2, E2-BSA, G1, PPT, or DPN for 10 mins, 20 mins, 30 mins, 60 mins and 2 hours. Cells were then fixed with 4% PFA and immunocytochemistry (Section S1.4) carried out with anti-ERα antibody. Cells were imaged and analysed using Image J for the nuclear: cytoplasmic ratio which delineates the amount of immunoreactive ERα in the nucleus and in the cytoplasm respectively. Results for every time point were normalised to the DMSO control. N=100 cells/time point

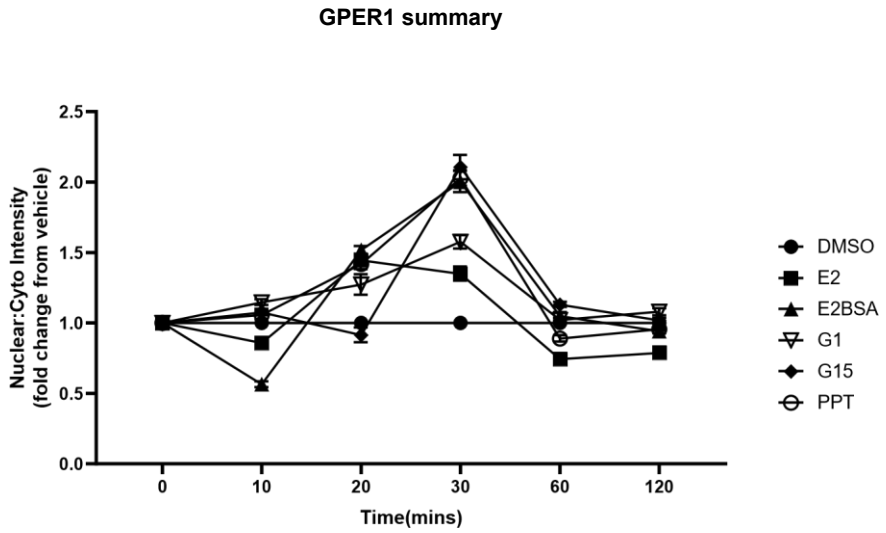

Figure 3.7. Optimisation of translocation of GPER1 in mES cells. Cells were treated with vehicle (1 %DMSO), 10-8M E2, E2-BSA, G1, PPT, or DPN for 10 mins, 20 mins, 30 mins , 60 mins and 2 hours. Cells were then fixed with 4% PFA and immunocytochemistry (Section S1.4) carried out with anti-GPER1 antibody. Cells were imaged and analysed using Image J for the nuclear: cytoplasmic ratio which delineates the amount of immunoreactive GPER1 in the nucleus and in the cytoplasm respectively. Results for every time point were normalised to the DMSO control. N=100 cells/time point

Goat anti -Mouse IgG (H+L) Cross Adsorbed Secondary Antibody, Alexa Fluor 568 (A-11004)	-Invitrogen, Thermo - Fisher Scientific, UK	Goat	1:300
Goat anti -Chicken IgY (H+L) Cross Adsorbed Secondary Antibody, DyLight 350 (SA5-10069)	-Invitrogen, Thermo -Fisher Scientific, UK	Goat	1:300
Goat anti -Chicken IgG (H+L) Cross Adsorbed Secondary Antibody, Alexa Fluor 647 (A-21449)	-Invitrogen, Thermo -Fisher Scientific, UK	Goat	1:300

Table S1.3 Details of primary and secondary antibodies used for immunocytochemistry in mES and mESn. Primary antibodies

4.Neurosteroids in the social behaviour network of the mouse

Chapter 4: This has been submitted for publication in Endocrinology.

Submitted publication: Neurosteroids in the social behaviour network of the mouse.

Dovey, Janine., Davis, DeAsia., Knight, P., and Vasudevan, N. Submitted to Endocrinology, November 2023.

Figures: All figures that relate to the male mouse represent data collected, analysed and generated by Ms. DeAsia Davis. All figures that relate to the female mouse represent data collected, analysed and generated by Ms. Janine Dovey, a student in the laboratory supervised by Nandini Vasudevan. Hence, this paper has equal contributions from Ms. Janine Dovey and Ms. DeAsia Davis and is submitted as such to Endocrinology.

Intellectual contribution: The work in the paper was originally conceived and supervised by Dr. Nandini Vasudevan and Professor Phil Knight. Ms. DeAsia Davis also independently optimised and validated the acute slice technique that is integral to this paper. Many of the ideas in this chapter was honed by discussion amongst Ms. Janine Dovey, Ms. DeAsia Davis and Dr. Nandini Vasudevan.

Writing: The results and methods were written by Ms. DeAsia Davis and Ms. Janine Dovey as well as parts of the introduction and discussion, in discussion with Nandini Vasudevan. Some

parts of the introduction and discussion were written by Dr. Nandini Vasudevan with discussion with both Ms. Janine Dovey and Ms. DeAsia Davis.

Neurosteroids in the social behaviour network of the mouse

Janine Dovey[1a], DeAsia Davis[1a], Philip G. Knight[1] and Nandini Vasudevan[1* 1]: School of Biological Sciences, University of Reading, Reading UK RG6 6AS. [a]: Both authors contributed equally to this paper.

*Corresponding author:
Dr. Nandini Vasudevan,
School of Biological Sciences, University of Reading, Reading UK RG6 6AS.
Email: n.vasudevan@reading.ac.uk

Keywords:
Neurooestrogen, hypothalamus, steroidogenesis, sexual dimorphism, neurotestosterone

Funding
JD was funded by the School of Biological Sciences, University of Reading UK.

Abstract

Neurosteroids are steroids made in the central nervous system. Of these, neurooestrogens are the best studied and have been shown to be synthesized *de novo* from cholesterol, at least in the rodent hippocampus. Moreover, deletion of aromatase in the mouse, the enzyme that converts testosterone to oestrogen has been shown to decrease cognition, neuronal spine density as well as some social behaviours such as sex behaviour in both sexes. However, the relevance of aromatase action has generally been more unequivocally shown in males.

The social behaviour network (SBN) that includes many hypothalamic areas is critical for the display of sexually dimorphic behaviours. Though several nodes of the SBN have been shown to express aromatase, the production of neurosteroids and the expression of steroidogenic enzymes in age-matched males and female rodents in different nodes of the SBN has not been characterized. Using a novel *ex vivo* slice culture system, we show that the production of neurooestrogen and neurotestosterone increases within 24 hours in all SBN nodes irrespective of sex, with males showing higher production of both testosterone and estrogen. In general, levels of steroidogenic enzymes are higher in males than in females in every SBN nuclei, independent of time. However, we show that expression of steroidogenic enzymes is sexually dimorphic with increased levels of *Stard1* and *cyp19a1* within 24 hours in some female SBN nuclei. Our data in the mouse show for the first time that sexual dimorphism in behaviour is possibly underpinned by sexual dimorphism in neurosteroid production.

4.1 Introduction

Steroid hormones have widespread effects on sexually dimorphic behaviours via nuclear hormone receptors that are abundantly expressed in the brain. The neural circuits underlying behaviour are found within the social behaviour network (SBN); a conserved, sexually dimorphic network of brain nuclei (Newman, 1999). The hypothalamus contributes several nuclei to the SBN, including the medial preoptic area (mPOA), anterior hypothalamus (AH), and ventromedial hypothalamus (VMH), and is a critical mediator of lordosis behaviour in female rodents (Pfaff, 1998) and aggressive behaviour in male rodents (Sano, Tsuda, et al., 2013) (Unger et al., 2015) when activated by sex hormones.

4.1.1 Expression of steroidogenic enzymes

Sex hormones not only originate from the gonads or adrenals but can be produced by the brain itself in *de novo* synthesis from cholesterol or *in situ* from haematogenous precursors (Giatti et al., 2019). *De novo* neurosteroidogenesis requires the expression of both steroidogenic acute regulatory protein (StAR), which mediates the transfer of cholesterol to the inner mitochondrial membrane, and the mitochondrial enzyme cytochrome P450 side-chain cleavage (P450scc), which converts cholesterol into pregnenolone. RT-PCR has demonstrated the regional and sexually dimorphic distribution of *Cyp11a1* (encoding P450scc) in the rat brain, where cortical expression is high amongst both male and female rats, but hippocampal expression is much higher in the female than the male (Mellon & Deschepper, 1993). Discrete cell populations in the mouse brain express P450scc and StAR proteins, suggesting that only a few cells can synthesise neurosteroids *de novo*, though co-immunoreactivity has been observed in the hypothalamus of both male and female mouse brains (King et al., 2002). Enzymes involved in further steroid metabolism, including 3β-hydroxysteroid dehydrogenase (3β-HSD), encoded by *Hsd3b1*, 17β-hydroxysteroid dehydrogenase (17β-HSD), encoded by *Hsd17b1*, and cytochrome P450 aromatase, encoded by the *Cyp19a1* gene, have also been demonstrated in the mammalian brain by means of immunohistochemistry, *in situ* hybridisation, Western blot, RT-PCR, and transgenes (Stanic et al., 2014) (Pelletier, 2010), (Stanic et al., 2014). Many of the steroidogenic enzymes show regional and sex differences in expression across the cerebral cortex, cerebellum, and hypothalamus. For example, female rats tend to express higher levels of *Stard1* encoding StAR mRNA in the cerebellum and *Hsd3b1* mRNA in the cerebral cortex (Giatti et al., 2019). Meanwhile, the female mouse hypothalamus expresses less *Hsd3b1* than the male (Nishida et al., 2005). In contrast, in the male hypothalamus, the bed nucleus of stria terminalis (BNST), preoptic area, and amygdala exhibit higher levels of aromatase expression than in the female (Tabatadze et al., 2014) (Stanic et al., 2014) (Wu et al., 2009), However, the dorsal hippocampus

and cingulate cortex did not show any sex dimorphisms in aromatase expression (Tabatadze et al., 2014).

4.1.2 The role of neurosteroids

Steroids made within the brain, i.e., neurosteroids, contribute to rapid signalling functions to exert a variety of effects on the nervous system, including myelin formation in peripheral nerves (Schumacher et al., 2001), synapse formation and maintenance in the hippocampus (Kretz et al., 2004; Prange-Kiel & Rune, 2006) , dendritic spine formation in the hippocampus (Murakami et al., 2018) (Kato et al., 2014), and promotion of GABAergic transmission in the VMH (Uddin et al., 2020). Many of these cellular or network effects have behavioural consequences. For example, 112euroestrogens rapidly modulate auditory processing circuits in the songbird brain to enhance song memory (Vahaba & Remage-Healey, 2018). In the mouse, neurooestrogen in the medial amygdala drives aggressive behaviour (Unger et al., 2015) and sexual motivation in male quail (Seredynski et al., 2013). In ovariectomised female mice, both intracerebroventricular and intra-VMH injections of E_2-benzoate can drive lordosis in a protein kinase-dependent pathway (Domínguez-Ordóñez et al., 2019), suggesting hypothalamic neurooestrogen is important for female sexual behaviour. In male mice with a forebrain-specific aromatase knockout (ArKO), sexual behaviour is decreased despite high levels of testosterone (Brooks et al., 2020). In the female rat hippocampus, 112euroestrogens fluctuate across the oestrous cycle, following a similar cyclicity in concentration to that in the plasma (Kato et al., 2013). However, the relative contribution of ovarian oestrogen and neurooestrogen to the overall concentrations measured in the brain remains unclear.

Concentrations of circulating sex hormones are not a direct representation of the concentrations present in the brain because of regional, and sexually dimorphic, changes in aromatase activity under certain physiological conditions. In the newborn rat, high aromatase activity in the hypothalamus correlates with higher levels of oestradiol and low levels of aromatase activity in the hippocampus and cortex correlates with lower levels of brain-derived oestradiol (Konkle & McCarthy, 2011). Neurosteroids have been measured to a greater extent in the songbird (Jalabert et al., 2022) (Thierry D. Charlier et al., 2010) (Saldanha et al., 2013), which contains the same SBN regions along with the caudal medial nidopallium (NCM); a steroid-responsive brain region important for song processing and social behaviours (Vahaba & Remage-Healey, 2018). In the rodent, neurosteroids have been measured mostly in the hippocampus (Hojo et al., 2004; Hojo & Kawato, 2018; Hojo et al., 2008) (Kretz et al., 2004), where they play an important role in learning and memory (Frick & Kim, 2018). Neurosteroids exist in higher concentrations than that of plasma steroids in both the songbird brain and the rodent hippocampus (T. D. Charlier et al., 2010) (Kato et al., 2013).

However, absolute concentrations of sex hormones and the regulation of their production within the adult SBN have not yet been demonstrated in the rodent.

Using a novel ex vivo slice culture method, we show differential expression between the sexes of steroidogenic enzymes and differences in local sex hormone concentrations that are important for the dynamics of neurooestrogen signalling *in vivo*, in response to stimuli. This will contribute to a greater understanding for the paracrine roles of locally produced hormones in sexually dimorphic brain processes.

4.2. Methods

4.2.1 Materials: Animals/Chemicals

Animal tissue was obtained from adult (7-8 week) male and female C57BL/6J mice that were purchased from either Charles River Laboratories, Inc or Envigo Laboratory, UK. Adult male and female mice were single-sex, group-housed and allowed access to water and food *ad libitum*. All chemicals are analytical grade and from Sigma, St Louis, MO or from Fisher Scientific, UK, unless otherwise mentioned.

4.2.2 Preparation of slice culture

This method is a modification of the (Loryan et al., 2013) protocol which has been shown to be effective for long-term drug incubation of acute brain slices. To ensure viability and healthy maintenance of brain tissue, artificial cerebrospinal fluid (aCSF) composed of 129 mM NaCl, 3mM KCl, 1.4mM CaCl2, 1.2 mM MgSO4, 0.4mM K2HPO4, 25mM HEPES, 10mM Glucose and 0.4mM ascorbic acid was used to mimic *in vivo* environments. Prior to decapitation, ascorbic acid from a 400 mM stock solution stored at 4°C, glucose in powder form and CaCl2 from a 200x stock solution was added to the appropriate volume of 10x stock aCSF solution to obtain the final concentrations above. The pH of this final aCSF solution was adjusted to 7.6, filtered using a 22 µm filter, 5mL placed in clean 5 mL glass vials and oxygenated with carbogen for at least 15 mins at 37C.

Following rapid decapitation of adult male mice, the brain was quickly removed from the skull and immediately placed in iced-cold oxygenated 30% sucrose solution. Trunk blood was collected at sacrifice in 1.5-microfuge tubes containing 10 µl of 0.5 M EDTA (Section 4.2.4). Upon removal of the brain from the sucrose solution, the anterior i.e. optic nerve and posterior areas i.e cerebellum respectively were removed with a sharp blade. The brain was placed back in oxygenated cold 30% sucrose solution in the microtome tray. Coronal sections (200µm) at the bregma level of 0.86 mm (lateral septum) to -2.06 mm (ventromedial hypothalamus) corresponding to a series of nuclei from the SBN were cut and immediately placed in each of the 5 ml oxygenated aCSF solution in the glass vials. These were then incubated at 37°C, 95%

O2, 5% CO2 for 45 minutes to 1 hour for recovery from the mechanical stress. Slices corresponding to discrete brain areas were then carefully transferred by pasteur pipette to wells in 12 well plates containing 1.5 mL of filtered aCSF. Slices were incubated at 37C°C in 5% C02 in a humidified tissue culture incubator for 0, 2, 8, 24 and 48 hours, or as stated for each experiment. At the end of the incubation period, aCSF was removed and stored at -20°C prior to neurosteroids measurement. Nuclei are punched out of the slices and used either for RNA isolation (Section 4.2.9) or steroid extraction (Section 4.2.6).

4.2.3 Determination of slice variability

Acute brain slices should remain viable to perform steroid biosynthesis throughout the duration of 24 hours incubation. Viability of brain slices may be assessed through electrophysiological parameters (Breen & Buskila, 2014) and/or measuring the release of lactate dehydrogenase (LDH) (Dos-Anjos et al., 2008). Here we used the trypan exclusion test to assess the viability of the slice, as per (Strober, 2015);(Legradi et al., 2011).

To determine viability after various incubation periods, brain slices were rinsed in prewarmed phosphate buffered saline (PBS), then fixed and stained simultaneously with 4% paraformaldehyde (PFA) and 0.5% trypan blue in PBS for 30 minutes. Slices were then rinsed with PBS for 30 seconds. Acute slices were carefully mounted on glass slides for imaging. Images were acquired using a Zeiss AxioImager Epiflourescent (Carl Zeiss MicroImaging GmbH) microscope with a 10x objective (brightfield) under identical exposure times. The live/dead cell ratio was determined using the ImageJ Fiji Particle Analyser plugin (Schindelin et al., 2012).

4.2.4 Blood Collection and Plasma Preparation

500 µl of 0.5 M sterile filtered EDTA was used to coat 1.5 ml microfuge tube for 2 mins/RT prior to being discarded. On decapitation, we applied gentle pressure to allow blood flow, and collected trunk blood into EDTA coated Eppendorf tubes which had 10 µl of 0.5M EDTA to prevent clotting. To mix, the tube was gently inverted 5-6 times and chilled on ice until plasma preparation. Samples were centrifuged for 10 mins at 10,000 g, 4°C. Supernatant (plasma) was transferred to a new microfuge tube and centrifuged for 1 minute at 5,000g at 4°C. Filtered plasma samples were aliquoted and stored at -80 C.

4.2.5 Palkovits punch technique for extraction of steroids and for real time PCR.

The Palkovits micropunch technique was first developed in rats by (Palkovits, 1973) and was used here with minor adaptions. After incubation of the slice for the desired times, brain slices were rinsed in prewarmed PBS, then fixed with 4% (PFA) for 30 minutes. Slices were then rinsed with PBS for 30 seconds. Acute slices were placed on a 0.01mm calibration slides and frozen briefly on dry ice. Sections of SBN were identified to closely match the Allen Mouse Brain Atlas, using a dissection scope. From each slice individual nuclei were isolated from both hemispheres using a 0.5mm diameter micropunch cannula (Fine Science Tools, USA) (Table 4.1). Multiple punches from SBN nuclei of individual animals are pooled and collected in microfuge tubes and subject to solid phase extraction. For real time PCR, multiple punches from each SBN nuclei from 3-4 animals were pooled to ensure adequate RNA concentration of high quality; these yields approximately at least 100-120 ng of RNA from 3 animals for each SBN nuclei.

Brain Area	Total # of slices/animal	Size of Punches (mm)	Total number of Punches (2 hemispheres)/animal
Lateral Septum	6	0.5	12
MPOA	5	0.5	10
BNST	2	0.5	4
Ventromedial Hypothalamus	3	0.5	6
Anterior Hypothalamus	3	0.5	8

Table 4.1. Punches from SBN Nuclei. 200 uM slices that span the nuclei of the social behaviour network were obtained from animals. After incubation, specific regions in the slices were punched using the Palkovits technique and punches used either for RNA extraction or for steroid extraction. Punches of SBN nuclei from multiple animals

were typically pooled for RNA extraction as detailed in Methods. For steroid extraction, pooled punches from a SBN nuclei from a single animal were used.

4.2.6 Solid Phase Extraction of steroids from plasma and punches

Solid phase extraction followed the protocol outlined in (T. D. Charlier et al., 2010);(Newman et al., 2008) with minor modifications for brain size. Brain punches from each individual animal were homogenized in 50 µl ice-cold deionized water: 250 µl ice-cold methanol mixture with a Pellet Pestle Cordless Motor (Fisher Scientific, UK) and left overnight at 4°C. For serum, an ice-cold mixture of 100 µl double distilled water: 900 µl methanol steroids was first added and then the mixture homogenized. 3mL C18 columns (Telos, Scientific Lab Supplies, UK) were primed with 3ml of absolute ethanol and equilibrated twice with 2.5mL of deionized water. 5mL of deionized water was added to the sample (punches or plasma) before it was loaded into the C18 column. The column was washed twice with 2.5mL of deionized water and steroids were eluted with 1.5 ml of HPLC-grade 90% methanol. Eluates were collected in glass vials and dried using a Speedvac before being resuspended in 350 µl of 0.1 M PBSG (0.1 M phosphate-buffered saline containing 0.1% gelatin) and 0.7% ethanol. These samples were stored at -20C prior to analyses using ELISA.

4.2.7 Determination of steroid concentration by ELISA

Concentrations of E2 and testosterone (T) in aCSF samples and from punches and serum (which had been subject to solid phase extraction) were measured using competitive in-house ELISAs. E2 ELISA was as outlined in (Cheewasopit et al., 2018). Detection limits of the estradiol and testosterone ELISAs were 10 and 15 pg/ml, respectively. Mean within- and between-plate CVs were <10% and <15%, respectively for both assays.

4.2.8 Determination of neurosteroid concentration in different brain areas

Concentrations of E2 and T per brain region were normalised from pg/ml obtained from the ELISA measurement to pg/mm^3 by the following protocol. First, we determined the total height by multiplying the number of punches used in each sample by the thickness of acute slice (Equation 1 below). Next, we determined the area of each region in µm^2 based on circular punch size (i.e 0.5 mm punch size) using the formula radius^2 X π . The total area in µm^3 was obtained by multiplying the total height (from equation 1) by this area and µm^3 was converted to mm^3 for ease and the concentration of the steroid obtained by ELISA (Section 4.2.7) expressed as [steroid]/mm^3 .

$Total\ Height\ (\ \mu m) = \#\ of\ punches\ X\ thickness\ of\ slice\ (\ um)$ --- Equation 1

4.2.9 Real time PCR for steroidogenic enzymes

0.5mm-1mm brain punches were pooled from each region of the SBN from either 3 or 4 animals and total RNA was extracted using RNeasy Plus Micro Kit (Qiagen Inc, UK) per manufacturers' instructions. DNase digestion was carried out using RNase-Free DNase Set (Qiagen Inc, GmBH) prior to RNA quantitation. RNA integrity and concentration was determined by the Nanodrop 2000 (ThermoScientific, UK) and samples at ratios different from 1.8-2.05 were discarded. 100 ng of total RNA/region was used for cDNA synthesis in a final volume of 20µl using Quanta cDNA synthesis kit (Qiagen Inc, GmBH) per manufacturer's instructions. cDNA was diluted to a final concentration of 1ng/µl in sterile RNase-free 1X TE (10mM Tris-HCl containing 1mM EDTA) and stored at -20°C until use. 5 ng cDNA was used for each real-time PCR reaction using Power Sybr green kit (Fisher Scientific, UK) in a 14 µl total volume, with 380 nM forward and reverse primers using StepOnePlus™ Real-Time PCR System (Applied Biosystems). Primers (Table 4.2) were designed using Primer-Blast (Ye et al., 2012), synthesized using IDT DNA technologies, dissolved at 5 µM in TE and stored at -20°C prior to use. PCR reactions for steroidogenic enzymes were carried out in triplicate using the following PCR profile: Initial Hold: 95ºC for 10 min and then denature at 94ºC, 15s, anneal/extend at 60ºC for 1min for 40 cycles including a standard melt curve at the end of the 40th cycle. Threshold cycles C_T were automatically determined by StepOne™ Software (Applied Biosystems). All samples were normalized to expression levels of an endogenous control gene, *ActB* encoding for β-actin.

Gene	Forward primer (5'to 3')	Reverse primer (5'to3')
Cytochrome P450, family 19, subfamily a, polypeptide 1 i.e. *Cyp19a1* (aromatase)	*GGACACCTCTAACATGCTC TTCCTGGG*	*TGATGAGGAGAGCTTG CCAGGC*
ActB (β-actin)	*TGTGCTGTCCCTGTATGCC TCTGG*	*GGGAGAGCATAGCCCT CGTAGATGG*
Cytochrome P450, family 11, subfamily a, polypeptide 1 i.e. *Cyp11a1* (P450scc)	*AGTCCTGGCTGCCCGGCG*	*GGTGGAGTCTCAGTGT CTCCTTGATGC*
Steroidogenic acute regulatory protein i.e. *Stard1* (StAR)	*GGAGAGGTGGCTATGCAG AAGGC*	*CCATCTTACTTAGCACT TCGTCCCCG*
Hydroxysteroid (3-beta) dehydrogenase 1 i.e. *Hsd3b1* (HSD3β1)	*CAGTATATGTGGAAAATGTG GCCTGGG*	*TGGCATTAGGGCGGAG CCC*
Hydroxysteroid (17-beta) dehydrogenase 1 i.e. *Hsd17b1* (HSD17β1)	*GTGCGAGAGTCTGGCGATC CTGC*	*CGCCCACCAGCTTTTC ATAGAAGG*

Table 4.2. Primers used in PCR reactions. Primer sequences for different steroidogenic enzymes were obtained as detailed in Methods and used to quantitate expression levels in different SBN nuclei in both male and female mice.

4.2.10 Statistical analyses

All data were analysed using Graph Pad Prism 8.4.3 (Graph Pad Prism Inc, USA) and graphs presented as mean ± SEM. All data were first analysed for distribution using the Shapiro-Wilk normality test. For steroid levels in the hypothalamus across time points, a one-way ANOVA followed by a Bonferroni multiple comparison posthoc test was used for parametric data. For

non-parametric data, a Kruskal-Wallis test followed by the Dunn's multiple comparison test was used to compare different time points. Relative gene expression was determined by using $2^{-\Delta\Delta C}{}_T$ method. (Livak & Schmittgen, 2001). The C_t values from each of triplicate samples was first normalized to the average C_t value of the endogenous control gene i.e. *Actb* to obtain the ΔCt value. This ΔC_t of each individual replicate was then normalized to the ΔC_t value of the control group i.e., the 0 hour time point or to the ovary, depending on the experiment. For the expression level of steroidogenic enzymes or for neurosteroid concentration, differences between regions in each sex were first shown by a two-way ANOVA comparing region, time, and the interaction between time and region. Within regions, parametric datasets for 0h *vs* 24h were analysed by an unpaired *t*-test; nonparametric datasets for 0h *vs* 24h were compared by a Mann-Whitney test. A p value of <0.05 was considered significant.

4.3. Results

4.3.1 The brain produces neurosteroids *ex vivo*

The concentrations of sex hormones E2 and T in *ex vivo* hypothalamic brain slices following incubation at different time points are shown in Figure. 4.1. Neurosteroids were measured in the incubation media, in females (Figure. 4.1A and 4.1C) and males (Figure. 4.1B and 4.1D). In female hypothalamic slices, E2 concentration was significantly increased by 8h (Figure. 4.1A, 0h *vs* 8h, $P = 0.0291$). In both females and males, there was a significant increase in E2 between 0h and 24h (Figure 4.1A, females, $P = 0.0373$; Figure. 4.1B, males, $P = 0.0456$), but no increase at 48h (Figure. 4.1A, females, 0h *vs* 48h, $P > 0.999$; Figure. 4.1B, males, 0h *vs* 48h, $P > 0.999$). In female hypothalamic slices, testosterone concentration increased significantly from 0h after 2h incubation (0h *vs* 2h, $P = 0.0067$), showing a continued increase at 8h (0h *vs* 8h, $P < 0.0001$) (Figure. 4.1C). After 24h incubation testosterone had increased significantly from 0h in both females (Fig. 4.1C, $P = 0.0109$) and males (Figure. 4.1D, $P = 0.0257$) and but did not increase resignificantly from 0h after 48h (0h *vs* 48h, $P > 0.999$ for both females (Figu. 4.1C) and males (Figure. 4.1D). Since there was a significant increase in the concentration of both E2 and testosterone at 24h in both males and females alongside satisfactory slice viability (Supp Figure. 3), a 24h incubation period was used for all subsequent experiments.

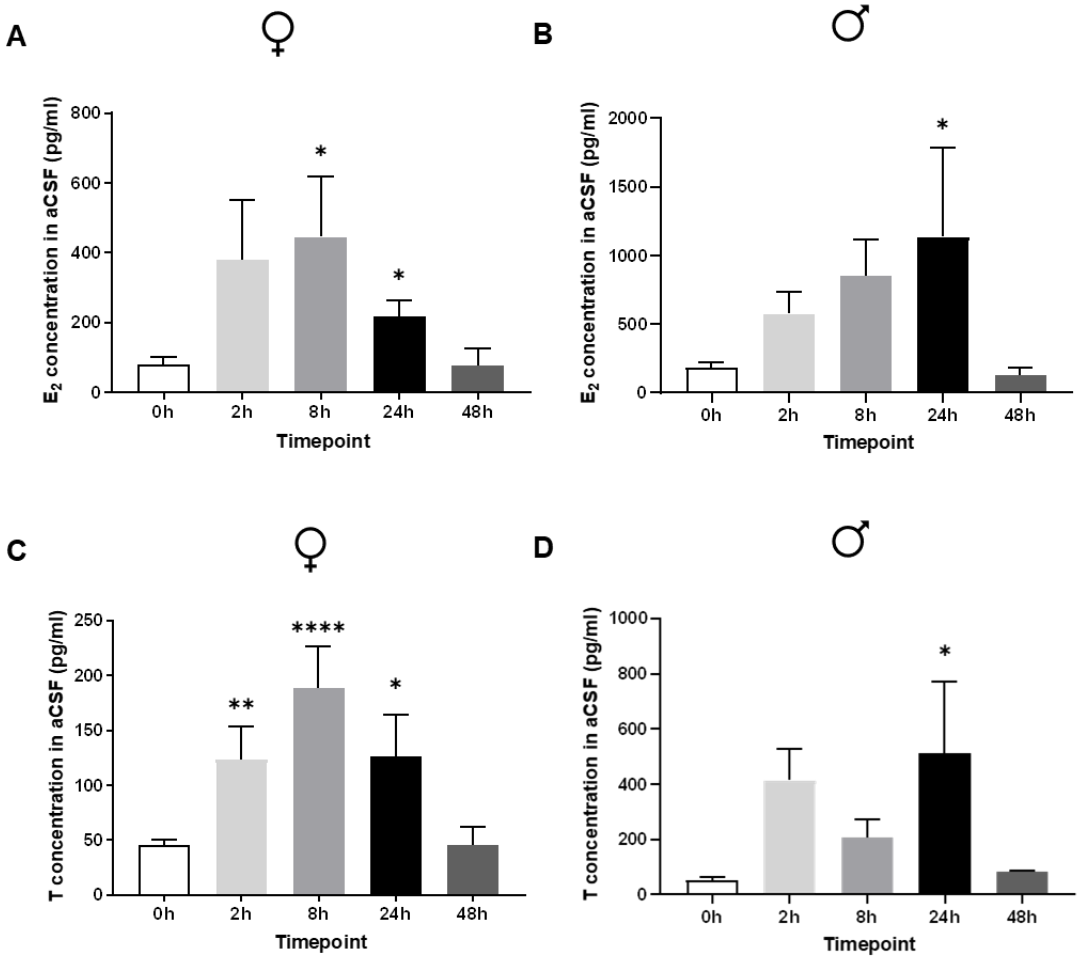

Figure 4.1. Neurosteroid concentrations in hypothalamic brain slices incubated for time points from adult male and female mice. A vibratome was used to take 200µm slices from hypothalamic brain regions of P38-44 C57Bl/6 mice, which were incubated in aCSF for different time points. Neurosteroid concentrations in the female hypothalamus were measured by using aCSF bathing female slices in an oestradiol-based ELISA (A) and a testosterone-based ELISA (C), n = 6 slices from 6 animals for all timepoints except 48h, where n = 3 slices from 3 animals. All animals and slices had a 0h timepoint, therefore n = 24 slices from 6 animals at 0h. The same method was used for the male hypothalamus to measure neuroestrogen (B) and neurotestosterone (D), n = 4 slices from 6 animals; all animals and slices had a 0h timepoint, therefore n = 24 slices from 6 animals at 0h. Differences were established by the Kruskal Wallis test with Dunn's multiple comparisons test post hoc (A and C), or by a one-way ANOVA with Bonferroni's multiple comparisons test post hoc (B and D), * $P < 0.05$ vs 0h, ** $P < 0.01$ vs 0h, **** $P < 0.0001$ vs 0h.

4.3.2 The capacity to synthesise neurosteroids in the social behaviour network is sexually dimorphic

To understand if males differed from females in neurosteroid synthesis, we investigated E2 and testosterone concentration at 0h and 24h across all SBN nuclei (Figure. 4.2). For both E2

(Figure. 4.2A) and testosterone (Figure. 4.2C), there was a significant effect of sex ($P < 0.0001$ for E2 and testosterone), timepoint ($P < 0.0001$ for E2 and testosterone), and the interaction between sex and timepoint ($P = 0.0002$ for E2, $P < 0.0001$ for testosterone). To compare punch dissected SBN nuclei between males and females, the concentrations of neurosteroids from the female mPOA, AH, and VMH was averaged and compared to the neurosteroids from the SBN nuclei of the male. There was a significant effect of sex ($P = 0.001$), timepoint ($P = 0.0005$), and the interaction between sex and timepoint ($P = 0.001$) on E2 concentration in SBN punches (Figure. 4.2B). There was a significant effect of timepoint on the concentration of testosterone in SBN nuclei ($P = 0.0002$), but no effect of sex or the interaction between sex and timepoint (Figure. 4.2D).

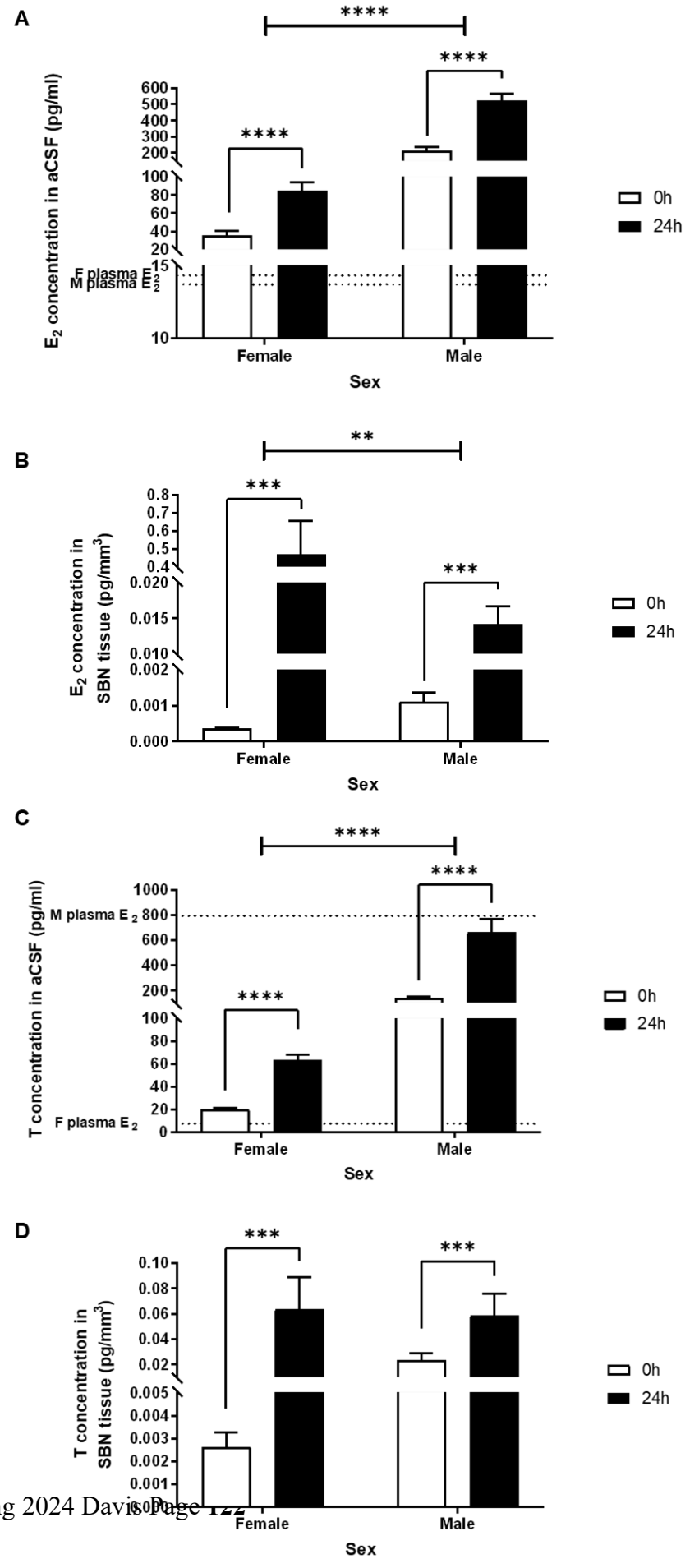
A
****
****
****
600
500
400
300
200
100
80
60
40
20
15
10
F plasma E2
M plasma E2
E2 concentration in aCSF (pg/ml)
Female
Male
Sex
0h
24h
B
**
***
***
0.8
0.7
0.6
0.5
0.4
0.020
0.015
0.010
0.002
0.001
0.000
E2 concentration in SBN tissue (pg/mm3)
Female
Male
Sex
0h
24h
C
****
****
****
1000
800
600
400
200
100
80
60
40
20
0
M plasma E2
F plasma E2
T concentration in aCSF (pg/ml)
Female
Male
Sex
0h
24h
D
***
***
0.10
0.08
0.06
0.04
0.02
0.005
0.004
0.003
0.002
0.001
0.000
T concentration in SBN tissue (pg/mm3)
Female
Male
Sex
0h
24h

Figure 4.2. Neurosteroid concentrations in pooled SBN nuclei of adult male and female mice. A vibratome was used to take 200µm slices from hypothalamic brain regions of P38-44 C57Bl/6 mice, which were incubated in aCSF for either 0h or 24h time points. Concentrations of neuroestrogen (A) and neurotestosterone (C) measured from the aCSF bathing male and female slices comprising the LS, mPOA, BNST, AH, MeA, and VMH after either 0h or 24h incubation were measured using an oestradiolbased ELISA assay or a testosterone-based ELISA assay, respectively. SBN nuclei were punch dissected from their slices after either 0h or 24h incubation in aCSF before being processed by C18 extraction to extract steroids. The steroid elution was used in an oestradiol-based ELISA assay to measure neuroestrogen (B) or a testosterone-based ELISA assay to measure neurotestosterone (D) in pooled male and female SBN nuclei, which were pooled for this analysis. Differences were established by a Kruskal-Wallis test with Dunn's multiple comparisons *post hoc.* * $P < 0.05$ *vs* 0h, ** $P < 0.01$ *vs* 0h, *** $P < 0.001$ *vs* 0h, **** $P < 0.0001$ *vs* 0h.

4.3.3 Neurosteroids are locally regulated across the social behaviour network and are significantly higher than plasma steroids

Across the SBN, neurosteroid production in *ex vivo* slices are locally regulated. Neurosteroids were measured from the incubation aCSF bathing hypothalamic slices containing SBN nuclei (Figure. 4.3A, 4.3C, 4.3E, and 4.3G). In females, there was a significant increase in E2 between 0h and 24h in all slices except those containing the mPOA/BNST (Figure. 4.3A, 0h vs 24h, LS/mPOA, P = 0.0097; AH/MeA, P <0.0001, MeA/VMH, P = 0.0253; mPOA/BNST, P = 0.0939). E2 measured in aCSF was at least 1.9x higher than that measured in plasma, shown by the dotted line (14.33 ±1.71 pg/ml) (Fig. 4.3A). Plasma steroids were lower than neurosteroids measured in aCSF regardless of oestrous stage (Supp Figure. 3). In male slices, there was a significant increase in E2 between 0h and 24h in all slice regions (Figure. 4.3C, 0h vs 24h, LS/mPOA, P <0.0001; mPOA/BNST, P = 0.0061; AH/MeA, P = 0.0014, MeA/VMH, P <0.0001). E2 measured in aCSF was considerably greater than that measured in plasma (13.7 ±0.07 pg/ml, shown by the dotted line), with a minimum difference of 11-fold (Fig. 4.3C).

For testosterone, there was a significant increase between 0h and 24h for all slice regions in both female (Figure 4.3E, 0h vs 24h, LS/mPOA, P <0.0001; mPOA/BNST, P = 0.0007; AH/MeA, P <0.0001; MeA/VMH, P = 0.0079) and male (Figure. 4.3G, 0h vs 24h, LS/mPOA, P <0.0001; mPOA/BNST, P = 0.0004; AH/MeA, P = 0.0157; MeA/VMH, P = 0.0048) ex vivo slices. This was most predominantly seen in male slices, where testosterone concentrations increased by up to 3.6-fold (Figure 4.3G). Plasma testosterone concentrations (shown by the dotted line) were less than that measured in aCSF in both females (7.49 ±1.34 pg/ml) (Figure. 4.3E) and males (660.21±15.07g/ml) (Figure 4.3G).

Since *ex vivo* hypothalamic slices contain steroid-producing cells outside of the SBN nuclei, individual nuclei were punch dissected and steroids were extracted by C18 extraction (Figure. 4.3B, 4.3D, 4.3E, and 4.3H). In the female, only 3 SBN nuclei were dissected, along with the arcuate nucleus of the hypothalamus, a non-SBN region that is important for the expression of lordosis during female reproductive behaviour. There was a significant increase in E2 between

0h and 24h in the female AH (0h vs 24h, P = 0.0095) and VMH (0h vs 24h, P = 0.0270) (Figure. 4.3B). In males, there was a significant increase in E_2 between 0h and 24h for all regions except the VMH (Figure 4.3D, 0h vs 24h, LS, P = 0.0357; mPOA, P = 0.0109; BNST, P = 0.0388; AH, P = 0.0135; MeA, P = 0.0163; VMH, P = 0.1509).

Testosterone concentrations within mPOA punch dissections showed a significant increase in females (Figure 4.3E, 0h vs 24h, P = 0.0152) and males (Figure. 4.3H, 0h vs 24h P = 0.0477). In male SBN punches, there was also a significant increase in testosterone between 0h and 24h in the VMH (Figure. 4.3H, 0h vs 24h, P <0.0001).

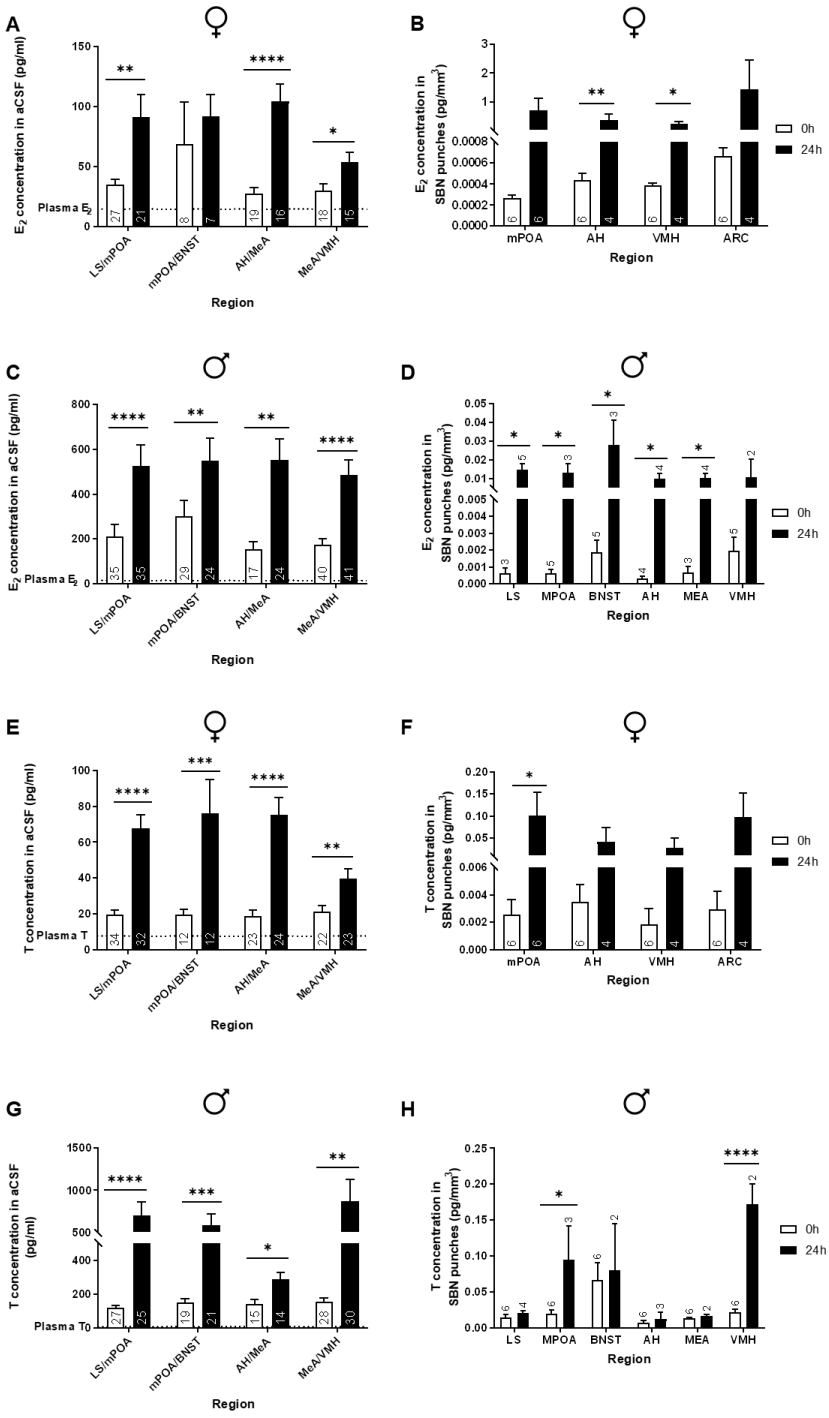

Figure 4.3. Neurosteroid concentrations in SBN nuclei of adult male and female mice. A vibratome was used to take 200µm slices from hypothalamic brain regions of P38-44 C57Bl/6 mice, which were incubated in aCSF for either 0h or 24h time points. Neuroestrogen concentrations were measured from the aCSF bathing female (A) and male (C) slices after either 0h or 24h incubation using an oestradiol-based ELISA assay. Neurotestosterone concentrations were measured from the aCSF bathing female (E) and male (G) slices after either 0h or 24h incubation using a testosterone-based ELISA assay. Dotted lines represent the average plasma levels of oestradiol

(A and C) and testosterone (E and G) of the animals used for neurosteroid analysis. SBN nuclei were punch dissected from their slices after either 0h or 24h incubation in aCSF before being processed by C18 extraction to extract steroids. The steroid elution was used in an oestradiol-based ELISA assay to measure neuroestrogen in female (B) and male (D) SBN nuclei, and in a testosterone-based ELISA assay to measure neurotestosterone in female (F) and male (H) SBN nuclei. Slice n is shown in bars for A-D, contributed by at least 5 animals per group. Animal n is shown in bars for E-H, where one animal contributed one whole SBN nucleus. Differences were established by a two-way ANOVA comparing region, time, and the interaction between time and region. Parametric datasets for 0h vs 24h were compared by an unpaired t-test; nonparametric datasets for 0h vs 24h were compared by a Mann-Whitney test. * $P < 0.05$ vs 0h, ** $P < 0.01$ vs 0h, *** $P < 0.001$ vs 0h, **** $P < 0.0001$ vs 0h.

4.4 Expression of steroidogenic enzymes varies between regions and is sexually dimorphic

4.4.1 Stard1 and Cyp11a1

Expression of *Stard1* mRNA encoding the cholesterol transport protein StAR and *Cyp11a1*, encoding the cytochrome P450 side chain cleavage enzyme, was measured in punch dissections of the SBN of male and female brain slices that had been incubated for 0h and 24h (Figure. 4.4), using real time PCR. In the female, there was a significant increase in *Stard1* expression in the LS (0h *vs* 24h, $P = 0.0266$), BNST (0h *vs* 24h, $P = 0.2179$), AH (0h *vs* 24h, $P = 0.0025$), and MeA (0h *vs* 24h, $P = 0.0125$) (Figure. 4.4A). *Cyp11a1* expression increased significantly between 0h and 24h in the female BNST (0h *vs* 24h, $P = 0.0179$) and AH (0h *vs* 24h, $P < 0.0001$) (Figure. 4.4B).

In male SBN punches, there was no significant difference in expression of either *Stard1* (Figure. 4.4C) or *Cyp11a1* (Figure. 4.4D) between 0h and 24h. However, the male SBN expressed significantly more *Stard1* than the female SBN at both time points (male *vs* female, 0h, $P = 0.0056$; 24h, $P < 0.0001$) (Supp. Figure. 3A). The same was true for *Cyp11a1* (male *vs* female, 0h, $P = 0.0134$; 24h, $P = 0.0031$) (Supp. Figure. 3B).

4.4.2 Hsd3b1 and Hsd17b1

In the female SBN, a significant increase in *Hsd3b1* expression was observed in the LS (0h *vs* 24h, $P = 0.0056$), AH (0h *vs* 24h, $P = 0.0027$), and VMH (0h *vs* 24h, $P = 0.0023$). There was a tendency for increase in the female BNST (0h *vs* 24h, $P = 0.0509$). The female BNST, AH, and MeA all showed a significant increase in *Hsd17b1* 17β-HSD expression between 0h and 24h (BNST, $P = 0.0035$; AH, $P = 0.0093$; MeA, $P = 0.0285$) (Figure. 4.5B).

The male mPOA showed a significant Increase in *Hsd3b1* expression between 0h and 24h (0h *vs* 24h, $P = 0.0177$), but this was not observed elsewhere in the SBN (Figure. 4.5C). There were

no significant changes in *Hsd17b1* expression between 0h and 24h in the male SBN (Figure. 4.5D). Sexual dimorphisms in enzyme expression were clear when the SBN nuclei were pooled per time point (Supp. Figure. 4). At 0h and 24h, the male SBN expressed more *Hsd3b1* than the female SBN (0h, $P = 0.0004$; 24h, $P = 0.0001$) (Supp. Figure. 4A). For *Hsd17b1*, expression was also significantly higher in the male SBN at 24h (male *vs* female, $P = 0.0001$) (Supp. Figure. 4B).

4.4.3 Cyp19a1 (aromatase)

Finally, the expression of *Cyp19a1*, encoding the aromatase enzyme that converts androgen to oestrogen, was measured in SBN punches, shown in Figure 4.6. In the female SBN, expression increased significantly in the mPOA (0h *vs* 24h, $P = 0.0025$), AH (0h *vs* 24h, $P = 0.0013$), and MeA (0h *vs* 24h, $P = 0.0265$) (Figure. 4.6A). There was no significant difference in expression between 0h and 24h in any SBN regions in the male (Figure. 4.6B), but sex dimorphisms in expression were clear when SBN punches were pooled per time point (Supp. Figure. 6). At both 0h and 24h, males expressed significantly more *Cyp19a1* than females at matched time points (Supp. Figure. 6, $P < 0.0001$ for both 0h and 24h).

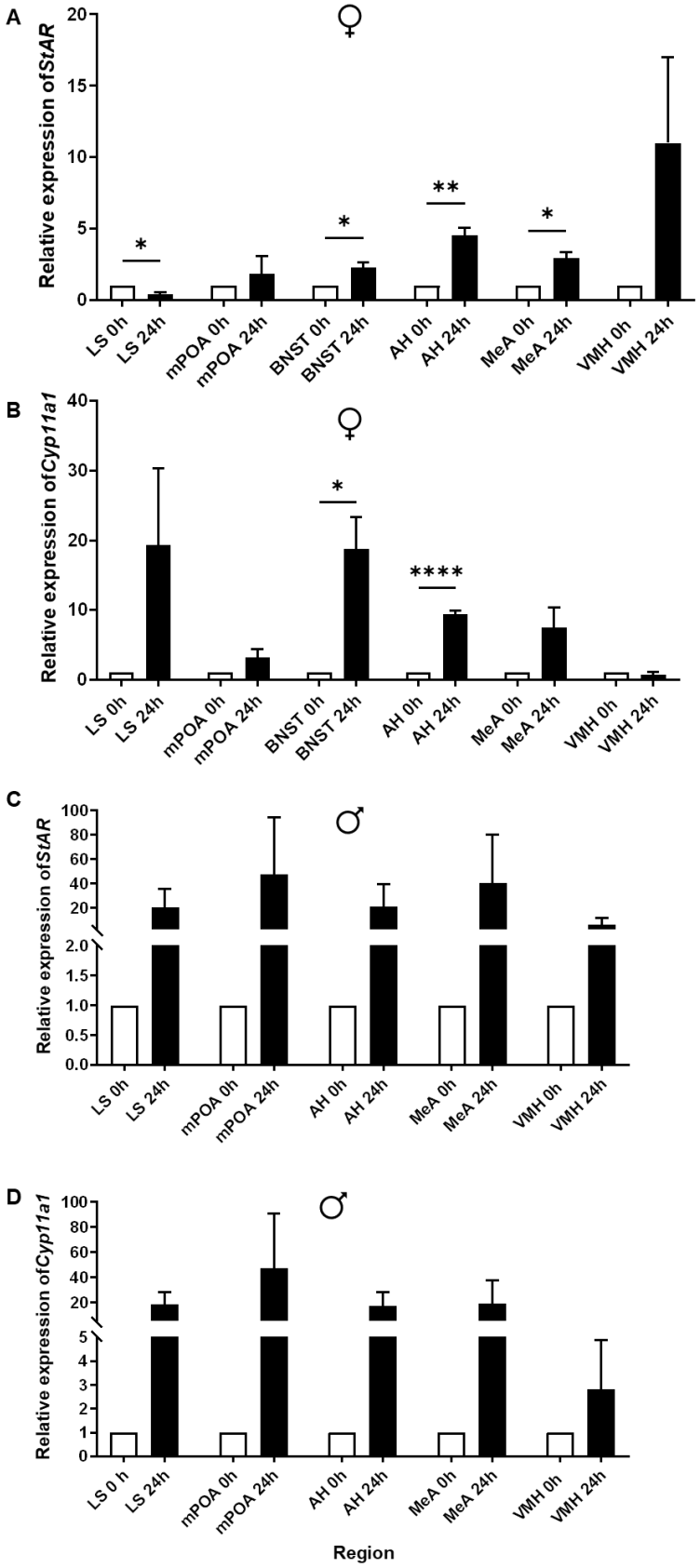

Figure 4.4. Expression of StAR and Cyp11a1 in adult male and female SBN nuclei after 0h and 24h slice incubation timepoints, measured by RT-qPCR. A vibratome was used to take 200μm slices from hypothalamic brain regions of P38-44 C57Bl/6 mice, which were incubated in aCSF for 0h or 24h time points. Following incubation, SBN nuclei were punch dissected, and nuclei from 4 animals were pooled into one, such that n = 3 from a total of 12 animals for A and B, and n = 2 from a total of 6 animals for C and D. Following RNA extraction, cDNA was synthesised and used in an RT-qPCR analysis. Relative expression to the housekeeping gene, β-actin, is shown for StAR (A) and Cyp11a1, encoding cytochrome P450 side-chain cleavage enzyme (B) within female SBN nuclei for 0h vs 24h slice incubation times. Relative expression to the housekeeping gene, β-actin, is shown for StAR (C) and Cyp11a1 (D) within male SBN nuclei for 0h vs 24h incubation times. Differences were established by a two-way ANOVA comparing region, time, and the interaction between time and region. Parametric datasets for 0h vs 24h were compared by an unpaired t-test; nonparametric datasets for 0h vs 24h were compared by a Mann-Whitney test. * $P < 0.05$ vs 0h, ** $P < 0.01$ vs 0h, **** $P < 0.0001$ vs 0h.

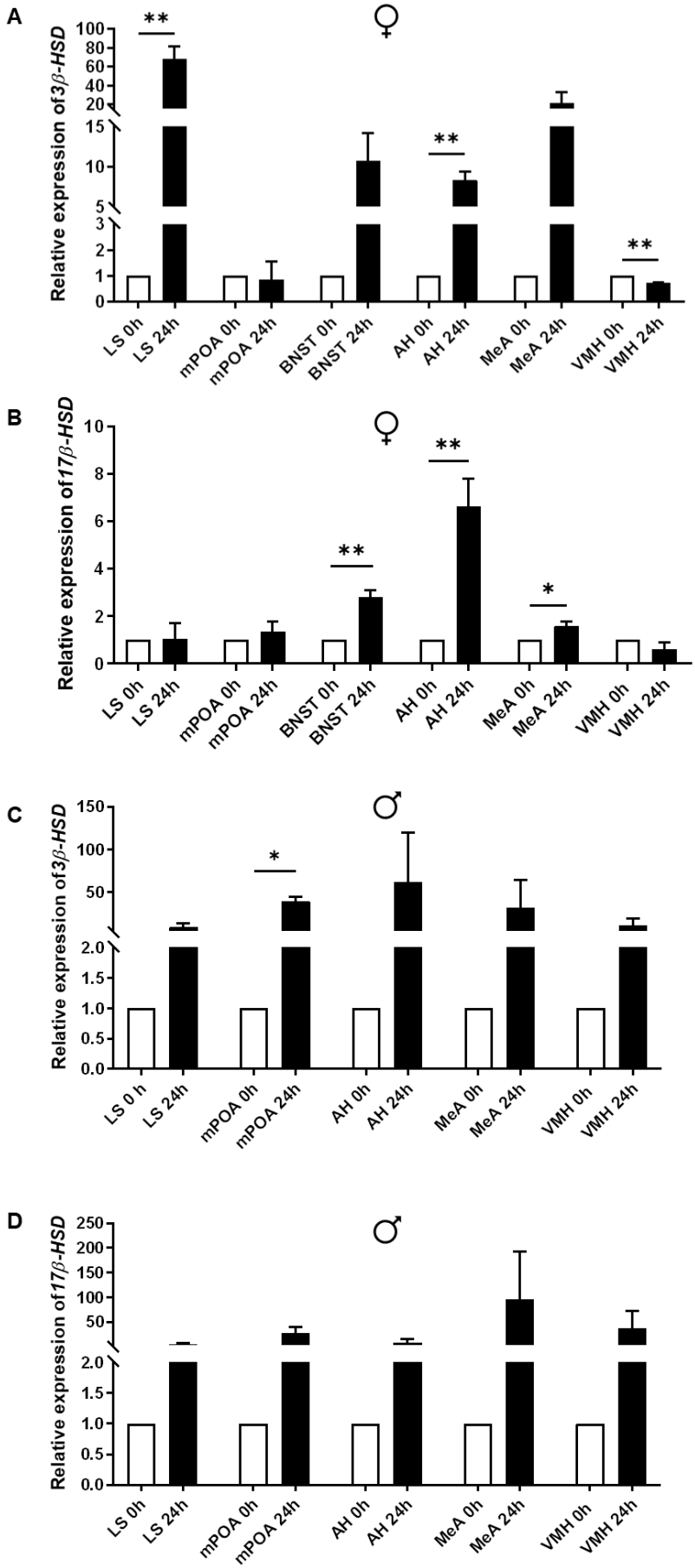
A
Relative expression of 3β-HSD
♀
**
**
**
LS 0h
LS 24h
mPOA 0h
mPOA 24h
BNST 0h
BNST 24h
AH 0h
AH 24h
MeA 0h
MeA 24h
VMH 0h
VMH 24h
B
Relative expression of 17β-HSD
♀
**
**
*
C
Relative expression of 3β-HSD
♂
*
D
Relative expression of 17β-HSD
♂

Figure 4.5. Expression of 3β-HSD and 17β-HSD in adult male and female SBN nuclei after 0h and 24h slice incubation timepoints, measured by RT-qPCR. A vibratome was used to take 200μm slices from hypothalamic brain regions of P38-44 C57Bl/6 mice, which were incubated in aCSF for 0h or 24h time points. Following incubation, SBN nuclei were punch dissected, and nuclei from 4 animals were pooled into one, such that $n = 3$ from a total of 12 animals for A and B, and $n = 2$ from a total of 6 animals for C and D. Following RNA extraction, cDNA was synthesised and used in an RT-qPCR analysis. Relative expression to the housekeeping gene, βactin, is shown for 3β-HSD (A) and 17βHSD (B) within female SBN nuclei for 0h *vs* 24h slice incubation times. Relative expression to the housekeeping gene, βactin, is shown for 3β-HSD (C) and 17βHSD (D) within male SBN nuclei for 0h *vs* 24h incubation times. Differences were established by a two-way ANOVA comparing region, time, and the interaction between time and region. Parametric datasets for 0h *vs* 24h were compared by an unpaired *t*-test; nonparametric datasets for 0h *vs* 24h were compared by a Mann-Whitney test.
* $P < 0.05$ *vs* 0h, ** $P < 0.01$ *vs* 0h.

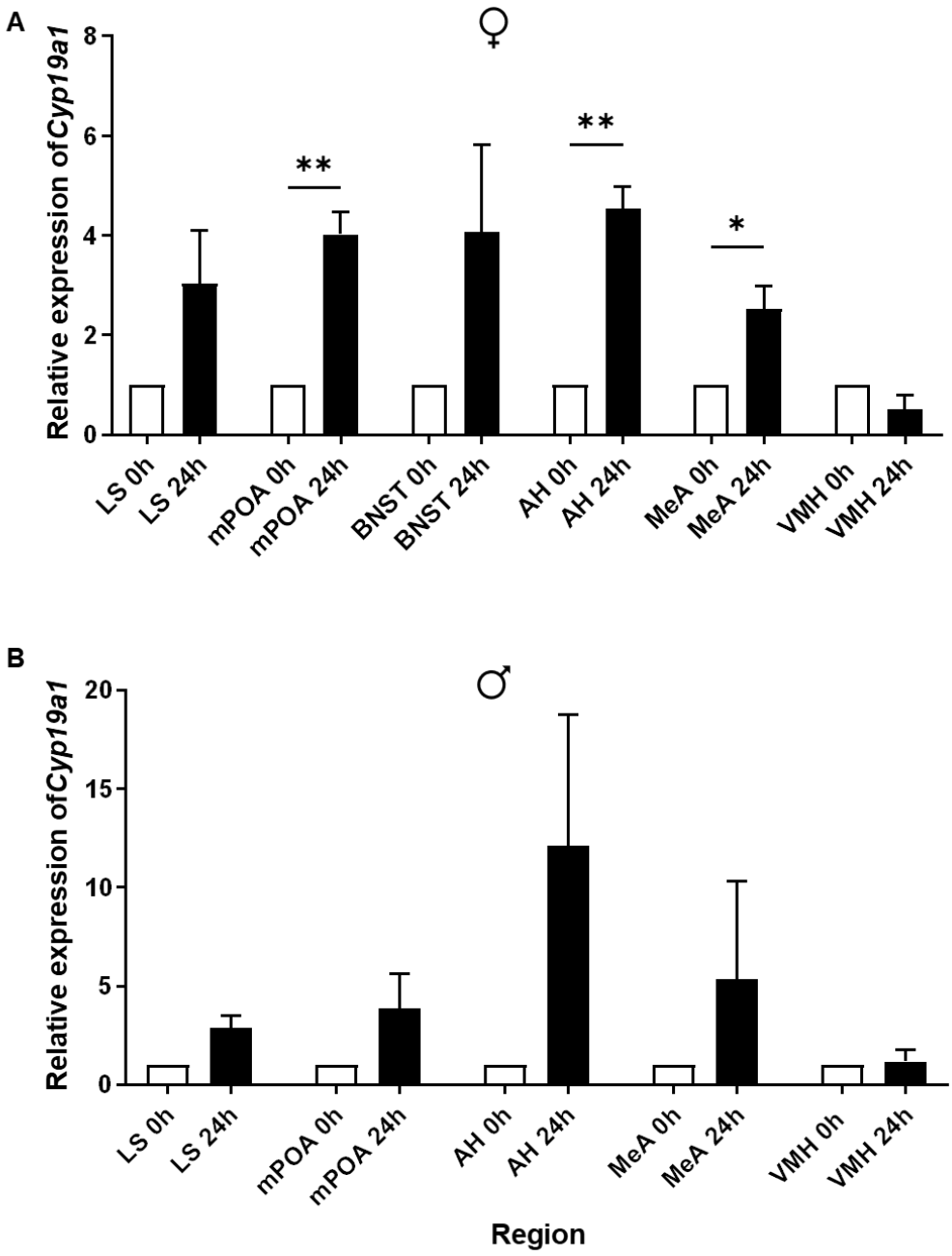

Figure 4.6. Expression of Cyp19a1 in adult male and female SBN nuclei after 0h and 24h slice incubation timepoints, measured by RT-qPCR. A vibratome was used to take 200µm slices from hypothalamic brain regions of P38-44 C57Bl/6 mice, which were incubated in aCSF for 0h or 24h time points. Following incubation, SBN nuclei were punch dissected, and nuclei from 4 animals were pooled into one, such that n = 3 from a total of 12 animals for A and B, and n = 2 from a total of 6 animals for C and D. Following RNA extraction, cDNA was synthesised and used in an RT-qPCR analysis. Relative expression to the housekeeping gene, β-actin, is shown for Cyp19a1, encoding the aromatase enzyme in female (A) and male (B) SBN nuclei for 0h vs 24h slice incubation times. Differences were established by a two-way ANOVA comparing region, time, and the interaction between time and region. Parametric datasets for 0h vs 24h were compared by an unpaired t-test; nonparametric datasets for 0h vs 24h were compared by a Mann-Whitney test. * $P < 0.05$ vs 0h, ** $P < 0.01$ vs 0h.

4.5 Discussion

In the present study, we used a novel method to measure steroid production by ex vivo hypothalamic brain slices from male and female mice. We punch-dissected specific nodes of the hypothalamus and SBN and found substantial sex differences in steroid production and expression of steroidogenic enzymes. In support of previous literature, the male brain was much more active in synthesising steroid hormones, as shown by higher levels of enzyme expression and greater concentrations of oestrogen and testosterone within the brain areas investigated (Hojo & Kawato, 2018; Roselli et al., 1984; Stanic et al., 2014) (Wu et al., 2009) (Tabatadze et al., 2014).

We investigated the synthesis of neurosteroids in male and female slices of the SBN using a modified method outlined in (Loryan et al., 2013), followed by a sensitive in-house assay for neurosteroids. This modified brain slice incubation model allows for the determination of neurosteroids concentration, not only in brain tissue, but also from the aCSF that served as the incubation media. It has been shown previously that, under optimal conditions that encapsulate the control of temperature, pH, bacterial growth and bacterial-induced glial nitric oxide production, acute brain slices can stay viable in aCSF for up to 36h (Buskila et al., 2014). In a series of optimization studies, we found that the volume of aCSF used initially during brain slice recovery has a high impact on viability and neurosteroid output. Using our system where we oxygenated vibratome cut brain slices in 5 ml aCSF, we demonstrate that not only are hypothalamic brain slices viable up to 48 hours, they are functional with secretion of steroids.

4.5.1 Timeline of neurosteroid production in the SBN

We have utilised an incubation system to show that steroid hormones can be measured from brain slices ex vivo after 24h in culture. Moreover, steroid hormone concentration increased over time in the absence of endocrine glands and peripheral steroid precursors. Steroid hormones are lipophilic and therefore cannot be stored in vesicles from which they would easily diffuse (Holst et al., 2004); this eliminates the possibility that the steroids measured were simply those that had originated from the periphery and were stored in the brain, thereby indicating true de novo synthesis. In male hypothalamic slices, both E2 and testosterone had increased by 24h incubation but in female hypothalamic slices, testosterone concentration increased significantly after 2h incubation. Hsd3b1 catalyses the biosynthesis of both progesterone from pregnenolone, and androstenedione from DHEA (Remage-Healey et al., 2008). The synthesis of both steroids is required for testosterone production, catalysed by 17β-HSD (Labrie et al., 1997). In zebra finches, the baseline activity of Hsd3b1 is higher in females than males (Soma et al., 2004). This could explain, at least in part, our observation of a much earlier increase in testosterone in female

hypothalamic slices compared to males. Despite an early increase in testosterone, E2 concentration in female hypothalamic slices did not significantly increase until 8h incubation, which could be due to the time required to synthesise de novo aromatisable precursors, which exist in much lower concentrations in the female brain and plasma (Caruso et al., 2013) (Konkle & McCarthy, 2011). This delayed increase in E2 was observed in a similar slice culture method using male rat brain, where application of tritiated (3H-) DHEA to slice culture medium resulted in the production of 3H-E2 after 5h (Hojo et al., 2004) . DHEA is an intermediate product between pregnenolone and testosterone. Therefore, it makes sense that in a slice without exogenously applied steroid precursors, concentrations of E2 and testosterone (further down the steroidogenic pathway) increase significantly after 8h, because they may be being synthesised de novo from cholesterol.

4.5.2 Sexual dimorphism in neurosteroid concentrations in the SBN

We found profound sex differences in E2 and testosterone concentrations across the SBN. Both oestrogen and testosterone measured from incubation aCSF were significantly higher in males compared to females at both 0h and 24h, and there was a significant increase over time within the same sex (Fig. 2). This highlights not only that the slices continued to synthesise steroids over time in incubation, but also that the basal levels of steroids and the capacity to produce and secrete them over time is significantly greater in male mouse hypothalamic slices. Using an EGFP transgene that is transcribed following the physiological activation of the aromatase gene, Cyp19A1, in male and female mice, it was shown that there are significantly more aromatase-positive fibres in the male BNST, posterodorsal and posteroventral medial amygdaloid nucleus, anterior hypothalamus and mPOA of male mice (Stanic et al., 2014). This would provide more avenues for steroid secretion; a possible reason for our observation of higher steroids in aCSF incubating male slices.

In the hippocampus, which is steroidogenically active (Hojo et al., 2004) and responsive to neurosteroids (Kretz et al., 2004), sophisticated LC-MS techniques revealed that the levels of basal testosterone and 17β-oestradiol were higher in male than in female rats at any stage of the estrous cycle (Hojo et al., 2009; Hojo & Kawato, 2018) consistent with the data that we see at the 0 hour timepoint. However, another study showed higher levels of testosterone in male hippocampus, cerebral cortex and cerebellum than in females but higher levels of E2 in these areas in females than in male rats (Caruso et al., 2013). This opposing sex dimorphism may

highlight regional and/or species differences to our data or could be due to methodological differences. Consistent with previous reports, we observed much higher concentrations of neurosteroids (oestrogen and testosterone) compared to concentrations of steroids measured in plasma (Caruso et al., 2013; T. D. Charlier et al., 2010; Hojo et al., 2009; Nilsson et al., 2015).

Few studies have made similar sex comparisons in the rodent SBN, but in a study comparing neurosteroid levels in male and female rats following acute swim stress, there was no significant difference in hypothalamic levels of corticosterone, deoxycorticosterone, dihydrodeoxycorticosterone, pregnenolone, or progesterone in non-stressed subjects (Sze et al., 2018). E2 was not measured, and testosterone could not be measured because concentrations in the female rat brain fell below the lower limit of quantification in all brain regions examined (Sze et al., 2018). Following swim stress testing, hypothalamic pregnenolone and progesterone increased to a significantly greater level in stressed female rats compared to stressed males (Sze et al., 2018), though this only highlights context-dependent changes in neurosteroids and not constitutive levels or typical synthesis rates in a non-stressed state.

When SBN regions were analysed separately, we found regional differences in steroid production in the male and female mouse brain (Fig. 3). E2 production increased significantly between 0h and 24h in both male and female hypothalamic slices corresponding to the LS/mPOA, AH/MeA, and MeA/VMH, and male slices corresponding to the mPOA/BNST. Testosterone production increased significantly in all slice regions of both male and female mice between 0h and 24h. In steroid extractions from punch dissections, the male SBN showed a significant increase in testosterone in both the mPOA and VMH and a significant increase in E2 across the whole SBN except the VMH, though there was a trend for increase. The female SBN showed a significant increase in E2 in the AH and VMH, and a significant increase in testosterone in the mPOA. Taken together, this suggests that some mouse SBN nuclei synthesise their own neurosteroids. Typically, neurooestrogen synthesis in the rodent is analysed by means of aromatase activity, which can be measured indirectly through the production of 3H2O in brain homogenates incubated with [1β-3H] androstenedione (Roselli et al., 1984). Hypothalamic preoptic area homogenates from male rats showed higher aromatase activity than homogenates of female rats, regardless of oestrous stage (Roselli et al., 1984). The same method has also shown that aromatase activity is greater in the male VMH, BNST, and MeA (Roselli et al., 1985) consistent with our observations of greater levels of E2 in these very same areas of the male mouse brain compared to females. To our knowledge, there are no detailed reports of

neurosteroid concentrations in the intact, non-hormone-primed female rodent SBN available to compare with our data.

Neurosteroid concentrations have been investigated more thoroughly in the bird SBN and caudal medial nidopallium (NCM): a node outside the SBN but responsive to steroid hormones and significant in the expression of complex and sexually dimorphic avian behaviour (Vahaba & Remage-Healey, 2018). Palkovits punch and C18 steroid extraction from behaviourally significant brain areas of sexually naïve male zebra finches also revealed regional differences in E2 concentration (Thierry D. Charlier et al., 2010). The NCM expresses high levels of aromatase (Saldanha et al., 2000), and unsurprisingly displayed the highest levels of E2, though this was not significantly different to the levels observed in the mPOA (Thierry D. Charlier et al., 2010). In male breeding song sparrows, E2 concentrations in micro dissected mPOA and AH did not differ from levels in the NCM, and whilst E2 was significantly lower in the VMH compared to the NCM and AH, it did not differ from levels observed in the mPOA (Jalabert et al., 2022). Despite the species difference, there is similarity in the regional steroidogenic activity in the SBN, at least in the male mouse where all regions of the SBN studied displayed higher levels of E2 at 24 hours.

Sex dimorphism is most easily visible when comparing secreted neurosteroids in the aCSF rather than punches of a SBN area, possibly due to methodological constraints of extraction or because of synthesis from overlapping brain regions in the slice. One caveat when comparing data, however, are the methodological differences and the units in which concentrations are measured. Studies measuring neurosteroids by LC-MS/MS or GC-MS/MS may present data as pg/mg protein (Caruso et al., 2013; Thierry D. Charlier et al., 2010; Hojo et al., 2004). Other studies have expressed neurosteroid concentrations in nM values (Kato et al., 2013). Our steroid concentrations were presented as pg/ml, given the liquid phase of incubation (aCSF) and pg/mm3 tissue, given the technical difficulty of accurately weighing ‘wet’ mouse brain punches. This further highlights the importance of having such comparisons between regions and sex carried out in one study.

4.5.3 Sexual dimorphism in the steroidogenic pathway in the SBN

Most studies investigate aromatase localisation and regulation as the main end enzyme that generates oestrogen, possibly from circulating testosterone in males. However, some studies have showed that other steroidogenic enzymes are present in the brain. In the male rat hippocampus, the presence of 5a-reductase, StAR, P450scc, 3b-HSD, 17b-HSD, P450(17a) and aromatase proteins have been localised using immunohistochemistry to the dentate gyrus granule cells and to neurons in the CA1-CA3 (Agís-Balboa et al., 2006; Furukawa et al., 1998; Hojo et al., 2004; Kawato et al., 2002; Mellon & Deschepper, 1993). Consistent with this, our data shows the presence of several steroidogenic enzymes, ranging from Cyp11a1 to Cyp19a1 in both male and female hypothalami. Comparison to the ovary shows that the female hypothalamus possesses lower levels of Hsd3b1, Hsd17b1, Stard1, Cyp11a1 but similar levels of Cyp19a1 as the ovary (Supplementary Figure 2-4). In addition, levels of mRNA of steroidogenic enzymes in the male at baseline (0 hours) are higher than in the female for all steroidogenic enzymes except Hsd17b1, suggesting that this might be a reason for higher steroidogenic capacity in the male brain. Transcriptomics data from the whole hypothalamus also shows that P450scc and 3b-HSD steroidogenic enzymes are lower in the female than male, consistent with our data (Nishida et al., 2005).

Though our data suggests that none of the steroidogenic enzymes measured in the whole hypothalamus show differences in mRNA level from the 0 hour to the 24-hour time point in either sex, sexual dimorphism is evident when individual SBN nuclei are investigated. There is both node-specific and enzyme specific regulation in females. For example, Stard1 mRNA increases within 24 hours in the AH, BNST and meA though such increases are not seen in the male. The AH and BNST also show increases of P450scc and Hsd17b1 mRNA at 24 hours in the female but not in the male. This is in contrast to the hippocampus where there appears to be no differences in Stard1, Hsd17b1 and aromatase expression between males and females (Hojo et al., 2014; Kato et al., 2013). In hippocampal dissociated cultures derived from mixed male and female pups, provision of cholesterol increases the amount of 17b-oestradiol produced, to a much larger extent than the provision of testosterone; this could be decreased with letrozole and by the knockdown of Stard1 with siRNA. These suggest that hippocampal cultures can synthesise oestradiol de novo from cholesterol and this is not sex-specific (Fester et al., 2009), in parallel with the lack of sexual dimorphism in steroidogenic enzymes. Similarly, in the cerebral cortex of the rat, there were no sex differences in the expression of several steroidogenic enzymes though Stard1 mRNA was higher in the female cerebellum than in the male rat cerebellum (Giatti et al., 2019). Consistent with these studies, our study also shows region and sex-specific levels of expression of steroidogenic enzymes.

In addition, there is very low expression of mRNA for the enzymes Cyp11a1 and Hsd3b1 when compared to the ovary and intermediate level of expression of mRNA for aromatase in adult male rat hippocampus (Hojo et al., 2004). This is not true for the hypothalamus where expression levels of Cyp11a1, Stard1, Hsd3b1 and Hsd17b1 are equivalent to the ovary in the male hypothalamus; this may be due to differences in methodology used in the previous study compared to ours or differences between mouse and rat.

We found a regional difference in Cyp19a1 expression in the female mouse mPOA over 24h incubation times, though there was a tendency for increase in the AH ($P = 0.0818$) and MeA ($P = 0.1$). It is interesting to note that, in steroids measured in the aCSF, E2 increased significantly between 0h and 24h in slices corresponding to the LS/mPOA, AH/MeA, and MeA/VMH. Regional differences were not observed in the male SBN, though there was a tendency for increase in the LS ($P = 0.0977$). This indicates that aromatase expression increases over time in incubation, though the mechanism underlying this is unclear. High levels of Cyp19a1 expression have also been found in the MeA, BNST, and mPOA (Tabatadze et al., 2014) consistent with our data. Aromatase mRNA (Tabatadze et al., 2014) and protein (Stanic et al., 2014) have been identified at high levels in the BNST and MeA, expressed in cell bodies and fibres (Wu et al., 2009). These studies have also shown a clear sex dimorphism in aromatase expression within these areas, where males typically express more aromatase mRNA and protein than females (Stanic et al., 2014; Tabatadze et al., 2014) (Wu et al., 2009) (Roselli & Klosterman, 1998) consistent with our data.

In male and female mice that express EGFP under the physiological activation of Cyp19a1 (Stanic et al., 2014), low densities of EGFP-positive cell bodies were found in the AH (male > female), ARC (male = female), and mPOA (male > female). EGFP-positive cell bodies were not detected at all in the VMH of male or female mice (Stanic et al., 2014) . Protein expression levels do not always correlate with mRNA expression levels, and aromatase activity is known to be post-translationally modified by phosphorylation and dephosphorylation (Ubuka et al., 2014). Cyp19a1 mRNA has been found in the rodent VMH, but it is worth noting that this was in male rats that had been treated with testosterone propionate for 1 week before sacrifice (Roselli & Klosterman, 1998).

Notably most previous studies have been performed in males due to the complications inherent in cycling females. One caveat is that we used very young females and males with most females in diestrous since it was difficult to source the required number of females in each phase of the

cycle for such analyses, especially when RNA amounts obtained from individual animals from each SBN nuclei is very low and we need to pool several animals together to obtain enough RNA for accurate analyses. However, mRNA levels of steroidogenic enzymes in the hippocampus do not change depending on the estrous cycle phase though the neurooestrogen levels show a peak in proestrous and a nadir at diestrous in the female (Hojo et al., 2014; Kato et al., 2013). Similarly, the increase in neurotestosterone and neurooestrogen levels in SBN nuclei at 24 hours in our study is not paralleled by an increase in the expression of steroidogenic enzymes. However, protein was not measured in these studies or ours and it is possible that activity levels are modulated independent of mRNA levels during this period.

4.6 Summary

This study is the first of its kind to measure steroid levels within nuclei of the mouse SBN and make direct comparisons in steroid synthesis and enzyme expression between age-matched, intact, and non-hormone-primed male and female subjects. We show that all SBN nuclei can show increased secretion of both oestrogen and testosterone within 24 hours, suggesting de novo synthesis. This is similar in both males and females (with the exception of slices that comprise the mPOA and BNST in the female) with levels of steroid secreted higher in males than in females for every SBN nuclei tested. In the hippocampus, increase in the concentration of E2, DHT and DHEA by addition of radiolabeled pregnenolone to hippocampal neurons, upon NMDA stimulation, suggests de novo steroidogenesis specifically in neurons (Hojo et al., 2004). The role of neurosteroids has been explored using both pharmacological and genetic manipulations, typically in the hippocampus. Aromatase inhibitor treatment to female rat hippocampal slice culture decreases synapse density, spine density and long term potentiation (LTP) (Kretz et al., 2004; Prange-Kiel & Rune, 2006). In vivo, central administration of an aromatase inhibitor decreased spatial memory in mice (Zhao et al., 2018) and the songbird (Bailey et al., 2013) and also decreased consolidation of novel object recognition memories in mice (Tuscher et al., 2016). Supporting this, conditional forebrain aromatase knockout male and ovariectomised female mice showed reduced LTP, spine density, novel object recognition memory and spatial memories (Lu et al., 2019). Our study provides a foundation to explore the physiological relevance of neurooestrogen synthesized in SBN nuclei to social behaviours in the mouse.

4.7 Supplementary data

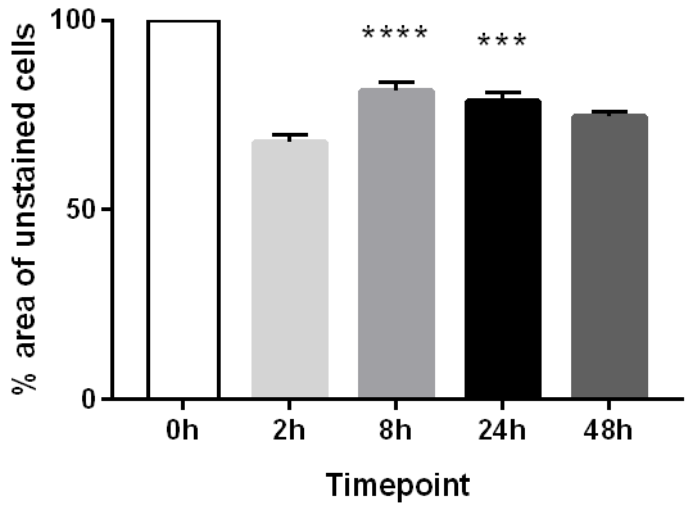

Supplementary Figure 3. Viability of hypothalamic brain slices incubated for different time points measured by the Trypan Blue exclusion assay. A vibratome was used to take 200µm slices from hypothalamic brain regions of P38-44 C57Bl/6 mice, which were incubated in aCSF for different time points. Following incubation, slices were fixed in 4% w/v PFA and incubated with 0.4% Trypan Blue Solution before being mounted on microscope slides and imaged under a light microscope. 10x images of four separate areas of each slice were taken, and each image was then divided into quadrants. The % area of unstained tissue is plotted, where 0h was assumed 100% viability. n = 1 slice per time point, where each slice contributed 16 images. Differences were established by a one-way ANOVA with Bonferroni's multiple comparisons test post hoc. *** $P < 0.001$ vs 2h, **** $P <$

0.0001 vs 2h.

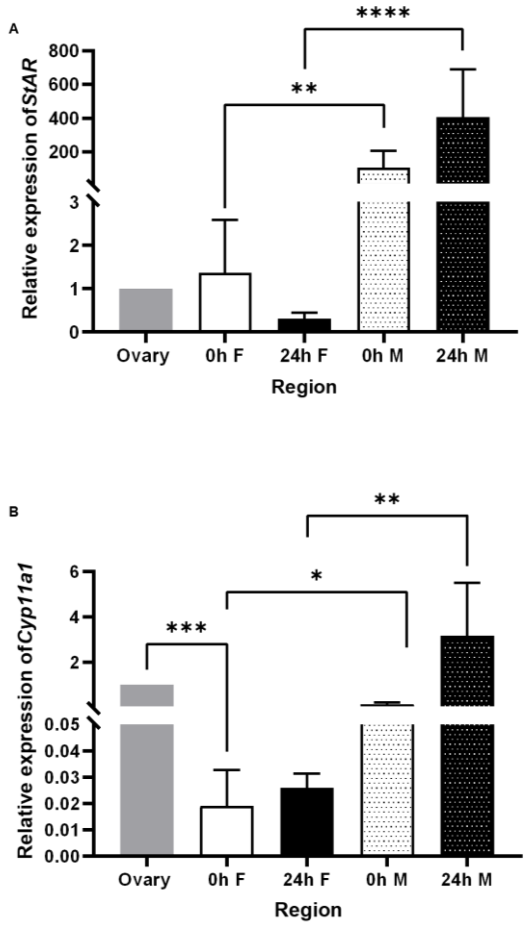

Supplementary Figure 4. Expression of StAR and Cyp11a1 in adult male and female pooled SBN nuclei after 0h and 24h slice incubation timepoints, measured by RT-qPCR. A vibratome was used to take 200µm slices from hypothalamic brain regions of P38-44 C57Bl/6 mice, which were incubated in aCSF for 0h or 24h time points. Following incubation, SBN nuclei were punch dissected, and nuclei from 4 animals were pooled into one, such that $n = 3$ from a total of 12 animals for female, and $n = 2$ from a total of 8 animals for male. Following RNA extraction, cDNA was synthesised and used in an RT-qPCR analysis. In this analysis, all SBN nuclei for each particular timepoint from male and female mice were pooled together. Relative expression to the housekeeping gene, β-actin, is shown for StAR (A) and Cyp11a1, encoding cytochrome P450 sidechain cleavage enzyme (B). Differences were established by a non-parametric one-way ANOVA with Dunn's multiple comparisons *post hoc*, * $P < 0.05$, ** $P < 0.01$, *** $P < 0.001$, **** $P < 0.0001$.

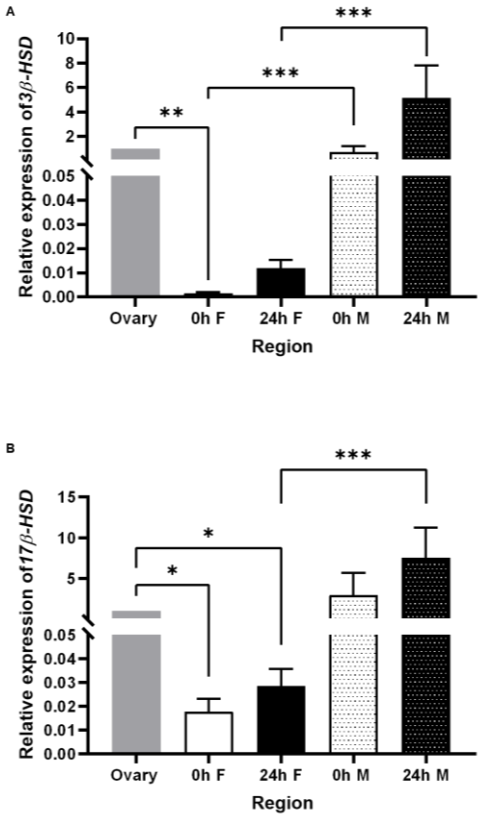

Supplementary Figure 5. Expression of 3β-HSD and 17β-HSD in adult male and female pooled SBN nuclei after 0h and 24h slice incubation timepoints, measured by RT-qPCR. A vibratome was used to take 200μm slices from hypothalamic brain regions of P38-44 C57Bl/6 mice, which were incubated in aCSF for 0h or 24h time points. Following incubation, SBN nuclei were punch dissected, and nuclei from 4 animals were pooled into one, such that $n = 3$ from a total of 12 animals for female, and $n = 2$ from a total of 8 animals for male. Following RNA extraction, cDNA was synthesised and used in an RT-qPCR analysis. In this analysis, all SBN nuclei for each particular timepoint from male and female mice were pooled together. Relative expression to the housekeeping gene, β-actin, is shown for 3β-HSD (A) and 17β-HSD (B). Differences were established by a non-parametric one-way ANOVA with Dunn's multiple comparisons *post hoc*, * $P < 0.05$, ** $P < 0.01$, *** $P < 0.001$.

Supplementary Figure 6. Expression of Cyp19ain adult male and female pooled SBN nuclei after 0h and 24h slice incubation timepoints, measured by RT-qPCR. A vibratome was used to take 200µm slices from hypothalamic brain regions of P38-44 C57Bl/6 mice, which were incubated in aCSF for 0h or 24h time points. Following incubation, SBN nuclei were punch dissected, and nuclei from 4 animals were pooled into one, such that n = 3 from a total of 12 animals for female, and n = 2 from a total of 8 animals for male. In this analysis, all SBN nuclei for each particular region, timepoint from male and female mice were pooled together. Following RNA extraction, cDNA was synthesised and used in an RT-qPCR analysis. Relative expression to the housekeeping gene, β-actin, is shown for Cyp19a1, encoding the aromatase enzyme. Differences were established by a nonparametric one-way ANOVA with Dunn's multiple comparisons post hoc, **** $P < 0.0001$.

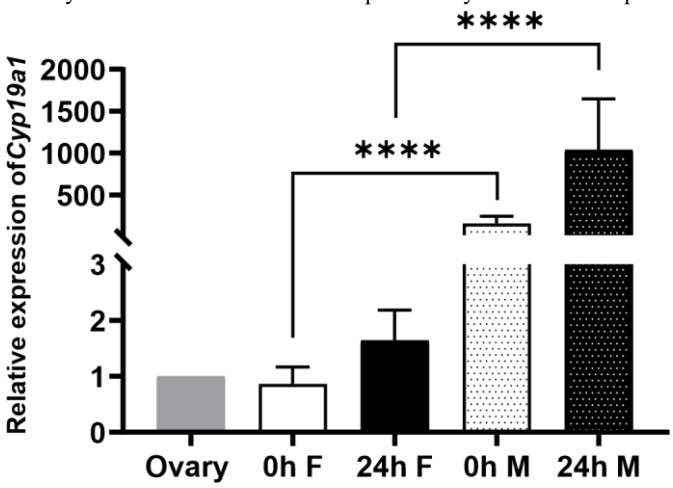

5.Summary of findings

Oestrogen is crucial for the development and maintenance of sexually dimorphic behaviours in the CNS(Bakker & Baum, 2008; Goodson, 2005; Goodson & Kabelik, 2009). Rapid non-genomic E2 responses can be mediated via classical ERs ERα and ERβ or by membrane receptors ERα36 and GPER1(Cheng, Quinn, et al., 2011; Filardo et al. 2000; Filardo et al., 2002; Filardo & Thomas, 2005) Unlike the genomic signalling, non -genomic signalling involves the activation of multiple protein kinase cascades. The activation of these protein kinases results in regulation of transcription, translation, and additional post- translational modifications of proteins(Levin, 2009b). The molecular interaction between these oestrogen receptors and their impact on social behaviour is not completely understood. Here, it was hypothesised that membrane oestrogen receptors (ERα and GPER1) bind to locally synthesized oestrogen in the social behaviour network to regulate sex-typical behaviours and that changes in oestrogen production in SBN can abolish or reduced such behaviours. In this thesis, we demonstrate, for the first time, the subcellular localization of oestrogen receptors (ERα, its variant ERα 36 and GPER1) and the regulation of aromatase using three cellular systems: 1) mouse embryonic cells (mES), 2) mES derived neurons (mESn)(Davis, Vajaria, et al., 2023), and 3) mouse hypothalamic neuronal cell line (mHypoE-42) . Investigating the subcellular colocalisation of these receptors also allows us to understand crosstalk between these receptors. Additionally, we used rodents to investigate the production and regulation of neurosteroids in the SBN of the male mouse.

In chapter 2, we developed a simple protocol for differentiating CGR8 mES cell line to motor neurons that express potent neuronal marker β Tublin III to quantify the subcellular localization of classical oestrogen receptor (ERα) and membrane receptors (GPER1and ERα-36) in mES and mESn at D7, D14, and D21 of neuronal development. We detected antigens in four distinct compartments of the cell: nucleus, endoplasmic reticulum, plasma membrane and Golgi apparatus. Based on previous literature we used comparative analysis to demonstrate that ERs are differentially distributed among cell types suggesting that receptors may play a specialized role that is cell dependent (Cammarata et al., 2004; Tecalco-Cruz et al., 2017). There was an increase in ERα localisation in the nucleus and plasma membrane in mESn compared to mES cells. In contrast, we found that as differentiation of neurons proceeds, there is a decrease in plasma membrane localisation of both ERα-36 and GPER1 to levels like those found in mES

cells. Although the localisation of these receptors has not been previous published, we know from current literature that oestrogen receptors localized at membrane are unique associated with rapid non genomic(Filardo et al., 2000; Filardo et al., 2002).Our results are partially consistent with those reported by some other authors(Filardo et al., 2002; Filardo & Thomas, 2005; Hammond et al., 2011; Hazell et al., 2009; Yu et al., 2010). However, there are no studies localising ERs in mESn cells at various stages of development. Development days D7-D21 do not correspond to specific embryonic or postnatal developmental stage but maintain the neuronal characteristics. More comparative research is needed to investigate the functional roles of these ERα-36 and GPER1 and what impact these two receptors have on critical neuronal stages. Although, our results show that ERs are present within 4 compartments of the cell, they are not colocalized. We used heat maps to observe differential distribution of these receptors within an organelle, they appear to occupy distinct spaces within the organelle, that is independent of cell type. The results of these studies demonstrate that ERα, ERα variant ERα 36 and GPER1 are differentially distributed between three cell types; suggesting that receptors may play a specialized role dependent on cell type.

In chapter 3, to understand the role of oestrogen receptors in rapid non-genomic regulation of aromatase expression, we treated mHypoE-42 with either vehicle (DSMO), E2, E2-BSA (membrane impermeable), G1 (GPER1 agonist), PPT (ERα agonist), or DPN (ERβ agonist) and measured aromatase expression at 20 mins. Preliminary studies show that aromatase expression increased nearly 20-fold after 20 mins of treatment with G1 and DPN, but not with PPT. Additional treatments with GPER1 antagonist and DPN reversed these effects, suggesting that increases in aromatase expression requires both GPER1 and ERβ to be active. Incubation with cAMP/PKA or Ca2+ inhibitors for 10 mins followed by 20 min incubation with G1 or DPN led to a significant decrease in aromatase expression, suggesting that these pathways might be important for upregulation of aromatase mRNA. Surprisingly, treatment with G1 and DPN together, decreased aromatase expression, suggesting that GPER1 and ERβ 'crosstalk' to mediate rapid increases in aromatase expression. Additionally, we show that within 20 minutes of adding GPER1 selective inhibitor G15 with GPER1 selective agonist G1, there is an increase in aromatase expression. G1 is an agonist for both GPER1 and ERα 36, but G15 is not an antagonist for ERα 36. This suggesting that ERα 36, not GPER1 may be acting in collaboration with ERα. GPER1 and ERα 36 has been shown to work in collaboration with one another and since ERα in similar in structure to ERα- 36 it is possible that actions associated with either ERα to GPER1 may be attributable to ERα 36(Lianguo Kang et al., 2010). In SKBR3 cells that express neither ERα or ERβ, but expresses GPER1, GPER1 expression was knocked down which decreased expression levels of ERα 36. This would suggest that GPER1 induces ERα 36

expression in SKBR3 cells. However, in MCF7 cells transfected with GPR30 siRNA then treated with agonist G1, there was an increase in ERK phosphorylation via ERα 36(Albanito et al., 2008; Pelekanou et al., 2011). Taken together, data would suggest that ERα 36 can act independently of GPER1, though this action may be cell dependent.

As stated previously the pattern of activity in each SBN node following or during a behavioural interaction is dependent on the availability of steroid hormone receptors in that region(Goodson, 2005; J. L. Goodson & Kabelik, 2009; Greenberg & Trainor, 2016). For example, in male rodents after engaging in sexual behaviour, the meAMY is the first to receive inputs from the olfactory bulb and signals are then relayed to the other regions of the SBN. However, in female sexual behaviour hypothalamic areas are proposed to receive inputs first, given the density of steroid hormone receptors available in the area (Li and Dulac,2018). In chapter 4, we used a novel ex vivo slice culture method to show differential expression between steroidogenic enzymes and differences in locally produced neuroestrogens and neurotestosterone. In general, across all SBN regions, we found regional differences in steroid production in the male and female mouse brain. Neuroestrogen production increased significant between 0 and 24 hours in both male and female LS/mPOA, AH/MeA, and MeA/VMH. However, there was only a significant increase in neuroestrogen production in males after 24 hours in the mPOA/BNST. This is not surprising considering the mPOA and BNST is considerable larger in males compared to females. Further research into the detailed molecular mechanisms of these signalling pathways will provide important insight into the role of oestrogen and which receptors are involved in regulation of aromatase and subsequent social behaviours.

Appendix 1

This is in support of Chapter 2 .Published with (Davis, Vajaria, et al., 2023)

These are statistics for Figure 2.5-2.7.

Supplementary data 1A: Statistical reporting for colocalisation of target antigens in different organelles. M1, M2 and M3 values obtained for colocalisation of different ERs in different values were compared to the MCC threshold of 0.5, indicating colocalisation, using the one sample t-test and Wilcoxon's test (Graph Pad Prism, CA). p values obtained in these tests that are <0.5 indicate that colocalisation is significantly different from the threshold value of 0.5.

For Figure 2.5A in mES cells, colocalisation of ERα-66 with ERα-36 in the nucleus and plasma membrane, reflected by M1, M2 and M3 values is significantly lower from the threshold of 0.5. Hence, Wilcoxon's test for M1 (nucleus) gives $t(48)=67.77$, $p<0.0001$ and for M1(plasma membrane) gives $t(47)=45.38$, $p<0.0001$. For M2 (nucleus), the value is $t(48)=68.20$, $p<0.0001$ while for M2 (plasma membrane), the value is $t(47)=44.56$, $p<0.0001$. For M3 (nucleus), the value is $t(48)=69.45$, $p<0.0001$ and for M3 (plasma membrane), the value is $t(47)=53.63$, $p<0.0001$. For Figure 5A in mES cells, colocalisation of ERα-66 with GPER1 in the nucleus and plasma membrane, reflected by M1, M2 and M3 values is significantly lower from the threshold of 0.5. Hence, for M1 (nucleus), $t(48)=29$; $p<0.0001$ and M1 (plasma membrane), the value is $t(47)=51.62$, $p<0.0001$. For M2 (nucleus), the value is $t(45)=35.34$, $p<0.0001$ and for M2 (plasma membrane), the value is $t(47)=49.39$, $p<0.0001$. Similarly, for M3 (nucleus), Wilcoxon's test reveals a value of $t(48)=28.36$, $p<0.0001$ while for M3 (plasma membrane), the value is $t(47)=48.03$, $p<0.0001$.

For Figure 2.5B in mES cells, colocalisation of ERα-66 with ERα-36 in the endoplasmic reticulum and Golgi apparatus, reflected by M1, M2 and M3 values is significantly lower from the threshold of 0.5. Hence, Wilcoxon's test for M1 (endoplasmic reticulum), the value is $t(48)=7.621$, $p<0.0001$ and M1 (Golgi apparatus), the value is $t(47)=11.64$, $p<0.0001$. For M2 (endoplasmic reticulum), the value is $t(47)=7.671$, $p<0.0001$ and for M2 (Golgi apparatus), the value is $t(47)=11.09$, $p<0.0001$. Similarly, for M3 (endoplasmic reticulum), the value is $t(48)=6.957$, $p<0.0001$ and for M3(Golgi apparatus), the value is $t(47)=11.91$, $p<0.0001$. For Figure 2.5B in mES cells, the colocalisation of ERα-66 with GPER1 in the endoplasmic reticulum and Golgi apparatus is also significantly lower than the MCC threshold of 0.5. Hence, for M1 (endoplasmic reticulum), the value is $t(46)=10.49$, $p<0.001$ while for M1 (Golgi apparatus), the value is $t(47)=10.95$, $p<0.001$. For M2 (endoplasmic reticulum), the value is $t(47)=9.012$, $p<0.0001$ and for M2 (Golgi apparatus), the value is $t(47)=10.81$,

p<0.0001. For M3 (endoplasmic reticulum), the value is t(47)=9.952, p<0.001 and for M3 (Golgi apparatus), t(47)=11.31, p<0.0001.

Supplementary data 1B: Low colocalisation in mESn of ERs is seen by statistical analyses. For Figure 2.6A in mESn cells, the colocalisation of ER□-66 with GPER1 in the nucleus and plasma membrane, reflected by M1, M2 and M3 values is significantly lower from the threshold of 0.5. Hence, Wilcoxon's test gives significantly lower values from the 0.5 threshold value for M1 (nucleus) at t(139)=50.27, p<0.0001 and for M1 (plasma membrane) at t(126)=29.72, p<0.001. For M2 (nucleus), the values are t(143)=43.21, p<0.0001 while for M2 (plasma membrane), the values are t(126)=29.16, p<0.0001. For M3 (nucleus), the values are t(140)=47.74 while for M3 (plasma membrane), the values are t(125)=34.76, p<0.0001.

For ERα-66 and ERα-36 (Figure 2.6A) in mESn cells, Wilcoxon's test reveals that colocalisation is also significantly lower from 0.5 in the nucleus and plasma membrane. Therefore, the value for M1 (nucleus) is t(141)=77.51, p<0.0001 while for M1 (plasma membrane), it is t(139)=82.50, p<0.001. For M2 (nucleus), it is t (142)=72.16, p<0.0001 and for M2 (plasma membrane), it its(139)=83.15, p<0.0001. For M3 (nucleus), it is t(142)=77.21, p<0.0001 while for M3 (plasma membrane), it is t(137)=93.59, p<0.0001.

For Figure 2.6B in mES cells, colocalisation of ERα-66 with ERα-36 in the endoplasmic reticulum and Golgi apparatus, reflected by M1, M2 and M3 values is significantly lower from the threshold of 0.5. Hence, Wilcoxon's test for M1 (endoplasmic reticulum), the value is, t(127)=8.327, p<0.0001 and M1 (Golgi apparatus), the value is t(116)=28.82, p<0.0001. For M2 (endoplasmic reticulum), the value is t(127)=7.948, p<0.0001 and for M2 (Golgi apparatus), the value is t(116)=28.85, p<0.0001. Similarly, for M3 (endoplasmic reticulum), the value is t(126)=9.576, p<0.0001 and for M3(Golgi apparatus), the value is t(115)=30.05, p<0.0001. For Figure 6B in mES cells, the colocalisation of ER□-66 with GPER1 in the endoplasmic reticulum and Golgi apparatus is also significantly lower than the MCC threshold of 0.5. Hence, for M1 (endoplasmic reticulum), the value is t(146)=12.71, p<0.001 while for M1 (Golgi apparatus), the value is t(146)=13.86, p<0.001. For M2 (endoplasmic reticulum), the value is t(146)=12.25, p<0.0001 and for M2 (Golgi apparatus), the value is t(145)=13.61, p<0.0001. For M3 (endoplasmic reticulum), the value is t(145)=12.62, p<0.001 and for M3 (Golgi apparatus), the value is t(144)=14.62 , p<0.0001.

Supplementary data 1C:Though there is ERα-36 and GPER1 in mES and mESn cells, there is no significant colocalisation of these two proteins in any organelle, as reflected by M1, M2 and M3 values that are significantly lower from the threshold of 0.5. Hence, Wilcoxon's test for colocalisation in mES cells (Figure 2.7A) gives significantly lower values from the 0.5

threshold value for M1 (nucleus) at $t(49)=83.96$, $p<0.0001$ and for M1 (plasma membrane) at $t(49)=48.58$, $p<0.001$. For M2 (nucleus), the values are $t(49)=94.03$, $p<0.0001$ while for M2 (plasma membrane), the values are $t(49)=52.40$, $p<0.0001$. For M3 (nucleus), the values are $t(43)=87.99$ while for M3 (plasma membrane), the values are $t(49)=50.74$, $p<0.0001$. For ERα-36 and GPER1 proteins in the endoplasmic reticulum and Golgi apparatus in mES cells (Figure 2.7B), Wilcoxon's test shows lower values from 0.5 threshold value for M1 (endoplasmic reticulum) at $t(49)=9.861$; $p<0.0001$ while for M2 (Golgi apparatus), the values are $t(49)=20.03$; $p<0.0001$. For M2(endoplasmic reticulum), the values are $t(49)=9.847$ while for M2(Golgi apparatus), the values are $t(49)=33.21$; $p<0.0001$. For M3 (endoplasmic reticulum), the values are $t(49)=9.948$; $p<0.0001$ while for M3 (Golgi apparatus), the values are $t(49)=18.61$; $p<0.0001$.

Similar lack of colocalisation in seen in mESn cells. Wilcoxon's Test (Figure 2.7A) reveals values for M1(nucleus) to be $t(46)=89.64$; $p<0.0001$ while values for M1 (plasma membrane) are $t(46)=133$; $p<0.0001$. For M2 (nucleus), the values are $t(46)=55.55$; $p<0.0001$ while for M2 (plasma membrane), the values are $t(46)=133.3$; $p<0.0001$. For M3 (nucleus), the values are $t(46)=55.95$; $p<0.0001$ while for M3 (plasma membrane), the values are $t(46)=224.1$; $p<0.0001$.

Figure 2.7B shows the colocalisation of ERα-36 and GPER1 in mESn cells. Wilcoxon's test shows lower values from 0.5 threshold value for M1 (endoplasmic reticulum) at $t(75)=24.97$; $p<0.0001$ while for M2 (Golgi apparatus), the values are $t(101)=498.4$; $p<0.0001$. For M2(endoplasmic reticulum), the values are $t(75)=24.99$ while for M2(Golgi apparatus), the values are $t(101)=518.7$; $p<0.0001$. For M3 (endoplasmic reticulum), the values are $t(75)=24.99$; $p<0.0001$ while for M3 (Golgi apparatus), the values are $t(101)=405.5$; $p<0.0001$.

These data show that in all organelles, regardless of the ERs present, no ER is colocalised with the other in that organelle.

Appendix 2

This section is in support Chapter 3

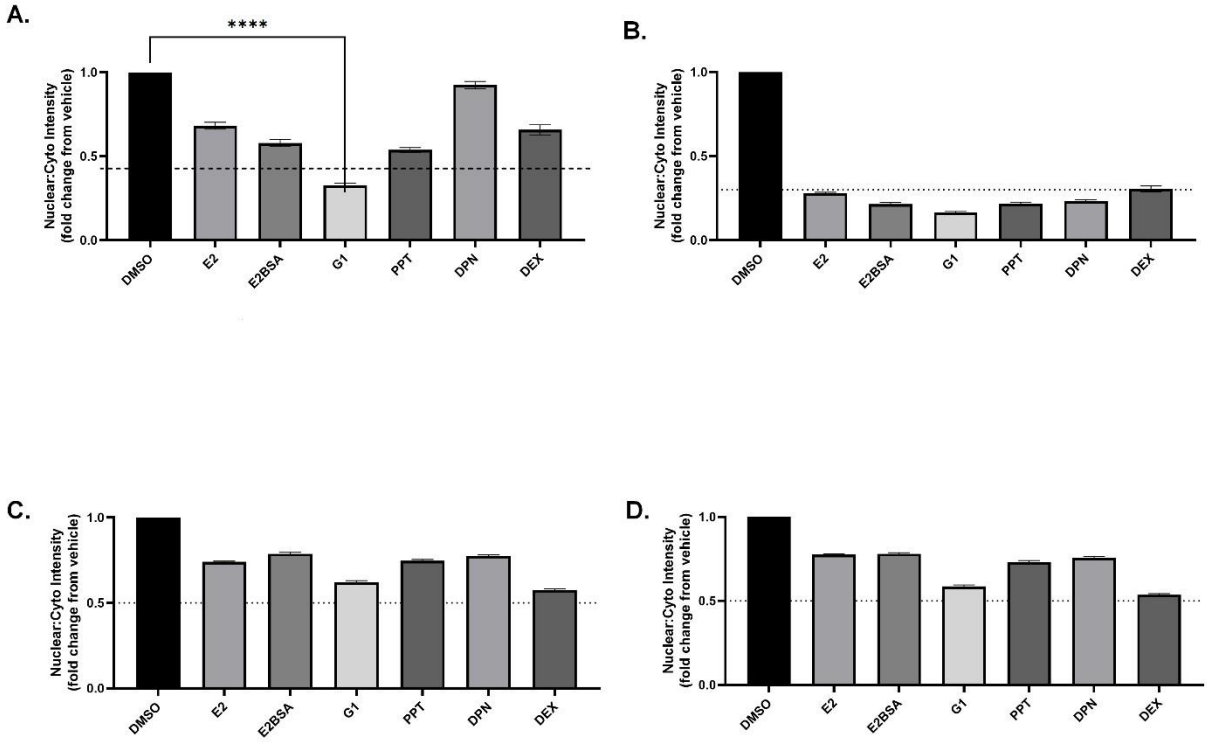

Supplementary Figure 2. Movement of oestrogen receptors in mES and N42 cells. (A) Nuclear-to Cytoplasmic Ratio of ERα in mES cells in control media DMSO- no treatment and media containing E2, E2-BSA, G1, PPT ,DPN, or DEX (dexamethasone) . G1 specific nuclear localization was seen following 20 mins of treatment (10-8M). (B) Nuclear-to Cytoplasmic Ratio of GPER1 in mES cells in control media (DMSO- no treatment) and media containing E2, E2-BSA, G1, PPT ,DPN or DEX. Non-specific localization of GPER1 seen in N42 cells to the cytoplasm. (C) Nuclear-to Cytoplasmic Ratio of ERα in N42 cells in control media (DMSO- no treatment) and media containing E2, E2-BSA, G1, PPT ,DPN, or DEX.(D) Nuclear-to Cytoplasmic Ratio of GPER1 in mES cells in control media (DMSO- no treatment) and media containing E2, E2-BSA, G1, PPT ,DPN or DEX. Non-specific localization of ERα and GPER1 seen in N42 cells. Results are expressed as the mean ± SEM, n=100 cells. Data is represented as the average of at least 2 independent experiments. ****$p \leq .0001$one-way ANOVA

Appendix 3

This section is in support of incomplete findings for the regulation of neurosteroids and the social behaviour network. These findings support need for additional work to establish the functional relevance of oestrogen receptors in the regulation of aromatase and subsequent oestrogen production.

We previously established that neurosteroids can be measured within the aCSF from slices incubated at 024 hours. We found that neurosteroids increase from 0-24 hours, suggesting de novo synthesis (Chapter 5). Based on this evidence we decided to determine if we could inhibit oestrogen production via aromatase inhibitor. We first tried the aromatase inhibitor letrozole seen in Figure 1 to increase the solubility of the lipophilic steroids we use BSA, however BSA causes interference with ELISA data not shown.

Concentrations of neuroestrogens and neurotestosterone following incubation with either vehicle with 0.1 % DMSO (Control) , Letrozole (10-7M) , Testosterone (10-8M) o Letrozole (10-7M) and Testosterone (10-8M) were measured in ex vivo SBN slices following 24 hours incubation. Two- way ANOVA yielded a non- significant treatment × region interaction effect on the production of neuroestrogens (Figure 1A, p=> 0.999) . In the LS/MPOA region there was a significant difference in testosterone concentration in the testosterone treated vs control and letrozole treated slices (Figure 1B).

Since we have previously shown that after 24-hour incubation neuroestrogens concentration can increase, which suggest de novo synthesis. We hypothesized that the additional of aromatase inhibitor, the enzyme response for the conversion of C19 steroids to C18 steroids, we would see a significant decrease in oestradiol production. – Studies have shown that even in concentrations as low as 0.05 % DMSO can interfere with brain excitability, based on this, we decided to use the more potent aromatase inhibitor fadrozole Figure 2, that could be dissolved in ethanol. Based on previous research, regions of SBN crucial for sexual and aggressive behaviour are the MPOA and the VMH. We decided to focus on these two regions for the remainder of our thesis.

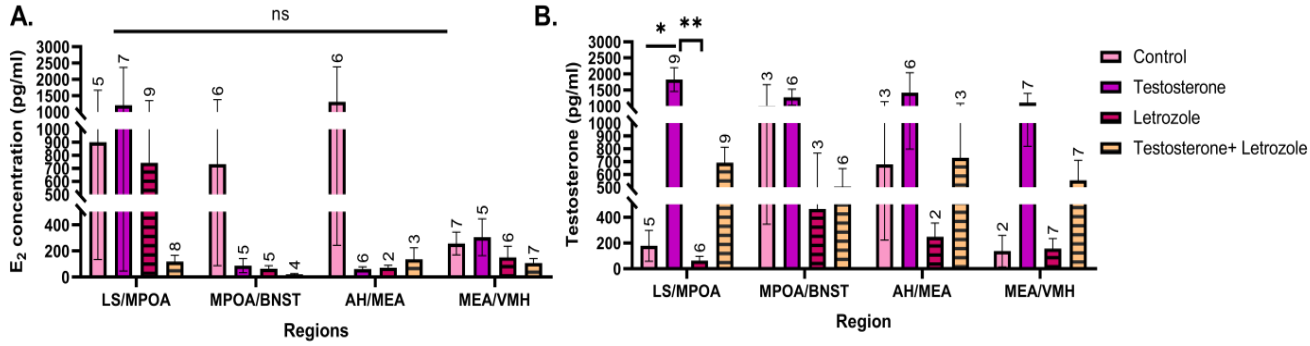

Figure 1. Neurosteroids concentrations in SBN nuclei of adult male mice. A vibratome was used to take 200µm slices from SBN of P38-44 C57Bl/6 mice, which were incubated in aCSF for 24 hours with 0.1 % (Control) , Letrozole (10-7M) , Testosterone (10-8M) o Letrozole (10-7M) and Testosterone (10-8M) . (A) Neuroestrogen concentrations were measured from aSCF of slices after a 45 minutes recovery followed by 24h incubation using an oestradiol-based ELISA assay (B) concentrations were measured from aSCF of slices after a 45 minutes recovery followed by 24h incubation using a testosterone-based ELISA assay. Differences were established by a two-way ANOVA comparing region, treatment, and the interaction between region and treatment . * $P < 0.05$,** $P < 0.01$.

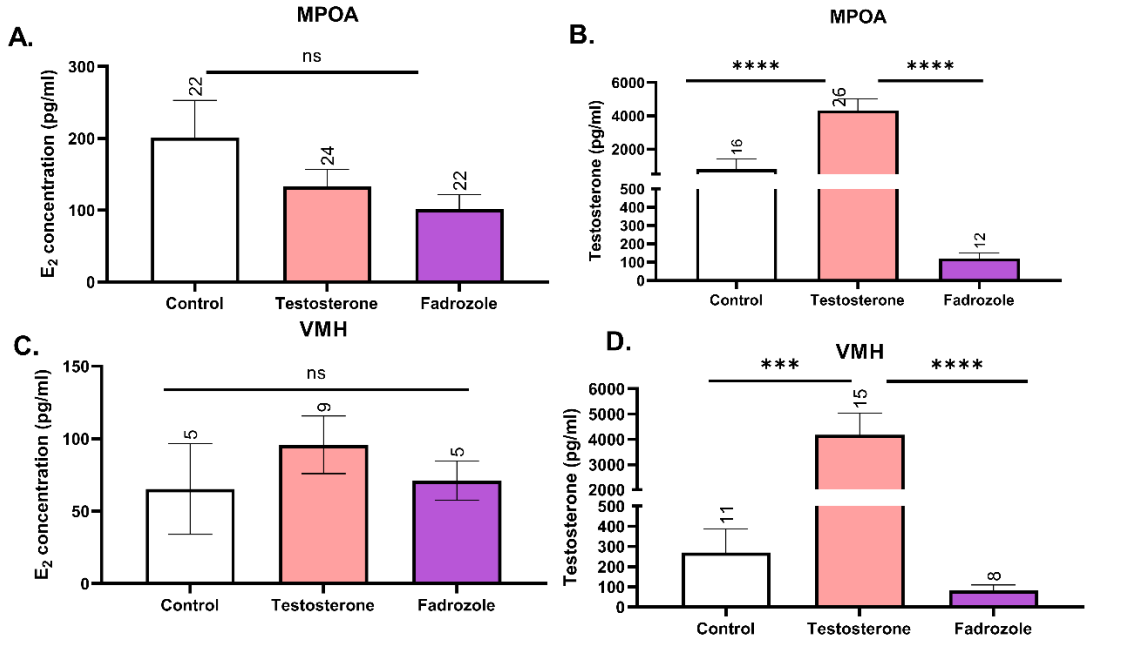

Figure 2. Neurosteroid concentrations in 200um coronal slices MPOA and VMH of adult male mice. A vibratome was used to take 200µm slices from the MPOA and VMH of P38-44 C57Bl/6 mice, which were incubated in aCSF for 24 hours with 0.01 % (Ethanol), Fadrozole (0.03µm) , Testosterone (0.01 µm). (A) Neuroestrogen concentrations were in the MPOA measured from aSCF of slices after a 45 minutes recovery followed by 24h incubation using an oestradiol-based ELISA assay. There were no significant differences in E2 concentrations. (B) concentrations were measured from aSCF of MPOA slices after a 45 minutes recovery followed by 24h incubation using a testosterone-based ELISA assay, There were significant differences between control and testosterone ; testosterone and fadrozole. (C) Neuroestrogen concentrations were in the VMH measured from aSCF of slices after a 45 minutes recovery followed by 24h incubation using an oestradiol-based ELISA assay.

There were no significant differences in E2 concentrations. (D) concentrations were measured in from aSCF of VMH slices after a 45 minutes recovery followed by 24h incubation using a testosterone-based ELISA assay, There were significant differences between control and testosterone ; testosterone and fadrozole. Differences were established by a one two-way ANOVA comparing control to treatment after 24 hours.

References

Aaron, J. S., Taylor, A. B., & Chew, T.-L. (2018). Image co-localization – co-occurrence versus correlation. *Journal of Cell Science*, *131*(3).

Abraham, I. M., Todman, M. G., Korach, K. S., & Herbison, A. E. (2004). Critical in vivo roles for classical estrogen receptors in rapid estrogen actions on intracellular signaling in mouse brain. *Endocrinology*, *145*(7), 3055-3061.

Acconcia, F., Ascenzi, P., Bocedi, A., Spisni, E., Tomasi, V., Trentalance, A., Visca, P., & Marino, M. (2005). Palmitoylation-dependent estrogen receptor alpha membrane localization: regulation by 17beta-estradiol. *Mol Biol Cell*, *16*(1), 231-237.

Acconcia, F., Fiocchetti, M., Busonero, C., Fernandez, V. S., Montalesi, E., Cipolletti, M., Pallottini, V., & Marino, M. (2021). The extra-nuclear interactome of the estrogen receptors: implications for physiological functions. *Molecular and Cellular Endocrinology*, *538*, 111452.

Agís-Balboa, R. C., Pinna, G., Zhubi, A., Maloku, E., Veldic, M., Costa, E., & Guidotti, A. (2006). Characterization of brain neurons that express enzymes mediating neurosteroid biosynthesis. *Proceedings of the National Academy of Sciences*, *103*(39), 14602-14607.

Akama, K. T., & McEwen, B. S. (2003). Estrogen stimulates postsynaptic density-95 rapid protein synthesis via the Akt/protein kinase B pathway. *J Neurosci*, *23*(6), 2333-2339.

Akama, K. T., Thompson, L. I., Milner, T. A., & McEwen, B. S. (2013). Post-synaptic density-95 (PSD-95) binding capacity of G-protein-coupled receptor 30 (GPR30), an estrogen receptor that can be identified in hippocampal dendritic spines. *J Biol Chem*, *288*(9), 6438-6450.

Albanito, L., Lappano, R., Madeo, A., Chimento, A., Prossnitz, E. R., Cappello, A. R., Dolce, V., Abonante, S., Pezzi, V., & Maggiolini, M. (2008). G-protein-coupled receptor 30 and estrogen receptor-alpha are involved in the proliferative effects induced by atrazine in ovarian cancer cells [Research Support, Non-U.S. Gov't]. *Environ Health Perspect*, *116*(12), 1648-1655.

Albers, J., & Offenhäusser, A. (2016). Signal propagation between neuronal populations controlled by micropatterning. *Frontiers in bioengineering and biotechnology*, *4*, 46.

Anchan, D., Gafur, A., Sano, K., Ogawa, S., & Vasudevan, N. (2014). Activation of the GPR30 Receptor Promotes Lordosis in Female Mice. *Neuroendocrinology*, *100*(1), 71-80.

Arai, Y., Sekine, Y., & Murakami, S. (1996). Estrogen and apoptosis in the developing sexually dimorphic preoptic area in female rats. *Neurosci Res*, *25*(4), 403-407.

Ariazi, E. A., Brailoiu, E., Yerrum, S., Shupp, H. A., Slifker, M. J., Cunliffe, H. E., Black, M. A., Donato, A. L., Arterburn, J. B., Oprea, T. I., Prossnitz, E. R., Dun, N. J., & Jordan, V. C. (2010). The G protein-coupled receptor GPR30 inhibits proliferation of estrogen receptor-positive breast cancer cells. *Cancer Res*, *70*(3), 1184-1194.

Bailey, D. J., Ma, C., Soma, K. K., & Saldanha, C. J. (2013). Inhibition of hippocampal aromatization impairs spatial memory performance in a male songbird. *Endocrinology*, *154*(12), 4707-4714.

Bakker, J., Baillien, M., Honda, S., Harada, N., & Balthazart, J. (2004). Relationships between aromatase activity in the brain and gonads and behavioural deficits in homozygous and heterozygous aromatase knockout mice. *J Neuroendocrinol*, *16*(5), 483-490.

Bakker, J., & Baum, M. J. (2008). Role for estradiol in female-typical brain and behavioral sexual differentiation. *Front Neuroendocrinol*, *29*(1), 1-16.

Bakker, J., Honda, S., Harada, N., & Balthazart, J. (2002). The aromatase knock-out mouse provides new evidence that estradiol is required during development in the female for the expression of sociosexual behaviors in adulthood. *J Neurosci*, *22*(20), 9104-9112.

Bakker, J., Honda, S., Harada, N., & Balthazart, J. (2003). The aromatase knockout (ArKO) mouse provides new evidence that estrogens are required for the development of the female brain. *Ann N Y Acad Sci*, *1007*, 251-262.

Bale, T. L., Davis, A. M., Auger, A. P., Dorsa, D. M., & McCarthy, M. M. (2001). CNS region-specific oxytocin receptor expression: importance in regulation of anxiety and sex behavior. *J Neurosci*, *21*(7), 2546-2552.

Bale, T. L., Dorsa, D. M., & Johnston, C. A. (1995). Oxytocin receptor mRNA expression in the ventromedial hypothalamus during the estrous cycle. *J Neurosci*, *15*, 5058-5064.

Balthazart, J., Absil, P., Foidart, A., Houbart, M., Harada, N., & Ball, G. F. (1996). Distribution of aromatase-immunoreactive cells in the forebrain of zebra finches (Taeniopygia guttata): implications for the neural action of steroids and nuclear definition in the avian hypothalamus. *J Neurobiol*, *31*(2), 129-148.

Balthazart, J., Baillien, M., Charlier, T. D., Cornil, C. A., & Ball, G. F. (2003a). Multiple mechanisms control brain aromatase activity at the genomic and non-genomic level [Research Support, Non-U.S. Gov't Research Support, U.S. Gov't, P.H.S.Review]. *J Steroid Biochem Mol Biol*, *86*(3-5), 367-379.

Balthazart, J., Baillien, M., Charlier, T. D., Cornil, C. A., & Ball, G. F. (2003b). The neuroendocrinology of reproductive behavior in Japanese quail [Research Support, Non-U.S. Gov't Research Support, U.S. Gov't, P.H.S.Review]. *Domest Anim Endocrinol*, *25*(1), 69-82.

Balthazart, J., & Surlemont, C. (1990). Copulatory behavior is controlled by the sexually dimorphic nucleus of the quail POA. *Brain Res Bull*, *25*(1), 7-14.

Baulieu, E.-E., Robel, P., & Schumacher, M. (1999). *Neurosteroids: a new regulatory function in the nervous system*. Humana Press.

Bayless, D. W., Yang, T., Mason, M. M., Susanto, A. A., Lobdell, A., & Shah, N. M. (2019). Limbic neurons shape sex recognition and social behavior in sexually naive males. *Cell*, *176*(5), 1190-1205. e1120.

Beyer, C. (1999). Estrogen and the developing mammalian brain [Review]. *Anatomy and Embryology*, *199*(5), 379-390.

Beyer, C., & Karolczak, M. (2000). Estrogenic stimulation of neurite growth in midbrain dopaminergic neurons depends on cAMP/protein kinase A signalling. *J Neurosci Res*, *59*(1), 107-116.

Bhosle, V. K., Rivera, J. C., & Chemtob, S. (2019). New insights into mechanisms of nuclear translocation of G-protein coupled receptors. *Small GTPases*, *10*(4), 254-263.

Bjornstrom, L., & Sjoberg, M. (2005). Mechanisms of estrogen receptor signaling: convergence of genomic and nongenomic actions on target genes. *Mol Endocrinol*, *19*(4), 833-842.

Blanchard, R. J., & Blanchard, D. C. (1977). Aggressive behavior in the rat. *Behavioral biology*, *21*(2), 197-224.

BOGIC, L., GERLACH, J. L., & McEWEN, B. S. (1988). The ontogeny of sex differences in estrogen-induced progesterone receptors in rat brain. *Endocrinology*, *122*(6), 2735-2741.

Boivin, B., Chevalier, D., Villeneuve, L. R., Rousseau, E., & Allen, B. G. (2003). Functional endothelin receptors are present on nuclei in cardiac ventricular myocytes. *Journal of Biological Chemistry*, *278*(31), 29153-29163.

Boivin, B., Vaniotis, G., Allen, B. G., & Hébert, T. E. (2008). G protein-coupled receptors in and on the cell nucleus: a new signaling paradigm? *Journal of Receptors and Signal Transduction*, *28*(1-2), 15-28.

Bondar, G., Kuo, J., Hamid, N., & Micevych, P. (2009). Estradiol-induced estrogen receptor-alpha trafficking. *J Neurosci*, *29*(48), 15323-15330.

Boon, W. C., Chow, J. D. Y., & Simpson, E. R. (2010). The multiple roles of estrogens and the enzyme aromatase [Article]. *Prog Brain Res*, *181*(C), 209-232.

Boulware, M. I., Kordasiewicz, H., & Mermelstein, P. G. (2007). Caveolin proteins are essential for distinct effects of membrane estrogen receptors in neurons. *J Neurosci*, *27*(37), 9941-9950.

Boulware, M. I., Weick, J. P., Becklund, B. R., Kuo, S. P., Groth, R. D., & Mermelstein, P. G. (2005). Estradiol activates group I and II metabotropic glutamate receptor signaling, leading to opposing influences on cAMP response element-binding protein. *J Neurosci*, *25*(20), 5066-5078.

Brailoiu, E., Dun, S. L., Brailoiu, G. C., Mizuo, K., Sklar, L. A., Oprea, T. I., Prossnitz, E. R., & Dun, N. J. (2007). Distribution and characterization of estrogen receptor G protein-coupled receptor 30 in the rat central nervous system [Research Support, N.I.H., ExtramuralResearch Support, Non-U.S. Gov't]. *J Endocrinol*, *193*(2), 311-321.

Brann, D., Raz, L., Wang, R., Vadlamudi, R., & Zhang, Q. (2012). Oestrogen signalling and neuroprotection in cerebral ischaemia. *J Neuroendocrinol*, *24*(1), 34-47.

Breen, P. P., & Buskila, Y. (2014). Braincubator: an incubation system to extend brain slice lifespan for use in neurophysiology. *Annu Int Conf IEEE Eng Med Biol Soc*, *2014*, 4864-4867.

Briz, V., Liu, Y., Zhu, G., Bi, X., & Baudry, M. (2015). A novel form of synaptic plasticity in field CA3 of hippocampus requires GPER1 activation and BDNF release. *J Cell Biol*, *210*(7), 1225-1237.

Brock, O., Baum, M. J., & Bakker, J. (2011). The development of female sexual behavior requires prepubertal estradiol. *J Neurosci*, *31*(15), 5574-5578.

Brooks, D. C., Coon V, J. S., Ercan, C. M., Xu, X., Dong, H., Levine, J. E., Bulun, S. E., & Zhao, H. (2020). Brain Aromatase and the Regulation of Sexual Activity in Male Mice. *Endocrinology*, *161*(10).

Brooks, D. C., Zhao, H., Yilmaz, M. B., Coon, V. J., & Bulun, S. E. (2012). Glucocorticoid-induction of hypothalamic aromatase via its brain-specific promoter. *Mol Cell Endocrinol*, *362*(1-2), 85-90.

Broselid, S., Berg, K. A., Chavera, T. A., Kahn, R., Clarke, W. P., Olde, B., & Leeb-Lundberg, L. M. (2014). G protein-coupled receptor 30 (GPR30) forms a plasma membrane complex with membrane-associated guanylate kinases (MAGUKs) and protein kinase A-anchoring protein 5 (AKAP5) that constitutively inhibits cAMP production. *J Biol Chem*, *289*(32), 22117-22127.

Buskila, Y., Breen, P. P., Tapson, J., van Schaik, A., Barton, M., & Morley, J. W. (2014). Extending the viability of acute brain slices. *Scientific Reports*, *4*(1), 5309.

Butler, M. J., Hildebrandt, R. P., & Eckel, L. A. (2018). Selective activation of estrogen receptors, ERα and GPER-1, rapidly decreases food intake in female rats. *Hormones and Behavior*, *103*, 54-61.

Buu, N. T., Hui, R.-t., & Falardeau, P. (1993). Norepinephrine in neonatal rat ventricular myocytes: association with the cell nucleus and binding to nuclear α1-and β-adrenergic receptors. *Journal of molecular and cellular cardiology*, *25*(9), 1037-1046.

Cammarata, P. R., Chu, S., Moor, A., Wang, Z., Yang, S.-H., & Simpkins, J. W. (2004). Subcellular distribution of native estrogen receptor α and β subtypes in cultured human lens epithelial cells. *Experimental eye research*, *78*(4), 861-871.

Caruso, D., Pesaresi, M., Abbiati, F., Calabrese, D., Giatti, S., Garcia-Segura, L. M., & Melcangi, R. C. (2013). Comparison of plasma and cerebrospinal fluid levels of neuroactive steroids with their brain, spinal cord and peripheral nerve levels in male and female rats. *Psychoneuroendocrinology*, *38*(10), 2278-2290.

Catalano, S., Giordano, C., Panza, S., Chemi, F., Bonofiglio, D., Lanzino, M., Rizza, P., Romeo, F., Fuqua, S. A., Maggiolini, M., Ando, S., & Barone, I. (2014). Tamoxifen through GPER upregulates aromatase expression: a novel mechanism sustaining

tamoxifen-resistant breast cancer cell growth. *Breast Cancer Res Treat*, *146*(2), 273-285.
Chaban, V. V., Lakhter, A. J., & Micevych, P. (2004). A membrane estrogen receptor mediates intracellular calcium release in astrocytes. *Endocrinology*, *145*(8), 3788-3795.
Chambliss, K. L., & Shaul, P. W. (2002). Estrogen modulation of endothelial nitric oxide synthase. *Endocr Rev*, *23*(5), 665-686.
Chan, H. J., Petrossian, K., & Chen, S. (2016). Structural and functional characterization of aromatase, estrogen receptor, and their genes in endocrine-responsive and -resistant breast cancer cells. *J Steroid Biochem Mol Biol*, *161*, 73-83.
Chan, M. Y., Huang, H., & Leung, L. K. (2010). 2, 3, 7, 8-Tetrachlorodibenzo-para-dioxin increases aromatase (CYP19) mRNA stability in MCF-7 cells. *Molecular and Cellular Endocrinology*, *317*(1-2), 8-13.
Charlier, T., Ball, G., & Balthazart, J. (2005). Sexual behavior activates the expression of the immediate early genes c-fos and Zenk (egr-1) in catecholaminergic neurons of male Japanese quail. *Neuroscience*, *131*(1), 13-30.
Charlier, T. D., Cornil, C. A., Ball, G. F., & Balthazart, J. (2010). Diversity of mechanisms involved in aromatase regulation and estrogen action in the brain [Research Support, N.I.H., Extramural Research Support, Non-U.S. Gov'tReview]. *Biochim Biophys Acta*, *1800*(10), 1094-1105.
Charlier, T. D., Po, K. W. L., Newman, A. E. M., Shah, A. H., Saldanha, C. J., & Soma, K. K. (2010). 17β-Estradiol levels in male zebra finch brain: Combining Palkovits punch and an ultrasensitive radioimmunoassay. *General and Comparative Endocrinology*, *167*(1), 18-26.
Cheewasopit, W., Laird, M., Glister, C., & Knight, P. G. (2018). Myostatin is expressed in bovine ovarian follicles and modulates granulosal and thecal steroidogenesis. *Reproduction*, *156*(4), 375-386.
Chen, G. G., Zeng, Q., & Tse, G. M. (2008). Estrogen and its receptors in cancer. *Medicinal research reviews*, *28*(6), 954-974.
Chen, P., & Hong, W. (2018). Neural Circuit Mechanisms of Social Behavior. *Neuron*, *98*(1), 16-30.
Cheng, S. B., Graeber, C. T., Quinn, J. A., & Filardo, E. J. (2011). Retrograde transport of the transmembrane estrogen receptor, G-protein-coupled-receptor-30 (GPR30/GPER) from the plasma membrane towards the nucleus. *Steroids*, *76*(9), 892-896.
Cheng, S. B., Quinn, J. A., Graeber, C. T., & Filardo, E. J. (2011). Down-modulation of the G-protein-coupled estrogen receptor, GPER, from the cell surface occurs via a trans-Golgi-proteasome pathway. *J Biol Chem*, *286*(25), 22441-22455.
Cheung, A. M.-Y., Wang, D., Liu, K., Hope, T., Murray, M., Ginty, F., Nofech-Mozes, S., Martel, A. L., & Yaffe, M. J. (2021). Quantitative single-cell analysis of immunofluorescence protein multiplex images illustrates biomarker spatial heterogeneity within breast cancer subtypes. *Breast Cancer Research*, *23*, 1-17.
Christensen, A., Dewing, P., & Micevych, P. (2011). Membrane-initiated estradiol signaling induces spinogenesis required for female sexual receptivity [Research Support, N.I.H., Extramural]. *J Neurosci*, *31*(48), 17583-17589.
Christensen, A., & Micevych, P. (2012). CAV1 siRNA reduces membrane estrogen receptor-alpha levels and attenuates sexual receptivity [Research Support, N.I.H., Extramural]. *Endocrinology*, *153*(8), 3872-3877.
Christensen, A., & Micevych, P. (2013). A Novel Membrane Estrogen Receptor Activated by STX Induces Female Sexual Receptivity through an Interaction with mGluR1a [Research Support, N.I.H., Extramural]. *Neuroendocrinology*, *97*(4), 363-368.
Cintra, A., Fuxe, K., Härfstrand, A., Agnati, L., Miller, L., Greene, J., & Gustafsson, J.-Å. (1986). Rapid important paper on the cellular localization and distribution of estrogen receptors in the rat tel-and diencephalon using monoclonal antibodies to human estrogen receptor. *Neurochem Int*, *8*(4), 587-595.

Cisternas, C. D., Cabrera Zapata, L. E., Arevalo, M. A., Garcia-Segura, L. M., & Cambiasso, M. J. (2017). Regulation of aromatase expression in the anterior amygdala of the developing mouse brain depends on ERβ and sex chromosome complement. *Scientific Reports*, *7*(1), 1-13.

Clancy, A. N., Coquelin, A., Macrides, F., Gorski, R. A., & Noble, E. (1984). Sexual behavior and aggression in male mice: involvement of the vomeronasal system. *Journal of Neuroscience*, *4*(9), 2222-2229.

Clancy, A. N., Zumpe, D., & Michael, R. P. (2000). Estrogen in the medial preoptic area of male rats facilitates copulatory behavior. *Hormones and Behavior*, *38*(2), 86-93.

Clark, S., Rainville, J., Zhao, X., Katzenellenbogen, B. S., Pfaff, D., & Vasudevan, N. (2014). Estrogen receptor-mediated transcription involves the activation of multiple kinase pathways in neuroblastoma cells. *J Steroid Biochem Mol Biol*, *139*, 45-53.

Commins, D., & Yahr, P. (1985). Autoradiographic localization of estrogen and androgen receptors in the sexually dimorphic area and other regions of the gerbil brain. *Journal of Comparative Neurology*, *231*(4), 473-489.

Coolen, L. M., Olivier, B., Peters, H. J., & Veening, J. G. (1997). Demonstration of ejaculation-induced neural activity in the male rat brain using 5-HT1A agonist 8-OH-DPAT. *Physiol Behav*, *62*(4), 881-891.

Coolen, L. M., Peters, H. J., & Veening, J. G. (1996). Fos immunoreactivity in the rat brain following consummatory elements of sexual behavior: a sex comparison. *Brain Res*, *738*(1), 67-82.

Coolen, L. M., Peters, H. J., & Veening, J. G. (1998). Anatomical interrelationships of the medial preoptic area and other brain regions activated following male sexual behavior: a combined fos and tract-tracing study. *J Comp Neurol*, *397*(3), 421-435.

Cornil, C. A., Ball, G. F., & Balthazart, J. (2012). Rapid control of male typical behaviors by brain-derived estrogens. *Frontiers in Neuroendocrinology*, *33*(4), 425-446.

Cornil, C. A., Ball, G. F., & Balthazart, J. (2012). Rapid control of male typical behaviors by brain-derived estrogens [Research Support, N.I.H., ExtramuralResearch Support, Non-U.S. Gov't]. *Front Neuroendocrinol*, *33*(4), 425-446.

Cornil, C. A., Ball, G. F., & Balthazart, J. (2018). Differential control of appetitive and consummatory sexual behavior by neuroestrogens in male quail. *Hormones and Behavior*, *104*, 15-31.

Cornil, C. A., Dalla, C., Papadopoulou-Daifoti, Z., Baillien, M., & Balthazart, J. (2006). Estradiol rapidly activates male sexual behavior and affects brain monoamine levels in the quail brain. *Behavioural brain research*, *166*(1), 110-123.

Cornil, C. A., Dalla, C., Papadopoulou-Daifoti, Z., Baillien, M., & Balthazart, J. (2006). Estradiol rapidly activates male sexual behavior and affects brain monoamine levels in the quail brain [Comparative Study Research Support, N.I.H., ExtramuralResearch Support, Non-U.S. Gov't]. *Behav Brain Res*, *166*(1), 110-123.

Court, L., Balthazart, J., Ball, G. F., & Cornil, C. A. (2022). Role of aromatase in distinct brain nuclei of the social behaviour network in the expression of sexual behaviour in male Japanese quail. *J Neuroendocrinol*, *34*(6), e13127.

Cross, E., & Roselli, C. E. (1999). 17beta-estradiol rapidly facilitates chemoinvestigation and mounting in castrated male rats. *Am J Physiol*, *276*(5 Pt 2), R1346-1350.

Cui, J., Shen, Y., & Li, R. (2013). Estrogen synthesis and signaling pathways during aging: from periphery to brain. *Trends in molecular medicine*, *19*(3), 197-209.

Dalla, C., Antoniou, K., Papadopoulou-Daifoti, Z., Balthazart, J., & Bakker, J. (2004). Oestrogen-deficient female aromatase knockout (ArKO) mice exhibit depressive-like symptomatology. *Eur J Neurosci*, *20*(1), 217-228.

Dalla, C., Antoniou, K., Papadopoulou-Daifoti, Z., Balthazart, J., & Bakker, J. (2005). Male aromatase-knockout mice exhibit normal levels of activity, anxiety and "depressive-like" symptomatology. *Behav Brain Res*, *163*(2), 186-193.

Davis, D., Dovey, J., Sagoshi, S., Thaweepanyaporn, K., Ogawa, S., & Vasudevan, N. (2023). Steroid hormone-mediated regulation of sexual and aggressive behaviour by non-genomic signalling. *Steroids*, *200*, 109324.

Davis, D., Vajaria, R., Delivopoulos, E., & Vasudevan, N. (2023). Localisation of oestrogen receptors in stem cells and in stem cell-derived neurons of the mouse. *Journal of Neuroendocrinology*, *35*(2), e13220.

Davis, E. C., Popper, P., & Gorski, R. A. (1996). The role of apoptosis in sexual differentiation of the rat sexually dimorphic nucleus of the preoptic area. *Brain Res*, *734*(1-2), 10-18.

Davis, P. G., McEwen, B., & Pfaff, D. W. (1979). Localized behavioral effects of tritiated estradiol implants in the ventromedial hypothalamus of female rats. *Endocrinology*, *104*, 893-903.

Davis, P. J., Davis, F. B., Lin, H. Y., & Bergh, J. (2004). Non genomic actions of thyroid hormone. Faseb Summer Research conferences: Steroid Hormone receptors: Integration of Plasma membrane and nuclear initiated signaling in hormone action., Tucson, Arizona.

de Bournonville, C., Dickens, M. J., Ball, G. F., Balthazart, J., & Cornil, C. A. (2013). Dynamic changes in brain aromatase activity following sexual interactions in males: where, when and why? [Research Support, N.I.H., Extramural Research Support, Non-U.S. Gov't Research Support, U.S. Gov't, Non-P.H.S.]. *Psychoneuroendocrinology*, *38*(6), 789-799.

de Valdivia, E. G., Broselid, S., Kahn, R., Olde, B., & Leeb-Lundberg, L. F. (2017). G protein-coupled estrogen receptor 1 (GPER1)/GPR30 increases ERK1/2 activity through PDZ motif-dependent and-independent mechanisms. *Journal of Biological Chemistry*, *292*(24), 9932-9943.

Delivopoulos, E., & Murray, A. F. (2011). Controlled adhesion and growth of long term glial and neuronal cultures on parylene-C. *PLoS One*, *6*(9), e25411.

Delivopoulos, E., Shakesheff, K. M., & Peto, H. (2015, 25-29 Aug. 2015). Neuralization of mouse embryonic stem cells in alginate hydrogels under retinoic acid and SAG treatment. 2015 37th Annual International Conference of the IEEE Engineering in Medicine and Biology Society (EMBC),

Dewing, P., Boulware, M. I., Sinchak, K., Christensen, A., Mermelstein, P. G., & Micevych, P. (2007). Membrane estrogen receptor-alpha interactions with metabotropic glutamate receptor 1a modulate female sexual receptivity in rats [Research Support, N.I.H., Extramural]. *J Neurosci*, *27*(35), 9294-9300.

Dewing, P., Christensen, A., Bondar, G., & Micevych, P. (2008). Protein kinase C signaling in the hypothalamic arcuate nucleus regulates sexual receptivity in female rats. *Endocrinology*, *149*(12), 5934-5942.

Dickens, M. J., Cornil, C. A., & Balthazart, J. (2011). Acute stress differentially affects aromatase activity in specific brain nuclei of adult male and female quail [Research Support, N.I.H., Extramural Research Support, Non-U.S. Gov'tResearch Support, U.S. Gov't, Non-P.H.S.]. *Endocrinology*, *152*(11), 4242-4251.

Do Rego, J. L., Seong, J. Y., Burel, D., Leprince, J., Luu-The, V., Tsutsui, K., Tonon, M. C., Pelletier, G., & Vaudry, H. (2009). Neurosteroid biosynthesis: enzymatic pathways and neuroendocrine regulation by neurotransmitters and neuropeptides. *Front Neuroendocrinol*, *30*(3), 259-301.

Dominguez-Ordonez, R., Garcia-Juarez, M., Lima-Hernandez, F. J., Gomora-Arrati, P., Blaustein, J. D., Etgen, A. M., & Gonzalez-Flores, O. (2016). Estrogen receptor alpha and beta are involved in the activation of lordosis behavior in estradiol-primed rats. *Horm Behav*, *86*, 1-7.

Domínguez-Ordoñez, R., Garcia-Juárez, M., Tapia-Hernández, S., Luna-Hernández, A., Galindo-Madrid, M. E., Tecamachaltzi-Silvarán, M. B., Hoffman, K. L., Pfaus, J. G., & González-Flores, O. (2021). Oxytocin induces lordosis behavior in female rats

through the prostaglandin E2/GnRH signaling system. *Hormones and Behavior*, *136*, 105081.

Domínguez-Ordóñez, R., García-Juárez, M., Lima-Hernández, F. J., Gómora-Arrati, P., Domínguez-Salazar, E., Luna-Hernández, A., Hoffman, K. L., Blaustein, J. D., Etgen, A. M., & González-Flores, O. (2019). Protein kinase inhibitors infused intraventricularly or into the ventromedial hypothalamus block short latency facilitation of lordosis by oestradiol. *Journal of Neuroendocrinology*, *31*(12), e12809.

Dominguez, R., Dewing, P., Kuo, J., & Micevych, P. (2013). Membrane-initiated estradiol signaling in immortalized hypothalamic N-38 neurons [Research Support, N.I.H., Extramural]. *Steroids*, *78*(6), 607-613.

Dominguez, R., Hu, E., Zhou, M., & Baudry, M. (2009). 17beta-estradiol-mediated neuroprotection and ERK activation require a pertussis toxin-sensitive mechanism involving GRK2 and beta-arrestin-1. *J Neurosci*, *29*(13), 4228-4238.

Dominguez, R., & Micevych, P. (2010). Estradiol rapidly regulates membrane estrogen receptor alpha levels in hypothalamic neurons [Research Support, N.I.H., Extramural]. *J Neurosci*, *30*(38), 12589-12596.

Doolan, C. M., & Harvey, B. J. (2003). A Galphas protein-coupled membrane receptor, distinct from the classical oestrogen receptor, transduces rapid effects of oestradiol on [Ca2+]i in female rat distal colon. *Mol Cell Endocrinol*, *199*(1-2), 87-103.

Dos-Anjos, S., Martínez-Villayandre, B., Montori, S., Salas, A., Pérez-García, C. C., & Fernández-López, A. (2008). Quantitative gene expression analysis in a brain slice model: influence of temperature and incubation media. *Anal Biochem*, *378*(1), 99-101.

Dovey, J. L., & Vasudevan, N. (2020). Does GPER1 play a role in sexual dimorphism? *Front Endocrinol (Lausanne)*, *11*, 595895.

Dulce Madeira, M., Ferreira-Silva, L., & Paula-Barbosa, M. M. (2001). Influence of sex and estrus cycle on the sexual dimorphisms of the hypothalamic ventromedial nucleus: stereological evaluation and Golgi study. *Journal of Comparative Neurology*, *432*(3), 329-345.

Efroni, S., Duttagupta, R., Cheng, J., Dehghani, H., Hoeppner, D. J., Dash, C., Bazett-Jones, D. P., Le Grice, S., McKay, R. D., & Buetow, K. H. (2008). Global transcription in pluripotent embryonic stem cells. *Cell Stem Cell*, *2*(5), 437-447.

Ellem, S. J., & Risbridger, G. P. (2009). The dual, opposing roles of estrogen in the prostate. *Annals of the New York Academy of Sciences*, *1155*(1), 174-186.

Enmark, E., & Gustafsson, J. A. (1999). Oestrogen receptors - an overview. *J Intern Med*, *246*(2), 133-138.

Ervin, K., Phan, A., Gabor, C., & Choleris, E. (2013). Rapid oestrogenic regulation of social and nonsocial learning. *Journal of Neuroendocrinology*, *25*(11), 1116-1132.

Ervin, K. S., Lymer, J. M., Matta, R., Clipperton-Allen, A. E., Kavaliers, M., & Choleris, E. (2015). Estrogen involvement in social behavior in rodents: Rapid and long-term actions. *Horm Behav*, *74*, 53-76.

Ervin, K. S., Mulvale, E., Gallagher, N., Roussel, V., & Choleris, E. (2015). Activation of the G protein-coupled estrogen receptor, but not estrogen receptor alpha or beta, rapidly enhances social learning. *Psychoneuroendocrinology*, *58*, 51-66.

Ervin, K. S., Phan, A., Gabor, C. S., & Choleris, E. (2013). Rapid oestrogenic regulation of social and nonsocial learning. *J Neuroendocrinol*, *25*(11), 1116-1132.

Falkner, A. L., Dollar, P., Perona, P., Anderson, D. J., & Lin, D. (2014). Decoding ventromedial hypothalamic neural activity during male mouse aggression. *Journal of Neuroscience*, *34*(17), 5971-5984.

Fannon, O. M., Bithell, A., Whalley, B. J., & Delivopoulos, E. (2020). A Fiber Alginate Co-culture Platform for the Differentiation of mESC and Modeling of the Neural Tube. *Front Neurosci*, *14*, 524346.

Feder, H. H., & Whalen, R. E. (1965). Feminine behavior in neonatally castrated and estrogen-treated male rats. *Science*, *147*(3655), 306-307.

Fernandez, S. M., Lewis, M. C., Pechenino, A. S., Harburger, L. L., Orr, P. T., Gresack, J. E., Schafe, G. E., & Frick, K. M. (2008). Estradiol-induced enhancement of object memory consolidation involves hippocampal extracellular signal-regulated kinase activation and membrane-bound estrogen receptors [Research Support, N.I.H., Extramural]. *J Neurosci*, *28*(35), 8660-8667.

Fester, L., Zhou, L., Butow, A., Huber, C., von Lossow, R., Prange-Kiel, J., Jarry, H., & Rune, G. M. (2009). Cholesterol-promoted synaptogenesis requires the conversion of cholesterol to estradiol in the hippocampus. *Hippocampus*, *19*(8), 692-705.

Filardo, E., Quinn, J., Pang, Y., Graeber, C., Shaw, S., Dong, J., & Thomas, P. (2007). Activation of the novel estrogen receptor G protein-coupled receptor 30 (GPR30) at the plasma membrane [Research Support, N.I.H., Extramural Research Support, Non-U.S. Gov't Research Support, U.S. Gov't, Non-P.H.S.]. *Endocrinology*, *148*(7), 3236-3245.

Filardo, E. J. (2002). Epidermal growth factor receptor (EGFR) transactivation by estrogen via the G-protein-coupled receptor, GPR30: a novel signaling pathway with potential significance for breast cancer. *J Steroid Biochem Mol Biol*, *80*(2), 231-238.

Filardo, E. J., Quinn, J. A., Bland, K. I., & Frackelton, A. R., Jr. (2000). Estrogen-induced activation of Erk-1 and Erk-2 requires the G protein-coupled receptor homolog, GPR30, and occurs via trans-activation of the epidermal growth factor receptor through release of HB-EGF [Research Support, Non-U.S. Gov't Research Support, U.S. Gov't, P.H.S.]. *Mol Endocrinol*, *14*(10), 1649-1660.

Filardo, E. J., Quinn, J. A., Bland, K. I., & Frackelton Jr, A. R. (2000). Estrogen-induced activation of Erk-1 and Erk-2 requires the G protein-coupled receptor homolog, GPR30, and occurs via trans-activation of the epidermal growth factor receptor through release of HB-EGF. *Molecular Endocrinology*, *14*(10), 1649-1660.

Filardo, E. J., Quinn, J. A., Frackelton, A. R., Jr., & Bland, K. I. (2002). Estrogen action via the G protein-coupled receptor, GPR30: stimulation of adenylyl cyclase and cAMP-mediated attenuation of the epidermal growth factor receptor-to-MAPK signaling axis. *Mol Endocrinol*, *16*(1), 70-84.

Filardo, E. J., & Thomas, P. (2005). GPR30: a seven-transmembrane-spanning estrogen receptor that triggers EGF release [Review]. *Trends Endocrinol Metab*, *16*(8), 362-367.

Flanagan-Cato, L. M., Calizo, L. H., & Daniels, D. (2001). The synaptic organization of VMH neurons that mediate the effects of estrogen on sexual behavior. *Horm Behav*, *40*(2), 178-182.

Frankfurt, M. (1994). Gonadal steroids and neuronal plasticity: Studies in the adult rat hypothalamus. *Ann NY Acad Sci*, *743*, 45-60.

Frankfurt, M., Gould, E., Woolley, C. S., & McEwen, B. S. (1990). Gonadal steroids modify dendritic spine density in ventromedial hypothalamic neurons: a Golgi study in the adult rat. *Neuroendocrinology*, *51*(5), 530-535.

Frick, K. M., & Kim, J. (2018). Mechanisms underlying the rapid effects of estradiol and progesterone on hippocampal memory consolidation in female rodents. *Horm Behav*.

Fuentes, N., & Silveyra, P. (2019). Estrogen receptor signaling mechanisms. *Adv Protein Chem Struct Biol*, *116*, 135-170.

Fukuchi, M., Tabuchi, A., & Tsuda, M. (2005). Transcriptional regulation of neuronal genes and its effect on neural functions: cumulative mRNA expression of PACAP and BDNF genes controlled by calcium and cAMP signals in neurons. *J Pharmacol Sci*, *98*(3), 212-218.

Funakoshi, T., Yanai, A., Shinoda, K., Kawano, M. M., & Mizukami, Y. (2006). G protein-coupled receptor 30 is an estrogen receptor in the plasma membrane [Research Support, Non-U.S. Gov't]. *Biochem Biophys Res Commun*, *346*(3), 904-910.

Furukawa, A., Miyatake, A., Ohnishi, T., & Ichikawa, Y. (1998). Steroidogenic acute regulatory protein (StAR) transcripts constitutively expressed in the adult rat central

nervous system: colocalization of StAR, cytochrome P-450SCC (CYP XIA1), and 3β-hydroxysteroid dehydrogenase in the rat brain. *Journal of neurochemistry*, *71*(6), 2231-2238.

Gabor, C., Lymer, J., Phan, A., & Choleris, E. (2015). Rapid effects of the G-protein coupled oestrogen receptor (GPER) on learning and dorsal hippocampus dendritic spines in female mice. *Physiol Behav*, *149*, 53-60.

Gabor, C., Lymer, J., Phan, A., & Choleris, E. (2015). Rapid effects of the G-protein coupled oestrogen receptor (GPER) on learning and dorsal hippocampus dendritic spines in female mice. *Physiology & behavior*, *149*, 53-60.

Galbiati, F., Volonte, D., Gil, O., Zanazzi, G., Salzer, J. L., Sargiacomo, M., Scherer, P. E., Engelman, J. A., Schlegel, A., Parenti, M., Okamoto, T., & Lisanti, M. P. (1998). Expression of caveolin-1 and -2 in differentiating PC12 cells and dorsal root ganglion neurons: caveolin-2 is up-regulated in response to cell injury. *Proc Natl Acad Sci U S A*, *95*(17), 10257-10262.

Garcia-Segura, L. M., Diz-Chaves, Y., Perez-Martin, M., & Darnaudery, M. (2007). Estradiol, insulin-like growth factor-I and brain aging. *Psychoneuroendocrinology*, *32 Suppl 1*, S57-61.

Gegenhuber, B., & Tollkuhn, J. (2022). Epigenetic mechanisms of brain sexual differentiation. *Cold Spring Harbor perspectives in biology*, *14*(11), a039099.

Gervais, N. J., Jacob, S., Brake, W. G., & Mumby, D. G. (2013). Systemic and intra-rhinal-cortical 17-β estradiol administration modulate object-recognition memory in ovariectomized female rats. *Hormones and Behavior*, *64*(4), 642-652.

Ghosh, D., Griswold, J., Erman, M., & Pangborn, W. (2009). Structural basis for androgen specificity and oestrogen synthesis in human aromatase. *Nature*, *457*(7226), 219-223.

Giatti, S., Garcia-Segura, L. M., Barreto, G. E., & Melcangi, R. C. (2019). Neuroactive steroids, neurosteroidogenesis and sex. *Prog Neurobiol*, *176*, 1-17.

Gilad, L. A., & Schwartz, B. (2007). Association of estrogen receptor β with plasma-membrane caveola components: Implication in control of vitamin D receptor. *Journal of molecular endocrinology*, *38*(6), 603-618.

Girgert, R., Emons, G., & Gründker, C. (2019). Estrogen signaling in ERα-negative breast cancer: ERβ and GPER. *Front Endocrinol (Lausanne)*, *9*, 781.

Goodson, J. L. (2005). The vertebrate social behavior network: evolutionary themes and variations. *Horm Behav*, *48*(1), 11-22.

Goodson, J. L., & Kabelik, D. (2009). Dynamic limbic networks and social diversity in vertebrates: from neural context to neuromodulatory patterning. *Front Neuroendocrinol*, *30*(4), 429-441.

Goodson, J. L., & Kabelik, D. (2009). Dynamic limbic networks and social diversity in vertebrates: from neural context to neuromodulatory patterning. *Frontiers in Neuroendocrinology*, *30*(4), 429-441.

Greenberg, G. D., & Trainor, B. C. (2016). Sex Differences in the Social Behavior Network and Mesolimbic Dopamine System. In *Sex differences in the central nervous system* (pp. 77-106). Academic Press.

Greenberg, G. D., & Trainor, B. C. (2016). Sex differences in the social behavior network and mesolimbic dopamine system. *Sex differences in the central nervous system*, 77-106.

Grove-Strawser, D., Boulware, M. I., & Mermelstein, P. G. (2010). Membrane estrogen receptors activate the metabotropic glutamate receptors mGluR5 and mGluR3 to bidirectionally regulate CREB phosphorylation in female rat striatal neurons. *Neuroscience*, *170*(4), 1045-1055.

Gu, Q., & Moss, R. L. (1996). 17beta estradiol potentiates kainate-induced currents via activation of the cAMP cascade. *J Neurosci*, *16*, 3620-3629.

Gu, Q., Tomaskovic-Crook, E., Lozano, R., Chen, Y., Kapsa, R. M., Zhou, Q., Wallace, G. G., & Crook, J. M. (2016). Functional 3D neural mini-tissues from printed gel-based bioink and human neural stem cells. *Advanced healthcare materials*, *5*(12), 1429-1438.

Hadjimarkou, M. M., & Vasudevan, N. (2018). GPER1/GPR30 in the brain: Crosstalk with classical estrogen receptors and implications for behavior. *J Steroid Biochem Mol Biol*, *176*, 57-64.

Hall, P. F. (1984). Cellular organization for steroidogenesis. *International review of cytology*, *86*, 53-95.

Hammond, R., Nelson, D., & Gibbs, R. B. (2011). GPR30 co-localizes with cholinergic neurons in the basal forebrain and enhances potassium-stimulated acetylcholine release in the hippocampus. *Psychoneuroendocrinology*, *36*(2), 182-192.

Hanafiah, A., Geng, Z., Wang, Q., & Gao, Z. (2020). Differentiation and characterization of neural progenitors and neurons from mouse embryonic stem cells. *JoVE (Journal of Visualized Experiments)*(159), e61446.

Harris, J., & Gorski, J. (1978). Evidence for a discontinuous requirement for estrogen in stimulation of deoxyribonucleic acid synthesis in the immature rat uterus. *Endocrinology*, *103*, 240-245.

Hart, D., Nilges, M., Pollard, K., Lynn, T., Patsos, O., Shiel, C., Clark, S. M., & Vasudevan, N. (2014). Activation of the G-protein coupled receptor 30 (GPR30) has different effects on anxiety in male and female mice. *Steroids*, *81*, 49-56.

Hashikawa, K., Hashikawa, Y., Falkner, A., & Lin, D. (2016). The neural circuits of mating and fighting in male mice. *Curr Opin Neurobiol*, *38*, 27-37.

Hayashi, S., Eguchi, H., Tanimoto, K., Yoshida, T., Omoto, Y., Inoue, A., Yoshida, N., & Yamaguchi, Y. (2003). The expression and function of estrogen receptor alpha and beta in human breast cancer and its clinical application. *Endocrine-Related Cancer*, *10*(2), 193-202.

Haynes, M. P., Sinha, D., Russell, K. S., Collinge, M., Fulton, D., Morales-Ruiz, M., Sessa, W. C., & Bender, J. R. (2000). Membrane estrogen receptor engagement activates endothelial nitric oxide synthase via the PI3-kinase-Akt pathway in human endothelial cells. *Circ Res*, *87*(8), 677-682.

Hazell, G. G., Yao, S. T., Roper, J. A., Prossnitz, E. R., O'Carroll, A. M., & Lolait, S. J. (2009). Localisation of GPR30, a novel G protein-coupled oestrogen receptor, suggests multiple functions in rodent brain and peripheral tissues. *J Endocrinol*, *202*(2), 223-236.

Heldring, N., Pike, A., Andersson, S., Matthews, J., Cheng, G., Hartman, J., Tujague, M., Ström, A., Treuter, E., Warner, M., & Gustafsson, J.-Å. (2007). Estrogen Receptors: How Do They Signal and What Are Their Targets. *Physiological Reviews*, *87*(3), 905-931.

Hines, M., Allen, L. S., & Gorski, R. A. (1992). Sex differences in subregions of the medial nucleus of the amygdala and the bed nucleus of the stria terminalis of the rat. *Brain Res*, *579*(2), 321-326.

Hines, M., Davis, F. C., Coquelin, A., Goy, R. W., & Gorski, R. A. (1985). Sexually dimorphic regions in the medial preoptic area and the bed nucleus of the stria terminalis of the guinea pig brain: a description and an investigation of their relationship to gonadal steroids in adulthood. *J Neurosci*, *5*(1), 40-47.

Hisasue, S., Seney, M. L., Immerman, E., & Forger, N. G. (2010). Control of cell number in the bed nucleus of the stria terminalis of mice: role of testosterone metabolites and estrogen receptor subtypes. *J Sex Med*, *7*(4 Pt 1), 1401-1409.

Hojo, Y., Hattori, T. A., Enami, T., Furukawa, A., Suzuki, K., Ishii, H. T., Mukai, H., Morrison, J. H., Janssen, W. G., Kominami, S., Harada, N., Kimoto, T., & Kawato, S. (2004). Adult male rat hippocampus synthesizes estradiol from pregnenolone by cytochromes P45017alpha and P450 aromatase localized in neurons. *Proc Natl Acad Sci U S A*, *101*(3), 865-870.

Hojo, Y., Higo, S., Ishii, H., Ooishi, Y., Mukai, H., Murakami, G., Kominami, T., Kimoto, T., Honma, S., & Poirier, D. (2009). Comparison between hippocampus-synthesized and circulation-derived sex steroids in the hippocampus. *Endocrinology*, *150*(11), 5106-5112.

Hojo, Y., & Kawato, S. (2018). Neurosteroids in adult hippocampus of male and female rodents: biosynthesis and actions of sex steroids. *Front Endocrinol (Lausanne)*, *9*, 183.
Hojo, Y., Murakami, G., Mukai, H., Higo, S., Hatanaka, Y., Ogiue-Ikeda, M., Ishii, H., Kimoto, T., & Kawato, S. (2008). Estrogen synthesis in the brain--role in synaptic plasticity and memory. *Mol Cell Endocrinol*, *290*(1-2), 31-43.
Hojo, Y., Okamoto, M., Kato, A., Higo, S., Sakai, F., Soya, H., Yamazaki, T., & Kawato, S. (2014). Neurosteroid synthesis in adult female rat hippocampus, including androgens and allopregnanolone. *J Steroids Hormon Sci S*, *4*, 2.
Holst, J. P., Soldin, O. P., Guo, T., & Soldin, S. J. (2004). Steroid hormones: relevance and measurement in the clinical laboratory. *Clinics in laboratory medicine*, *24*(1), 105-118.
Honda, S.-i., Harada, N., Ito, S., Takagi, Y., & Maeda, S. (1998). Disruption of sexual behavior in male aromatase-deficient mice lacking exons 1 and 2 of thecyp19Gene. *Biochemical and biophysical research communications*, *252*(2), 445-449.
Honda, S.-I., Wakatsuki, T., & Harada, N. (2011). Behavioral analysis of genetically modified mice indicates essential roles of neurosteroidal estrogen. *Front Endocrinol (Lausanne)*, *2*, 40.
Hong, S. H., Nah, H. Y., Lee, Y. J., Lee, J. W., Park, J. H., Kim, S. J., Lee, J. B., Yoon, H. S., & Kim, C. H. (2004). Expression of estrogen receptor-α and-β, glucocorticoid receptor, and progesterone receptor genes in human embryonic stem cells and embryoid bodies. *Molecules and cells*, *18*(3), 320-325.
Hull, E. M., & Dominguez, J. M. (2007). Sexual behavior in male rodents. *Hormones and Behavior*, *52*(1), 45-55.
Ivanova, T., Karolczak, M., & Beyer, C. (2001). Estrogen stimulates the mitogen activated protein kinase pathway in midbrain astroglia. *Brain Res*, *889*(1-2), 264-269.
Jalabert, C., Shock, M. A., Ma, C., Bootsma, T. J., Liu, M. Q., & Soma, K. K. (2022). Ultrasensitive quantification of multiple estrogens in songbird blood and microdissected brain by LC-MS/MS. *eNeuro*, *9*(4).
Juneja, D. S., Nasuto, S., & Delivopoulos, E. (2020). Fast and efficient differentiation of mouse embryonic stem cells into ATP-responsive astrocytes. *Front Cell Neurosci*, *13*, 579.
Kalinichev, M., Rosenblatt, J. S., Nakabeppu, Y., & Morrell, J. I. (2000). Induction of c-fos-like and fosB-like immunoreactivity reveals forebrain neuronal populations involved differentially in pup-mediated maternal behavior in juvenile and adult rats. *Journal of Comparative Neurology*, *416*(1), 45-78.
Kallen, C. B., Billheimer, J. T., Summers, S. A., Stayrook, S. E., Lewis, M., & Strauss, J. F. (1998). Steroidogenic acute regulatory protein (StAR) is a sterol transfer protein. *Journal of Biological Chemistry*, *273*(41), 26285-26288.
Kang, L., Zhang, X., Xie, Y., Tu, Y., Wang, D., Liu, Z., & Wang, Z.-Y. (2010). Involvement of estrogen receptor variant ER-α36, not GPR30, in nongenomic estrogen signaling. *Molecular Endocrinology*, *24*(4), 709-721.
Kang, L., Zhang, X., Xie, Y., Tu, Y., Wang, D., Liu, Z., & Wang, Z. Y. (2010). Involvement of estrogen receptor variant ER-alpha36, not GPR30, in nongenomic estrogen signaling. *Mol Endocrinol*, *24*(4), 709-721.
Kato, A., Hojo, Y., Higo, S., Komatsuzaki, Y., Murakami, G., Yoshino, H., Uebayashi, M., & Kawato, S. (2013). Female hippocampal estrogens have a significant correlation with cyclic fluctuation of hippocampal spines. *Front Neural Circuits*, *7*, 149.
Kato, K., Nakagawa, C., Murabayashi, H., & Oomori, Y. (2014). Expression and distribution of GABA and GABAB-receptor in the rat adrenal gland. *Journal of Anatomy*, *224*(2), 207-215.
Katsetos, C. D., Herman, M. M., & Mörk, S. J. (2003). Class III β-tubulin in human development and cancer. *Cell motility and the cytoskeleton*, *55*(2), 77-96.
Kawato, S., Hojo, Y., & Kimoto, T. (2002). Histological and metabolism analysis of P450 expression in the brain.

Kelly, M. J., & Levin, E. R. (2001). Rapid actions of plasma membrane estrogen receptors. *Trends Endocrinol Metab*, *12*(4), 152-156.

Kendrick, A. M., Rand, M. S., & Crews, D. (1995). Electrolytic lesions to the ventromedial hypothalamus abolish receptivity in female whiptail lizards, Cnemidophorus uniparens. *Brain Research*, *680*(1-2), 226-228.

Khbouz, B., de Bournonville, C., Court, L., Taziaux, M., Corona, R., Arnal, J. F., Lenfant, F., & Cornil, C. A. (2020). Role for the membrane estrogen receptor alpha in the sexual differentiation of the brain. *Eur J Neurosci*, *52*(1), 2627-2645.

Kim, J., Szinte, J. S., Boulware, M. I., & Frick, K. M. (2016). 17beta-Estradiol and Agonism of G-protein-Coupled Estrogen Receptor Enhance Hippocampal Memory via Different Cell-Signaling Mechanisms. *J Neurosci*, *36*(11), 3309-3321.

King, S. R., Manna, P. R., Ishii, T., Syapin, P. J., Ginsberg, S. D., Wilson, K., Walsh, L. P., Parker, K. L., Stocco, D. M., & Smith, R. G. (2002). An essential component in steroid synthesis, the steroidogenic acute regulatory protein, is expressed in discrete regions of the brain. *Journal of Neuroscience*, *22*(24), 10613-10620.

Kirn, J., & Floody, O. R. (1985). Differential effects of lesions in three limbic areas on ultrasound production and lordosis by female hamsters. *Behav Neurosci*, *99*(6), 1142.

Koh, S., Lee, W., Park, S. M., & Kim, S. H. (2021). Caveolin-1 deficiency impairs synaptic transmission in hippocampal neurons. *Molecular brain*, *14*, 1-10.

Kollack-Walker, S., & Newman, S. (1995). Mating and agonistic behavior produce different patterns of Fos immunolabeling in the male Syrian hamster brain. *Neuroscience*, *66*(3), 721-736.

Konkle, A. T., & McCarthy, M. M. (2011). Developmental time course of estradiol, testosterone, and dihydrotestosterone levels in discrete regions of male and female rat brain [Research Support, N.I.H., Extramural Research Support, Non-U.S. Gov't]. *Endocrinology*, *152*(1), 223-235.

Koolhaas, J. M., Coppens, C. M., de Boer, S. F., Buwalda, B., Meerlo, P., & Timmermans, P. J. (2013). The resident-intruder paradigm: a standardized test for aggression, violence and social stress. *J Vis Exp*(77), e4367.

Kotula-Balak, M., Pawlicki, P., Milon, A., Tworzydlo, W., Sekula, M., Pacwa, A., Górowska-Wójtowicz, E., Bilinska, B., Pawlicka, B., & Wiater, J. (2018). The role of G-protein-coupled membrane estrogen receptor in mouse Leydig cell function—in vivo and in vitro evaluation. *Cell Tissue Res*, *374*, 389-412.

Kow, L.-M., & Pfaff, D. (1988). Transmitter and peptide actions on hypothalamic neurons in vitro: Implications for lordosis. *Brain Res Bull*, *20*, 857-861.

Kow, L.-M., & Pfaff, D. W. (2004). The membrane actions of estrogens can potentiate their lordosis behavior-facilitating genomic actions. *Proceedings of the National Academy of Sciences*, *101*(33), 12354-12357.

Kretz, O., Fester, L., Wehrenberg, U., Zhou, L., Brauckmann, S., Zhao, S., Prange-Kiel, J., Naumann, T., Jarry, H., Frotscher, M., & Rune, G. M. (2004). Hippocampal synapses depend on hippocampal estrogen synthesis. *J Neurosci*, *24*(26), 5913-5921.

Kuiper, G. G., Carlsson, B., Grandien, K., Enmark, E., Häggblad, J., Nilsson, S., & Gustafsson, J.-A. k. (1997). Comparison of the ligand binding specificity and transcript tissue distribution of estrogen receptors α and β. *Endocrinology*, *138*(3), 863-870.

Kuiper, G. G., Enmark, E., Pelto-Huikko, M., Nilsson, S., & Gustafsson, J. A. (1996). Cloning of a novel receptor expressed in rat prostate and ovary. *Proc Natl Acad Sci U S A*, *93*(12), 5925-5930.

Kumar, P., Kamat, A., & Mendelson, C. R. (2009). Estrogen receptor α (ERα) mediates stimulatory effects of estrogen on aromatase (CYP19) gene expression in human placenta. *Molecular Endocrinology*, *23*(6), 784-793.

Kuo, J., Hariri, O. R., Bondar, G., Ogi, J., & Micevych, P. (2009). Membrane estrogen receptor-alpha interacts with metabotropic glutamate receptor type 1a to mobilize intracellular calcium in hypothalamic astrocytes. *Endocrinology*, *150*(3), 1369-1376.

Labrie, F., Luu-The, V., Lin, S.-X., Claude, L., Simard, J., Breton, R., & Bélanger, A. (1997). The key role of 17β-hydroxysteroid dehydrogenases in sex steroid biology. *Steroids*, *62*(1), 148-158.

Laredo, S. A., Villalon Landeros, R., Dooley, J. C., Steinman, M. Q., Orr, V., Silva, A. L., Crean, K. K., Robles, C. F., & Trainor, B. C. (2013). Nongenomic effects of estradiol on aggression under short day photoperiods. *Horm Behav*, *64*(3), 557-565.

Lauber, A. H., Romano, G. J., Mobbs, C. V., Howells, R. D., & Pfaff, D. W. (1990). Estradiol induction of proenkephalin messenger RNA in hypothalamus: dose-response and relation to reproductive behavior in the female rat. *Mol Brain Res*, *8*, 47-54.

Lee, H., Kim, D. W., Remedios, R., Anthony, T. E., Chang, A., Madisen, L., Zeng, H., & Anderson, D. J. (2014). Scalable control of mounting and attack by Esr1+ neurons in the ventromedial hypothalamus. *Nature*, *509*(7502), 627-632.

Legradi, A., Varszegi, S., Szigeti, C., & Gulya, K. (2011). Adult rat hippocampal slices as in vitro models for neurodegeneration: Studies on cell viability and apoptotic processes. *Brain Res Bull*, *84*(1), 39-44.

Lenz, K., Nugent, B., & McCarthy, M. (2012). Sexual Differentiation of the Rodent Brain: Dogma and Beyond [Review]. *Front Neurosci*, *6*.

Lephart, E. D. (1996). A review of brain aromatase cytochrome P450. *Brain research reviews*, *22*(1), 1-26.

Leroy, F., Park, J., Asok, A., Brann, D. H., Meira, T., Boyle, L. M., Buss, E. W., Kandel, E. R., & Siegelbaum, S. A. (2018). A circuit from hippocampal CA2 to lateral septum disinhibits social aggression. *Nature*, *564*(7735), 213-218.

Levin, E. R. (2009a). G protein-coupled receptor 30: estrogen receptor or collaborator? *Endocrinology*, *150*(4), 1563-1565.

Levin, E. R. (2009b). Membrane oestrogen receptor alpha signalling to cell functions. *J Physiol*, *587*(Pt 21), 5019-5023.

Li, L., Haynes, M. P., & Bender, J. R. (2003). Plasma membrane localization and function of the estrogen receptor alpha variant (ER46) in human endothelial cells. *Proc Natl Acad Sci U S A*, *100*(8), 4807-4812.

Li, L., Haynes, M. P., & Bender, J. R. (2003). Plasma membrane localization and function of the estrogen receptor α variant (ER46) in human endothelial cells. *Proceedings of the National Academy of Sciences*, *100*(8), 4807-4812.

Li, Y., & Dulac, C. (2018). Neural coding of sex-specific social information in the mouse brain. *Curr Opin Neurobiol*, *53*, 120-130.

Lin, S.-L., Yan, L.-Y., Zhang, X.-T., Yuan, J., Li, M., Qiao, J., Wang, Z.-Y., & Sun, Q.-Y. (2010). ER-α36, a variant of ER-α, promotes tamoxifen agonist action in endometrial cancer cells via the MAPK/ERK and PI3K/Akt pathways. *PLoS One*, *5*(2), e9013.

Lind, G. J., & Cavanagh, H. D. (1993). Nuclear muscarinic acetylcholine receptors in corneal cells from rabbit. *Investigative ophthalmology & visual science*, *34*(10), 2943-2952.

Liu, S. B., Zhang, N., Guo, Y. Y., Zhao, R., Shi, T. Y., Feng, S. F., Wang, S. Q., Yang, Q., Li, X. Q., Wu, Y. M., Ma, L., Hou, Y., Xiong, L. Z., Zhang, W., & Zhao, M. G. (2012). G-protein-coupled receptor 30 mediates rapid neuroprotective effects of estrogen via depression of NR2B-containing NMDA receptors. *J Neurosci*, *32*(14), 4887-4900.

Liu, Y. Y., & Brent, G. A. (2005). Thyroid hormone-dependent gene expression in differentiated embryonic stem cells and embryonal carcinoma cells: identification of novel thyroid hormone target genes by deoxyribonucleic acid microarray analysis. *Endocrinology*, *146*(2), 776-783.

Livak, K. J., & Schmittgen, T. D. (2001). Analysis of relative gene expression data using real-time quantitative PCR and the 2(-Delta Delta C(T)) Method. *Methods*, *25*(4), 402-408.

S1046-2023(01)91262-9 [pii]

Long, N., Long, B., Mana, A., Le, D., Nguyen, L., Chokr, S., & Sinchak, K. (2017). Tamoxifen and ICI 182,780 activate hypothalamic G protein-coupled estrogen receptor 1 to rapidly facilitate lordosis in female rats. *Horm Behav*, *89*, 98-103.

Long, N., Serey, C., & Sinchak, K. (2014). 17beta-estradiol rapidly facilitates lordosis through G protein-coupled estrogen receptor 1 (GPER) via deactivation of medial preoptic nucleus mu-opioid receptors in estradiol primed female rats. *Horm Behav*, *66*(4), 663-666.

Loryan, I., Fridén, M., & Hammarlund-Udenaes, M. (2013). The brain slice method for studying drug distribution in the CNS. *Fluids and Barriers of the CNS*, *10*(1), 6.

Losel, R. M., Falkenstein, E., Feuring, M., Schultz, A., Tillmann, H.-C., Rossol-Haseroth, K., & Wehling, M. (2003). Nongenomic steroid action: controversies, questions, and answers. *Physiological Reviews*, *83*(3), 965-1016.

Lu, Y., Sareddy, G. R., Wang, J., Wang, R., Li, Y., Dong, Y., Zhang, Q., Liu, J., O'Connor, J. C., Xu, J., Vadlamudi, R. K., & Brann, D. W. (2019). Neuron-Derived Estrogen Regulates Synaptic Plasticity and Memory. *J Neurosci*, *39*(15), 2792-2809.

Łuczak, M., & Jagodziński, P. (2009). Trichostatin A down-regulates CYP19 transcript and protein levels in MCF-7 breast cancer cells. *Biomedicine & pharmacotherapy*, *63*(4), 262-266.

Luo, W., & Wiltbank, M. C. (2006). Distinct regulation by steroids of messenger RNAs for FSHR and CYP19A1 in bovine granulosa cells. *Biology of Reproduction*, *75*(2), 217-225.

Luoma, J. I., Boulware, M. I., & Mermelstein, P. G. (2008). Caveolin proteins and estrogen signaling in the brain. *Mol Cell Endocrinol*, *290*(1-2), 8-13.

Lymer, J., Robinson, A., Winters, B. D., & Choleris, E. (2017). Rapid effects of dorsal hippocampal G-protein coupled estrogen receptor on learning in female mice. *Psychoneuroendocrinology*, *77*, 131-140.

Lymer, J. M., Sheppard, P. A. S., Kuun, T., Blackman, A., Jani, N., Mahbub, S., & Choleris, E. (2018). Estrogens and their receptors in the medial amygdala rapidly facilitate social recognition in female mice. *Psychoneuroendocrinology*, *89*, 30-38.

Madeo, A., & Maggiolini, M. (2010). Nuclear alternate estrogen receptor GPR30 mediates 17β-estradiol–induced gene expression and migration in breast cancer–associated fibroblasts. *Cancer Res*, *70*(14), 6036-6046.

Manders, E., Verbeek, F., & Aten, J. (1993). Measurement of co-localization of objects in dual-colour confocal images. *Journal of microscopy*, *169*(3), 375-382.

Mangelsdorf, D. J., Thummel, C., Beato, M., Herrlich, P., Schultz, G., Umeseno, K., Blumber, B., Kastner, P., Mark, M., Chambon, P., & Evans, R. M. (1995). Overview: the nuclear receptor superfamily: the second decade. *Cell*, *83*, 835-840.

Marrocco, R., & Davidson, M. (1996). Neurochemistry of Attention. In R. Parasuraman (Ed.), *Mechanisms of Attention* (pp. 35-50).

Martin, L. A., Farmer, I., Johnston, S. R., Ali, S., Marshall, C., & Dowsett, M. (2003). Enhanced estrogen receptor (ER) alpha, ERBB2, and MAPK signal transduction pathways operate during the adaptation of MCF-7 cells to long term estrogen deprivation. *J Biol Chem*, *278*(33), 30458-30468.

Martini, M., Di Sante, G., Collado, P., Pinos, H., Guillamon, A., & Panzica, G. (2008). Androgen receptors are required for full masculinization of nitric oxide synthase system in rat limbic–hypothalamic region. *Hormones and Behavior*, *54*(4), 557-564.

Martini, M., Pradotto, M., & Panzica, G. (2011). Synergic effects of estradiol and progesterone on regulation of the hypothalamic neuronal nitric oxide synthase expression in ovariectomized mice. *Brain Research*, *1404*, 1-9.

Matsuda, K., Sakamoto, H., Mori, H., Hosokawa, K., Kawamura, A., Itose, M., Nishi, M., Prossnitz, E. R., & Kawata, M. (2008). Expression and intracellular distribution of the G protein-coupled receptor 30 in rat hippocampal formation. *Neurosci Lett*, *441*(1), 94-99.

Matthews, J., & Gustafsson, J.-Å. (2003). Estrogen signaling: a subtle balance between ERα and ERβ. *Molecular interventions*, *3*(5), 281.
Mazzucco, C. A., Walker, H. A., Pawluski, J. L., Lieblich, S. E., & Galea, L. A. (2008). ERalpha, but not ERbeta, mediates the expression of sexual behavior in the female rat. *Behav Brain Res*, *191*(1), 111-117.
Mccarthy, M. M. (2008). Estradiol and the Developing Brain. *Physiological Reviews*, *88*(1), 91-134.
McCarthy, M. M., Schlenker, E. H., & Pfaff, D. W. (1993). Enduring consequences of neonatal treatment with antisense oligodeoxynucleotides to estrogen receptor messenger ribonucleic acid on sexual differentiation of rat brain. *Endocrinology*, *133*(2), 433-439.
McDevitt, M. A., Glidewell-Kenney, C., Jimenez, M. A., Ahearn, P. C., Weiss, J., Jameson, J. L., & Levine, J. E. (2008). New insights into the classical and non-classical actions of estrogen: evidence from estrogen receptor knock-out and knock-in mice. *Mol Cell Endocrinol*, *290*(1-2), 24-30.
Meattini, I., Bicchierai, G., Saieva, C., De Benedetto, D., Desideri, I., Becherini, C., Abdulcadir, D., Vanzi, E., Boeri, C., & Gabbrielli, S. (2017). Impact of molecular subtypes classification concordance between preoperative core needle biopsy and surgical specimen on early breast cancer management: Single-institution experience and review of published literature. *European Journal of Surgical Oncology (EJSO)*, *43*(4), 642-648.
Meitzen, J., & Mermelstein, P. G. (2011). Estrogen receptors stimulate brain region specific metabotropic glutamate receptors to rapidly initiate signal transduction pathways. *J Chem Neuroanat*, *42*(4), 236-241.
Mellon, S. H., & Deschepper, C. F. (1993). Neurosteroid biosynthesis: genes for adrenal steroidogenic enzymes are expressed in the brain. *Brain Research*, *629*(2), 283-292.
Merchenthaler, I., Lane, M. V., Numan, S., & Dellovade, T. L. (2004). Distribution of estrogen receptor α and β in the mouse central nervous system: in vivo autoradiographic and immunocytochemical analyses. *Journal of Comparative Neurology*, *473*(2), 270-291.
Micevych, P., & Christensen, A. (2012). Membrane-initiated estradiol actions mediate structural plasticity and reproduction. *Front Neuroendocrinol*, *33*(4), 331-341.
Micevych, P., & Sinchak, K. (2008). Synthesis and function of hypothalamic neuroprogesterone in reproduction. *Endocrinology*, *149*(6), 2739-2742.
Micevych, P. E., Chaban, V., Ogi, J., Dewing, P., Lu, J. K., & Sinchak, K. (2007). Estradiol stimulates progesterone synthesis in hypothalamic astrocyte cultures [Research Support, N.I.H., Extramural]. *Endocrinology*, *148*(2), 782-789.
Micevych, P. E., & Dewing, P. (2011). Membrane-initiated estradiol signaling regulating sexual receptivity. *Front Endocrinol (Lausanne)*, *2*, 26.
Miller, W. L. (2007). Steroidogenic acute regulatory protein (StAR), a novel mitochondrial cholesterol transporter. *Biochimica et Biophysica Acta (BBA)-Molecular and Cell Biology of Lipids*, *1771*(6), 663-676.
Mosselman, S., Polman, J., & Dijkema, R. (1996). ERβ: Identification and characterization of a novel human estrogen receptor. *FEBS Letters*, *392*(1), 49-53.
Mueller, S. O., & Korach, K. S. (2001). Estrogen receptors and endocrine diseases: lessons from estrogen receptor knockout mice. *Curr Opin Pharmacol*, *1*(6), 613-619.
Murakami, G., Hojo, Y., Kato, A., Komatsuzaki, Y., Horie, S., Soma, M., Kim, J., & Kawato, S. (2018). Rapid nongenomic modulation by neurosteroids of dendritic spines in the hippocampus: androgen, oestrogen and corticosteroid. *Journal of Neuroendocrinology*, *30*(2), e12561.
Murray, A. F., & Delivopoulos, E. (2021). Adhesion and Growth of Neuralized Mouse Embryonic Stem Cells on Parylene-C/SiO2 Substrates. *Materials*, *14*(12), 3174.
Musatov, S., Chen, W., Pfaff, D. W., Kaplitt, M. G., & Ogawa, S. (2006). RNAi-mediated silencing of estrogen receptor α in the ventromedial nucleus of hypothalamus

abolishes female sexual behaviors. *Proceedings of the National Academy of Sciences*, *103*(27), 10456-10460.
Naftolin, F., & MacLusky, N. J. (1982). Aromatase in the central nervous system. *Cancer Res*, *42*(8 Suppl), 3274s-3276s.
Naveh-Many, T., & Nechama, M. (2007). Regulation of parathyroid hormone mRNA stability by calcium, phosphate and uremia. *Current opinion in nephrology and hypertension*, *16*(4), 305-310.
Nelson, L. R., & Bulun, S. E. (2001). Estrogen production and action. *Journal of the American Academy of Dermatology*, *45*(3), S116-S124.
Nelson, R. J., & Trainor, B. C. (2007). Neural mechanisms of aggression. *Nat Rev Neurosci*, *8*(7), 536-546.
Nes, W. D. (2011). Biosynthesis of cholesterol and other sterols. *Chemical reviews*, *111*(10), 6423-6451.
Newman, A., Chin, E., Schmidt, K., Bond, L., Wynne-Edwards, K., & Soma, K. (2008). Analysis of steroids in songbird plasma and brain by coupling solid phase extraction to radioimmunoassay. *General and Comparative Endocrinology*, *155*(3), 503-510.
Newman, S. W. (1999). The medial extended amygdala in male reproductive behavior. A node in the mammalian social behavior network. *Ann N Y Acad Sci*, *877*, 242-257.
Nilsson, M. E., Vandenput, L., Tivesten, Å., Norlén, A.-K., Lagerquist, M. K., Windahl, S. H., Börjesson, A. E., Farman, H. H., Poutanen, M., & Benrick, A. (2015). Measurement of a comprehensive sex steroid profile in rodent serum by high-sensitive gas chromatography-tandem mass spectrometry. *Endocrinology*, *156*(7), 2492-2502.
Nilsson, S., & Gustafsson, J. A. (2011). Estrogen receptors: therapies targeted to receptor subtypes. *Clin Pharmacol Ther*, *89*(1), 44-55.
Nilsson, S., Makela, S., Treuter, E., Tujague, M., Thomsen, J., Andersson, G., Enmark, E., Pettersson, K., Warner, M., & Gustafsson, J. (2001). Mechanisms of estrogen action. *Physiol Rev*, *81*(4), 1535-1565.
Nishida, Y., Yoshioka, M., & St-Amand, J. (2005). Sexually dimorphic gene expression in the hypothalamus, pituitary gland, and cortex. *Genomics*, *85*(6), 679-687.
Nomura, M., Andersson, S., Korach, K. S., Gustafsson, J. A., Pfaff, D. W., & Ogawa, S. (2006). Estrogen receptor-beta gene disruption potentiates estrogen-inducible aggression but not sexual behaviour in male mice. *Eur J Neurosci*, *23*(7), 1860-1868.
Nomura, M., Durback, L., Chan, J., Gustafsson, J.-A., Smithies, O., Korach, K. S., Pfaff, D. W., & Ogawa, S. (2002). Genotype/age interactions on aggressive behavior in gonadally intact estrogen receptor b knockout (bERKO) male mice. *Horm Behav*, *41*(3), 288-296.
Norman, A. W., & Litwack, G. (1997). General considerations of hormones. *Hormones*, *1*, 2-49.
Notas, G., Panagiotopoulos, A., Vamvoukaki, R., Kalyvianaki, K., Kiagiadaki, F., Deli, A., Kampa, M., & Castanas, E. (2021). ERα36-GPER1 Collaboration Inhibits TLR4/NFκB-Induced Pro-Inflammatory Activity in Breast Cancer Cells. *Int J Mol Sci*, *22*(14).
O'Connell, L. A., & Hofmann, H. A. (2011). The vertebrate mesolimbic reward system and social behavior network: a comparative synthesis. *J Comp Neurol*, *519*(18), 3599-3639.
Ogawa, S., Chan, J., Chester, A. E., Gustafsson, J. A., Korach, K. S., & Pfaff, D. W. (1999). Survival of reproductive behaviors in estrogen receptor beta gene-deficient (betaERKO) male and female mice. *Proc Natl Acad Sci USA*, *96*(22), 12887-12892.
Ogawa, S., Eng, V., Taylor, J., Lubahn, D. B., Korach, K. S., & Pfaff, D. W. (1998). Roles of estrogen receptor-alpha gene expression in reproduction-related behaviors in female mice. *Endocrinology*, *139*(12), 5070-5081.

Ogawa, S., & Pfaff, D. (1999). Genes participating in the control of reproductive behaviors. In D. W. Pfaff, W. Berrettini, T. Joh, & S. Maxson (Eds.), *Genetic Influences on Neural and Behavioral Function*. CRC Press.

Ogawa, S., Tsukahara, S., Choleris, E., & Vasudevan, N. (2020). Estrogenic regulation of social behavior and sexually dimorphic brain formation. *Neurosci Biobehav Rev*, *110*, 46-59.

Orikasa, C., Mizuno, K., Sakuma, Y., & Hayashi, S. (1996). Exogenous estrogen acts differently on production of estrogen receptor in the preoptic area and the mediobasal hypothalamic nuclei in the newborn rat. *Neurosci Res*, *25*(3), 247-254.

Otto, C., Rohde-Schulz, B., Schwarz, G., Fuchs, I., Klewer, M., Brittain, D., Langer, G., Bader, B., Prelle, K., Nubbemeyer, R., & Fritzemeier, K. H. (2008). G protein-coupled receptor 30 localizes to the endoplasmic reticulum and is not activated by estradiol. *Endocrinology*, *149*(10), 4846-4856.

Paisley, J. C., Huddleston, G. G., Carruth, L. L., Petrulis, A., Grober, M. S., & Clancy, A. N. (2012). Sexual responses of the male rat medial preoptic area and medial amygdala to estrogen I: site specific suppression of estrogen receptor alpha. *Horm Behav*, *62*(1), 50-57.

Palkovits, M. (1973). Isolated removal of hypothalamic or other brain nuclei of the rat. *Brain Res*, *59*, 449-450.

Parsons, B., Rainbow, T., Pfaff, D., & McEwen, B. (1982). Hypothalamic protein synthesis essential for the activation of the lordosis reflex in the female rat. *Endocrinology*, *110*, 620-624.

Patisaul, H. B., Whitten, P. L., & Young, L. J. (1999). Regulation of estrogen receptor beta mRNA in the brain: opposite effects of 17β-estradiol and the phytoestrogen, coumestrol. *Molecular Brain Research*, *67*(1), 165-171.

Pawlak, J., Karolczak, M., Krust, A., Chambon, P., & Beyer, C. (2005). Estrogen receptor-alpha is associated with the plasma membrane of astrocytes and coupled to the MAP/Src-kinase pathway. *Glia*, *50*(3), 270-275.

Pedram, A., Razandi, M., & Levin, E. R. (2006). Nature of functional estrogen receptors at the plasma membrane. *Molecular Endocrinology*, *20*(9), 1996-2009.

Pedram, A., Razandi, M., & Levin, E. R. (2006). Nature of Functional Estrogen Receptors at the Plasma Membrane. *Mol Endocrinol*.

Pedram, A., Razandi, M., Sainson, R. C., Kim, J. K., Hughes, C. C., & Levin, E. R. (2007). A conserved mechanism for steroid receptor translocation to the plasma membrane. *Journal of Biological Chemistry*, *282*(31), 22278-22288.

Pelekanou, V., Notas, G., Kampa, M., Tsentelierou, E., Radojicic, J., Leclercq, G., Castanas, E., & Stathopoulos, E. (2011). ERα36, a new variant of the ERα is expressed in triple negative breast carcinomas and has a specific transcriptomic signature in breast cancer cell lines. *Steroids*, *77*, 928-934.

Peljto, M., Dasen, J. S., Mazzoni, E. O., Jessell, T. M., & Wichterle, H. (2010). Functional diversity of ESC-derived motor neuron subtypes revealed through intraspinal transplantation. *Cell Stem Cell*, *7*(3), 355-366.

Peljto, M., Dasen, J. S., Mazzoni, E. O., Jessell, T. M., & Wichterle, H. (2010). Functional diversity of ESC-derived motor neuron subtypes revealed through intraspinal transplantation. *Cell Stem Cell*, *7*(3), 355-366.

Pelletier, G. (2010). Steroidogenic enzymes in the brain: morphological aspects. *Prog Brain Res*, *181*, 193-207.

Penot, G., Le Péron, C., Mérot, Y., Grimaud-Fanouillere, E., Ferriere, F., Boujrad, N., Kah, O., Saligaut, C., Ducouret, B., & Métivier, R. (2005). The human estrogen receptor-α isoform hERα46 antagonizes the proliferative influence of hERα66 in MCF7 breast cancer cells. *Endocrinology*, *146*(12), 5474-5484.

Petrie, W. K., Dennis, M. K., Hu, C., Dai, D., Arterburn, J. B., Smith, H. O., Hathaway, H. J., & Prossnitz, E. R. (2013). G protein-coupled estrogen receptor-selective ligands modulate endometrial tumor growth. *Obstet Gynecol Int*, *2013*.

Pettersson, K., Delaunay, F., & Gustafsson, J. A. (2000). Estrogen receptor beta acts as a dominant regulator of estrogen signaling. *Oncogene*, *19*(43), 4970-4978.

Pfaff, D. (1973). Luteinizing hormone releasing factor (LRF) potentiates lordosis behavior in hypophysectomized ovariectomized female rats. *Science*, *182*, 1148-1149.

Pfaff, D. (1998). Hormonal and environmental control of lordosis behavior: Neural and molecular mechanisms. *Eur J Neurosci*, *10*, 330.

Pfaff, D. W., McCarthy, M., Schwartz-Giblin, S., & Kow, L. M. (1994). Female reproductive behavior. In E. Knobil & J. Neill (Eds.), *The Physiology of Reproduction* (Vol. 2, pp. 107-220.). Raven.

Pfaff, D. W., & Sakuma, Y. (1979). Deficit in the lordosis reflex of female rats caused by lesions in the ventromedial nucleus of the hypothalamus. *J Physiol (Lond)*, *288*, 203-210.

Phan, A., Gabor, C. S., Favaro, K. J., Kaschack, S., Armstrong, J. N., MacLusky, N. J., & Choleris, E. (2012). Low doses of 17beta-estradiol rapidly improve learning and increase hippocampal dendritic spines. *Neuropsychopharmacology*, *37*(10), 2299-2309.

Phan, A., Lancaster, K. E., Armstrong, J. N., MacLusky, N. J., & Choleris, E. (2011). Rapid effects of estrogen receptor alpha and beta selective agonists on learning and dendritic spines in female mice. *Endocrinology*, *152*(4), 1492-1502.

Phoenix, C. H., Goy, R. W., Gerall, A. A., & Young, W. C. (1959). Organizing Action Of Prenatally Administered Testosterone Propionate On The Tissues Mediating Mating Behavior In The Female Guinea Pig1. *Endocrinology*, *65*(3), 369-382.

Pierman, S., Sica, M., Allieri, F., Viglietti-Panzica, C., Panzica, G. C., & Bakker, J. (2008). Activational effects of estradiol and dihydrotestosterone on social recognition and the arginine-vasopressin immunoreactive system in male mice lacking a functional aromatase gene. *Horm Behav*, *54*(1), 98-106.

Pike, A. C. W., Brzozowski, A. M., & Hubbard, R. E. (2000). A structural biologist's view of the oestrogen receptor. *The Journal of Steroid Biochemistry and Molecular Biology*, *74*(5), 261-268.

Prange-Kiel, J., Jarry, H., Schoen, M., Kohlmann, P., Lohse, C., Zhou, L., & Rune, G. M. (2008). Gonadotropin-releasing hormone regulates spine density via its regulatory role in hippocampal estrogen synthesis. *J Cell Biol*, *180*(2), 417-426.

Prange-Kiel, J., & Rune, G. M. (2006). Direct and indirect effects of estrogen on rat hippocampus. *Neuroscience*, *138*(3), 765-772.

Prange-Kiel, J., Wehrenberg, U., Jarry, H., & Rune, G. M. (2003). Para/autocrine regulation of estrogen receptors in hippocampal neurons. *Hippocampus*, *13*(2), 226-234.

Prossnitz, E. R., & Maggiolini, M. (2009a). Mechanisms of estrogen signaling and gene expression via GPR30 [Research Support, N.I.H., Extramural Research Support, Non-U.S. Gov't Review]. *Mol Cell Endocrinol*, *308*(1-2), 32-38.

Prossnitz, E. R., & Maggiolini, M. (2009b). Non-genomic signaling by steroids [Editorial Introductory]. *Mol Cell Endocrinol*, *308*(1-2), 1-2.

Pupo, M., Vivacqua, A., Perrotta, I., Pisano, A., Aquila, S., Abonante, S., Gasperi-Campani, A., Pezzi, V., & Maggiolini, M. (2013). The nuclear localization signal is required for nuclear GPER translocation and function in breast Cancer-Associated Fibroblasts (CAFs). *Molecular and Cellular Endocrinology*, *376*(1-2), 23-32.

Qiu, J., Bosch, M. A., Jamali, K., Xue, C., Kelly, M. J., & Ronnekleiv, O. K. (2006). Estrogen upregulates T-type calcium channels in the hypothalamus and pituitary. *J Neurosci*, *26*(43), 11072-11082.

Qiu, J., Bosch, M. A., Tobias, S. C., Krust, A., Graham, S. M., Murphy, S. J., Korach, K. S., Chambon, P., Scanlan, T. S., Ronnekleiv, O. K., & Kelly, M. J. (2006). A G-protein-coupled estrogen receptor is involved in hypothalamic control of energy homeostasis. *J Neurosci*, *26*(21), 5649-5655.

Qu, C., Ma, J., Zhang, Y., Han, C., Huang, L., Shen, L., Li, H., Wang, X., Liu, J., & Zou, W. (2019). Estrogen receptor variant ER-α36 promotes tamoxifen agonist activity in glioblastoma cells. *Cancer Science*, *110*(1), 221-234.

Qu, Q., Li, D., Louis, K. R., Li, X., Yang, H., Sun, Q., Crandall, S. R., Tsang, S., Zhou, J., Cox, C. L., Cheng, J., & Wang, F. (2014). High-efficiency motor neuron differentiation from human pluripotent stem cells and the function of Islet-1. *Nat Commun*, *5*(1), 3449.

Rainville, J., Pollard, K., & Vasudevan, N. (2015). Membrane-initiated non-genomic signaling by estrogens in the hypothalamus: cross-talk with glucocorticoids with implications for behavior [Review]. *Front Endocrinol (Lausanne)*, *6*.

Rainville, J. R., Weiss, G. L., Evanson, N., Herman, J. P., Vasudevan, N., & Tasker, J. G. (2019). Membrane-initiated nuclear trafficking of the glucocorticoid receptor in hypothalamic neurons. *Steroids*, *142*, 55-64.

Ray, J., Peterson, D. A., Schinstine, M., & Gage, F. H. (1993). Proliferation, differentiation, and long-term culture of primary hippocampal neurons. *Proceedings of the National Academy of Sciences*, *90*(8), 3602-3606.

Razandi, M., Alton, G., Pedram, A., Ghonshani, S., Webb, P., & Levin, E. R. (2003). Identification of a structural determinant necessary for the localization and function of estrogen receptor alpha at the plasma membrane. *Mol Cell Biol*, *23*(5), 1633-1646.

Razandi, M., Pedram, A., Merchenthaler, I., Greene, G. L., & Levin, E. R. (2004). Plasma membrane estrogen receptors exist and functions as dimers. *Molecular Endocrinology*, *18*(12), 2854-2865.

Razandi, M., Pedram, A., Merchenthaler, I., Greene, G. L., & Levin, E. R. (2004). Plasma membrane estrogen receptors exist and functions as dimers. *Mol Endocrinol*, *18*(12), 2854-2865.

Remage-Healey, L., Maidment, N. T., & Schlinger, B. A. (2008). Forebrain steroid levels fluctuate rapidly during social interactions. *Nat Neurosci*, *11*(11), 1327-1334.

Revankar, C. M., Cimino, D. F., Sklar, L. A., Arterburn, J. B., & Prossnitz, E. R. (2005). A transmembrane intracellular estrogen receptor mediates rapid cell signaling. *Science*, *307*(5715), 1625-1630.

Revankar, C. M., Cimino, D. F., Sklar, L. A., Arterburn, J. B., & Prossnitz, E. R. (2005). A Transmembrane Intracellular Estrogen Receptor Mediates Rapid Cell Signaling. *Science*, *307*(5715), 1625-1630.

Romano, G. J., Mobbs, C. V., Lauber, A., Howells, R. D., & Pfaff, D. W. (1990). Differential regulation of proenkephalin gene expression by estrogen in the ventromedial hypothalamus of male and female rats: implications for the molecular basis of a sexually differentiated behavior. *Molecular Brain Research*, *536*, 63-68.

Roselli, C., Cross, E., Poonyagariyagorn, H., & Stadelman, H. (2003). Role of aromatization in anticipatory and consummatory aspects of sexual behavior in male rats. *Hormones and Behavior*, *44*(2), 146-151.

Roselli, C. E. (1995). Subcellular localization and kinetic properties of aromatase activity in rat brain. *J Steroid Biochem Mol Biol*, *52*(5), 469-477.

Roselli, C. E., Ellinwood, W. E., & Resko, J. A. (1984). Regulation of brain aromatase activity in rats. *Endocrinology*, *114*(1), 192-200.

Roselli, C. E., Horton, L. E., & Resko, J. A. (1985). Distribution and regulation of aromatase activity in the rat hypothalamus and limbic system. *Endocrinology*, *117*(6), 2471-2477.

Roselli, C. E., & Klosterman, S. A. (1998). Sexual differentiation of aromatase activity in the rat brain: effects of perinatal steroid exposure. *Endocrinology*, *139*(7), 3193-3201.

Rosenfeld, C. S., Shay, D. A., & Vieira-Potter, V. J. (2018). Cognitive effects of aromatase and possible role in memory disorders. *Front Endocrinol (Lausanne)*, *9*, 610.

Rosie, R., Wilson, H., & Fink, G. (1993). Testosterone Induces an All-or-None, Exponential Increase in Arginine Vasopressin mRNA in the Bed Nucleus of Stria Terminalis of the Hypogonadal Mouse. *Mol Cell Neurosci*, *4*(1), 121-126.

Sa, S. I., Pereira, P. A., Malikov, V., Ferreira, I. M., & Madeira, M. D. (2014). Role of plasma membrane estrogen receptors in mediating the estrogen induction of progesterone receptors in hypothalamic ventromedial neurons. *J Comp Neurol*, *522*(2), 298-307.

Saczko, J., Michel, O., Chwiłkowska, A., Sawicka, E., Mączyńska, J., & Kulbacka, J. (2017). Estrogen Receptors in Cell Membranes: Regulation and Signaling. *Adv Anat Embryol Cell Biol*, *227*, 93-105.

Sagoshi, S., Maejima, S., Morishita, M., Takenawa, S., Otubo, A., Takanami, K., Sakamoto, T., Sakamoto, H., Tsukahara, S., & Ogawa, S. (2020). Detection and Characterization of Estrogen Receptor Beta Expression in the Brain with Newly Developed Transgenic Mice. *Neuroscience*, *438*, 182-197.

Sakamoto, H., Matsuda, K., Hosokawa, K., Nishi, M., Morris, J. F., Prossnitz, E. R., & Kawata, M. (2007). Expression of G protein-coupled receptor-30, a G protein-coupled membrane estrogen receptor, in oxytocin neurons of the rat paraventricular and supraoptic nuclei. *Endocrinology*, *148*(12), 5842-5850.

Saldanha, C. J., Burstein, S. R., & Duncan, K. A. (2013). Induced synthesis of estrogens by glia in the songbird brain. *J Neuroendocrinol*.

Saldanha, C. J., Tuerk, M. J., Kim, Y. H., Fernandes, A. O., Arnold, A. P., & Schlinger, B. A. (2000). Distribution and regulation of telencephalic aromatase expression in the zebra finch revealed with a specific antibody. *Journal of Comparative Neurology*, *423*(4), 619-630.

Sandén, C., Broselid, S., Cornmark, L., Andersson, K., Daszkiewicz-Nilsson, J., Mårtensson, U. E., Olde, B., & Leeb-Lundberg, L. F. (2011). G protein-coupled estrogen receptor 1/G protein-coupled receptor 30 localizes in the plasma membrane and traffics intracellularly on cytokeratin intermediate filaments. *Molecular pharmacology*, *79*(3), 400-410.

Sano, K., Tsuda, M. C., Musatov, S., Sakamoto, T., & Ogawa, S. (2013). Differential effects of site-specific knockdown of estrogen receptor alpha in the medial amygdala, medial pre-optic area, and ventromedial nucleus of the hypothalamus on sexual and aggressive behavior of male mice [Research Support, Non-U.S. Gov't]. *Eur J Neurosci*, *37*(8), 1308-1319.

Sano, K., Vasudevan, N., Nagata, K., Nakata, M., Uchimura, T., Xiao, K., Tsuda, M. C., & Ogawa, S. (2013). Loss of neuronal ERα abolishes sexual and aggressive behaviors in male mice. *Tsukuba Psychol Res*, *45*, 1-9.

Schindelin, J., Arganda-Carreras, I., Frise, E., Kaynig, V., Longair, M., Pietzsch, T., Preibisch, S., Rueden, C., Saalfeld, S., & Schmid, B. (2012). Fiji: an open-source platform for biological-image analysis. *Nat Methods*, *9*(7), 676-682.

Schlegel, A., Wang, C., Katzenellenbogen, B. S., Pestell, R. G., & Lisanti, M. P. (1999). Caveolin-1 Potentiates Estrogen Receptor α (ERα) Signaling: Caveolin-1 Drives Ligand-Independent Nuclear Translocation And Activation Of ERα*. *Journal of Biological Chemistry*, *274*(47), 33551-33556.

Schneider, C. A., Rasband, W. S., & Eliceiri, K. W. (2012). NIH Image to ImageJ: 25 years of image analysis. *Nat Methods*, *9*(7), 671-675.

Schumacher, M., Guennoun, R., Mercier, G., Désarnaud, F., Lacor, P., Bénavides, J., Ferzaz, B., Robert, F., & Baulieu, E. E. (2001). Progesterone synthesis and myelin formation in peripheral nerves. *Brain research reviews*, *37*(1-3), 343-359.

Scott, C. J., Tilbrook, A. J., Simmons, D. M., Rawson, J. A., Chu, S., Fuller, P. J., Ing, N. H., & Clarke, I. J. (2000). The distribution of cells containing estrogen receptor-alpha (ERalpha) and ERbeta messenger ribonucleic acid in the preoptic area and

hypothalamus of the sheep: comparison of males and females. *Endocrinology*, *141*(8), 2951-2962.
Seredynski, A. L., Balthazart, J., Ball, G. F., & Cornil, C. A. (2015). Estrogen Receptor beta Activation Rapidly Modulates Male Sexual Motivation through the Transactivation of Metabotropic Glutamate Receptor 1a. *J Neurosci*, *35*(38), 13110-13123.
Seredynski, A. L., Balthazart, J., Christophe, V. J., Ball, G. F., & Cornil, C. A. (2013). Neuroestrogens rapidly regulate sexual motivation but not performance [Research Support, N.I.H., Extramural Research Support, Non-U.S. Gov't]. *J Neurosci*, *33*(1), 164-174.
Sheppard, P. A. S., Koss, W. A., Frick, K. M., & Choleris, E. (2018). Rapid actions of oestrogens and their receptors on memory acquisition and consolidation in females. *J Neuroendocrinol*, *30*(2).
Sheridan, P. J. (1979). The nucleus interstitialis striae terminalis and the nucleus amygdaloideus medialis: prime targets for androgen in the rat forebrain. *Endocrinology*, *104*(1), 130-136.
Shparberg, R. A., Glover, H. J., & Morris, M. B. (2019). Modeling mammalian commitment to the neural lineage using embryos and embryonic stem cells. *Frontiers in physiology*, *10*, 447012.
Shughrue, P., Komm, B., & Merchenthaler, I. (1996). The distribution of estrogen receptor b mRNA in the rat hypothalamus. *Steroids*, *61*, 678-681.
Shughrue, P., Scrimo, P., Lane, M., Askew, R., & Merchenthaler, I. (1997). The distribution of estrogen receptor-beta mRNA in forebrain regions of the estrogen receptor-alpha knockout mouse. *Endocrinology*, *138*(12), 5649-5652.
Simerly, R. B. (1990). Hormonal control of neuropeptide gene expression in sexually dimorphic olfactory pathways. *Trends Neurosci*, *13*(3), 104-110.
Simerly, R. B., Chang, C., Muramatsu, M., & Swanson, L. W. (1990). Distribution of androgen and estrogen receptor mRNA-containing cells in the rat brain: an in situ hybridization study. *J Comp Neurol*, *294*(1), 76-95.
Simerly, R. B., Swanson, L. W., Handa, R. J., & Gorski, R. A. (1985). Influence of perinatal androgen on the sexually dimorphic distribution of tyrosine hydroxylase-immunoreactive cells and fibers in the anteroventral periventricular nucleus of the rat. *Neuroendocrinology*, *40*(6), 501-510.
Simoncini, T., Fornari, L., Mannella, P., Varone, G., Caruso, A., Liao, J. K., & Genazzani, A. R. (2002). Novel non-transcriptional mechanisms for estrogen receptor signaling in the cardiovascular system. Interaction of estrogen receptor alpha with phosphatidylinositol 3-OH kinase. *Steroids*, *67*(12), 935-939.
Sinchak, K., Eckersell, C., Quezada, V., Norell, A., & Micevych, P. (2000). Preproenkephalin mRNA levels are regulated by acute stress and estrogen stimulation. *Physiol Behav*, *69*(4-5), 425-432.
Singewald, G. M., Rjabokon, A., Singewald, N., & Ebner, K. (2011). The modulatory role of the lateral septum on neuroendocrine and behavioral stress responses. *Neuropsychopharmacology*, *36*(4), 793-804.
Sirianni, R., Chimento, A., Ruggiero, C., De Luca, A., Lappano, R., Ando, S., Maggiolini, M., & Pezzi, V. (2008). The novel estrogen receptor, G protein-coupled receptor 30, mediates the proliferative effects induced by 17beta-estradiol on mouse spermatogonial GC-1 cell line. *Endocrinology*, *149*(10), 5043-5051.
Snyder, M. A., Smejkalova, T., Forlano, P. M., & Woolley, C. S. (2010). Multiple ERbeta antisera label in ERbeta knockout and null mouse tissues. *J Neurosci Methods*, *188*(2), 226-234.
Snyder, M. A., Smejkalova, T., Forlano, P. M., & Woolley, C. S. (2010). Multiple ERβ antisera label in ERβ knockout and null mouse tissues. *J Neurosci Methods*, *188*(2), 226-234.

Sodersten, P., & Eneroth, P. (1981). Serum levels of oestradiol-17β and progesterone in relation to sexual receptivity in intact and ovariectomized rats. *Journal of Endocrinology*, *89*(1), 45-54.

Sohrabji, F. (2015). Estrogen-IGF-1 interactions in neuroprotection: ischemic stroke as a case study. *Front Neuroendocrinol*, *36*, 1-14.

Soma, K. K., Alday, N. A., Hau, M., & Schlinger, B. A. (2004). Dehydroepiandrosterone metabolism by 3β-hydroxysteroid dehydrogenase/Δ5-Δ4 isomerase in adult zebra finch brain: sex difference and rapid effect of stress. *Endocrinology*, *145*(4), 1668-1677.

Sparks, P. D., & LeDoux, J. E. (1995). Septal lesions potentiate freezing behavior to contextual but not to phasic conditioned stimuli in rats. *Behav Neurosci*, *109*(1), 184.

Stanic, D., Dubois, S., Chua, H. K., Tonge, B., Rinehart, N., Horne, M. K., & Boon, W. C. (2014). Characterization of aromatase expression in the adult male and female mouse brain. I. Coexistence with oestrogen receptors alpha and beta, and androgen receptors. *PLoS One*, *9*(3), e90451.

Stauffer, W., Sheng, H., & Lim, H. N. (2018). EzColocalization: An ImageJ plugin for visualizing and measuring colocalization in cells and organisms. *Scientific Reports*, *8*(1), 1-13.

Stocco, C. (2012). Tissue physiology and pathology of aromatase. *Steroids*, *77*(1-2), 27-35.

Strober, W. (2015). Trypan blue exclusion test of cell viability. *Current protocols in immunology*, *111*(1), A3. B. 1-A3. B. 3.

Sze, Y., Gill, A. C., & Brunton, P. J. (2018). Sex-dependent changes in neuroactive steroid concentrations in the rat brain following acute swim stress. *Journal of Neuroendocrinology*, *30*(11), e12644.

Szego, C. M., & Davis, J. S. (1967). Adenosine 3',5'-monophosphate in rat uterus: acute elevation by estrogen. *Proc Natl Acad Sci U S A*, *58*(4), 1711-1718.

Tabatadze, N., Sato, S. M., & Woolley, C. S. (2014). Quantitative analysis of long-form aromatase mRNA in the male and female rat brain. *PLoS One*, *9*(7), e100628.

Tabatadze, N., Smejkalova, T., & Woolley, C. S. (2013). Distribution and posttranslational modification of synaptic ERalpha in the adult female rat hippocampus. *Endocrinology*, *154*(2), 819-830.

Taziaux, M., Cornil, C. A., Dejace, C., Arckens, L., Ball, G. F., & Balthazart, J. (2006). Neuroanatomical specificity in the expression of the immediate early gene c-fos following expression of appetitive and consummatory male sexual behaviour in Japanese quail [Research Support, N.I.H., Extramural Research Support, Non-U.S. Gov't]. *Eur J Neurosci*, *23*(7), 1869-1887.

Taziaux, M., Lopez, J., Cornil, C. A., Balthazart, J., & Holloway, K. S. (2007). Differential c-fos expression in the brain of male Japanese quail following exposure to stimuli that predict or do not predict the arrival of a female [Research Support, N.I.H., Extramural Research Support, Non-U.S. Gov't]. *Eur J Neurosci*, *25*(9), 2835-2846.

Tecalco-Cruz, A. C., Pérez-Alvarado, I. A., Ramírez-Jarquín, J. O., & Rocha-Zavaleta, L. (2017). Nucleo-cytoplasmic transport of estrogen receptor alpha in breast cancer cells. *Cellular Signalling*, *34*, 121-132.

Thomas, P., Pang, Y., Filardo, E. J., & Dong, J. (2005). Identity of an estrogen membrane receptor coupled to a G protein in human breast cancer cells. *Endocrinology*, *146*(2), 624-632.

Thompson, R., Goodson, J., Ruscio, M., & Adkins-Regan, E. (1998). Role of the archistriatal nucleus taeniae in the sexual behavior of male Japanese quail (Coturnix japonica): a comparison of function with the medial nucleus of the amygdala in mammals. *Brain Behavior and Evolution*, *51*(4), 215-229.

Trainor, B. C., Crean, K. K., Fry, W. H., & Sweeney, C. (2010). Activation of extracellular signal-regulated kinases in social behavior circuits during resident-intruder aggression tests. *Neuroscience*, *165*(2), 325-336.

Trainor, B. C., Finy, M. S., & Nelson, R. J. (2008). Rapid effects of estradiol on male aggression depend on photoperiod in reproductively non-responsive mice. *Horm Behav*, *53*(1), 192-199.

Trainor, B. C., Greiwe, K. M., & Nelson, R. J. (2006). Individual differences in estrogen receptor alpha in select brain nuclei are associated with individual differences in aggression. *Horm Behav*, *50*(2), 338-345.

Trainor, B. C., Lin, S., Finy, M. S., Rowland, M. R., & Nelson, R. J. (2007). Photoperiod reverses the effects of estrogens on male aggression via genomic and nongenomic pathways [Comparative Study Research Support, N.I.H., Extramural]. *Proc Natl Acad Sci U S A*, *104*(23), 9840-9845.

Trainor, B. C., Rowland, M. R., & Nelson, R. J. (2007). Photoperiod affects estrogen receptor alpha, estrogen receptor beta and aggressive behavior. *Eur J Neurosci*, *26*(1), 207-218. https://doi.org/EJN5654 [pii]

10.1111/j.1460-9568.2007.05654.x

Turner, B. M. (2008). Open chromatin and hypertranscription in embryonic stem cells. *Cell Stem Cell*, *2*(5), 408-410.

Tuscher, J. J., Szinte, J. S., Starrett, J. R., Krentzel, A. A., Fortress, A. M., Remage-Healey, L., & Frick, K. M. (2016). Inhibition of local estrogen synthesis in the hippocampus impairs hippocampal memory consolidation in ovariectomized female mice. *Horm Behav*, *83*, 60-67.

Tzeng, H.-H., Hsu, C.-H., Chung, T.-H., Lee, W.-C., Lin, C.-H., Wang, W.-C., Hsiao, C.-Y., Leu, Y.-W., & Wang, T.-H. (2015). Cell signaling and differential protein expression in neuronal differentiation of bone marrow mesenchymal stem cells with hypermethylated Salvador/Warts/Hippo (SWH) pathway genes. *PLoS One*, *10*(12), e0145542.

Ubuka, T., Haraguchi, S., Tobari, Y., Narihiro, M., Ishikawa, K., Hayashi, T., Harada, N., & Tsutsui, K. (2014). Hypothalamic inhibition of socio-sexual behaviour by increasing neuroestrogen synthesis. *Nat Commun*, *5*, 3061.

Uddin, M. M., Ibrahim, M. M., & Briski, K. P. (2020). Sex-dimorphic neuroestradiol regulation of ventromedial hypothalamic nucleus glucoregulatory transmitter and glycogen metabolism enzyme protein expression in the rat. *BMC Neurosci*, *21*, 1-18.

Unger, E. K., Burke, K. J., Jr., Yang, C. F., Bender, K. J., Fuller, P. M., & Shah, N. M. (2015). Medial amygdalar aromatase neurons regulate aggression in both sexes. *Cell Rep*, *10*(4), 453-462.

Vahaba, D. M., & Remage-Healey, L. (2018). Neuroestrogens rapidly shape auditory circuits to support communication learning and perception: Evidence from songbirds. *Hormones and Behavior*, *104*, 77-87.

Vajaria, R., & Vasudevan, N. (2018). Is the membrane estrogen receptor, GPER1, a promiscuous receptor that modulates nuclear estrogen receptor-mediated functions in the brain? *Horm Behav*, *104*, 165-172.

Vajaria, R., & Vasudevan, N. (2018). Is the membrane estrogen receptor, GPER1, a promiscuous receptor that modulates nuclear estrogen receptor-mediated functions in the brain? *Hormones and Behavior*, *104*, 165-172.

Vasudevan, N., & Pfaff, D. W. (2007). Membrane-initiated actions of estrogens in neuroendocrinology: emerging principles. *Endocr Rev*, *28*(1), 1-19.

Vasudevan, N., & Pfaff, D. W. (2008). Non-genomic actions of estrogens and their interaction with genomic actions in the brain. *Front Neuroendocrinol*, *29*(2), 238-257.

Veening, J. G., Coolen, L. M., Spooren, W. J., Joosten, H., van Oorschot, R., Mos, J., Ronken, E., & Olivier, B. (1998). Patterns of c-fos expression induced by fluvoxamine are different after acute vs. chronic oral administration. *Eur Neuropsychopharmacol*, *8*(3), 213-226.

Veillat, V., Sengers, V., Metz, C. N., Roger, T., Leboeuf, M., Mailloux, J., & Akoum, A. (2012). Macrophage migration inhibitory factor is involved in a positive feedback loop increasing aromatase expression in endometriosis. *The American journal of pathology*, *181*(3), 917-927.

Vierk, R., Glassmeier, G., Zhou, L., Brandt, N., Fester, L., Dudzinski, D., Wilkars, W., Bender, R. A., Lewerenz, M., Gloger, S., Graser, L., Schwarz, J., & Rune, G. M. (2012). Aromatase inhibition abolishes LTP generation in female but not in male mice. *J Neurosci*, *32*(24), 8116-8126.

Villee, D. B. (1972). The development of steroidogenesis. *Am J Med*, *53*(5), 533-544.

Vranic, S., Gatalica, Z., Deng, H., Frkovic-Grazio, S., Lee, L. M., Gurjeva, O., & Wang, Z.-Y. (2011). ER-α36, a novel isoform of ER-α66, is commonly over-expressed in apocrine and adenoid cystic carcinomas of the breast. *Journal of clinical pathology*, *64*(1), 54-57.

Vrtačnik, P., Ostanek, B., Mencej-Bedrač, S., & Marc, J. (2014). The many faces of estrogen signaling. *Biochem Med (Zagreb)*, *24*(3), 329-342.

Wagner, C. K., & Morrell, J. I. (1997). Neuroanatomical distribution of aromatase MRNA in the rat brain: indications of regional regulation. *J Steroid Biochem Mol Biol*, *61*(3-6), 307-314.

Wallacides, A., Chesnel, A., Ajj, H., Chillet, M., Flament, S., & Dumond, H. (2012). Estrogens promote proliferation of the seminoma-like TCam-2 cell line through a GPER-dependent ERα36 induction. *Mol Cell Endocrinol*, *350*(1), 61-71.

Wang, B., Zhang, Y., Zhang, H., & Lin, Q. (2015). Complete mitochondrial genome sequence of the Barbour's seahorse Hippocampus barbouri Jordan & Richardson, 1908 (Gasterosteiformes: Syngnathidae). *Mitochondrial DNA*, *26*(6), 851-852.

Wang, L. (2018). *The Mediation of Conspecific Self-Defense in the Ventromedial Hypothalamus* New York University].

Wang, Z., Zhang, X., Shen, P., Loggie, B. W., Chang, Y., & Deuel, T. F. (2005). Identification, cloning, and expression of human estrogen receptor-α36, a novel variant of human estrogen receptor-α66. *Biochemical and biophysical research communications*, *336*(4), 1023-1027.

Wang, Z., Zhang, X., Shen, P., Loggie, B. W., Chang, Y., & Deuel, T. F. (2006). A variant of estrogen receptor-{alpha}, hER-{alpha}36: transduction of estrogen- and antiestrogen-dependent membrane-initiated mitogenic signaling. *Proc Natl Acad Sci U S A*, *103*(24), 9063-9068.

Watanabe, M., Noda, M., & Nakajin, S. (2007). Aromatase expression in a human osteoblastic cell line increases in response to prostaglandin E2 in a dexamethasone-dependent fashion. *Steroids*, *72*(9-10), 686-692.

Waters, E. M., Thompson, L. I., Patel, P., Gonzales, A. D., Ye, H. Z., Filardo, E. J., Clegg, D. J., Gorecka, J., Akama, K. T., McEwen, B. S., & Milner, T. A. (2015). G-protein-coupled estrogen receptor 1 is anatomically positioned to modulate synaptic plasticity in the mouse hippocampus. *J Neurosci*, *35*(6), 2384-2397.

Watters, J. J., Campbell, J. S., Cunningham, M. J., Krebs, E. G., & Dorsa, D. M. (1997). Rapid membrane effects of steroids in neuroblastoma cells: effects of estrogen on mitogen activated protein kinase signalling cascade and c-fos immediate early gene transcription. *Endocrinology*, *138*(9), 4030-4033.

Watters, J. J., & Dorsa, D. M. (1998). Transcriptional effects of estrogen on neuronal neurotensin gene expression involve cAMP/protein kinase A dependent mechanisms. *J Neurosci*, *18*(7), 6672-6680.

Wehling, M., & Lösel, R. (2006). Non-genomic steroid hormone effects: membrane or intracellular receptors? *The Journal of Steroid Biochemistry and Molecular Biology*, *102*(1-5), 180-183.

Weiser, M. J., Foradori, C. D., & Handa, R. J. (2008). Estrogen receptor beta in the brain: from form to function. *Brain research reviews*, *57*(2), 309-320.

Wichterle, H., & Peljto, M. (2008). Differentiation of mouse embryonic stem cells to spinal motor neurons. *Current protocols in stem cell biology*, *5*(1), 1H. 1.1-1H. 1.9.

Woolley, C. S., & McEwen, B. S. (1992). Estradiol mediates fluctuation in hippocampal synapse density during the estrous cycle in the adult rat [published erratum appears in J Neurosci 1992 Oct; 12 (10): following table of contents]. *Journal of Neuroscience*, *12*(7), 2549-2554.

Wu, M. V., Manoli, D. S., Fraser, E. J., Coats, J. K., Tollkuhn, J., Honda, S., Harada, N., & Shah, N. M. (2009). Estrogen masculinizes neural pathways and sex-specific behaviors [Research Support, N.I.H., Extramural Research Support, Non-U.S. Gov't

Research Support, U.S. Gov't, Non-P.H.S.]. *Cell*, *139*(1), 61-72.

Wu, M. V., & Shah, N. M. (2011). Control of masculinization of the brain and behavior. *Curr Opin Neurobiol*, *21*(1), 116-123.

Wu, W.-f., Maneix, L., Insunza, J., Nalvarte, I., Antonson, P., Kere, J., Yu, N. Y.-L., Tohonen, V., Katayama, S., & Einarsdottir, E. (2017). Estrogen receptor β, a regulator of androgen receptor signaling in the mouse ventral prostate. *Proceedings of the National Academy of Sciences*, *114*(19), E3816-E3822.

Wullimann, M. F., & Mueller, T. (2004). Teleostean and mammalian forebrains contrasted: Evidence from genes to behavior. *J Comp Neurol*, *475*(2), 143-162.

Xu, X., Coats, J. K., Yang, C. F., Wang, A., Ahmed, O. M., Alvarado, M., Izumi, T., & Shah, N. M. (2012). Modular genetic control of sexually dimorphic behaviors. *Cell*, *148*(3), 596-607.

Yang, C. F., Chiang, M. C., Gray, D. C., Prabhakaran, M., Alvarado, M., Juntti, S. A., Unger, E. K., Wells, J. A., & Shah, N. M. (2013). Sexually dimorphic neurons in the ventromedial hypothalamus govern mating in both sexes and aggression in males. *Cell*, *153*(4), 896-909.

Yang, T., Yang, C. F., Chizari, M. D., Maheswaranathan, N., Burke, K. J., Jr., Borius, M., Inoue, S., Chiang, M. C., Bender, K. J., Ganguli, S., & Shah, N. M. (2017). Social Control of Hypothalamus-Mediated Male Aggression. *Neuron*, *95*(4), 955-970 e954.

Ye, J., Coulouris, G., Zaretskaya, I., Cutcutache, I., Rozen, S., & Madden, T. L. (2012). Primer-BLAST: a tool to design target-specific primers for polymerase chain reaction. *BMC bioinformatics*, *13*, 1-11.

Yilmaz, M. B., Wolfe, A., Cheng, Y. H., Glidewell-Kenney, C., Jameson, J. L., & Bulun, S. E. (2009). Aromatase promoter I.f is regulated by estrogen receptor alpha (ESR1) in mouse hypothalamic neuronal cell lines. *Biol Reprod*, *81*(5), 956-965.

Yilmaz, M. B., Wolfe, A., Zhao, H., Brooks, D. C., & Bulun, S. E. (2011). Aromatase promoter I.f is regulated by progesterone receptor in mouse hypothalamic neuronal cell lines. *J Mol Endocrinol*, *47*(1), 69-80.

Yilmaz, M. B., Zhao, H., Brooks, D. C., Fenkci, I. V., Imir-Yenicesu, G., Attar, E., Akbal, E., Kaynak, B. A., & Bulun, S. E. (2015). Estrogen receptor alpha (Esr1) regulates aromatase (Cyp19a1) expression in the mouse brain. *Neuro Endocrinol Lett*, *36*(2), 178-182.

Yin, Y., Huang, P., Han, Z., Wei, G., Zhou, C., Wen, J., Su, B., Wang, X., & Wang, Y. (2014). Collagen nanofibers facilitated presynaptic maturation in differentiated neurons from spinal-cord-derived neural stem cells through MAPK/ERK1/2-Synapsin I signaling pathway. *Biomacromolecules*, *15*(7), 2449-2460.

Yu, X., Filardo, E. J., & Shaikh, Z. A. (2010). The membrane estrogen receptor GPR30 mediates cadmium-induced proliferation of breast cancer cells. *Toxicol Appl Pharmacol*, *245*(1), 83-90.

Yun, S. P., Ryu, J. M., Kim, M. O., Park, J. H., & Han, H. J. (2012). Rapid actions of plasma membrane estrogen receptors regulate motility of mouse embryonic stem cells through a profilin-1/cofilin-1-directed kinase signaling pathway. *Molecular Endocrinology*, *26*(8), 1291-1303.

Zajda, K., & Gregoraszczuk, E. (2020). Environmental polycyclic aromatic hydrocarbons mixture, in human blood levels, decreased oestradiol secretion by granulosa cells via ESR1 and GPER1 but not ESR2 receptor. *Human & Experimental Toxicology*, *39*(3), 276-289.

Zhang, L., Ma, Y., Liu, M., Ma, Y., & Guo, H. (2019). The effects of various estrogen doses on the proliferation and differentiation of cultured neural stem cells. *General Physiology & Biophysics*, *38*(5).

Zhang, M., Cho, E. J., Burstein, G., Siegel, D., & Zhang, Y. (2011). Selective inactivation of a human neuronal silencing phosphatase by a small molecule inhibitor. *ACS Chem Biol*, *6*(5), 511-519.

Zhao, Y., Long, L., Xu, W., Campbell, R. F., Large, E. E., Greene, J. S., & McGrath, P. T. (2018). Changes to social feeding behaviors are not sufficient for fitness gains of the Caenorhabditis elegans N2 reference strain. *Elife*, *7*.

Zhou, K., Sun, P., Zhang, Y., You, X., Li, P., & Wang, T. (2016). Estrogen stimulated migration and invasion of estrogen receptor-negative breast cancer cells involves an ezrin-dependent crosstalk between G protein-coupled receptor 30 and estrogen receptor beta signaling. *Steroids*, *111*, 113-120.

Zhou, Y., Watters, J. J., & Dorsa, D. M. (1996). Estrogen rapidly induces the phosphorylation of the cAMP response element binding protein in rat brain. *Endocrinology*, *137*(5), 2163-2166.

Zivadinovic, D., & Watson, C. S. (2005). Membrane estrogen receptor-alpha levels predict estrogen-induced ERK1/2 activation in MCF-7 cells. *Breast Cancer Res*, *7*(1), R130-144.